

# Fixtureless automated incremental sheet metal forming

by

BALAJI ILANGO VAN

Submitted as

A Doctoral Thesis

Submitted in partial fulfilment of the requirements for the award  
of Doctor of Philosophy of Loughborough University

**24<sup>th</sup> May 2016**

**EPSRC Centre for Innovative Manufacturing in Intelligent  
Automation**

Wolfson School of Mechanical and Manufacturing Engineering

©by **Balaji Ilangovan (2016)**

## ABSTRACT

Die-based forming is a technology used by many industries to form metal panels. However, this method of forming lacks flexibility and cost effectiveness. In such cases, manual panel beating is typically undertaken for incremental forming of metal panels. Manual panel forming is a highly skilled operation with very little documentation and is disappearing due to non-observance and a lack of interest.

Confederation of British Metal forming (CBM) and Institution of Sheet Metal Engineering (ISME) have realised the need for capturing and understanding manual skills used by panel beaters to preserve the knowledge. At the same time, industries seek for alternative panel forming solutions to produce high quality and cost-effective parts at low volume and reduce the repetitive, yet adaptive parts of the panel forming process to free up skilled workers to concentrate on the forming activities that are more difficult to automate. Incremental forming technologies, currently in practice, lack adaptability as they require substantial fixtures and dedicated tools.

In this research a new proof-of-concept fixtureless automated sheet metal forming approach was developed on the basis of human skills captured from panel beaters. The proposed novel approach, named Mechatroforming®, consists of integrated mechanisms to form simple sheet metal parts by manipulating the workpiece using a robotic arm under a repetitive hammering tool. Predictive motion planning based on FEA was analysed and the manual forming skills were captured using a motion capture system. This facilitated the coordinated hammering and motion of the part to produce the intended shape accurately. A 3D measurement system with a vertical resolution of 50µm was also deployed to monitor the formation of the parts and make corrections to the forming path if needed. Therefore, the developed mechatronic system is highly adjustable by robotic motion and was closed loop via the 3D measurement system.

The developed automated system has been tested rigorously, initially for bowl shape parts to prove the principle. The developed system which is 98% repeatable for depth and diameter, is able to produce targeted bowl shape parts with  $\pm 1\%$  dimensional accuracy, high surface quality, and uniform material thickness of 0.95mm when tested with aluminium. It is envisaged that by further research, the proposed approach can be extended to form irregular and more complicated shapes that are highly in demand in various industries.

# ACKNOWLEDGEMENTS

The work produced in this thesis is one of the most significant achievements in my academic career. I would like to thank the God Almighty for providing me with all the strength and will power to achieve this feat.

I owe my profound gratitude to my supervisor **Dr. Radmehr Monfared** for all his guidance and encouragement to deliver this thesis successfully. He has been one of my best critiques both technically and professionally. I am very thankful to him for his time, constant encouragement and willingness to teach. He has been a very inspiring and resourceful person in introducing Mechatroforming.

My sincere thanks to my supervisor and research head **Prof. Mike Jackson** for providing me with an opportunity to pursue my doctorate. I am grateful to him for his time and encouragement.

I would like to thank **EPSRC centre for Innovative Manufacturing in Intelligent Automation** (grant reference number EP/IO33467/1) and **Wolfson School of Mechanical & Manufacturing Engineering** for providing me with the essential research facilities. I express my sincere gratitude to all the staff, supporting staff, technicians and administration staff who have contributed to the completion of this thesis.

I would like to acknowledge the efforts of my colleagues **Dr. Mitul Tailor** and **Dr. Taufiq Widjanarko** who guided me and contributed to the set-up of laser scanner. I like to thank my colleague **Mr. Angel Sanchez** for his support with human skill capturing. I am thankful to all my research colleagues for their continuous support and encouragement to complete this thesis successfully.

My heart-felt appreciations and thankfulness goes to all my **friends** who have been a great pillar of support during my doctoral studies. I am obliged to thank all my friends for being my source of motivation and constant progression.

I am very thankful to my **family members** who have always been a constant source of encouragement. I am grateful to my parents **Mr. Ilangovan Palaniappan** and **Mrs. Mallika Ilangovan** for their love, care and support throughout my life. My father has always been my inspiration and his inputs have been very significant towards completing this thesis.

I am very pleased to thank my lovable wife **Dr. Meenal Balaji** who understood the importance of my doctoral studies and has sacrificed her time to let me complete my thesis successfully. I am obliged to thank her for her patience and perseverance.

Finally, I am very happy to bestow this work on my lovable one year old son **Srihari Balaji** for all the happiness and peace of mind whilst writing up my thesis.

## Table of Contents

1.	Introduction .....	1
1.1	Background.....	2
1.2	Need for the research .....	5
1.3	Aim and Objectives .....	7
1.4	Research Scope .....	9
1.5	Research Approach.....	9
1.6	Thesis overview .....	10
2.	State of the art.....	12
2.1	Introduction.....	12
2.2	Product and process design factors .....	13
2.3	Traditional panel forming .....	16
2.3.1	Manual forming process .....	17
2.4	Incremental panel forming - an overview .....	19
2.4.1	Commercial methods available in incremental forming .....	21
2.5	State of the art research in incremental forming by stretching/ pulling.....	23
2.6	State of the art in incremental forming by hammering.....	26
2.7	Research gap .....	33
2.8	Selection of the power hammer and the motion capture system .....	35
2.8.1	Selection of the power hammer.....	35
2.8.2	Selection of the motion capture system.....	37
3.	Research methodology .....	39
3.1	Introduction.....	39
3.2	The process of Mechatroforming.....	41
3.3	Control system for Mechatroforming .....	45
3.4	Research challenges .....	47
3.4.1	Learning from a skilled operator .....	48



3.4.2	Impact force and energy required for sheet metal forming .....	48
3.4.3	Gripping the sheet metal.....	48
3.4.4	Manipulating the sheet metal.....	49
3.4.5	Size and shape of the support .....	49
3.4.6	Effect of residual stresses .....	49
3.5	Research plan to develop Mechatroforming.....	50
4.	Modelling and analysis of the manual sheet metal deformation process .....	53
4.1	Introduction.....	53
4.2	Specification of the experiments.....	54
4.3	Experiment 1 – Measuring the impact velocity using a high speed camera and wooden hammer .....	56
4.4	Experiment 2 – Measuring the impact velocity using high speed camera and instrumented hammer .....	56
4.4.1	High speed camera set-up.....	57
4.4.2	Impact velocity measurement and the kinetic energy .....	58
4.5	Experiment 3 – Determining the impact force using instrumented hammer...61	
4.5.1	Selection of hammer head to be mounted on the hammer .....	62
4.5.2	Instrumented hammer set-up .....	63
4.5.3	Impact force calculation using instrumented hammer.....	66
4.6	Experimental results .....	66
4.6.1	Experiment 1 .....	66
4.6.2	Experiment 2 .....	68
4.6.3	Summary of results.....	69
5.	Modelling deformation through FEA .....	70
5.1	Introduction.....	70
5.2	FEA modelling of aluminium workpiece .....	71
5.3	FEA modelling of the hammer .....	72
5.4	Applying constraints .....	73

5.5	Formulating the contact (impact) between rigid body and the aluminium structure .....	74
5.6	FEA modelling results .....	75
5.7	Discussion and comparison of experimental results and FEA results .....	76
5.7.1	FEA material input problem.....	76
6.	Development of automated solution based on captured human skills .....	79
6.1	Introduction.....	79
6.2	Envisaged automated system.....	79
6.3	Manual panel forming skills .....	83
6.4	Target artefact.....	87
6.5	Transfer of human skills to the human operated hammering machine.....	87
6.5.1	Parameter settings of the hammering machine.....	89
6.6	Human motion capture using Vicon system.....	91
6.7	Determination of the best pattern and path.....	96
6.8	Summary of human skills transferable to the automated system.....	98
7.	Automation approach and system integration .....	100
7.1	Introduction.....	100
7.2	Robot manipulation of the sheet metal .....	100
7.3	Development of the gripping unit for the automated system.....	101
7.3.1	Experiments using a standard gripper and standard finger design .....	101
7.3.2	Gripper with the required force and modified finger design .....	102
7.4	Transfer of human skills to the robot-operated hammering machine .....	104
7.5	Integration of hammering machine to the robotic system .....	107
7.6	Assembly and experiments on the integrated system .....	109
7.6.1	Findings from the preliminary tests.....	109
7.6.2	Improving the compliance of the gripping unit.....	112
7.7	Summary of the integrated system and initial test results .....	113

8.	Synchronisation and path planning for the robotic automation system .....	115
8.1	Introduction.....	115
8.2	Initial tests using robotic manipulation.....	115
8.3	Synchronising part motions with the impact frequency .....	117
8.4	Path planning algorithm.....	118
8.4.1	45 degree step angle resulting in hexagonal shape.....	122
8.4.2	Modifications to the algorithm .....	123
8.4.3	Perpendicular positioning of the sheet metal relative to the hammer's origin	126
8.4.4	Further enhancement of the algorithm .....	127
8.5	Results based on the successful manipulation algorithm.....	129
8.5.1	Experiment 1 .....	131
8.5.2	Experiment 2 .....	134
8.6	Limitations of the automated system.....	136
8.7	Summary of the results achieved.....	138
9.	In-process measurement of forming.....	139
9.1	Introduction.....	139
9.2	Laser scanner set-up.....	139
9.2.1	Experimental set-up.....	141
9.2.2	Calibration .....	145
9.3	Image acquisition and point cloud data generation .....	150
9.3.1	Image acquisition.....	151
9.3.2	Point cloud data generation .....	153
9.4	Image processing for depth/ area measurement and experimental validation	154
9.4.1	Validation of results on comparison with CMM measurement.....	157
9.5	Shape and feature detection experiments.....	158
9.6	Discussion of results and proposed method for error rectification.....	161

9.6.1	Method proposed for error identification and rectification .....	161
9.7	Summary.....	163
10.	Conclusions .....	164
10.1	Research overview .....	164
10.2	Research achievements .....	165
10.3	Contribution to the knowledge.....	166
10.4	Further discussions.....	168
10.5	Recommended Future work .....	169
REFERENCES .....		171
LIST OF APPENDICES .....		180
LIST OF PUBLICATIONS.....		181

## List of Figures

Fig 1 - Schematic representation of an Industrial Die [1] .....	2
Fig 2 -Schematic representation of manual panel beating - modified [1] .....	4
Fig 3 - Incremental sheet metal forming by stretching.....	5
Fig 4 - Panel beater using a hammer and dolly .....	16
Fig 5 - Traditional manual forming .....	17
Fig 6 - Plan view of peaks and troughs drawn on the sheet metal to form the tucks .....	18
Fig 7 - finer refinements using metal hammer and dolly .....	18
Fig 8 - Using a wheeling machine for contour finish.....	19
Fig 9 - Single point incremental forming [43].....	21
Fig 10 - Application of Incremental Sheet Forming (ISF) at AMINO [48].....	22
Fig 11 - Ford F3T technology [51].....	22
Fig 12 - Single point incremental forming - modified from [53].....	23
Fig 13 - DPIF process – modified from [53].....	24
Fig 14 – Roboforming [54].....	24
Fig 15 - Servo hammering unit [70] .....	26
Fig 16 - Linear servo hammering unit and linear servo motor with hammer head – modified [33].....	27
Fig 17 - Sensitivity to the neighbouring deformation - modified [33] .....	28
Fig 18 - System set up used by Asakawa [71].....	28
Fig 19 - Hammering unit with gas burner [72].....	29
Fig 20 - Hammering tool without counter balance (a) and with counter balance (b) [32] .....	30
Fig 21 - Shrinking using kraftformer - modified [74] .....	31
Fig 22 - 'Co-Drive' by Co-Tesys [76].....	32
Fig 23 - Hammering machine - Eckold Kraftformer KF170PD [77].....	37
Fig 24 - The Vicon system .....	38
Fig 25 - Proposed solution (Envisaged) .....	39
Fig 26 - Mechatroforming .....	41
Fig 27 – Mechatroforming – Ideal forming strategy .....	42
Fig 28 - Mechatroforming – Implemented forming strategy.....	44
Fig 29 – Control system for Mechatroforming (implemented).....	46
Fig 30 - Research challenges.....	47

Fig 31 - Research plan .....	51
Fig 32 - Experimental set-up .....	54
Fig 33 - Support used for initial experimental studies .....	55
Fig 34 - Cross-sectional view of impact applied on the aluminium test piece.....	55
Fig 35 – High speed camera set-up .....	57
Fig 36 – PFV software.....	58
Fig 37 - Theoretical calculation of impact force based on the impact velocity measured .....	59
Fig 38 - IH-10 instrumented hammer .....	61
Fig 39 - Hammer head material types .....	63
Fig 40 - IC with BNC connections in working mode.....	64
Fig 41 - Instrumented hammer set-up .....	64
Fig 42 – Accelerator mounted upon impact hammer .....	65
Fig 43 - Accelerator mounted on the sheet metal surface .....	65
Fig 44 - Sheet deformation - Experiment 1 .....	67
Fig 45 - Experiment 1 - Instrumented hammer data.....	67
Fig 46 - Sheet deformation - Experiment 2.....	68
Fig 47 - Experiment 2 - Instrumented hammer data.....	68
Fig 48 - Quad meshed 3D structure.....	71
Fig 49 - Rigid body placed 0.8 m above the aluminium structure .....	72
Fig 50 - Constraints - front view .....	73
Fig 51 - Constraints - orthogonal view.....	73
Fig 52 - Contact table – example.....	74
Fig 53 - Finite element analysis of deformation.....	75
Fig 54 - Dog bone samples .....	77
Fig 55 - Instron tensile testing machine .....	77
Fig 56 - Stress/ strain curve obtained based on tensile test .....	78
Fig 57 - Process flow diagram.....	80
Fig 58 - Enhanced control system .....	82
Fig 59 - Illustration of human skills related to hammer (skills 1 – 4).....	84
Fig 60 - Compliant gripping of the sheet metal (human skill 5) .....	84
Fig 61 - Position and Skewing of the sheet metal (human skills 6 and 7) .....	85
Fig 62 – Human Skills based on forming strategy of the sheet metal (skills 8 - 10) .....	85
Fig 63 - Target artefact .....	87

Fig 64 - Hammering machine reconfigurable settings .....	88
Fig 65 - Doming tool (dimensions are in mm) .....	89
Fig 66 – The Vicon system.....	92
Fig 67 - Simulink model.....	93
Fig 68 - Manipulation path (data from Matlab processing) .....	94
Fig 69 - Hammering frequency .....	95
Fig 70 - Yaskawa Motoman SDA10 .....	101
Fig 71 - Experiments using a standard gripper.....	102
Fig 72 - Gripper with modified finger design .....	103
Fig 73 - Tool centre point.....	105
Fig 74 - Translational directions of the robot.....	105
Fig 75 - User co-ordinate set up for transfer of human skills 6 and 7 .....	106
Fig 76 - Solenoid valve replacing foot pedal in the hammering machine.....	108
Fig 77 - Solenoid actuation through robot controller .....	109
Fig 78 - Path taken by the robot .....	110
Fig 79 - Preliminary test strategy (flowchart) .....	110
Fig 80 - Smooth path transition in continuous stroke.....	111
Fig 81 - Shore hardness test.....	112
Fig 82 - Initial test results on forming a bowl shape .....	116
Fig 83 - Significance of automation over manual forming .....	118
Fig 84 - Archimedean spiral and initial increase of step angle .....	119
Fig 85 - Conical helix to form bowl shape and the quadrant segmentation.....	121
Fig 86 - Results obtained with 45 deg step angle.....	122
Fig 87 - Additional segmentations for skewing .....	124
Fig 88 - Results based on 8 segments.....	124
Fig 89 - Minimising the step angle to 10 deg.....	125
Fig 90 - Results of minimising the step angle to 10 degrees.....	125
Fig 91 - Sheet metal's point of impact always perpendicular to the centre of hammer	126
Fig 92 - Results based on skewing sheet metal perpendicular to the hammer's centre	127
Fig 93 - Planar surface of the bowl .....	128
Fig 94 - Excess impact due to constant step size determinant .....	128
Fig 95 - Gradual decrement of step size.....	129
Fig 96 - Improved finish.....	129
Fig 97 - Successful algorithm for forming a bowl shape .....	130

Fig 98 - Accuracy of the bowl diameter formed (Exp 1 - trials).....	133
Fig 99 - Geometrical error of the final bowl shape formed (Exp 1 – trials).....	133
Fig 100 - Cycle time for forming a bowl shape (Exp 1 – trials) .....	133
Fig 101 - Result of Experiment 1 - 1st Trial .....	134
Fig 102 - Accuracy of the bowl diameter formed (Exp 2 - trials).....	135
Fig 103 - Geometrical error of the final bowl shape formed (Exp 2 – trials).....	136
Fig 104 - Cycle time for forming a bowl shape (Exp 2 – trials) .....	136
Fig 105 - Results of Experiment 2 – 1st trial.....	136
Fig 106 - Limitations of the automated system.....	137
Fig 107 - Triangulation angle .....	141
Fig 108 - Camera view of laser stripe with and without filter.....	141
Fig 109 - Laser scanner set-up illustration .....	143
Fig 110 - Laser scanner experimental set-up.....	144
Fig 111 - Calibration grid .....	145
Fig 112 - Principle of sheet of light.....	147
Fig 113 – Calibration images at lowest reference plane.....	148
Fig 114 - Calibration images at highest reference plane .....	148
Fig 115 - Defining measurement volume .....	149
Fig 116 - Cross section of the bowl shape formed .....	151
Fig 117 - Camera interface with robot controller .....	151
Fig 118 - Algorithm for camera trigger sequence .....	152
Fig 119 - Re-constructed model in Halcon.....	153
Fig 120 - Deformation on single impact measured under laser scanner .....	154
Fig 121 - Reference plane ambiguity in depth measurement .....	155
Fig 122 - Reference plane ambiguity - illustration.....	155
Fig 123 - Depth map of spherical depression.....	156
Fig 124 - Circumference and depth of the deformation determined .....	156
Fig 125 - CMM measurement of the deformation.....	157
Fig 126 - Shape to be measured .....	158
Fig 127 - Shape measurement results .....	159
Fig 128 - Angle of the gradient .....	159
Fig 129 - Increasing the precision of measurement.....	162
Fig 130 - Buckle identification.....	162



## List of Tables

Table 1 - Summary of experimental results .....	69
Table 2 - FEA dimensioning standards .....	70
Table 3 - Experimental and FEA results .....	76
Table 4 - Skills determined.....	86
Table 5 - Optimum position and stroke length (for optimum impact force).....	90
Table 6 - Patterns and paths tested* .....	97
Table 7 - Inputs for forming the target artefact with 45 deg step angle .....	122
Table 8 - Experimental trails with 45 deg step angle .....	123
Table 9 - Experiment 1 - 1st trial.....	132
Table 10 - Experiment 2 - 1st trial.....	135
Table 11 - Laser scanner and CMM measurement comparison .....	158
Table 12 - Shape and feature detection experimental results .....	160

# 1. Introduction

---

Industrial research in metal forming has always been in demand to meet the ever evolving needs for new technologies in the manufacturing industry, especially in automotive and aerospace industries.

Despite the highly sophisticated metal forming facilities currently used in industries, many sheet metal parts are still formed through the manual forming process known as ‘panel beating’. Such manual processes are not only used for repairs and one-off products but also used as part of production lines in some industries such as aerospace. Consequently, such industries are heavily reliant on the recruitment and training of highly skilled manual workers and therefore, they have been seeking alternative automated solutions, especially for prototyping and producing complex sheet metal panels.

Increases in production rate and demands for reducing manufacturing costs in the past decades have led to the development of automated manufacturing systems. Since then, robots have become an integral part of manufacturing facilities to create bespoke solutions. Robots have increased the manufacturing accuracy and precision leading to minimal errors and an increase in throughput. Acknowledging this fact, manufacturing industries have been changing their facilities to use mechatronic systems involving robots to produce customised solutions in a shorter lead time. To increase manufacturing standards, feedback systems are being used to ensure that the manufacturing quality is maintained through continuous monitoring.

This thesis discusses an innovative methodology to form the sheet metal using an integrated automation system. Sheet metals which are mostly 1mm thick are usually used in automotive industries to produce car panels. Sheet metals are also used in aerospace and rail industries. Most commonly sheet metal panels are produced using conventional manually operated processes such as drawing, stretching, stamping and roll forming. Comparing these processes, each method has got its own significance over the others. However, due to die usage, all these manufacturing methods lack flexibility: which is essential for producing customised products. A flexible sheet metal forming approach is required to cater to ever-changing industrial requirements, and to enable the prototyping of new designs at a lower production cost. Developing such a flexible

approach would also benefit other specific applications such as metal sculpturing and sheet metal manufactured for electronic hardware, apart from being highly beneficial to automotive and aerospace industries generally. Such a flexible, automated solution would also be able to carry out laborious repetitive work; freeing up the manual worker to concentrate on difficult-to-automate features. This research is focussed on developing a flexible sheet metal forming approach by using integrated manufacturing and mechatronics systems.

### 1.1 Background

In many industries, dies are used to form sheet metal panels of different contours. The production of dies involves huge costs and consumes more time as they need to meet the necessary industrial standards. Industrial data provided by the Confederation of British Metal forming [1] indicates that a lead time of 8 months and a cost of £1 million is required to produce a panel of a car's side door and its corresponding die. Despite such huge investment and a high lead time, it is very unlikely that the same die could be used to produce two different panels. Though tool flexibility can be introduced, any detailed design modification to the panels will either require a new die or post-production modification of the existing die which incurs extra costs. Producing low-volume, sophisticated panels and prototyping different models are not feasible using a die due to its huge manufacturing costs and lack of flexibility. Dies are used for mass production and rollers/ benders used for low-volume production, as they are not able to provide flexibility which would require substantial fixtures to produce the sheet metal into the required shape. Furthermore, the use of fixtures leads to non-uniform thickness in the final sheet metal panel produced due to stretching. This may also lead to cracks and fractures in the panel, often during die proving. Fig 1 illustrates a forming die.

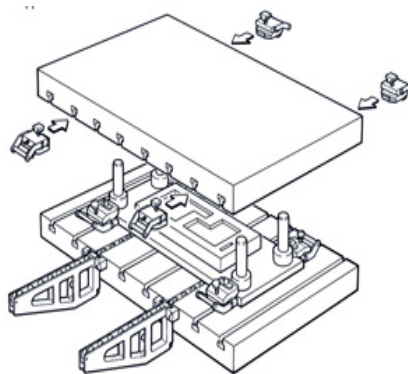


**Fig 1 - Schematic representation of an Industrial Die [1]**

As in-process feedback is not possible in die forming due to the very short forming time, process failures in the die operation can only be prevented by pre and post-processing analyses before any scrap components are produced. Thus, any failure in production above the tolerance limits will incur costly rectifications. Also, dies need a high force in closely bounded surfaces to manufacture parts precisely. In order to be able to produce such high pressures, die forming machines are built as huge structures which consume considerable space in the industrial shop-floor. Therefore, dies lack flexibility and cost-effectiveness when in low-volume production, or when repair or prototyping is required.

In such cases where complex panels are required to be produced in low volumes, or where prototyping is required, manual panel beating is typically undertaken for the incremental forming of metal panels. Manual panel beating is a highly skilled operation with very little documentation. Manual panel beaters use a step by step process to incrementally form the sheet metal using a hammer and an anvil. The process includes many tools and techniques to achieve the shape required. Unlike die-based forming, the sheet metal panels produced using the manual panel forming process has almost uniform thickness. Hand-eye co-ordination and human sensory perception (e.g. vision, sound, touch) assists a panel beater to assess the strategy for achieving the target shape. Using these sensory elements, panel beaters make decisions based on prior knowledge gained through their experiences. Apart from this, panel beaters use templates to check their forming progress towards the target shape. This provides feedback to optimise the forming strategy to achieve the required shape. This could be considered as an in-process inspection technique used in manual operations. Fig 2 illustrates a manual panel forming process.

Unfortunately, due to recruitment issues, high cost and sporadic industrial applications, manual panel beating is being isolated and gradually forgotten. There is not enough research carried out to fully understand and capture the skills of experienced panel beaters and how these human skills link to formal, sheet metal forming theories. It is essential to capture these highly skilled processes and preserve the knowledge of the metal forming practice.

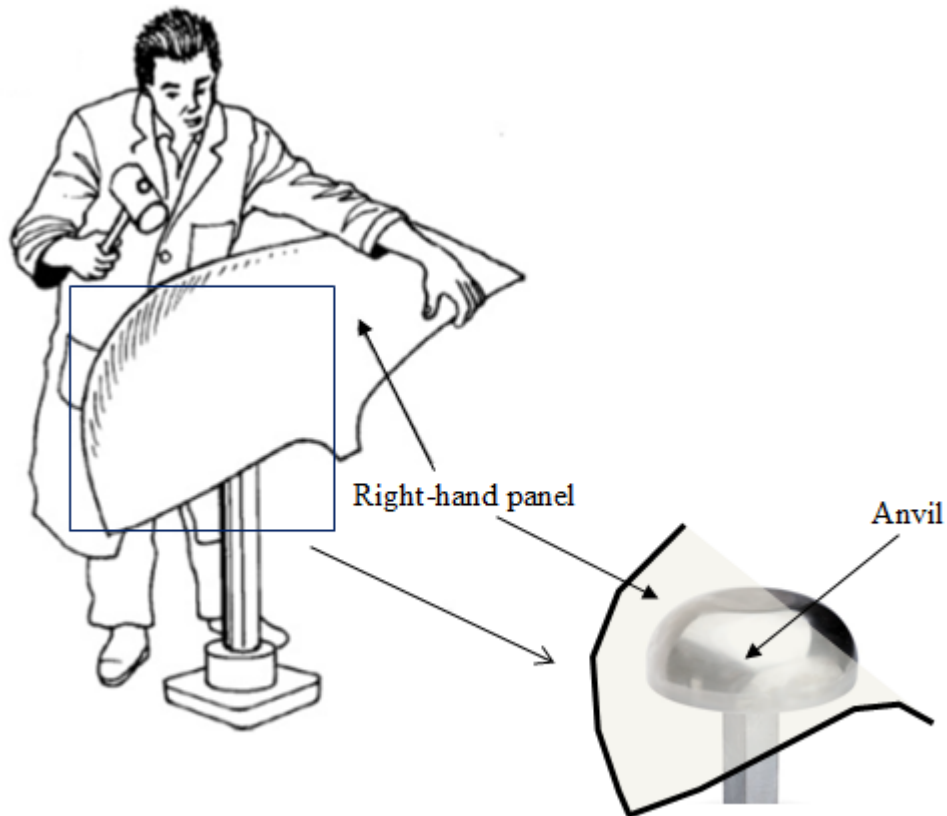


**Fig 2 -Schematic representation of manual panel beating - modified [1]**

Evaluating the need for the modernisation of die forming and understanding the need for pre-processing and in-process analysis, many new studies have been carried out in the field of panel-forming. Some of the technologies in sheet metal forming - which have come into existence with the primary aim of improving flexibility - are superplastic forming, hydroforming, electro-magnetic sheet metal forming, shot peening and laser sheet metal forming. Some of the methodologies which are being used are electro-hydraulic forming, stretching using grippers and the use of a digitized die for sheet metal forming. The most effective research in achieving the required precision and accuracy in sheet metal forming has been through incremental sheet metal forming.

The majority of the proposed incremental sheet metal forming methods uses either stretching or drawing techniques with or without an anvil's support. The sheet metal is formed by using a round-headed tool which moves down vertically (i.e. in the Z-axis). The sheet metal is typically held by fixtures along the edges to avoid movement caused by the tool. Either the sheet metal or the tool is moved along XY axes (i.e. the

horizontal plane) to achieve the required contour as shown in Fig 3. The forming is often computer controlled. Employing this technique achieves a smooth finish, but may result in fractures due to excessive stretching and often fails while forming complex contours (e.g. having more than a  $55^\circ$  wall angle [2]). These methods use fixtures to hold the sheet and typically result in a non-uniform thickness of the formed sheet metal, hence, affecting the quality.

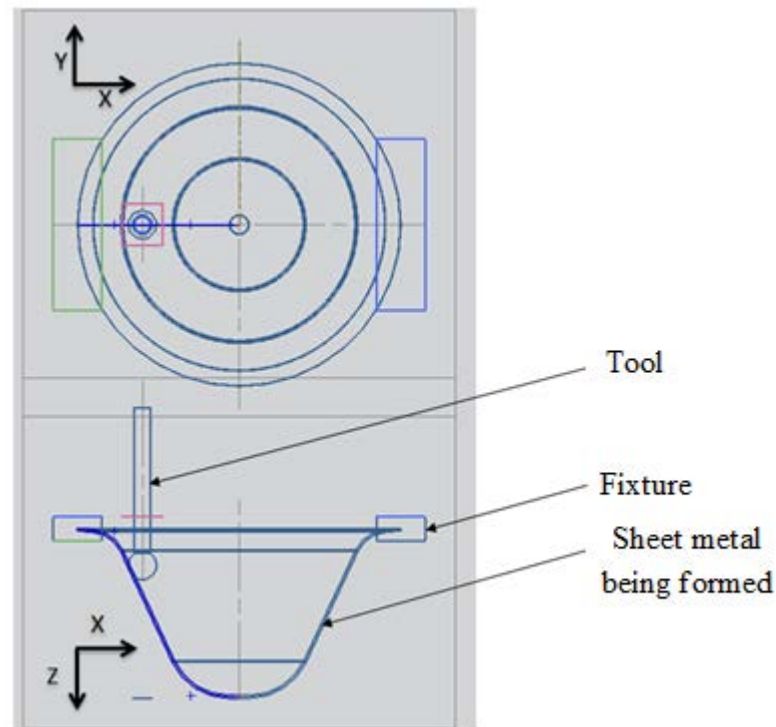


**Fig 3 - Incremental sheet metal forming by stretching**

The use of fixtures limits the part complexity and size dramatically. They also apply additional forces to the forming process that result in a reduction of the thickness (via non-uniform stretching) and change the physical properties and dimensions in an almost unpredictable manner (e.g. the spring back action). Hence, the incremental forming methods proposed are neither able to provide uniform thickness nor able to provide the required flexibility. This has increased the need for further research in the field of incremental sheet metal forming.

### **1.2 Need for the research**

In addition to the large-scale and high-volume panel forming in automotive industries, various industrial sectors often utilise panel beating for sheet metal forming on a

smaller scale. Due to the low-volume production in these sectors and a decline in the availability of skilled workers, the incremental forming, rather than the die-based approaches, are naturally more cost-effective

However, the manual incremental forming i.e. the panel beating, is a non-standard, non-descriptive and relatively undocumented craftsmanship that varies from one skilled worker to another. Nonetheless incremental forming is still being used, inevitably due to its lower cost in comparison to the alternative solutions.

On this basis, the industry has recognised its need to investigate alternative solutions. This is primarily focused on the need to: a) understand, capture, and document manual panel forming skills before they become completely obsolete, and b) develop semi or fully automated approaches for panel forming to improve consistency and the repeatability of the products, and reduce reliance on rare individuals' skills.

The author has recognised the above-mentioned industrial needs and interests, and primarily focused this research on understanding and capturing the manual forming processes. Furthermore, the major investigation of this research is the reproduction of those skills through the development of an automated robotic panel beating system.

In this regard, various application scenarios for such automated systems are realised. For instance, the automotive sector aims at using high-strength, lightweight materials in car body parts [3]. It is aimed at using aluminium and magnesium alloys. These materials are high-strength but are low-ductility, which affects the material during the thinning process. When their capability for material forming is analysed, the Incremental Sheet Metal Forming (ISMF) is believed to have the ability to form such materials more effectively than the traditional die forming.

From a different perspective, the importance of incremental forming can be found in reforming retro/vintage cars. These cars come under the category of one off cars which need high maintenance. In order to retain the artistic skills with which they were built, Incremental sheet metal forming is believed to be the most appropriate solution for such applications, if not the only one.

Perhaps the most commonly known application for incremental forming is the reconditioning of sheet metal panels, for example, the reconditioning of dents on

vehicle bodies such as automobiles or aircrafts. Additionally, incremental forming is also used in customising cars to the customer's requirements. Incremental forming could also be utilised in the field of medicine for applications such as reconstructing steel structures to be used as exo-skeletons for paralysed patients. Such shapes are complicated and need high levels of accuracy and precision in production.

Comparing the conventional die-based methods and the incremental methods, incremental methods have greater advantages since they can form non-uniform shapes, shapes with higher wall angles and contours of larger depth with a nose edge [4]. Considering low batch production, which needs high variability, incremental sheet metal forming has a paramount advantage as it allows customisation at low cost [5]. As incremental sheet metal forming is an iterative process, there is a potential for in-process inspection and modifications via the feedback achieved after the iterations. In view of these factors, transformation from conventional to incremental forming in industries could be easily envisaged [6]. For example, the incremental method increases the dimensional accuracy when forming sheet metal by electromagnetic-assisted stamping.

The necessity to undertake further research in the field of incremental forming is evident from the above discussion. It can also be concluded that further research in the area will require the development of a proof-of-concept automated system to enable the theoretical development to be put into practice. Such system could facilitate the assessment of the progress made in this field of research.

### **1.3 Aim and Objectives**

Incremental sheet metal forming is a wide research area and cannot be defined through one principle or method. Extensive research has been carried out in the field of incremental sheet metal forming and a critical review of this research has been presented in the literature review.

Based on literature review it was understood that much of the research carried out in this area does not provide an adequate solution for flexibility in incremental sheet metal forming, which is the main theme of this research. It was also observed that the significance of a skilled human operator forming a sheet metal has largely been overlooked when considering an automated incremental forming approach. Therefore



developing an automated incremental sheet metal forming process based on manual panel forming skills is the subject matter of this research.

### ***Research Aim***

To investigate manual sheet metal forming and develop an automated solution to replicate the manual forming of a simple sheet metal part using a fixtureless automated robotic system through an incremental impact forming approach.

### ***Main Objectives***

- To understand the human skills involved in traditional sheet metal forming and formulate each human skill into a robotic skill (refer table 4 in section 6.3), based on the human skills observed
- To develop a proof-of-concept automated panel forming system through incremental sheet metal forming without using fixtures
- To investigate the possibility of producing parts with a uniform thickness distribution through automated incremental forming, which will eventually increase the quality of the sheet metal part being formed.

### ***Sub-objectives***

- To conduct a series of experiments to understand and measure individual techniques used in manual forming processes, such as forming patterns, force, and the angle of impacts.
- To measure and calculate the impact force/ energy required for forming the sheet metal (based on human skills) using an instrumented hammer and a high speed camera
- To investigate prediction of impact sheet metal forming through modelling (via finite element analysis (FEA)) and to compare the measured and calculated impact force results with the corresponding results of the finite element analysis of the forming process.
- To capture human skills using motion capture systems to determine the best path and pattern for forming the experimental parts,
- To transform the human skills into a parametric automated solution, by integrating an impact hammer with a robotic unit to develop a proof-of-concept integrated manufacturing system for incremental sheet metal forming

- To use a 3D vision measurement system based on laser triangulation for determining the depth and circumference of the sheet metal being formed and provide in-line on-process feedback to the automated system for the envisioned optimisation of the forming path

#### **1.4 Research Scope**

To provide a manageable research scope, this study was restricted to the use of aluminium sheet (grade 1050) with 1mm thickness (most commonly used material thickness in the automotive and aerospace industries). The study was also limited to forming a bowl shape using a Motoman robot and an Eckold hammering machine.

#### **1.5 Research Approach**

This research was initiated by reviewing the current state-of-the-art equipment within the academic and industrial domains. It was acknowledged that, thus far, not enough emphasis has been placed on the understanding and the acquisition of individual techniques in manual skills – such as specific hammering patterns. It was rightly stated by Leacock A.G [7] that sheet metal forming incorporates the skills of an artisan, engineer, metallurgist and mathematician. It is not possible to avoid any of these areas, as accuracy and precision can be achieved only when all these human skills are integrated. Therefore, the main theme of this research is based on understanding these essential manual skills and developing automation systems according to what is learned from them.

Initially, a panel forming course was undertaken by the author at Contour Autocraft, Peterborough, United Kingdom. The course provided a systematic insight into the sheet metal forming from its initial uncoiling stage to the final wheeling stage. The need for each human skill was clearly evident during the training. The detail of the course attended is reported in Appendix 1.

It was observed that a large number of variables are greatly influential in the forming of sheet metal parts using manual panel beating techniques. Some of these include the angle and force of the impact, the shape of the hammer and the supporting tool (anvil), the movement of the part and the pattern (spiral pattern) in which the impacts are applied.

It was therefore hypothesised that it may be possible to eliminate or merge some of the variables to facilitate the development of an automated system, independent of the individuals' techniques.

A robotic panel manipulation device was envisaged to place and move a sheet metal part under a vertical hammering machine, impacting continuously. Such a system should be supported by a vision system to monitor the intermediate forming stages of the part. The unfinished parts could be compared with the intermediate CAD model of the part to prescribe rectification to the automated forming process if required.

It was also envisaged that the process of forming could be modelled based on using FEA approach to predict the forming behaviour of the part at each stage.

A series of experiments were conducted to understand and develop the automated system in three phases. These include fully manual forming, manual part movement under a hammering machine, and finally fully automated part manipulation with a hammering machine.

## **1.6 Thesis overview**

This thesis documents in detail on how an automated incremental sheet metal forming solution was achieved through a systematic theoretical and experimental approach.

The literature review is presented in Chapter 2. The chapter discusses the product and process design factors involved in sheet metal forming. A brief overview of traditional manual forming and a critical review of existing incremental forming methods are presented. A comparison of existing methods and the research gap is also presented in this chapter. This chapter also includes the selection of impact hammers.

The proposed incremental forming approach, research challenges and research plan to overcome the challenges are discussed in Chapter 3.

Chapter 4 presents a detailed discussion of experimental analysis involved in determining the impact force. Experiments based on instrumented hammer and the high speed camera is discussed in detail.

Chapter 5 explains in detail the use of finite element analysis for determining the impact force of sheet metal forming. The chapter also presents a comparison of the experiments' results with the numerical analysis results.

Chapter 6 explains in detail the human skill capture using a motion capture system. The human skills observed when forming the sheet metal utilising the impact hammer and the transformation of these human skills into a parametric solution is explained in detail in this chapter. The selection of the target artefact and an overview of the envisaged automated system are also presented in Chapter 6.

The transformation from a semi-automated system to an automated system is discussed in Chapter 7. Selecting a gripper and the modification of finger design based on the initial experiment's results is presented in this chapter. The integration of the robot and the impact hammer is discussed in detail in the chapter - including the initial experiment's results.

Chapter 8 explains the path planning algorithm developed and the synchronisation of robotic manipulation with pertinent impacts of the impact hammer. The chapter presents a detailed discussion about the progressive stages in achieving the desired solution. The results based on achieving the target shape are also presented in this chapter.

The 3D vision measurement system installed and the laser triangulation principle are explained in Chapter 9. This chapter presents a detailed discussion about the shape and feature detection using laser triangulation. The results achieved through image processing and envisioned path modification are also presented in this chapter.

Chapter 10 presents a conclusion of the research work explaining the results achieved based on the aim and objectives. Recommendations for future work are also presented in this chapter.

## 2. State of the art

---

### 2.1 Introduction

Sheet metal forming is a wide research area; significant research has been carried out to improve the process of sheet metal forming. Research has been investigated on several incremental sheet metal forming methodologies to increase the accuracy of the materials formed. The current state-of-the-art methodologies used in sheet metal forming have been studied. It was recognised that most of the new technologies developed did not consider traditional manual forming techniques from which the conventional and current state of the art technologies evolved.

As mentioned in Section 1.3, the main theme of this research is to develop an automated incremental sheet metal forming methodology based on the traditional panel forming methodology. Therefore, it is necessary to understand the basic principles and techniques involved in sheet metal forming. As mentioned earlier, training was undergone to observe the traditional manual forming skills. Observing a skilled panel former's approach towards forming a sheet metal was significant in the analysis of existing technologies involved in sheet metal forming. The techniques involved in traditional panel forming are briefly presented in this chapter.

Understanding the techniques involved in sheet metal forming provided an insight of the process and product design factors to be analysed prior to beginning the process of sheet metal forming. These product and process design factors are discussed in this chapter.

The commercial technologies currently available in the incremental sheet metal forming industry have been reviewed to understand the industrial requirements and how this research could contribute to meet those requirements. Current state-of-the-art research technologies in incremental sheet metal forming were studied and a critical review has been presented specifying the problems involved in those techniques and the benefits of impact forming.

As the major objective of this research is to use the impact forming technique, a detailed review of the few methodologies that have been researched on forming a sheet metal using impact has been presented. The lack of flexibility in forming three

dimensional shapes using these techniques and the research gap based on the comparison of these methodologies has been discussed in this chapter. The research focus formulation based on the research gap is also presented in this chapter.

The requirement and the selection of a power hammer, based on the results of the experiment's analysis (discussed in Chapter 4 and 5) are presented in this chapter. The requirement for a motion capture system and the selection of the motion capture system used for capturing the human skills are also presented in this chapter.

## **2.2 Product and process design factors**

Sheet metal forming involves several factors of consideration before, after and during the forming of sheet metals. There are certain products and process design factors which affect the sheet metal forming. These factors are mainly based on the incremental sheet metal forming. However, the conventional process factors were also analysed.

For instance, material properties of the sheet metals such as its crystallographic structure and thickness influence its forming. It is understood that plastic anisotropy condition of the material can cause non-assumed flow of material [8]. It is also important to know the material thickness distribution: to avoid wrinkling and tear while forming [9]. Both thickness and crystallographic structure of the material have a related influence in the forming of sheet metal. It is found that thinner materials with larger grain size are ideal for producing complex shapes [10]. Irrespective of the sheet metal's properties, the material of tools used to form the sheet metal can also influence the formability of the sheet metal with respect to the wear and friction between tools and parts. Typically coated tools may have better results than powder tools as the latter have resistance to wear - which could cause irregular forming in parts [11].

Once the material aspects have been considered, to start the sheet metal forming, it is necessary to design the pattern of the initial contour. Usually the sheet metal is cut along the edges to produce the initial pattern. Nonetheless, cutting along the edges of the material to achieve the initial pattern may cause stress on the edges, which can lead to fracture [12]. To avoid this, the pattern can be designed first through reverse engineering, either by geometrical modelling [13] which flattens the CAD model of final contour to predict the initial design, or by a feature detection algorithm which uses

stereo lithographic (STL) parts' specifications to identify the part parameters and to design the initial pattern using an expert computer aided process planning (CAPP) system [14].

The plasticity and elasticity of the material has to be pre-determined usually before the initial deformation. These are two major properties based on which the sheet deforms. The plastic deformation usually results in a deformed shape due to the dislocation caused. The distortion caused in the material due to elasticity does not result in a deformed shape, so the material attains a spring back. It is therefore essential to know the plastic and elastic behaviours of the sheet metal in order for it to be formed. The Young's Modulus relative to elasticity and stress/strain relation relative to plasticity have already been predetermined for a particular material. However, it is more effective to calculate them practically rather depending on the predetermined values.

The sheet metal forming is always under the limitations of the stress/strain index of that specific material termed as forming limit curve. The index indicates the maximum stress that can be induced in the material and the maximum strain that the material can form under. Several techniques are used to predict the strain rates of the material to be formed [15, 16]. Understanding the forming limit curves (FLC) and rescaling the stress induced in the direction of the impact is crucial to form the material without any fractures [17]. Though FLC was used in most cases, based on experiments in different types of incremental forming, it was also suggested that incremental forming should be based on forming fracture limit (FFL) instead of using FLC [18]. Forming fracture limit is similar to FLC but indicates the fracture limits of the material instead of the maximum limits.

While forming the material incrementally, it is important to understand the yield stress/strain of the material being formed. It was suggested that the elastic recovery of the material could be differentiated into two phases, namely, linear elastic recovery and non-linear elastic recovery. The non-linear elastic recovery has no effect as it is proportional to unloading. However, the linear elastic recovery affects the sheet metal formed as it is a function on residual stress formed due to deformation (due to loading) and stress at the point of unloading [19]. Therefore, it is essential to account for the development of residual stress which may cause deviations in the forming [20].

A few parametric models were suggested to predict the forming of the material based on loading conditions [21, 22]. Nevertheless, once the impact has been made to form the sheet metal, the actual intended deformation may not be achieved due to occurrence of spring back. The stress/strain response due to the plastic modulus of the material influences the spring back behaviour [23]. It was also found that wall surfaces are more prone to spring back in incremental forming [24].

To realise the relation between impact force and deformation, it is vital to understand the kinetic energy involved in deforming the material. Studies done on impact loading suggest that kinetic energy should be calculated as the difference between external energy imparted and the internal energy (plastic & elastic) of the material. It was also suggested that during dynamic impacts there are non-smooth contacts due to friction and induced impulse which causes oscillation. If these oscillations are damped, the maximum kinetic energy will be dissipated onto the workpiece [25]. Another study on impact loading suggested that the plastic deformation caused in the sheet metal is a factor of the tool diameter (used for impacting), the sheet thickness and the impact velocity [26]. Studies also suggest that friction and lubrication of the tool are also influential in the quality of sheet metal being formed [27, 28].

Once these factors have been considered, the subsequent step in incremental forming is planning the path of forming and monitoring. Helical convolution, outward, scanning, zig-zag, outward-in, inward-out, approaches based on the tool's centre point were analysed to be the best techniques used in incremental forming based on studies [29-33]. The path will have to be decided based on the sheet metal's initial and final contour using CAD and integrated with feedback systems. Few process development approaches [34-36] were studied to learn about integrating the systems together required for forming the sheet metal. When path deviations occur, they can be optimised by using 3D vision feedback to monitor the forming. 3D vision systems can use the stereo cameras to measure the grid patterns of deformation [37]. Based on the feedback, the tool path for forming could be optimised to increase the part accuracy based on various approaches [38-42].

All these product and process design factors were considered to develop the automated incremental sheet metal forming process.



### **2.3 Traditional panel forming**

The knowledge and practise of traditional panel forming techniques gained during the training evolve to be the basis and foundations of sheet metal forming. The sheet metals are formed using cold rolling/forming technologies to ensure that the quality of the material is not lost and the material remains durable for years. There are several factors involved in sheet metal forming starting from uncoiling the non-formed sheet to the final finish of the formed sheet metal. Each and every step of the sheet metal forming technology has got a design consideration. Considering sheet metal forming as an incremental forming technology, each step has got its own importance. If the steps are not designed, worked out properly or eluded, the final shape attained will not be of perfect dimensions and desired shape.

Wooden mallets, anvils, hammers and dollies (refer to Appendix 1) are the basic tools used, while different forming strategies are formulated by a panel beater to acquire a final desired shape. At times, there is more than one particular strategy to attain the final shape. Correspondingly, there are different tool sets involved in achieving a required shape. During the training, it was observed that tooling plays an important role determining the progress of the final desired shape. Several traditional, semi-automatic and automatic tooling methodologies that exist in the sheet metal forming industry were studied during the training course. Fig 4 illustrates the use of hammer and dolly (small anvil) by a panel beater.



**Fig 4 - Panel beater using a hammer and dolly**

Undertaking training in the traditional manual forming techniques was helpful in understanding the behaviour of sheet metal under different forming methodologies. The characteristics of sheet metal during its forming stages were studied and their design engineering and finite element aspects were analysed during the training. The learning formed the basis of research due to which constructive analysis was possible in developing an automated system for incremental sheet metal forming. A brief of the forming procedure is discussed below and a detailed study is included as Appendix 1.

### 2.3.1 Manual forming process

The manual forming as a conventional method of sheet metal forming was analysed by observing experienced panel beaters with the aim of capturing the human skills, and to then apply them to the automated approach. In manual forming, the parts are initially formed using a hammer (wooden mallet) and an anvil (support). Later, the metal hammer and dollies are used to finish the forming. The sheet metal is held between the hammer and support. The support is typically held stationary and hammer is used to apply impact repetitively at the same point with gradual movement of the part. The part is moved gradually and skewed over the dolly to produce the required contour. The methodology for forming a double curvature is illustrated below in Fig 5. The methodology and equipment for forming are almost common for any contour required.

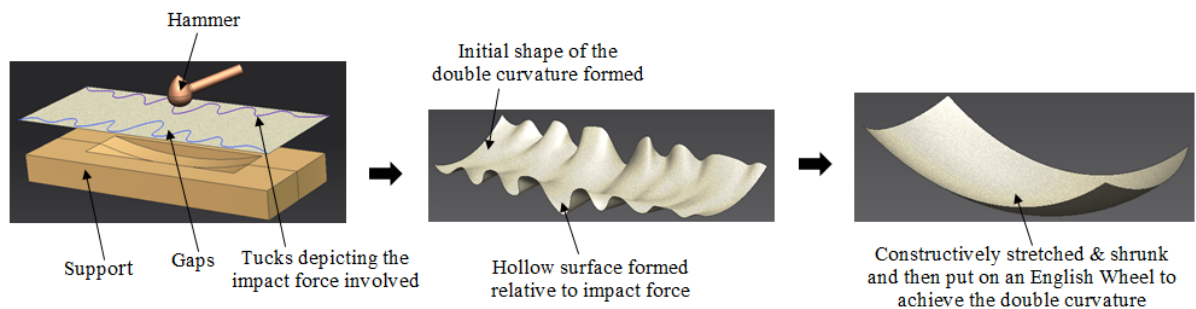


**Fig 5 - Traditional manual forming**

Initially tucks (larger impact forces resulting in larger deformations) were formed to introduce the basic shape required. The tucks are formed with reasonable gaps to avoid affecting the earlier formed tucks. Fig 6 shows the Plan view of peaks and troughs outlined by a panel beater to form the tucks of varied deformation. Peaks represent a larger impact force to be applied to achieve a hollower shape and troughs represent a smaller impact force resulting in shallower shape. The varied impact force required is

achieved by varying the pivot position of the hammer (relative to the hammer head) held by the panel beater. It was understood that farther the pivot position, the greater the force. Forming the tucks results in the basic shape required as shown in Fig 5.

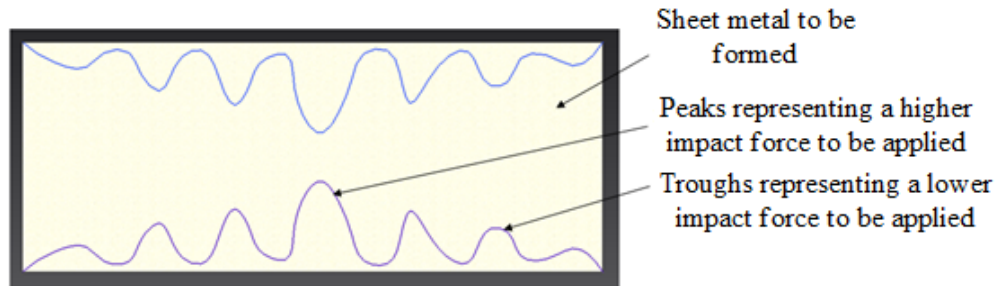


**Fig 6 - Plan view of peaks and troughs drawn on the sheet metal to form the tucks**

Constructing on the formed tucks, the sheet metal is shrunk and stretched consecutively to produce the required contour. Initially the consecutive shrinking and stretching is performed using the hammer and support. Different patterns and paths are used to consecutively shrink and stretch the sheet metal. The pattern and path used are very significant in the final shape achieved; using same pattern with two different path directions could yield different shapes. For finer refinements, a metal hammer and a dolly are used, as shown in Fig 7. There are different types of metal hammers such as the cross pein hammer, flat faced hammer and the curve faced hammer. Also, there are different types of dollies such as heel, curved, toe and a utility dolly that could be used.

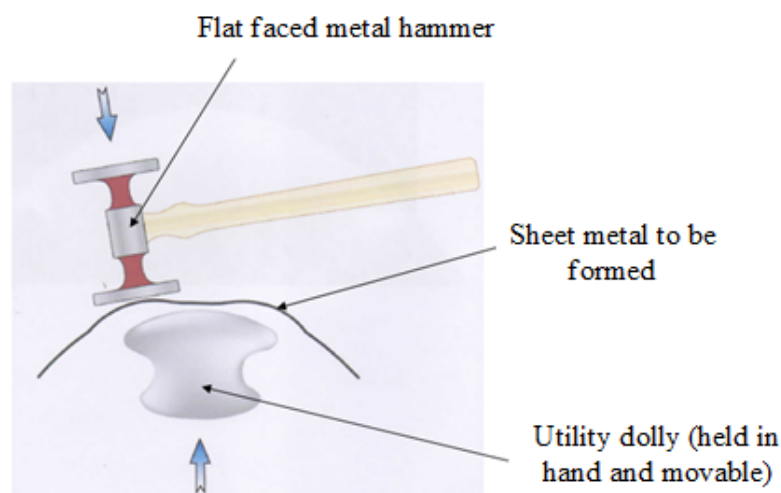


**Fig 7 - finer refinements using metal hammer and dolly**

The sheet metal is held in the hand while forming. The hand also acts as a damper bearing the vibration produced on the workpiece. The damping action enhances the dissipation of kinetic energy on the sheet metal and allows better prediction of deformation based on the impact force applied. However, a panel beater used different templates to analyse the progression towards achieving the target shape. Finally, the formed sheet metal is finished using a wheel machine which smoothens the acquired contour as shown in Fig 8.



**Fig 8 - Using a wheeling machine for contour finish**

The above discussed technique is the most general technique used to form any required contour. Nevertheless, there are several other tools and techniques involved in traditional forming. These have been comprehensively presented as a report in Appendix 1.

The traditional manual forming skills observed formed the basis of this research and contributed significantly to develop the automated system. The conversion of these human skills into parametric solutions that could be given as input to the automated system is discussed in Chapter 6.

#### **2.4 Incremental panel forming - an overview**

With a need for further accuracy and precision in sheet metal forming, incremental sheet metal forming techniques were developed. There are several ongoing researches in the field of incremental sheet metal forming as discussed by Echrif, S.B.M [43]. Several technologies are being used in incremental sheet metal forming which has

provided a wider perspective of research in this field. Most of the techniques use prediction analysis, based on material mechanics which has been instrumental in increasing the accuracy and precision. Occasionally, a combination of conventional and incremental sheet metal forming is also executed to achieve the optimal forming strategy to improve accuracy and precision.

Although several technologies are used, the theory involved in incremental sheet metal forming is the same. The final three dimensional shape is sliced into several contours to be specified as intermediate target shapes for incrementally forming the sheet metal. Based on the target shapes, trajectories are planned and executed. An advantage of incremental forming is that any deviation in the incremental steps compared to the planned trajectory is easily identifiable. This offers the manufacturer the ability to modify the trajectory, optimising the forming path and minimising the forming errors.

Some of the techniques include incremental sheet metal forming through shearing, considering that shearing provides a better strain result [44]. Water Jet Incremental Sheet Metal Forming (WJISMF) [45] is an innovative approach in which high pressurised water is sprayed through the nozzle to deform a sheet metal. Computational Fluid Dynamics (CFD) and Finite Element Analysis (FEA) are pivotal in determining the pressure required for deforming the sheet metal. Research is also being carried out on laser-supported incremental sheet metal forming [46].

However, Single Point Incremental Forming (SPIF) [47] is the especially widely used technique to note in incremental sheet metal forming, as it was able to provide the required process variations. In SPIF, usually a rotating mandrel moves down incrementally in the Z-axis, forming the sheet metal fixed to a blank holder which is able to move in the XY-axes as shown in Fig 9. Radial displacement tools were also used instead of a rotating mandrel. Later, these tools were replaced by Computer Numerical Controlled (CNC) tools which improved both cost and time efficiency. State-of-the-art research in incremental forming by using NC tools is further discussed in section 2.5.

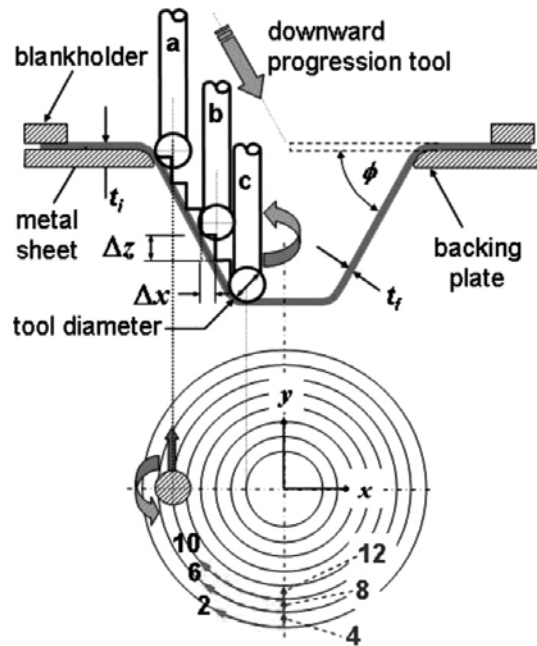


**Fig 9 - Single point incremental forming [43]**

Apart from using a linearly displacing tool to incrementally form the sheet metal, some research is also being carried out on using an impacting mechanism for incremental sheet metal forming. Incremental sheet metal forming through impacting is the core subject area of the research presented in this thesis. A detailed discussion of using impacting mechanism for incremental sheet metal forming is presented in Section 2.6.

#### **2.4.1 Commercial methods available in incremental forming**

Incremental sheet metal forming is being used in industries very sparsely in terms of large manufacturing sectors. Small scale industries are slowly transforming to ISMF methods because of cost-saving factors and high flexibility. However, most of the large scale manufacturers are using robots for flanging and bending operations. Using robots has increased the part accuracy and decreased the cycle time involved in manufacturing.

AMINO North America Corporation [48] has produced a commercial die-less numerical controlled incremental forming machine. The technology was used to produce a section of Shinkansen (Bullet Train, Japan) as shown in Fig 10.



An example application of ISF – a 1/8 scale model of the front section of a Shinkansen (Bullet Train) made by Amino in Japan.

**Fig 10 - Application of Incremental Sheet Forming (ISF) at AMINO [48]**

OCAS BV [49] and ASCAMM Technology Centre [50] have also been researching on rapid prototyping methodologies for metal forming. FORD [51] has been researching on the flexible forming technology and has introduced Freeform Fabrication Technology (F3T) which could be helpful in producing the prototypes in days. In this method, a computer controlled stylus is used to incrementally form the sheet metal which is held in fixture as shown in Fig 11. Airbus, St. Eloi has been researching on Asymmetric Incremental Sheet Forming (AISF) for producing the Pylons for aircrafts [52]. The pylons are made of titanium which makes it a complex task to shape them by traditional forming processes. Hence, the process involving FE modelling of AISF is being researched.

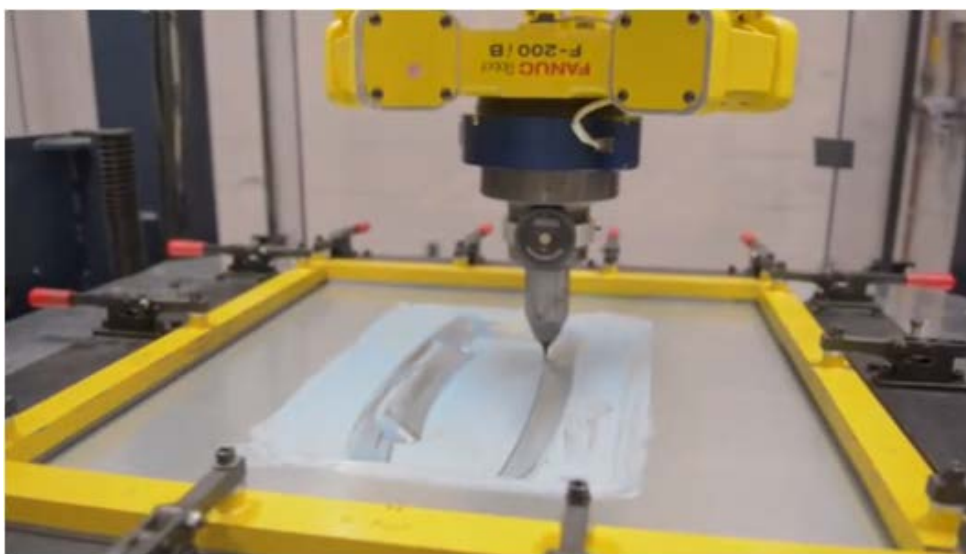


**Fig 11 - Ford F3T technology [51]**



All these processes are based on the incremental sheet metal forming, by either drawing or stretching, which affects the thickness distribution of the material formed. Also, the use of fixtures limits the freedom of forming. As it could be noted, all the discussed commercial methods are used for the rapid prototyping purposes of the sheet metal which is the most significant requirement for automotive, aerospace and sheet metal industries.

### **2.5 State of the art research in incremental forming by stretching/ pulling**

Most of the researches in incremental sheet metal forming are based on stretching and pulling. Incremental sheet metal forming (ISMF) are also termed as die-less incremental sheet metal forming as die is not used in the forming process. Single point incremental forming (SPIF) [47], double pass incremental forming (DPIF) or two point incremental forming (TPIF) [53] are some of the well-known ISMF techniques proposed.

In SPIF, the sheet metal is constrained in its boundaries using a blank holder which has motion in XY axes or back-plate, which allows the sheet to be drawn, and a rotating tool incrementally moving down in the Z axis, forming the sheet metal. The SPIF process with a back-plate is shown in Fig 12.

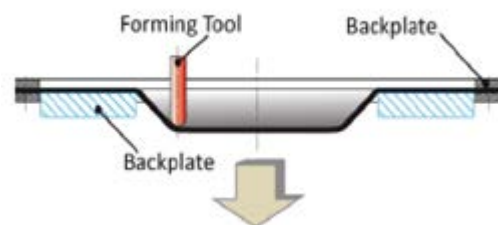


**Fig 12 - Single point incremental forming - modified from [53]**

DPIF uses the same technology as SPIF with a partial die supporting the forming of sheet metal (AKA, TPIF). If the partial die is replaced with a periphery supporting tool - which is known as duplex incremental forming with periphery support (DPIF-P). If the local support replaces the partial die, the process is known as duplex incremental forming with local support (DPIF-L). All these processes use numerically controlled tooling. These processes are shown in Fig 13 where (a) is DPIF with partial die, (b) is DPIF-P and (c) is DPIF-L.



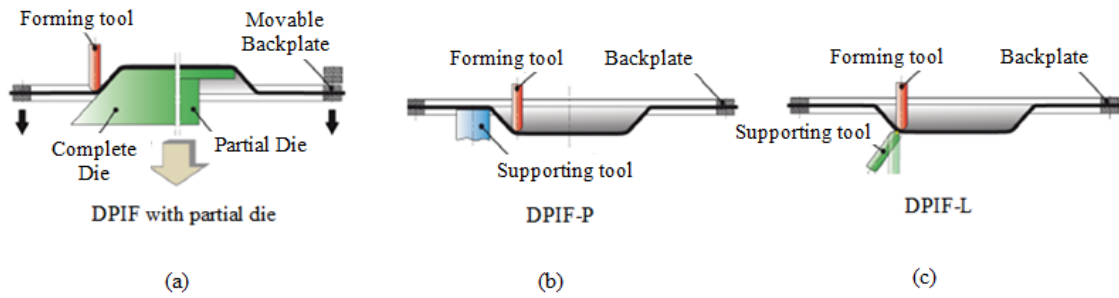


**Fig 13 - DPIF process – modified from [53]**

In the DPIF-L process, if the tools are held by the robot the process is known as Roboforming [54] as shown in Fig 14.

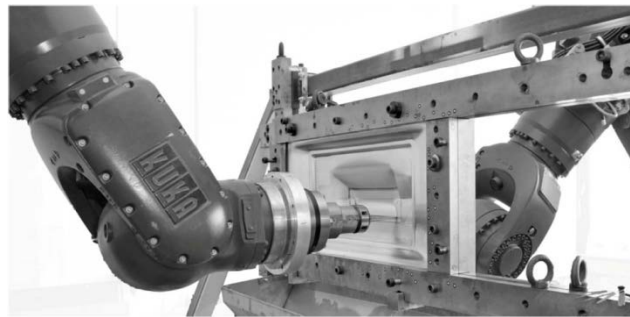


**Fig 14 – Roboforming [54]**

SPIF using numerical controlled tool was widely used in Research. IMRC, Bath University [55] and AFRC, University of Strathclyde Engineering [56] have been researching the die-less incremental forming using numerically controlled machines. IMRC have been able to achieve results with respect to tool speed, tool-path generation and numerical modelling of the deformation. RWTH (IBF) at Aachen University [57] is researching on 5-axis and 3 axis CNC incremental forming units.

Kuleuven University, Germany [58] has researched on SPIF using both CNC controlled tool and Robot controlled tool and had achieved results on force measurements for forming the sheet metal. MTA, SZTAKI, Hungary [59] has been researching on SPIF using a FANUC Robot which holds the tool to form the sheet metal. Polytechnic University of Marche, Ancona, Italy [60] used a hybrid mechanism by mounting a parallel kinematic Tricept HP1 upon a COMAU robot. The system was used to experiment on the kinetostatic model in incremental forming.

Apart from the numerical controlled and robot controlled, there are other prototypes based on incremental forming. Fatronik, Spain [61] has developed a prototype for metal forming by incrementally forming the sheet metal using an adapted milling process. AMPL, Northwestern University, US [62] has come up with a Double Sided Incremental Forming prototype for forming the sheet metal and predicted the failures in forming the metal in comparison with results achieved using numerical methods.

It was studied that complicated shapes such as pyramids with six sides can be produced using die-less incremental forming [63]. The pyramids formed are of 60 mm depth with their deepest point having a 2.5 mm radius curve. A wall angle up to  $80^\circ$  and twisting half- apex angle up to  $10^\circ$  were formable. This was a major feat using a die-less forming method. Using DPIF, it was observed that superimposing pressure with the counter tool (DPIF-L) could produce an increased wall angle of 12.5% when compared to duplex forming with peripheral support (DPIF-P). The observation was based on forming an aluminium alloy. DPIF-P produced a wall angle of  $64^\circ$  whereas DPIF-L resulted in a wall angle of  $72^\circ$  [64].

Based on these studies, further investigations were carried out on sheet metal formed using SPIF methods [2, 47, 65-68] and DPIF methods. The studies suggest that

- Knowledge of maximum draw angle particular to the thickness of the sheet metal is important.
- The incremental step size of the tool is significant in forming the sheet metal.
- Lubrication helps improve tribological factors of forming.
- Mostly, the critical wall angle was determined to be  $45^\circ$ ,  $51^\circ$ ,  $55^\circ$  and  $61^\circ$  under various experimental conditions using SPIF process. DPIF results suggested that wall angles of  $64^\circ$ ,  $72^\circ$  and  $80^\circ$  could be formed.
- Surface roughness of both the sheet metal and the tool seems to have effect on the formability.
- DPIF process provided much control on the sheet metal forming compared to SPIF.

However, all the above discussed techniques use a stretching/pulling method to form the sheet metal. These are likely to result in non-uniform thickness of sheet metal and often lead to fracture. Though higher wall angles were possible using DPIF methods, they decreased the flexibility in forming drastically.

## 2.6 State of the art in incremental forming by hammering

As mentioned earlier, sheet metals are traditionally formed using a hammering process. However, there have been only a few studies using the hammering or impact forming method.

Comparing the incremental forming by stretching and hammering techniques, a study carried out by researchers in Cambridge University has found that the hammering process had a steady impulse response in comparison to incremental stretch forming [69]. It was also found that hammering is better for forming a widespread region rather than using incremental stretching as it tends to be more localised. Higher wall angles and a deeper curvature could not be produced using stretching process as it often leads to fracture of the material. Nonetheless, hammering creates a noisy environment and for an equally smoother surface further process may be required (e.g. planishing).

Tanaka [70] initially proposed a servo hammering unit to produce the incremental deformation required as illustrated below in Fig 15.

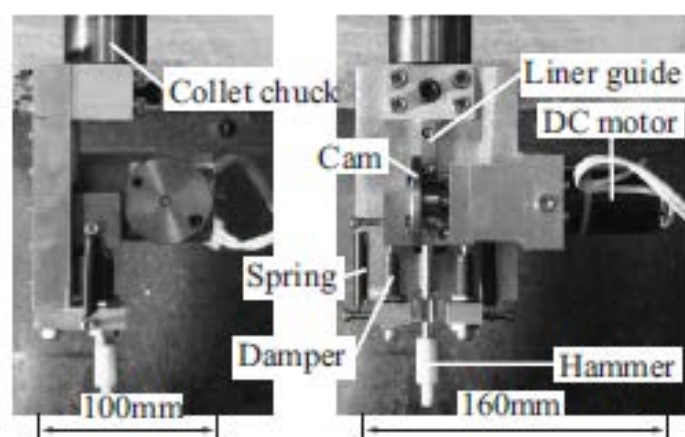


**Fig 15 - Servo hammering unit [70]**

The mechanism used a DC motor with a linear guide and Cam arrangement. When the DC motor is triggered, the Cam raises and releases the hammer which is accelerated by

a spring to have an increased impact. A damper has been included in the set up to bear the retracting forces. With a tool diameter of 6 mm and a frequency of 10 times per second, a terminal velocity of 10 m/s and an impact force of about 400 N were achieved.

By enhancing from the previous system to reduce the risk of crack, the DC motor was replaced by the linear servo motor [33]. The linear servo motor was developed using a slide bearing, stator coil, magnet shaft, stopper and a hammer head as shown in Fig 16 (b). This hammering unit was mounted on the XY axes movable robot as shown in Fig 16 (a). The hammer was 6 mm in diameter with a round tip of 1 mm to avoid fracture. It could be inferred that a velocity of up to 1 m/s could be produced using this. It was also suggested that most of the kinetic energy is consumed in deforming the material rather than shaping the material to the required contour. There is not enough information about whether the tool has reached its bottom dead centre in order to produce the required deformation.

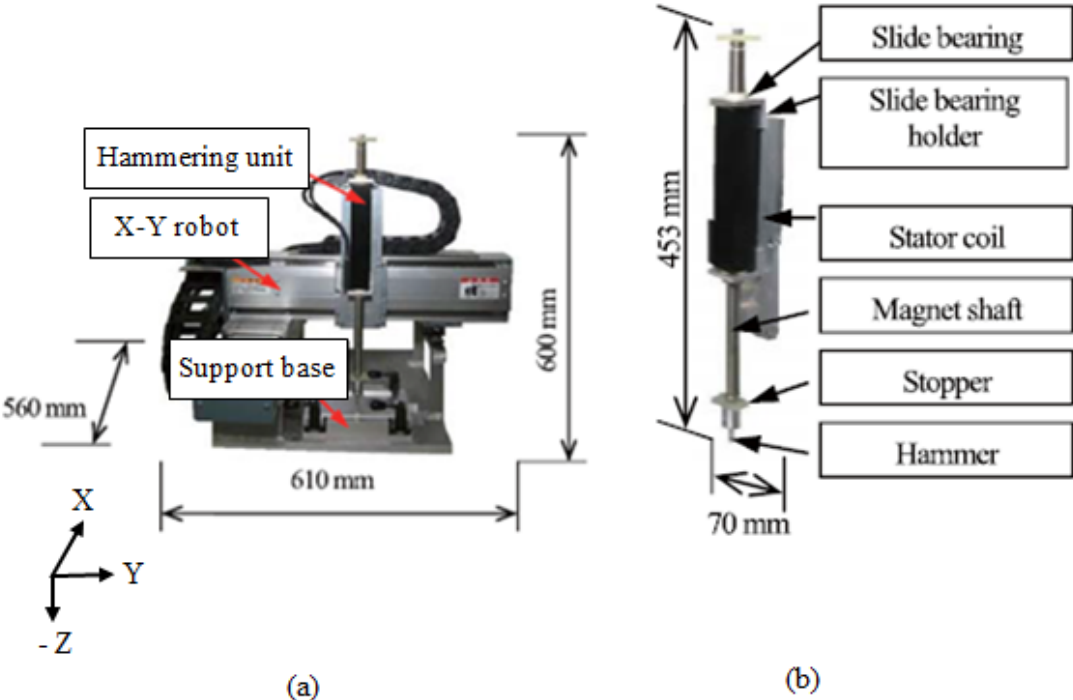


**Fig 16 - Linear servo hammering unit and linear servo motor with hammer head – modified [33]**

It was also found that successive impacts were partially sensitive to the region of earlier impacts and can consequently influence the deformation achieved as shown in Fig 17.

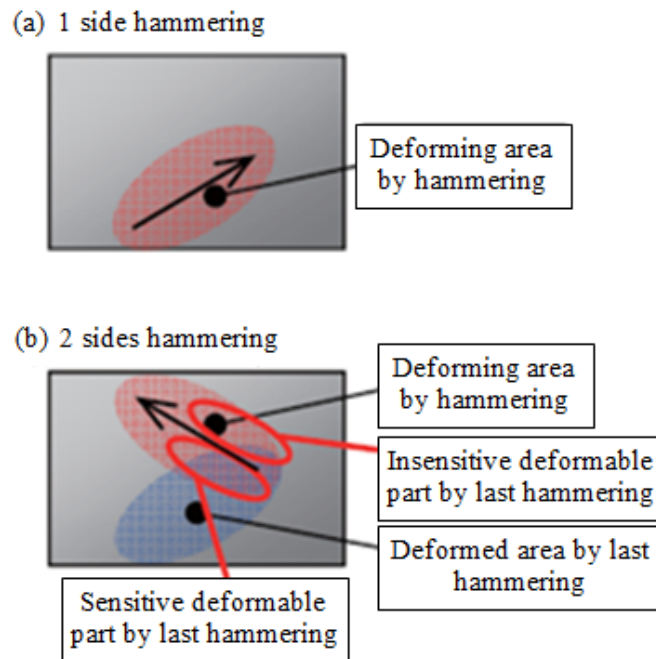


**Fig 17 - Sensitivity to the neighbouring deformation - modified [33]**

Improving on Tanaka’s system, Asakawa [71] proposed a servo hammering unit mounted on a Kawasaki 6-DOF industrial robot to form the sheet metal. The system set up used by Asakawa is shown in Fig 18.

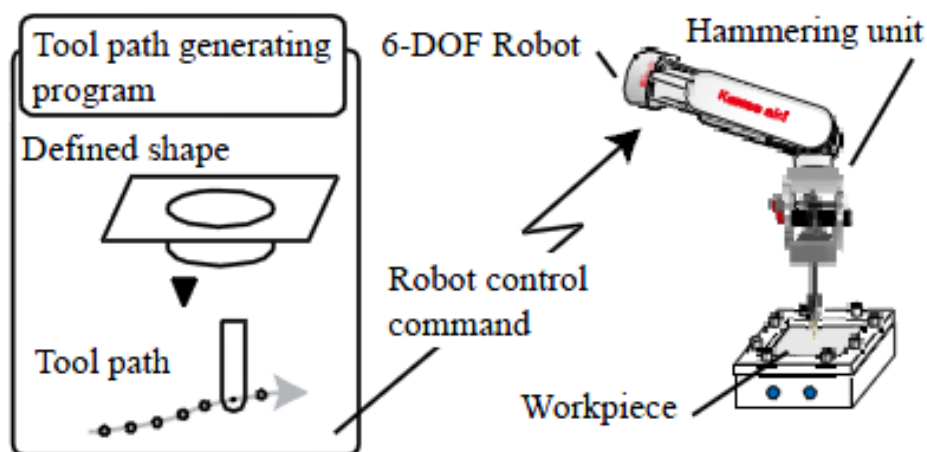


**Fig.8 Configuration of the system**

**Fig 18 - System set up used by Asakawa [71]**

Investigations were carried out on the existing tool path and based on the investigation results, a new tool path based on the parametric curve interpolation was proposed. The new system proposed that the sheet metal being formed is free from sudden deformation in the corners. The proposed system indicated that the deformation is gradual, which minimises the cracks in the sheet metal. However, the forming process was performed using stretching and was prone to non-uniform thickness distribution in the sheet metal being formed.

Furthermore, Yamamoto [72] suggested that a tool path may have an influence on the formability and so proposed a local heating of the sheet metal by using a gas burner during the hammering process, as shown in Fig 19. In this annealing process, the metal is melted to the recrystallisation temperature or higher. This has a significant benefit in analysing the boundary line between the hammered portion and unprocessed portion. The proposed local heating methodology improved the formability and thickness distribution in the sheet metal. However, effects of spring back during the cooling down were not taken into account in analysing the forming path during the process.

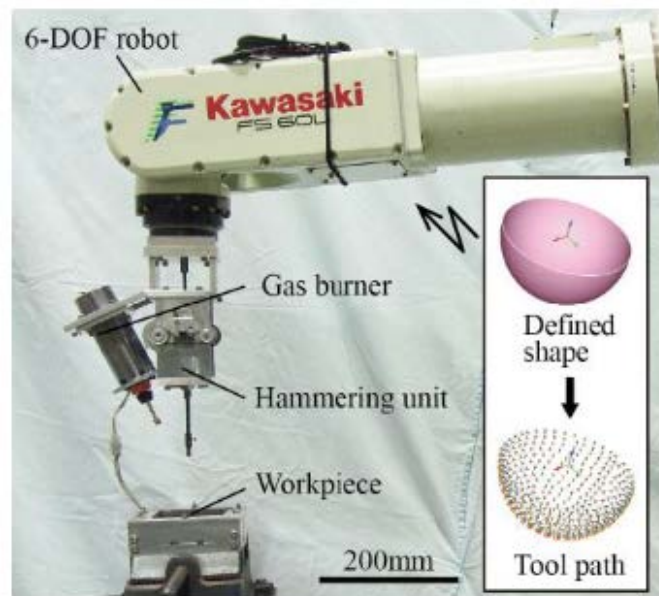


**Fig 19 - Hammering unit with gas burner [72]**

Luo [73] suggested an incremental punching approach to form the sheet metal. In this method, the punch was controlled using a hydraulic unit with Programmable Logic Controller (PLC). The sheet to be formed was held in a fixture which is fixed to a movable XY table. It was determined that the shape formation depends on the radius of

the punch ball, the distance between two consecutive punches and radius of the punch that is in contact with the sheet while impacting (over its duration, the impact was not always in the centre of the punch, it varied in radii depending on the surface geometry of the sheet metal). Depending on all these criteria, a geometry error model was developed and the incremental punching was performed. The experiment was carried out for a 10mm punch diameter with 1 mm thick 300x300 mm steel. The method was used with a 1 mm thick sheet with a varying vertical punch feed steps of 1 mm – 4 mm and was used in 3 mm thick sheet with constant vertical feed step of 3 mm. It was found that the method with significantly shorter feed steps of 1 mm achieved a better accuracy. It was also found that holding the sheet too tight might fracture it and holding it too loose might result in deviations.

Schafer [32] introduced an eccentric cam to the hammering method with two counter balancing masses to balance the masses as shown in Fig 20.

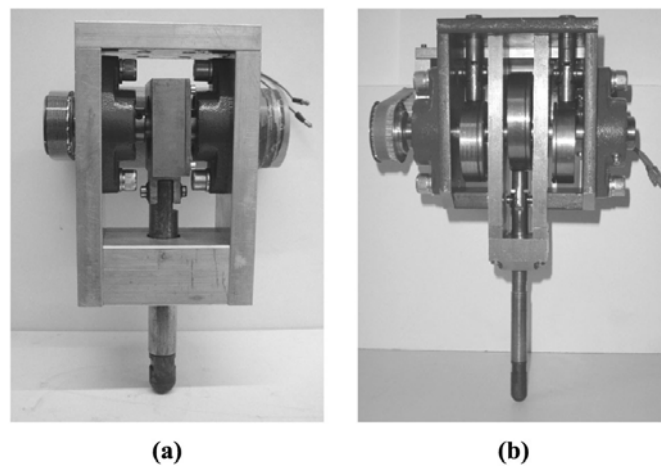


**Fig 20 - Hammering tool without counter balance (a) and with counter balance (b) [32]**

The sheet metal was formed by means of punches produced by the hammering unit reciprocating due to the eccentricity of the cam. Without the counter balancing masses, the mechanism produced 60 impacts/s. Introducing counter balancing masses to increase the hammering frequency resulted in producing 100 impacts/s, with a 1.2 mm hammering amplitude. The tool centre point (TCP) could either be defined at the point where the tool impacts the surface or as the centre of the spherical tool used. In this methodology, calculations were based on defining the centre of spherical tool as the tool centre point (TCP) since the motion of tool is always vertical in the z-axis of the

workpiece. This was helpful in predicting the hammering impact point. It has to be noted that the mechanism had very high friction losses.

Both Schafer's and Yamamoto's techniques used motion of tool to achieve the required contour (two dimensional motions by a robot in the servo mechanism and a six-axis robot in the eccentric cam mechanism) while the sheet metal was held in a fixture. Forming the sheet metal by motion of the tool has got a significant effect in forming; the vibration caused may affect the hammering unit and may cause inaccuracy in forming.

Replacing the motion of tool, Opritescu [74] introduced 'kraftformer' for shrinking the edges of the sheet metal using a shrinking machine and a six axis robot which held the sheet metal, as shown in Fig 21. The sheet was guided by the robot and all the transformations required at the tool centre point (hammering impact point) were defined relative to the robot's base. The sheet metal was driven by the robot in the path that was tracked and imparted from the human motions of shrinking the sheet metal. Based on this, three dimensional stopping points for the robot and stroke depths for the "Kraftformer" were calculated using the two dimensional linear transformation. In this method, tests were made only to shrink the sheet metal on the edges by 'kraftformer' which measured a 6% deviation to that shrunk by human.

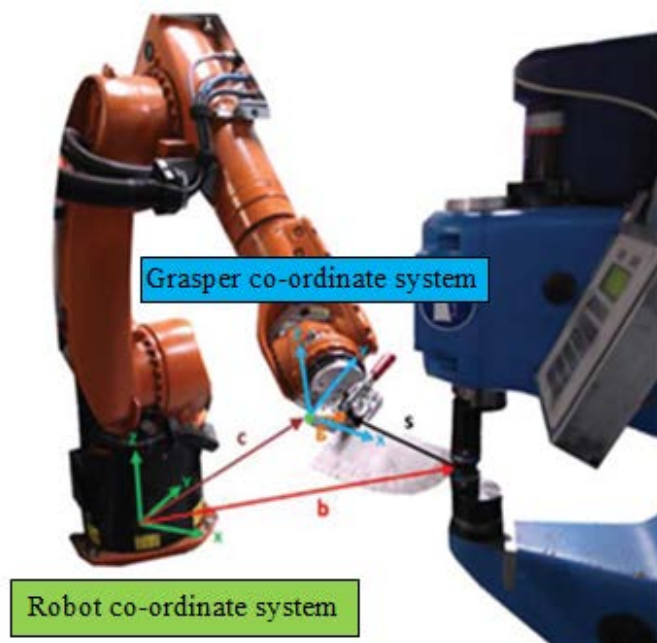
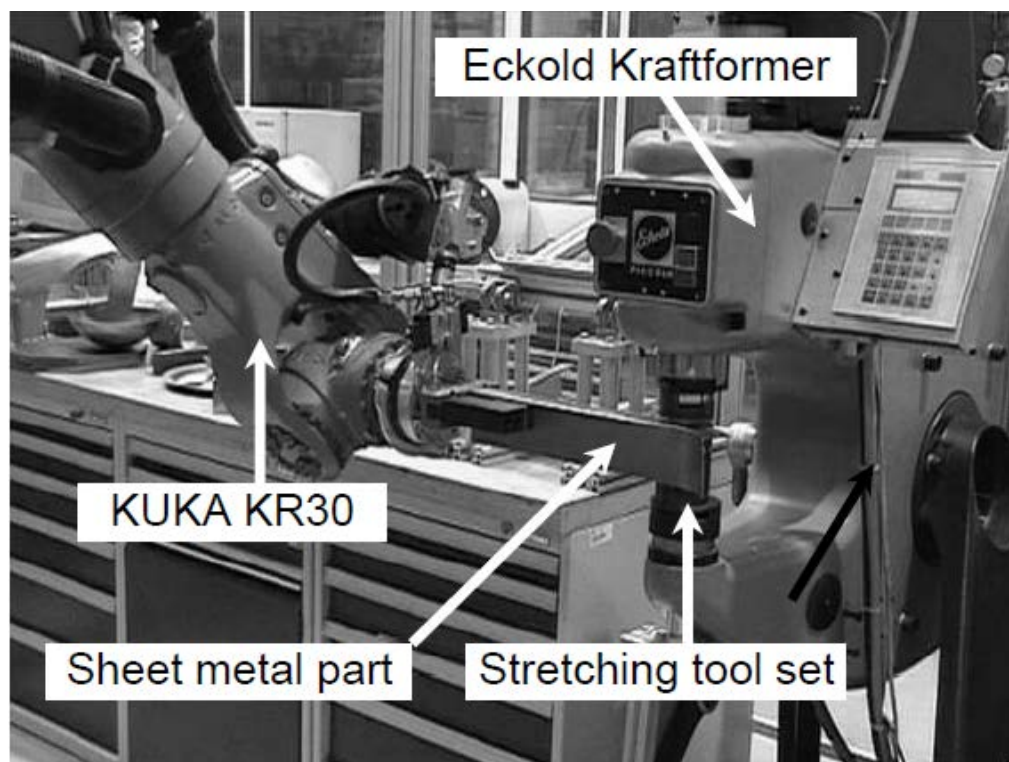


Fig 21 - Shrinking using kraftformer - modified [74]



Removing the use of fixtures and progressing further on Opritescu's methodology, the CoTesys research project [75] used a six-axis robot to hold the sheet metal while the sheet metal was formed by using an Eckold Kraftformer electric hammer as shown in Fig 22. The research was aimed at capturing the cognitive knowledge - to form the sheet metal using incremental forming method which was termed as driving [76]. The research named 'CoDrive' has provided a significant contribution towards incremental sheet metal forming using the kraftformer. Incremental impact stretch forming was implemented using the kraftformer to form the sheet metal, which was held by the robot. The research was about understanding how the robot motion alters itself (learning from the human) to the geometrical changes, in particular, the bending radii in the sheet metal while stretching or shrinking. Though the research has made a significant contribution to incremental sheet metal forming using the Kraftformer, the focus of research was confined to either shrinking or stretching on a 2D contour [74].



**Fig 22 - 'Co-Drive' by Co-Tesys [76]**

Though CoTesys made a significant impact through their project CoDrive, they did not focus learning from highly skilled panel beaters and transforming the human skills into a parametric solution that could be used as a universal solution to form any 3D geometrical shape from a defined 2D sheet metal contour.

## 2.7 Research gap

On reviewing the existing commercial, and the state-of-the-art methods for research in incremental sheet metal forming, it was concluded that most of the incremental sheet metal forming processes are based on the principle of stretching or pulling. The accuracy of forming has increased through these processes. However, in most of the existing methodologies, the sheet metal forming uses substantial fixtures and the main principle involved in sheet metal forming is either stretching or drawing. This causes a significant thinning effect resulting in non-uniform thickness distribution and an increased possibility of failures due to fracture. Also, due to the use of fixtures, the existing processes do not provide flexibility in forming. Moreover, as discussed earlier in Section 1.2, the automotive industries are progressing towards using light-weight alloys for manufacturing. In which case, the incremental forming by stretching or pulling will be prone to a much more thinning effect. Hence, there is a high possibility of failure.

As discussed, the roboforming incremental sheet metal forming method could produce a higher wall angle. Nevertheless, the process requires a very complex algorithm to manage the counter force or super imposed pressure when forming complex contours, and also due to the fact that the process causes thinning of the sheet metal. The discussed hammering methods which use a hammer mounted on an axial servo motor or six-axis robot, mostly constrain the sheet using fixtures. This causes a thinning effect and reduces the freedom of forming.

While forming the sheet metal using an impacting method, the hammer should reach the bottom dead centre of the anvil. Reaching the bottom dead centre of the anvil ensures that the required shape and deformation is achieved locally at the point of impact. Studies related to impact force and kinetic energy involved in the sheet metal forming have not considered whether the hammer reaches the bottom dead centre of the anvil. This is significant to be determined since it gives the information on the energy delivered and the shape formed. In most cases, the kinetic energy applied does not deform the material to the required depth. The energy lost in the process and the impact force required to achieve the required deformation have not been analysed.

The residual stresses that occur during sheet metal forming and its influence on the local and global deformation has not been recognised in the proposed approaches. The

sheet metal's material properties change upon each impact due to the effect of yield stress produced upon impact. The studies involved in sheet metal forming have not considered the significance of yield stress. Also, the prediction of forming was always based on the pre-defined standard stress/strain relation or forming limits of the material. It was not recognised that using pre-defined data might mislead predictions. Material stress/ strain relation or forming limits were not calculated using tensile tests.

3D vision systems have been very sparsely used in sheet metal forming. Its significance on optimising the sheet metal forming process has not been explored.

The co-tesys project contributed significantly to the incremental sheet metal forming process by impacting. The use of robot to hold the sheet metal introduced flexibility into forming. However, the process was confined to either shrinking or stretching a 2D contour. The process focussed on capturing the cognitive knowledge to form the sheet metal. The research did not provide a solution to incrementally form a 3D contour. The research was also not focussed on learning the panel forming skills from highly skilled operators and converting them into an automated solution.

On reviewing the traditional panel forming, it was apparent from the manual sheet metal forming methodologies that higher flexibility and adaptability can be achieved. It was also observed that the sheet metal formed has a uniform thickness distribution increasing the quality of the part produced. Nevertheless, the significance of manual panel forming skills was not considered by incremental sheet metal forming researchers.

Based on the literature review, the research gap identified is summarised below.

- Flexibility of forming was only introduced for shrinking or stretching a 2D contour. However, flexibility of forming is not available to form a 3D contour.
- The proposed studies did not recognise the panel forming skills of highly skilled panel beaters and their techniques were almost not considered for automating the forming approach.
- Thinning effects cannot produce good rigidity and when lightweight materials replace the materials that are currently being used, it is very hard to control the

formability. Good sheet metal forming practice is to maintain uniform thickness while forming.

- Residual stresses and their effects on sensitivity of deformation have not been considered.
- 3D vision system's capability on sheet metal forming process monitoring and contour feedback has not been utilised.
- Installing a 3D vision measurement system to monitor the shape of the sheet metal being formed and provide feedback on shape features detected to optimise the process of forming

## **2.8 Selection of the power hammer and the motion capture system**

### **2.8.1 Selection of the power hammer**

Based on the research focus discussed in Chapter 3, the impact force and energy involved in the sheet metal forming were analysed. The impact force required for sheet metal forming was determined using experimental analyses, as discussed in Chapters 4 and 5. On determining the impact force required, investigation was done on the power hammers that could be used in the automated system for forming a 3D contour. The detailed investigation into power hammers is included in Appendix 2. The investigations lead to the following conclusions:

- Power hammers are mostly operated using electric motors
- An eccentric cam is used to guide the reciprocating motion of the hammer
- A flywheel can be used to store and produce a much higher impact energy
- Power hammers are pedal-operated and they act as a clutch (could be replaced using a switch)
- A leaf spring mechanism or linkage mechanism is needed to provide the final push
- The action of power hammer needs to stop (using a break) as soon as the mechanism is switched off

As electrical power hammers were not commercially available for the required specifications (as concluded on the investigation above), inquiries were made on pneumatic power hammers that could produce the required impact force. The Eckold Kraftformer manufactured by the German and Swiss was investigated in detail. On the basis of detailed study, Eckold Kraftformer KF170PD [77] was used in the automated system as it met the investigated requirements and produced the impact force required. The Kraftformer provided a large number of tooling sets. However, a doming tool was determined as the best tool to be used in the automated system. The doming tool was chosen as it was similar in shape to the hammer (wooden mallet) used by the manual panel beater. The doming tool provided the significance of forming any 3D shape using the Kraftformer.

It could be noted that CoTesyS research project also used the Eckold Kraftformer. However, only the shrinking and stretching tools were used which either shrank or stretched a 2D contour. Using a doming tool for forming a 3D contour using an automated approach was a significant development and a novel method used in this research.

The hammering machine, Eckold Kraftformer KF170 PD (shown in Fig 23) was pneumatically operated at a pressure of 6 bar. The hammering machine was capable of being operated at a maximum of 60KN impact force producing 150-250 impacts/minute and capable of forming aluminium sheet metal of 2mm thickness. Varied impact force could be produced on varying the stroke length and RAM of the hammering machine. The stroke length could be adjusted in the range of 2 mm – 6 mm with fine adjustments of 0.05 mm. The RAM could be adjusted in the range of 0 – 8 mm with fine adjustments of 0.01 mm.

The Kraft Former was operated using a pedal (acting as a clutch). The mechanism stops immediately once the foot is taken off the pedal. The hammer also has the ability to be operated in single stroke or multiple stroke conditions producing the same impact force which was a specific requirement for this research. The detailed spec of the Kraft Former is given in Appendix 3.

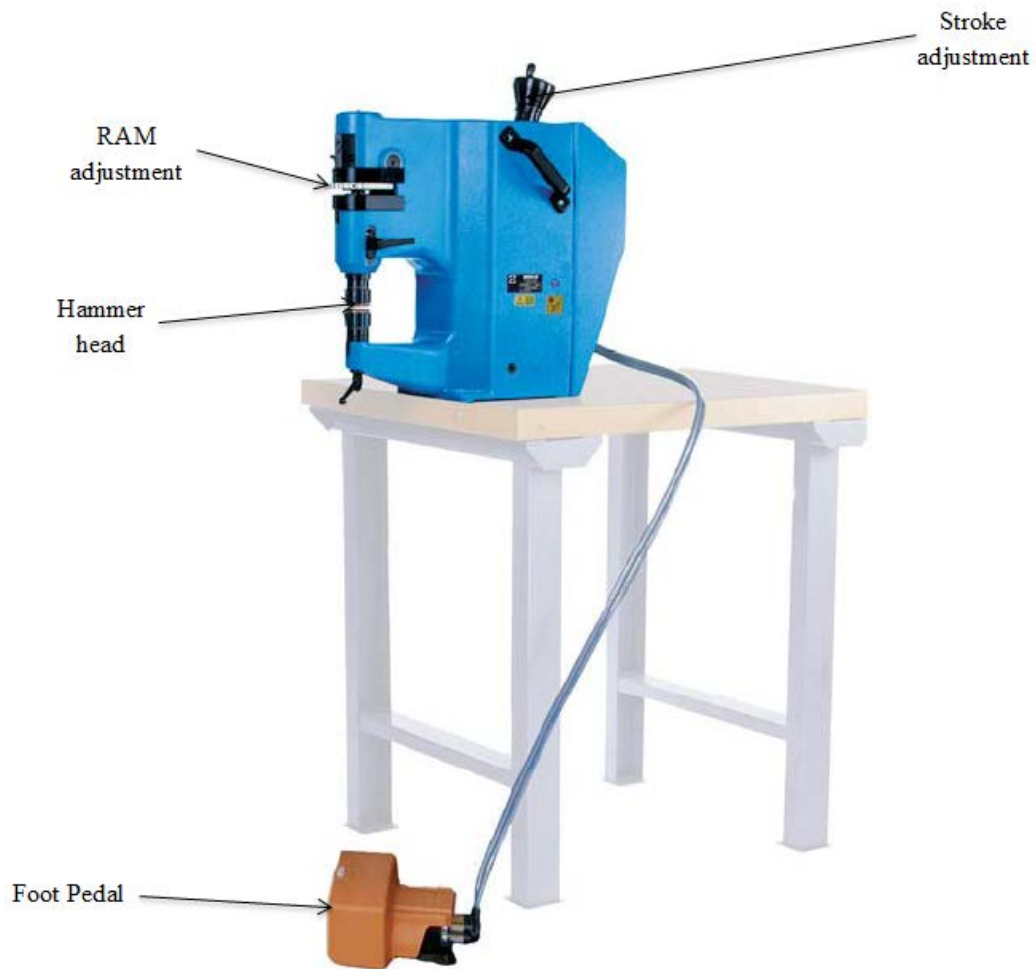


**Fig 23 - Hammering machine - Eckold Kraftformer KF170PD [77]**

### **2.8.2 Selection of the motion capture system**

As one of the research focuses (discussed in Chapter 3) was to capture and interpret the panel forming skills of a human skilled operator, a motion capture technology was required. Though many motion capture technologies are available commercially, motion capture using the Vicon system [78] was chosen, as precise and accurate measurements were required in a closely bounded volume of the hammering and sheet metal manipulation.

The Vicon system used for motion capture of sheet metal manipulation and hammering included two 2MP Vicon T-Series camera [79] for motion capture. The cameras were mounted on the tripod as shown in Fig 24 to focus the cameras at the required angles. The cameras had a resolution of 0.5mm. Passive reflective markers were used to track the motion of the sheet metal and hammer. A gigaset-ethernet switch was used for the

fast transfer of tracking data into the PC host. The Vicon Tracker Analyser software was used for three dimensional object tracking and analyses purposes. The Vicon system is illustrated in Fig 24.

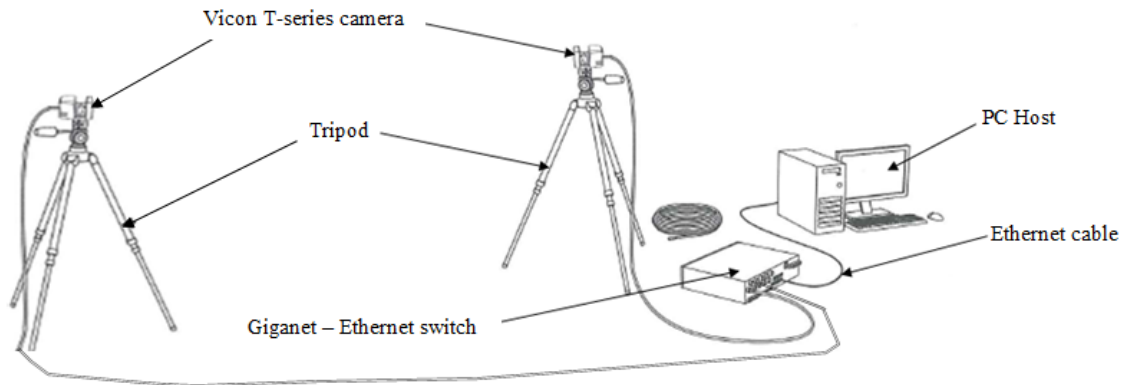


**Fig 24 - The Vicon system**

### 3. Research methodology

---

#### 3.1 Introduction

It was determined that manual panel forming provides sufficient flexibility and part quality through incremental sheet metal forming. The proposed research focusses on capturing and transforming the manual panel forming skills into an automated system for incrementally forming sheet metal parts.

The research was initiated by developing the following hypothesis:

*If the skill used by a manual panel beater is understood correctly, an automated system could be developed based on adopting the essential human skills and eliminating some steps involved in panel beating. A motion capture system is envisioned to be used for capturing the human skills of a panel beater.*

*It is envisaged that a robot could be used to manipulate the sheet metal and an impact hammer could be used to form the 3D shape of the sheet metal.*

*FEA is envisaged to be used for forming path prediction of the sheet metal to be formed. 3D vision measurement and CAD are anticipated to be used for shape measurement and comparative analysis of the sheet metal formed using the automated process.*

The hypothesis developed is illustrated in Fig 25.

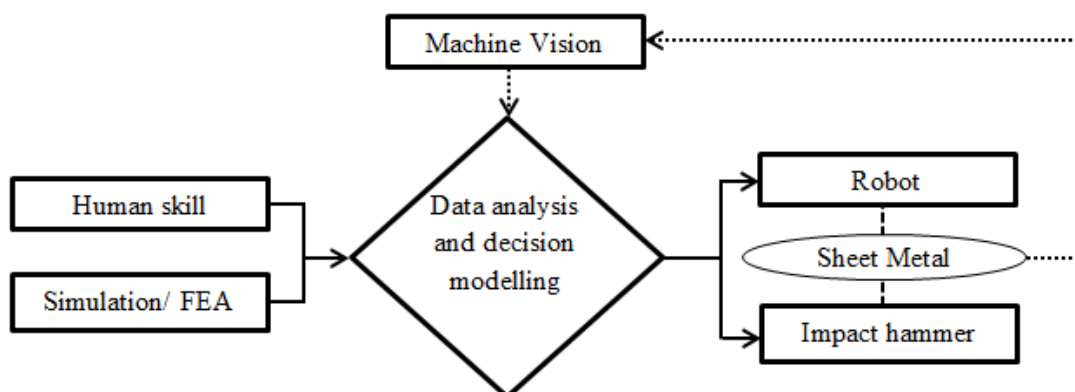


**Fig 25 - Proposed solution (Envisaged)**



Based on the research gap identified in Section 2.7, this research was focussed on achieving the following:

- Determination of impact force for sheet metal forming by experimental analysis
- Determination of impact force for sheet metal forming by finite element analysis
- Determination of human skills involved in sheet metal forming and interpreting them into parametric inputs for the automated system. Specifically focussing on determining the pattern, path and sheet metal manipulation skills of a human operator
- Designing and developing the Mechatroforming system by using a hammering machine and a robot to form a 3D contour.
- Developing the automated system to provide high flexibility in sheet metal forming by designing a suitable gripper and increase the uniform thickness distribution of the material being formed
- Installing a 3D vision measurement system for shape measurement and contour feedback

Based on the hypothesis and research focus, Mechatroforming was developed to provide the following attributes:

- Sheet metal forming by impact
- Forming without fixtures
- Generic incremental forming approach for forming any 3D contour
- Integrated system for automation feasibility considering factors involved in forming
- Continuous monitoring and feedback for process optimisation

### 3.2 The process of Mechatroforming

Based on the observation of manual panel beating by skilled labourers and analysing the different factors affecting the sheet metal forming, the Mechatroforming method was developed. As shown in Fig 26, a robot holds the sheet metal similarly to the manual operator and the hammering unit forms the sheet by impacting the sheet which is held upon a support (i.e. the anvil). The support was universal to provide flexibility in forming different contours. The robot provides the motion and angle for incrementally forming the sheet metal under the hammer.

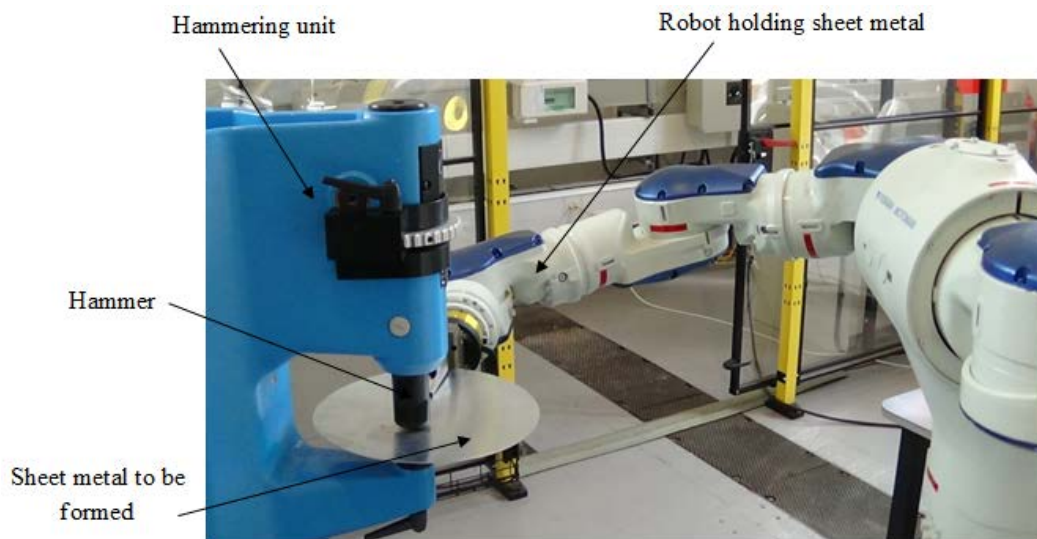


**Fig 26 - Mechatroforming**

Based on the requirements for predicting the forming of sheet metal, a forming strategy was developed as shown in Fig 27. This strategy enables an in-line off-process monitoring of the forming following each iteration to configure the impacting pattern accordingly to achieve the required shape of the sheet metal.

The robot and the hammering unit are integrated using the following components,

- **Database** – consisting of human skills captured and Pre-processing FEA
- **Robot Controller** – to control the motion of sheet metal to achieve the shape required
- **Hammering control** – to control the motion of hammer to achieve the deformation required

- **3D Shape Measurement** – to monitor the forming of desired shape and deformation
- **Force Sensor** – to measure the deformation achieved after each impact

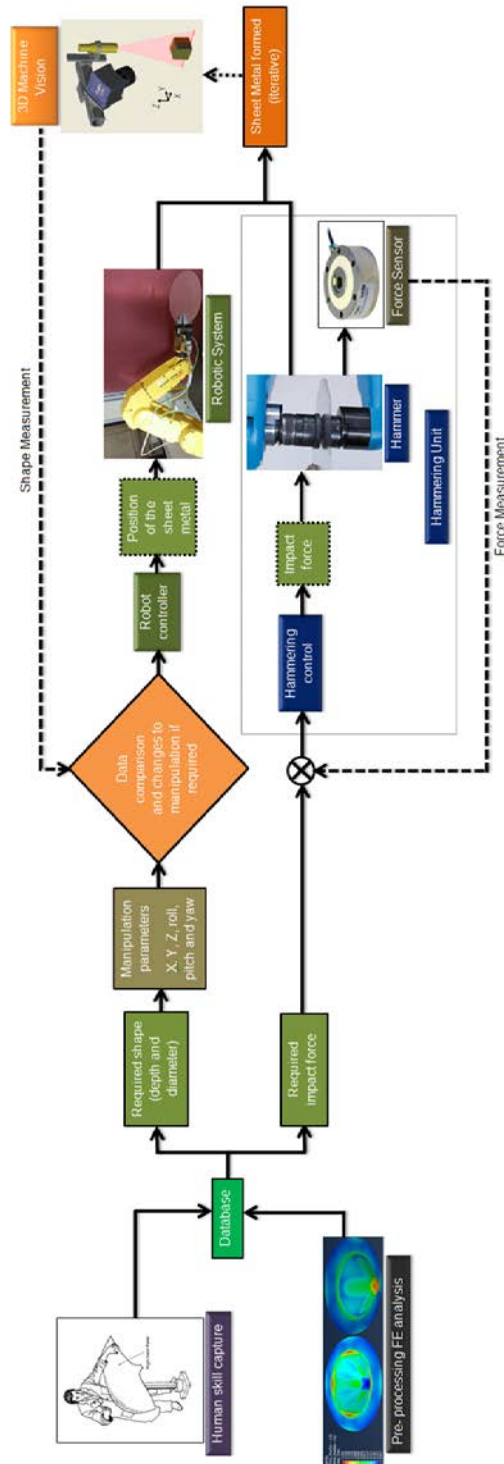


**Fig 27 – Mechatroforming – Ideal forming strategy**

### **The ideal process**

Ideally, the initial contour to start the forming is designed by reverse engineering the CAD model of final shape to be achieved.

In the ideal process, the initial process has tucks being formed (as discussed in Section 2.3.1) to produce the basic formability shape of the required contour. The location and force of the first impact is based on the combined database of FE analysis and system parameters observed from human skills (referred as system parameters here). Once the first impact has been made, impact force sensor will feedback the impact force to predict the deformation achieved. The pre-processing FE analysis will provide the region sensitive to residual stresses because of that impact; hence, the next impact could be made away from the sensitive region based on the system parameters.

After the initial formable shape is achieved, the consecutive shrinking and stretching will lead to the contour required. The pre-processing FE analysis and the system parameters combined will generate contour slices based on which the sheet metal will have to be formed. Each contour slice will follow a perceived path and will need to achieve the required shape and deformation.

The 3D shape measurement scans the sheet metal and produces the depth and the shape information that is fed back into the control system. The achieved contour will be compared to the pre-defined path. Any error in the path will be rectified by the feature detection algorithm (developed using Matlab [80] programming) in the control system (i.e. by comparing with the CAD model). The algorithm which is embedded with the processing unit will make the decision about the forming path, considering the initial pre-defined contour path, current contour of the sheet metal and the final contour to be achieved. Once the error has been rectified, the usual process is continued until the final shape has been achieved.

### **The implemented process**

The research was aimed at implementing the ideal strategy, however, only a part of the strategy was implemented as shown in Fig 28 due to constraints in time and resources.

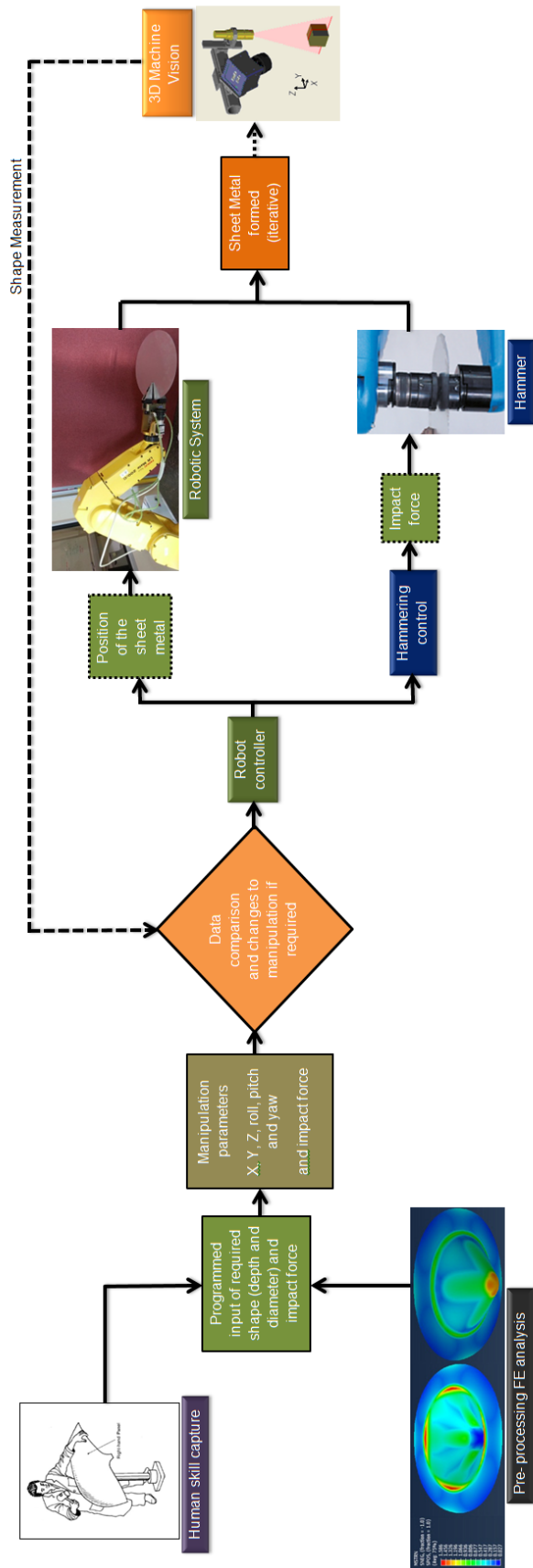


**Fig 28 - Mechatroforming – Implemented forming strategy**

In the implemented strategy, the knowledge of FE analysis and humans skills captured was used to program the forming path and pattern to be fed into the robot controller for sheet metal manipulation. The required force for forming was also analysed based on FEA to be fed into the hammering control. The hammering sequence was synchronised with the sheet metal manipulation by controlling the hammer using the robot controller.

The 3D shape measurement system was implemented to measure the shape of the sheet metal being formed in-between the iterations of the forming process. The shape of the sheet metal formed was compared with the dimensions of the original shape parameters programed as input. On comparison, the error in forming relative to the final shape required was found and used for rectification. However, the rectification algorithm was not implemented in the automated process. Instead, rectification was performed manually and fed into the program for the next iteration to enhance the shape being formed to achieve the required contour.

### **3.3 Control system for Mechatroforming**

The skills observed from manual operator are interpreted as system parameters and provided as input. These system parameters include: (a) Clearance between the surface of forming and surface where the sheet metal is held, (b) Force of the hammer required to form the contour, (c) Pattern and path in which the required shape could be easily achieved, (d) Space in between the impacts to achieve the required contour, and (e) Co-ordinate points according to which the sheet will have to be moved and skewed.

The forming process was simulated using FEA and used for pre-processing analysis. The magnitude of force required to achieve the required contour was predicted based on the FEA modelling and instrumented hammer measurements. The path, pattern, forming dimensions (depth, diameter and angle) and force were then programed to be fed as input to the robot controller to initiate the iterations in forming the sheet metal.

Based on the iterations, the robot controller manipulates the robot to locate the sheet metal in the required position and orientation between hammer and the support. The robot controller and the hammering control were integrated to communicate the input parameters. This allowed the robot controller (Master) to feed the required magnitude of force into the hammering control (Slave) for forming the sheet metal to the required contour as shown in Fig 29.

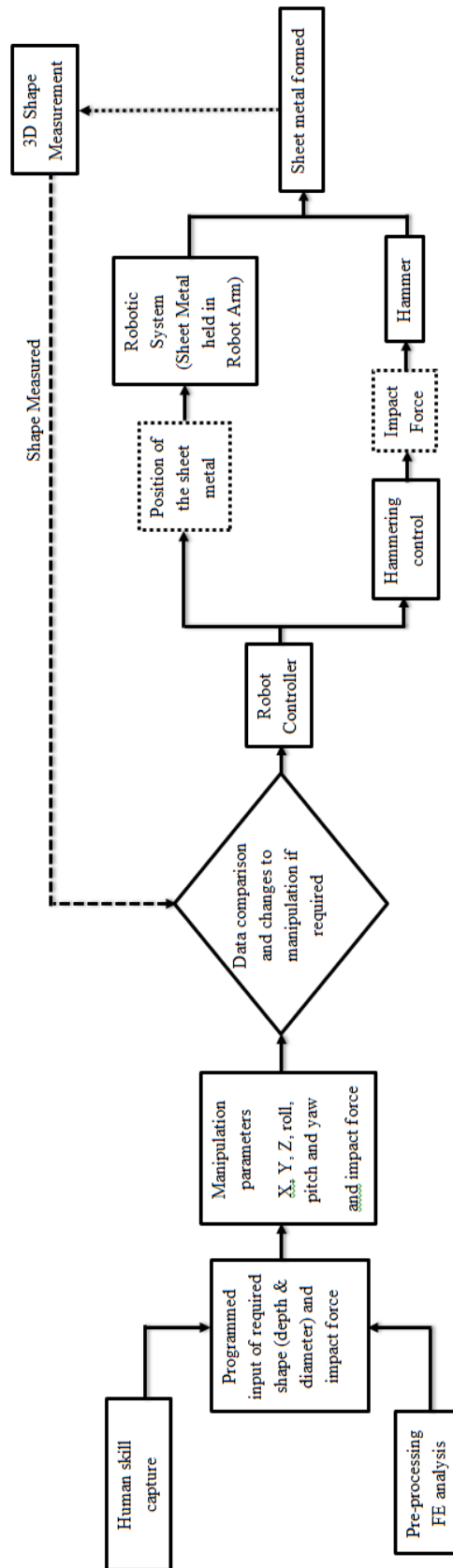


Fig 29 – Control system for Mechatroforming (implemented)

On completion of each iteration, the 3D shape measurement system scans the sheet metal to create a point cloud data with depth and shape information about the formed contours. The point cloud data is then fed back into the control system to be compared with the desired contour which is usually a CAD model of the final shape required.

With the existing arrangement of the prototype system as shown in Fig 29, it is rather a time-consuming process to scan the part after moving it away from the hammering unit. However, it is anticipated that the process is optimised to be faster by refining the forming strategy based on the shape measurement and the calculated depth/ diameter after each iteration.

The iterations continue until the desired shape of the sheet metal is achieved as compared to CAD model of the same.

### 3.4 Research challenges

The literature review, observation of the manual forming process, and a number of initial experiments indicate a number of challenges in developing the proposed forming solution. These include understanding forming techniques and predicting the material deformation, in addition to the technological challenges to build the proposed automated system. Fig 30 illustrates some of the forming parameters that have to be monitored and controlled which are discussed in the following sections.

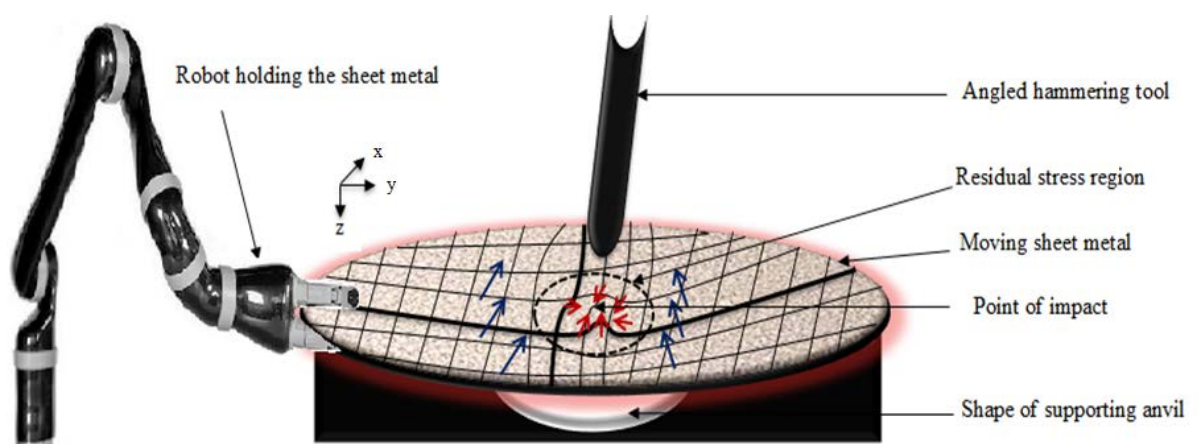


**Fig 30 - Research challenges**

The robot manipulates the sheet metal to locate it in the required position and orientate between the hammer and the support. The sheet metal will have to be moved along the



XY plane (horizontal plane) and skewed about the X or Y axis according to the shape required to be formed.

#### **3.4.1 Learning from a skilled operator**

The primary challenge in this process was to learn the manual process from skilled operators and apply it to the automated solution. Training was undergone to observe, perform and completely understand the forming parameters that are significant from a skilled operator's perspective. The techniques learned have been briefed in Section 2.3.1 and a detailed document on the training is provided in Appendix 1. The key skills observed from a skilled operator have been transformed into parametric solutions to be given as input to the automated system. The transformation of human skills is discussed in detail in Chapter 6.

However, it was understood that some of the manual operations are habitual and are developed over years by skilled operators. These may not be necessarily essential for an automated solution. For instance, hammering in angle is commonly used to achieve the required shape in a manual process. An angled tool introduces substantial computational restraints for modelling and prediction of the deformations, therefore, the angular motion of the hammer is eliminated in the proposed automated solution.

#### **3.4.2 Impact force and energy required for sheet metal forming**

Based on the traditional manual forming skills observed, it was noted that a varied energy and impact force are involved in sheet metal forming. As discussed earlier in Section 2.2, the energy delivered does not necessarily form the sheet metal, as it may be lost in just deforming the material. It is vital to analyse the impact force and energy involved in sheet metal forming. Therefore, the measurement of the impact force and kinetic energy involved in panel beating of sheet metal was carried out using an instrumented mallet and high speed video to capture data during manual hammering tests conducted in a structured laboratory environment. The experimental analysis performed and the test artefact used is discussed in detail in Chapter 4.

#### **3.4.3 Gripping the sheet metal**

The primary control characteristic of Mechatroforming is to grip the sheet metal by means of a robotic gripper. Adaptability of the gripper is essential to adjust relative to the continuously changing contour. The gripper and robot will have to bear the

oscillation or vibration caused due to dynamic impact. Failing to damp will affect the gripper as well as dissipation of kinetic energy in the sheet metal. Damping will also provide the required compliance in the gripper to adapt relative to the impact force. Therefore, a damper is provided at the intersection of the gripper and the sheet metal which is discussed in Section 7.6.2. Damping is applied by using a medium soft gripping material. The gripper finger design was also designed appropriately such that it could provide the required compliance and also applies the force required for gripping the sheet metal.

#### **3.4.4 Manipulating the sheet metal**

The robot manipulates the sheet metal to locate it in the required position and orientation between the hammer and the support. The sheet metal will have to be moved along the XY plane and skewed about the X or Y axis (refer to Fig 30) according to the necessity. This technique is inferred from the manual panel beating method and provides higher formability.

Though skewing the sheet provides a better control, sometimes angled tooling will be required to achieve the required shape. As the angled tooling introduces computational complexity, this is also provided by orientation of parts. If the sheet is not skewed to an appropriate angle, all the energy dissipated might go into deforming the sheet metal rather than shaping it to required contour. The transformation of manipulation and skewing skills into the automated system is discussed in Section 7.4 and the implementation of manipulation and skewing techniques has been discussed in Sec. 8.4.

#### **3.4.5 Size and shape of the support**

Designing the size and shape of the support is important to determine the deformation achieved as it has a direct influence on the impact force applied on the sheet metal. Through experimentation, it is anticipated that by reducing the size of support, the deformation achieved will be more predictable and the shape of deformation can be well defined as the region of reaction force will be reduced. The significance of size and shape of the support is discussed in Section 8.6.

#### **3.4.6 Effect of residual stresses**

Soon after an impact, residual stresses get developed around the point of impact. These residual stresses cause changes to the material properties as discussed in section 2.2.

The sheet metal will need to be analysed both locally and globally before making the next impact as it is sensitive to the residual stress region and will have consecutive effect in forming the sheet metal. It is difficult to feedback the material properties of the sheet metal after each impact in real time. This requires high computations and a longer time duration which is commercially not viable. Therefore, the monitoring process should be carried out frequently - in accordance with the system's computational processing power. This was also experienced through the manual panel beating and applied using the system's parameters. However, finite element analysis was performed to determine the impact force in a simulated environment. The analysis was performed to develop confidence in the finite element analysis to be used as a prediction tool that could predict consecutive impact points based on residual stress. The determination of impact force using FEA is discussed in detail in Chapter 5.

### **3.5 Research plan to develop Mechatroforming**

The development of Mechatroforming was based on a number of laboratory experiments to determine the process parameters involved in sheet metal forming. The research was developed in three key stages. These consist of human skill capture, which involves understanding human skills and calculating the impact force using an instrumented hammer, developing a semi-automated system and a fully automated system. The research plan is illustrated in Fig 31.

Initially, experimental studies were carried out to understand the energy involved in the sheet metal forming. The impact force involved in sheet metal forming was determined using an instrumented hammer. Simultaneously, impact force was also determined theoretically by decomposing the hammering motion captured from the high speed camera. The time-based analysis also helped to determine the kinetic energy involved in sheet metal forming. Furthermore, impact force was also predicted using Finite Element Analysis (FEA) in a simulation environment recreated to emulate the experimental environment. The analysis was useful to gain confidence to be able to use FEA as a prediction model in the future control system.

On determining the impact force involved in the sheet metal forming, the hammering machine essential to produce the required impact force in the automated panel forming system that was selected. An automated system was designed and developed,

constructing on the proposed methodology. The experimental artefact to be tested in the automated system for a proof of concept was determined.

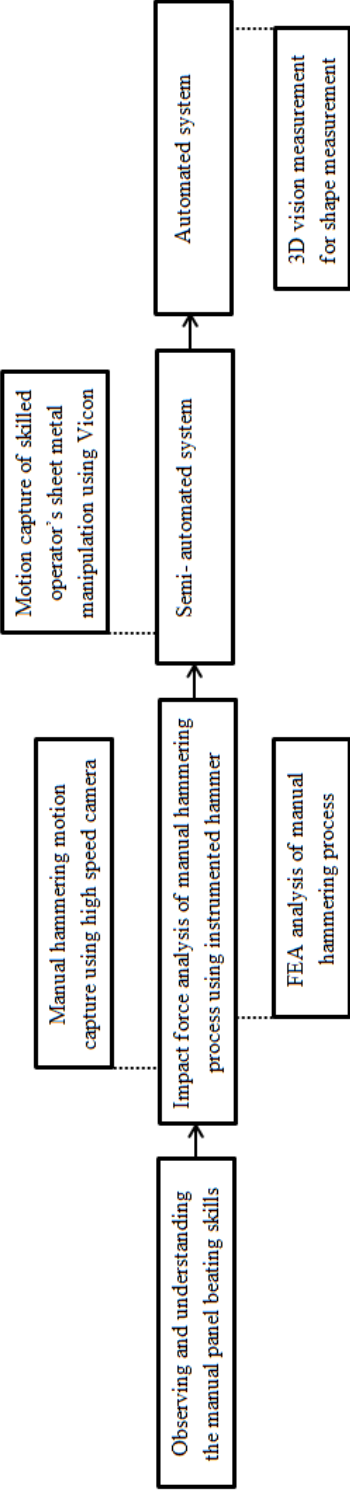


**Fig 31 - Research plan**

Based on the traditional panel forming skills observed, the significant human skills involved in sheet metal forming were categorised. The human skills were transformed into a parametric solution that could be provided as input to the automated system. The skilled operator's skills on pattern and paths involved in sheet metal forming were tested in a semi-automated environment utilising the hammering machine. Motion capture technology was used to track the skilled operator's manipulation techniques and the best pattern and paths for forming the target artefact. On understanding the flexibility required in sheet metal manipulation, the human skilled operator was replaced by a multi-axis robot. The gripping unit, with the specifically designed finger, along with the required damping, compliance was integrated into the robot to grip the sheet metal.

The parametric solutions were provided as input to the hammering machine and the robot, to execute the sheet metal forming in the fully automated system. The hammering machine and the robot were synchronised to automatically form the sheet metal to achieve the required quality. A path planning algorithm was developed to form the target artefact and several modifications were done on the algorithm to optimise the forming strategy.

A 3D vision measurement system was installed to monitor the sheet metal forming. The 3D vision system using laser triangulation principle was used in-line off-process to scan the sheet metal being formed. The shape and features detected were converted into a point cloud data using a code developed in the Halcon image processing software [81]. Analyses on the point cloud data were carried out using Matlab and an envisioned path modification is presented.

Due to the computational complexity involved, the in-process impact force prediction based on FEA was not implemented. The hammering machine was operated at optimum impact force, thus, eliminating the requirements for impact force feedback using force sensor.

## 4. Modelling and analysis of the manual sheet metal deformation process

---

### 4.1 Introduction

This research was initiated by understanding the manual deformation process. As discussed in Section 2.3.1, the author was trained by professional panel beaters and gained the skill required to form simple sheet metal parts through incremental deformation.

The first stage of this research was aimed at measuring the main parameters of the deformation process for the artefact used in this research. In parallel, a FEA modelling approach was taken to support and predict the deformation.

A number of laboratory tests were carried out to study the deformation of sheet metal parts through the proposed approach. The objectives of the experiments were:

- to find the required hammering weight and velocity and to calculate the kinetic energy using a high speed camera, hence, determining the impact force required
- to determine the impact force in real-time using an instrumented hammer (i.e. a hammer equipped with a load cell)
- to develop a FEA model of the previous experiments in order to determine the impact force using finite element analysis
- to compare the results of impact force achieved using the above said experiments and to validate the measured parameters, so that FEA can confidently be used for material flow prediction

It was understood that incremental deformation achieved on the sheet metal, relative to the impact force, will have to be determined in terms of kinetic energy applied within a short period of time (i.e. the impact time). Therefore, it was necessary to perform a time-based analysis to find the kinetic energy required for deforming the sheet metal during each impact. This was measured in an experimental manual hammering while recording the process using a high speed camera. This analysis was also necessary to develop a system to set the frequency of impacts based on the duration of impact.

It was also necessary to validate the theoretical findings as the impact occurs over a very short duration of about 0.2 seconds. Therefore, an instrumented hammer with an embedded force transducer was used to measure the impact force in this test.

Experiments were carried out using the high speed camera and the instrumented hammer. As the deformation achieved would be same, the impact force determined in each case could be compared for validation.

The FEA model was developed to provide pre-processing analysis to determine the impact force based on the deformation that should be achieved similar to the previous experimental method. The objective was to ensure that FEA results align with the results achieved using time-based analysis and the instrumented hammer. In which case, FEA could be used to simulate the process and predict the forming at each contour monitoring stage, combined with the analysis obtained from 3D shape measurement system.

#### 4.2 Specification of the experiments

Both experiments of the high speed camera and instrumented hammer were performed using the same experimental set-up, so that the experiments can be performed simultaneously and confidently compared. The experimental set-up is shown in Fig 32.



**Fig 32 - Experimental set-up**

The experimental set-up includes a high speed camera set-up and an instrumented hammer set-up, which are explained in Sections 4.4.1 and 4.5.2 respectively.

Investigations were carried out to select the suitable material for experiments. Steel and aluminium discs were tested to be used for the impact force determination experiments. The material properties of both materials were studied and their formability was determined by using test pieces. Comparing both, aluminium was found to be easily formable for the relatively limited equipment available in the lab.

Therefore, all the experiments were performed on aluminium of 1 mm thickness and 275 mm diameter. The sheet was held in circular wooden block, hollow at its centre to about 135 mm diameter as shown in Fig 33. In the case of FEA, a nearly similar set-up was made virtually. This support was chosen to be similar to those used during the manual processes (traditional manual forming) to minimise the test variability. However, a smaller size support is used in the automated process as discussed in 3.4.5.



**Fig 33 - Support used for initial experimental studies**

The cross-sectional view of the impact applied on the aluminium test piece held on the support is shown in Fig 34.

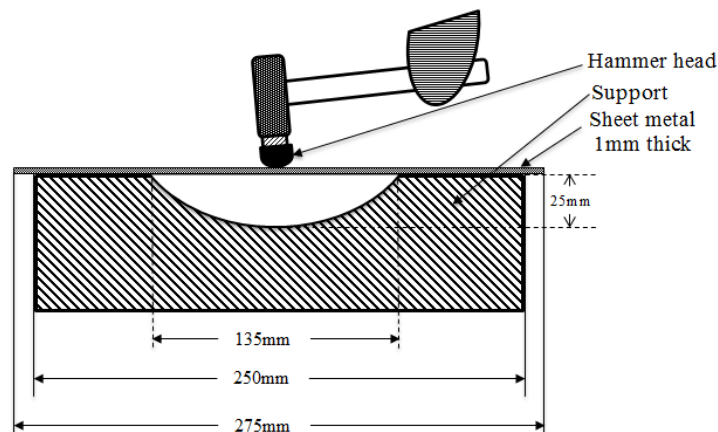


**Fig 34 - Cross-sectional view of impact applied on the aluminium test piece**



#### **4.3 Experiment 1 – Measuring the impact velocity using a high speed camera and wooden hammer**

Initially a steel plate of 1 mm thickness was impacted using a wooden hammer of 0.42 Kg from a height of 0.8 m. These values were chosen to be close to the manual panel beating practices. A high speed camera was used to record the motion and hence the velocity of the hammer.

A calibration grid (5 x 5 cm – Black & White grids 0.80 m high), as shown in Fig 32, was placed in the background. This was in close proximity to the hammering action, so that the motion of the hammer could be framed using the high speed camera at 200 fps (frames per second) and also at 400 fps.

The high speed camera was tested for both 200 fps and 400 fps. The camera was triggered to capture the motion of the hammer. The hammer's motion was detected every 5 milliseconds and the distance travelled was also identified. The objective was to determine the distance travelled and the time taken at regular intervals. This enabled the calculation of the variable velocity and acceleration. Consequently, the impact velocity and force were calculated (the theoretical calculation is discussed in Section 4.4.2).

The results achieved were sporadic (2-6 KN force) and therefore not reliable, as the frame rate of the camera was not enough relative to the speed of hammer (discussed in Appendix 4). Therefore, it was found that a camera with a higher resolution and frame rate is required to detect the motion of the hammer with sufficient accuracy.

#### **4.4 Experiment 2 – Measuring the impact velocity using high speed camera and instrumented hammer**

Following the unsatisfactory results from the last experiment, the second experiment was performed using a higher resolution camera and an instrumented hammer with force sensor. However, it was understood that the consistency of the manual hammering is essential both in terms of speed and angle of impact. A ball dropping mechanism was considered to be used instead of a hammer, but was soon realised to be

impractical<sup>1</sup>. Therefore, multiple tests were performed and the results' average was used to minimise the inconsistency that may occur in manual hammering.

#### 4.4.1 High speed camera set-up

A Fastcam ultima APX high speed camera (black & white – 2 GB high definition data at 1000 fps) was connected to a frame grabbing unit and the frame grabbing unit was connected to a the laptop running PFV software which triggers and captures the image data. This is illustrated in Fig 35.

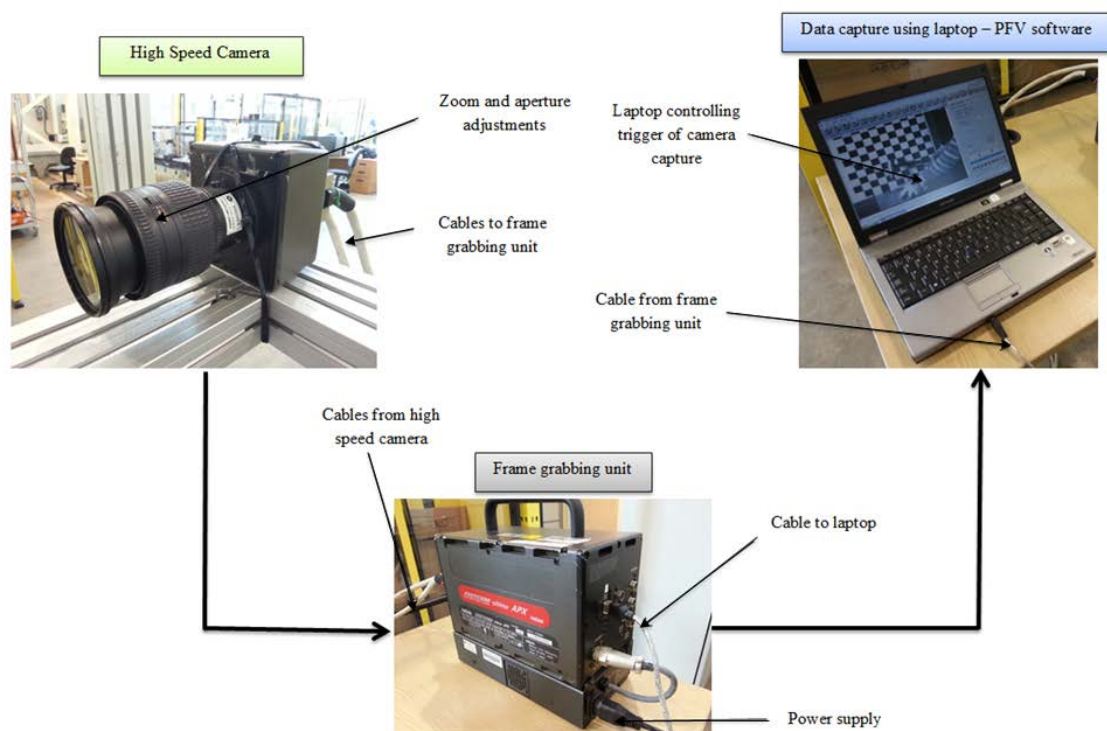


**Fig 35 – High speed camera set-up**

To capture the action of hammer using a high speed camera, a 5 x 5 cm black and white grid, lines separated by a 2.5 cm dotted line along the length and breadth was used (as shown in Fig 32). The grid lines were 0.80 m high to ensure the measurements were made from start point of the hammer till the datum point of impact. If initial hammer action cannot be read, some initial velocity involved in creating impact force will be missed in the measurement. This loss of data can cause measurement issues. To ensure

<sup>1</sup> Experiment 1 showed that the impact force will be in range of 2000 N and 6000 N. For a ball dropping mechanism to generate 2KN force, a very large steel ball would have been required, or a very high dropping point. This was decided to be impractical due to the health and safety restrictions within the laboratory.

the accuracy of the measurements, the grid lines were focussed on by an 800 W flash light source (as shown in Fig 32) to ensure the lines were visible for diagnosis purposes.

The PFV software (provided by the camera's manufacturer as shown in Fig 36) connected to the frame grabbing unit had the ability to trigger the camera for capturing at 1000 frames per second. It produced a 2 GB data while capturing the action for 2 seconds. Each step in action could be measured frame by frame to detect the motion of hammer. For this experiment, the resolution was set to 1024 x 1024 PPI (pixel per inch) and the frame rate to 1000 fps.

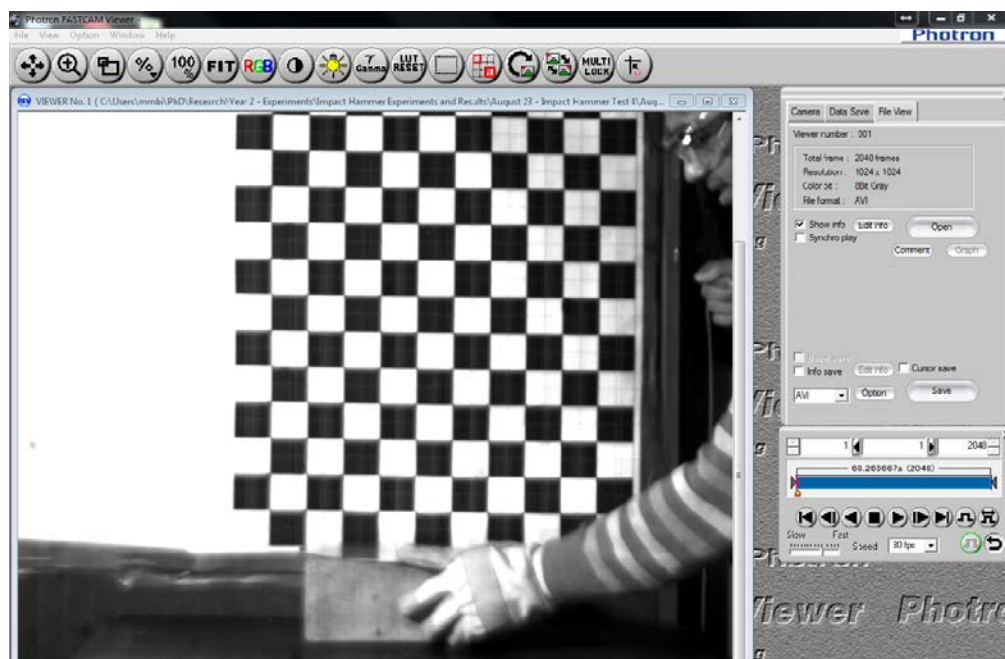


**Fig 36 – PFV software**

#### **4.4.2 Impact velocity measurement and the kinetic energy**

While impacting the sheet metal with impact hammer, time-based analysis was also carried out by using a high speed camera. With 5×5 cm black and white grid lines, 0.80 m high at the backdrop, the hammering action was captured at 1000 frames per second. A total of 33 data points were collected while the hammer moved from a 0.80 m distance to a 0.00 datum plane, where it impacted the sheet. These time and distance data were interpreted in Matlab software to find the fourth order polynomials. The formula used is given below:

$$P(x) = P_1 x^n + P_2 x^{n-1} + \dots + P_n x + P_{n+1} \quad \dots \text{(Equ 1) [82]}$$

Finds the coefficient of polynomial  $p(x)$  of degree  $n$ .

Since the motion of the hammer is accelerated, the velocity and acceleration of the hammer are variable with time. Hence, calculations were made based on time-dependent acceleration. The equations for calculations were based on:

$$\text{Position, } x(t) = x_0 + v_0 t + b \frac{t^2}{2} + c \frac{t^3}{6} + d \frac{t^4}{12} = x_0 + \int_0^t v \partial t \quad \dots \text{(Equ 2) [82]}$$

$$\text{Velocity, } \frac{\partial x}{\partial t} = v(t) = v_0 + bt + c \frac{t^2}{2} + d \frac{t^3}{3} = v_0 + \int_0^t a \partial t \quad \dots \text{(Equ 3) [82]}$$

$$\text{Acceleration, } \frac{\partial^2 x}{\partial t^2} = a(t) = b + ct + dt^2 \quad \dots \text{(Equ 4)}$$

[82]

Using (Equ 3) the impact velocity of the hammer at the point of impact could be found. The impact kinetic energy was found using the equation:

$$K.E = \frac{1}{2} mV^2 \quad \dots \text{(Equ 5)}$$

Where,  $m$  is the mass of the hammer used and  $V$  is the impact velocity of the hammer.

Fig 37 illustrates the kinetic energy delivered to the sheet metal.

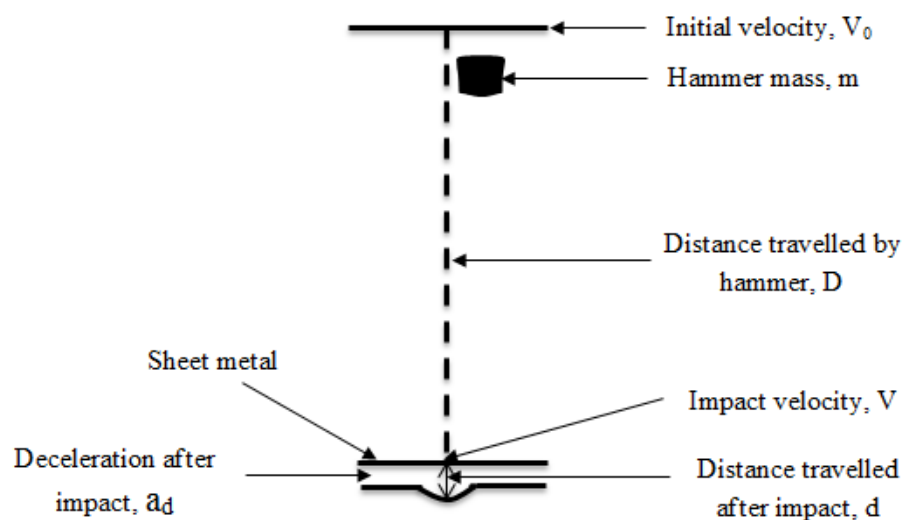


**Fig 37 - Theoretical calculation of impact force based on the impact velocity measured**

From the above illustration, it could be noted that kinetic energy K.E delivered to the sheet metal is directly proportional to the distance travelled by the hammer after impact,  $d$ . Energy lost by friction due to air and impact are negligible as they have very minor error factor compared to the larger impact force. The hammer's deceleration effect and material displacement effect have been neglected as energy delivery is not the prime scope of this research. The consistency of manual hammering was calibrated in advance by practicing a uniform hammering on different workpieces. Therefore, the direction of the impact was considered to be perpendicular to the surface of the work sheet.

Equating kinetic energy is equivalent to work done:

$$K.E = F \times d \quad \dots\dots (Equ 6)$$

The force,  $F$  calculated will be the impact force.

As the theory discussed above is applied in static loading, the theory behind the dynamic impacts was also studied. Based on the hertz theory of contact [83], there is some elastic energy transferred as vibration in the sheet metal during dynamic impact, it is necessary to find this vibrational energy to determine the actual kinetic energy spent in deforming the sheet metal. Calculation of vibrational energy is by means of pressure pulse and it depends on the Poisson's ratio and mass density of both the hammer and the sheet metal. Then the equation could be related as,

$$K.E - \text{Vibrational Energy} = F \times d \quad \dots\dots (Equ 7)$$

During experiments, the energy calculated in comparison to the deformation achieved suggested that vibrational energy has no significant influence on the energy delivered if the sheet was held securely. Hence, the vibrational energy was considered to be negligible considering the scope of the experiments.

In addition, some of the data regarding the material mechanics generated by the FEA model was also considered to be beyond the scope of this experiment and therefore was disregarded. It was envisaged that such an assumption will have negligible impacts on the results of the experiments. The prime purpose was to develop a comparative time-

based analysis and it was proved that Equ 6 was adequate since the impact force was also measured in real time using an instrumented hammer.

Equating impact force “F” as the product of mass of the hammer “m” and deceleration after impact “ $a_d$ ”, deceleration after the impact can be found.

$$F = ma_d \quad \dots\dots \text{Equ (8)}$$

#### 4.5 Experiment 3 – Determining the impact force using instrumented hammer

Recreating the 2000N impact force (refer section 4.3) using the instrumented impact hammer also proved to be challenging. Initially investigations were made to embed a force transducer in the wooden hammer used for testing. This idea was proved to be impractical. Hence, a commercial impact hammer was purchased<sup>2</sup> equipped with impact force transducer.

The instrumented impact hammer (shown in Fig 38) was equipped with a force transducer just above the impacting material.

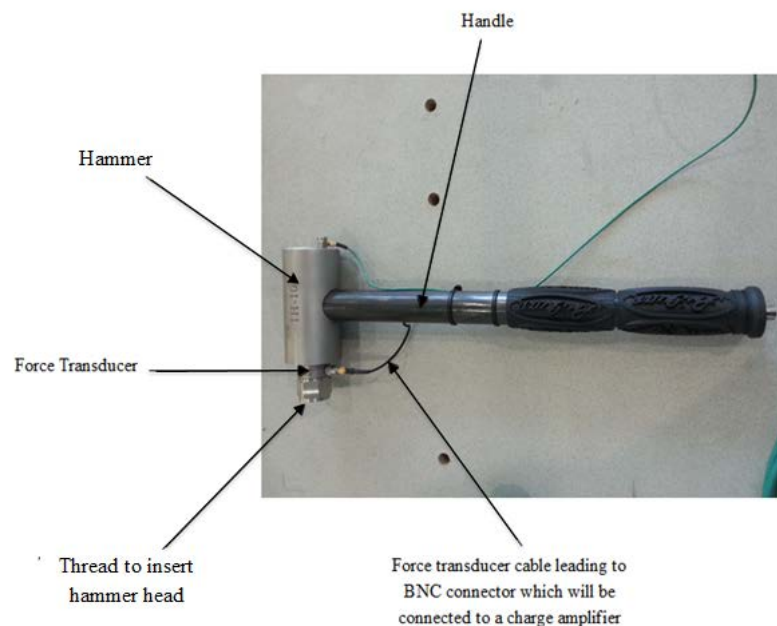


**Fig 38 - IH-10 instrumented hammer**

---

<sup>2</sup> There are only very few commercial products available for impact force measurement and the need to recreate the 2000 N impact force meant that the hammer should have higher mass. Therefore, “IH-10” range instrumented impact hammer by DJB instruments [84] was selected, weighing 1 Kg with ability to measure up to 10000 N.

The force transducer changes the mechanical energy into an equivalent voltage pulse which is measured using an amplification unit and a pulse measuring instrument such as oscilloscope (set-up is discussed in Section 4.5.2). Measuring the voltage pulse will lead to the calculation of impact force as the sensitivity of the force transducer is known as  $0.499 \text{ mVN}^{-1}$ . The data sheet of the instrumented hammer is provided in Appendix 5.

The difference between using a large weighing ball for experiment and just a 1 Kg instrumented hammer has been carefully analysed. The ball drop occurs due to a gravitational force, but the impacting action of instrumented hammer occurs by accelerating the hammer. As discussed in section 2.3, the change in acceleration due to the distance between the pivot of the hammer and holding point of the handle makes the difference in creating a larger impact force when compared to a ball drop. The handle length of the “IH-10” impact hammer is 370 mm and the hammer has a 50 mm diameter.

Hence, it was decided that the hammering action was very important - as the hammering action will have to be repetitive in order to have consistency in the results achieved. The hammering motion is usually made between the operator’s head and hip. The datum plane alongside the hip is considered to be an appropriate position to hit with the maximum force (that can be applied pertaining to the action performed). Hence, the support was held at the operator’s hip height. From the hip, the height to operator’s head was measured to be 0.80 m (as shown in Fig 32). Therefore, all the hammering actions were standardised to make an impact after travelling 0.80 m. The operator was able to have a consistent hammering action as he had undergone training in sheet metal forming.

#### **4.5.1 Selection of hammer head to be mounted on the hammer**

The hammer head’s material was understood to have influence in the forming process through friction, vibration, and its elastic deformation.

Three different materials were tested to be mounted on the hammer. They include steel, softer plastic and harder plastic. It was understood that a balance has to be reached in selection of material in order to achieve the necessary deformation and required damping. Using steel was inappropriate as it caused large vibration and a significant

noise in the measured data. Softer plastic was also inappropriate as it did not create the expected deformation due to its own elastic deformation.

Tests made using harder plastic created the expected deformation and the vibration was minimised in comparison with steel. The different types of hammer head are as shown in what Fig 39. Hence, harder plastic was decided to be used as the hammer head for the experimental purposes.

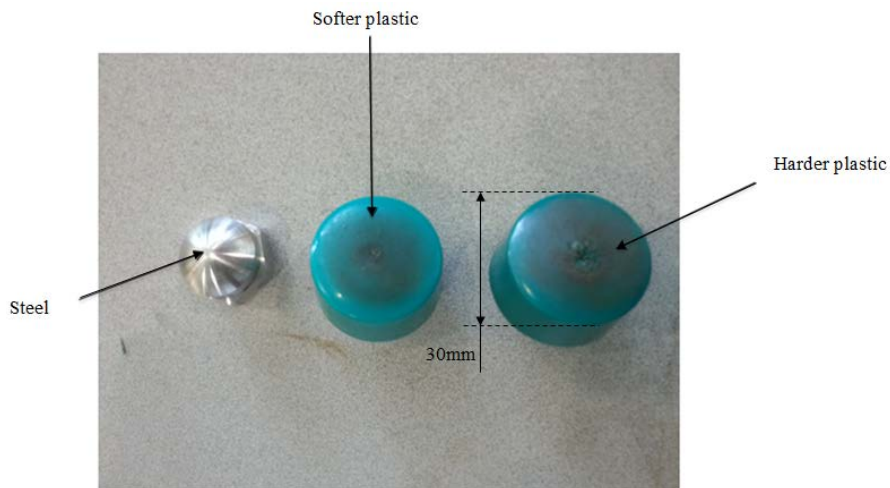


**Fig 39 - Hammer head material types**

#### **4.5.2 Instrumented hammer set-up**

The instrumented hammer “IH-10” was set up using the following:

- Integrated Chip (IC) voltage source amplifier
- Four channel digital storage oscilloscope TDS 2014
- BNC connectors
- Accelerometers

The force transducer of instrumented hammer was connected to the IC voltage source amplifier using BNC connectors. The IC voltage source amplifier strengthens the signal and sends it to the oscilloscope using BNC connectors. The IC voltage source amplifier has only a single input/output BNC lead as shown in Fig 40. Therefore, multiple IC voltage source amplifiers were used to acquire different outputs as shown in Fig 41.





**Fig 40 - IC with BNC connections in working mode**



**Fig 41 - Instrumented hammer set-up**

The accelerometers were used to validate the results of force transducer and also to validate the acceleration calculated by determining the velocity of hammer from a high speed camera. For this purpose, accelerometers were mounted on top of the hammer (shown in Fig 42) and also on the surface of the sheet metal to be impacted (shown in Fig 43).

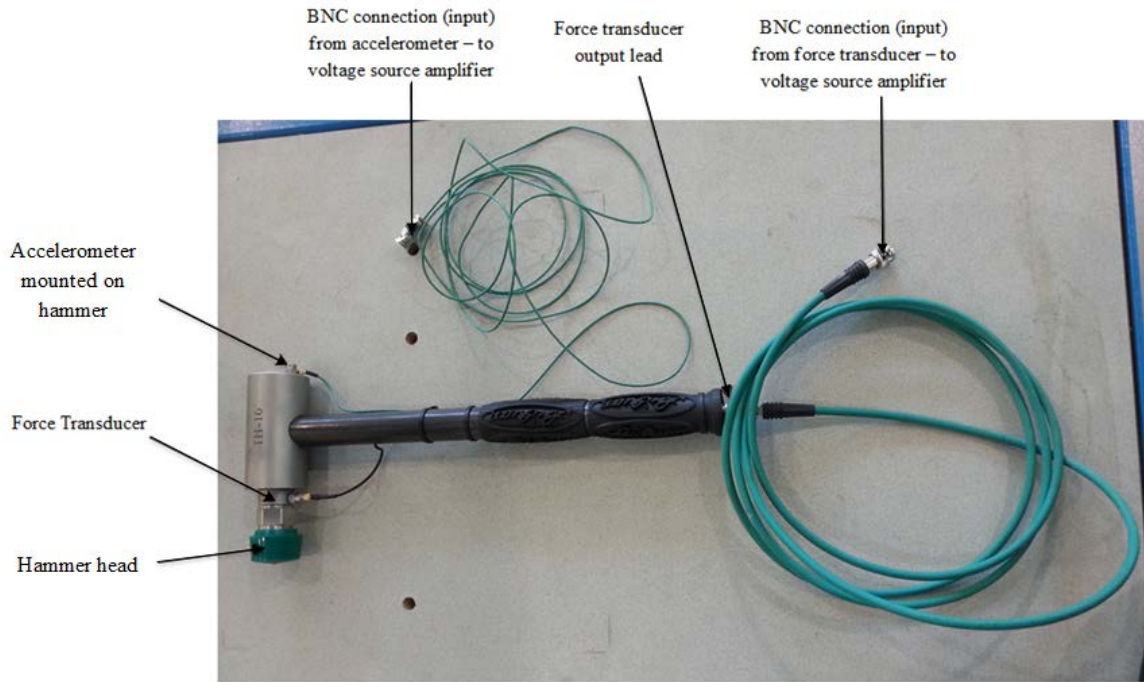


**Fig 42 – Accelerator mounted upon impact hammer**

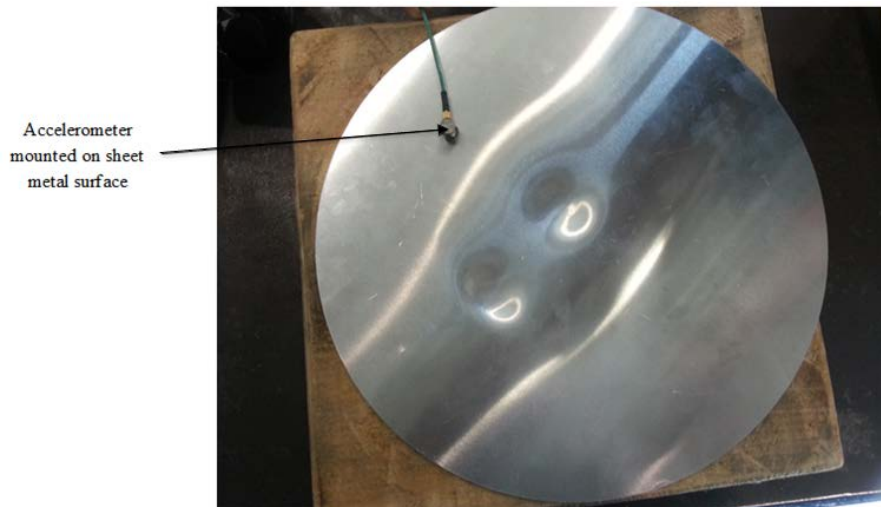


**Fig 43 - Accelerator mounted on the sheet metal surface**

The acceleration results of the accelerometer were corresponding to the impact force results of the force transducer. Also, the acceleration results, determined using the accelerometer, coincided with the acceleration results calculated using the velocity which was determined from the high speed camera. This validation was important to perform the experiments concurrently and compare their results.

The accelerometers were connected to the voltage source amplifier and then to the oscilloscope to measure the output. The connections were made using BNC connectors as shown in Fig 41. From the measured output voltage, the acceleration was calculated to be  $34.5 \text{ ms}^{-2}$  on the accelerometer mounted on top of the hammer. The acceleration measurement was exactly the opposite on the accelerometer mounted on the surface of the sheet metal. The results validated the experimental calculations of impact force using the instrumented hammer.

### 4.5.3 Impact force calculation using instrumented hammer

The force transducer of the instrumented hammer measures the impact force as a voltage signal under time. The sensitivity of impact hammer is  $0.499 \text{ mVN}^{-1}$ . So, knowing the voltage signal (V) after impact, impact force (N) can be calculated as:

$$\text{Impact Force, } F = \frac{V}{0.499 \text{ mVN}^{-1}} \quad (10^3 \text{ N}) \quad \dots\text{Equ (9)}$$

While measuring the voltage signal in oscilloscope, the peak signal has to be selected in order to calculate the maximum impact force imparted to the sheet metal in deforming it.

## 4.6 Experimental results

The hammering test was performed using the instrumented hammer to measure the actual impact force applied on to the sheet metal. At the same time, the high speed camera was triggered to capture the hammering action to measure the velocity based on time and distance to calculate the kinetic energy, hence the impact force. The experiments were performed concurrently to compare and validate their results.

Several experiments were conducted, of which four sets of experiments accounted for the comparison between different experimental methods. Amongst those, only two experimental data were adequate for analysis purposes. These experiments are discussed below.

### 4.6.1 Experiment 1

The set-up was similar to the one discussed in section 4.2 and the impact hammer of mass 1 kg was used to impact the sheet metal (refer Fig 37). The hammer travelled 0.212 sec (t) for a distance of 0.8065 m (D+d) producing a deformation with depth (d)

of 0.0065 m as shown in Fig 44. The impact velocity of the hammer was determined by the high speed camera and was calculated using Equ (3) as  $7.17 \text{ ms}^{-1}$ . The impact kinetic energy was calculated using Equ (5) as 25.70 J. The impact force was calculated using Equ (6) as 3954.5 N.



**Fig 44 - Sheet deformation - Experiment 1**

Similarly, using the impact hammer, a voltage of 2.08 V (refer Fig 45) was measured upon impact. Calculating the impact force based on the sensitivity of  $0.499 \text{ mVN}^{-1}$  using Equ (9), the impact force was calculated as 4168 N.

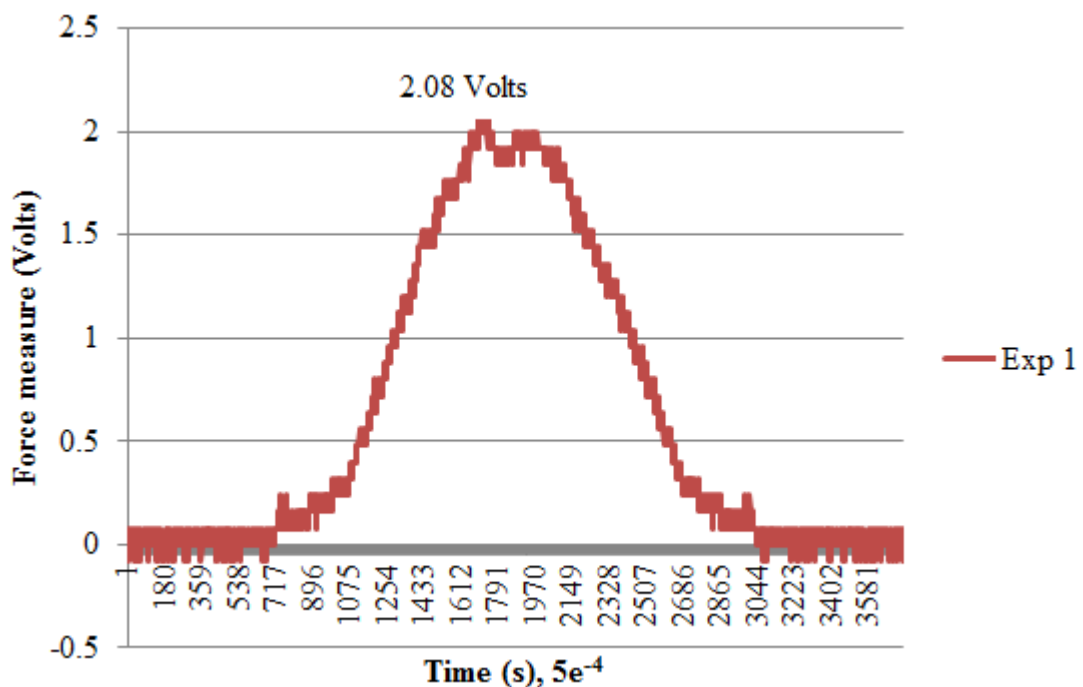


**Fig 45 - Experiment 1 - Instrumented hammer data**

#### 4.6.2 Experiment 2

The set-up was similar to the one discussed in Section 4.2, and the impact hammer of mass 1 kg was used to impact the sheet metal. The hammer travelled 0.210 sec (t) for a distance of 0.8037 m (D+d) producing a deformation, d of 0.0037 m as shown in Fig 46. The impact velocity of the hammer was determined by the high speed camera and was calculated using Equ (3) as  $6.02 \text{ ms}^{-1}$ . The impact kinetic energy was calculated using Equ (5) as 18.1 J. The impact force was calculated using Equ (6) as 4897.35 N.



Fig 46 - Sheet deformation - Experiment 2

Similarly, using the impact hammer, a voltage of 2.64 V (refer Fig 47) was measured upon impact. Calculating the impact force based on the sensitivity of  $0.499 \text{ mVN}^{-1}$  using Equ (9), the impact force was calculated as 5290.5 N.

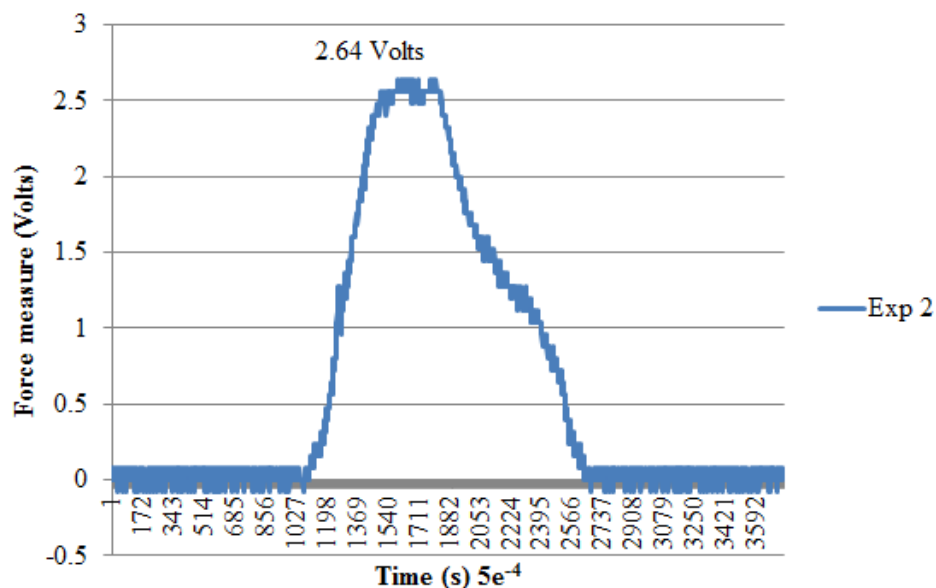


Fig 47 - Experiment 2 - Instrumented hammer data

### 4.6.3 Summary of results

The impact velocity was measured using the high speed camera and the kinetic energy and impact force involved were calculated. The impact force was also measured using an instrumented hammer. The results obtained in the two experiments are summarised below in Table 1.

Experiment No.	Time travelled by hammer (s)	Distance travelled by hammer (D+d) (m)	Deformation achieved (d) (m)	Instrumented impact hammer results		High speed camera results		
				Measured Voltage* (V)	Impact Force** (N)	Impact Velocity* (ms <sup>-1</sup> )	Kinetic Energy* (J)	Impact Force* (N)
1	0.212	0.8065	0.0065	2.08 (refer Fig 45)	4168	7.17	25.70	3954.5
2	0.210	0.8037	0.0037	2.64 (refer Fig 47)	5290.5	6.02	18.1	4897.35

Note: \*denotes measured values, \*\*denotes calculated values

**Table 1 - Summary of experimental results**

Comparing experiments 1 & 2 (refer to Table 1), the impact force applied in experiment 1 is less than the impact force produced in experiment 2, but the deformation produced is larger in experiment 1 when compared to experiment 2. This is because deformation depends on the impact kinetic energy. Higher impact kinetic energy produces larger deformation (experiment 1), similarly, smaller impact kinetic energy produces smaller deformation (experiment 2). This can also be observed from the area under curve of the voltage measured for experiments 1 & 2. By inspection, the area under the curve for experiment 1 is larger than the area under the curve for experiment 2, suggesting that a higher impact kinetic energy produces higher deformation and vice-versa. However, the impact force applied depends on angular contact with the surface of the support based on the support's size and shape (refer Fig 34).

The impact force required for the sheet metal forming was determined as 5KN (average impact force based on the experiments) using the above discussed experiments.

Subsequently, impact force was also determined using finite element analysis which is discussed in Chapter 5.



## 5. Modelling deformation through FEA

### 5.1 Introduction

The FEA modelling was used to predict the impact velocity and impact force involved in the sheet metal forming. The main objective was to validate the results on comparison with the results obtained in experimental analysis. Achieving which, FEA could be confidently used for predicting the incremental forming of parts.

The FEA modelling was performed using MSC MARC software [85] as it was understood to be an efficient software in determining time-based dynamic impacts. In addition, it was the software application available to this research. The FE analysis was carried out for the same set of data as used in the previous manual experiments. All the material properties were specified in the simulation model using the pre-defined parameters defined by the software. The dimensions of the sheet and the hammer were given relatively as FEA is a dimensionless modelling system. The dimensioning was given using the standards values as given in Table 2.

Quantity	SI	mm/tonne/s/K or SI-mm	Imperial	US Common
Length	m	mm	in	in
Time	s	s	s	s
Mass	kg	tonne Mg	lbf-s <sup>2</sup> /in	pound (lb)
Force	kg-m/s <sup>2</sup> N	tonne-mm/s <sup>2</sup> N	lbf	pound force (lbf)
Density	kg/m <sup>3</sup>	tonne/mm <sup>3</sup> Mg/mm <sup>3</sup>	lbf-s <sup>2</sup> /in <sup>4</sup>	lb/in <sup>3</sup>
Stress	kg/m/s <sup>2</sup> N/m <sup>2</sup>	tonne/mm/s <sup>2</sup> MPa or N/mm <sup>2</sup>	lbf/in <sup>2</sup>	p.s.i.
Energy	kg-m <sup>2</sup> /s <sup>2</sup> J	tonne-mm <sup>2</sup> /s <sup>2</sup> MJ or N-mm	lbf-in	lbf-in
Temperature	°K	°C	°R	°F
Spec. Heat Capacity	m <sup>2</sup> /s <sup>2</sup> /°K J/kg/°C	mm <sup>2</sup> /s <sup>2</sup> /°C	in <sup>2</sup> /s <sup>2</sup> /°R	Btu/lb/°F
Heat Convection	kg/s <sup>3</sup> /°K W/m <sup>2</sup> /°C	tonne/s <sup>3</sup> /°C N/s/°K/mm	lbf/in/s/°R	Btu/in <sup>2</sup> /s/°F
Thermal Conductivity	kg-m/s <sup>3</sup> /°K W/m/°C	tonne-mm/s <sup>3</sup> /°C N/s/°K	lbf/s/°R	Btu/in/s/°F
Thermal Expansion	m/m/°K	mm/mm/°C	in/in/°R	in/in/°F

**Table 2 - FEA dimensioning standards**

## 5.2 FEA modelling of aluminium workpiece

Initially, a surface was created with 275 mm diameter, similar to the disc used in manual experiments. The surface was then meshed to create elements in order to perform detailed analysis. It was understood that quad mesh is the meshing most appropriate for the required experimental purposes as the model is developed using solid shell elements (discussed in section 5.2). Therefore, the surface was meshed using quad mesh. Therefore, 50 elements and 101 nodes were formed. As the sheet metal was 1mm thick, the surface created was converted to a 3D structure by raising it 1 mm in the Z-axis. This formed 100 elements and 202 nodes for a 3D structure with 1mm thickness and 275 mm diameter as shown in Fig 48.

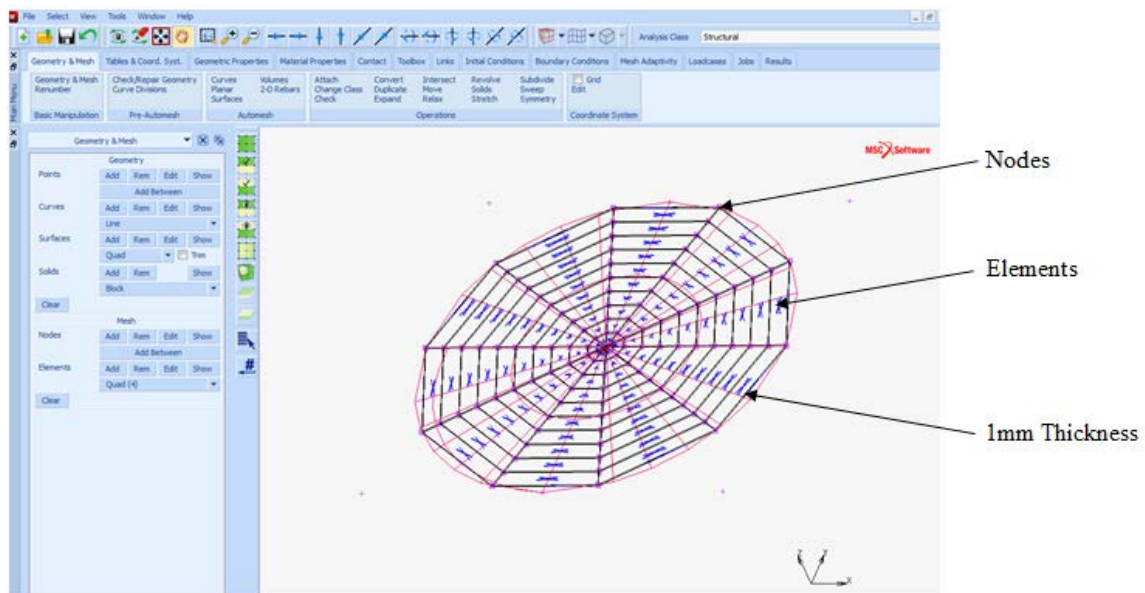


**Fig 48 - Quad meshed 3D structure**

In finite element analysis, it is necessary to identify the geometrical type of 3D-structure for the purpose of analysis. There are different types of elements such as solid element, shell element and solid shell element. The solid elements have complicated analysis and are prone to long time analysis but are very accurate. The shell elements are easier to analyse and are faster with less accuracy in comparison to solid elements. Due to the purpose of experiments, it was understood that both solid element analysis properties and shell element analysis properties are required. So, a combination of both was used in modelling which was provided by solid shell elements.



Once the geometrical element properties were defined, material properties were required to be specified. Material properties of aluminium such as Poisson's ratio (0.334), young's modulus (69), mass density (2700), and mass (0.19) were defined similar to aluminium used in manual experiments. The material was specified as elasto-plastic since the aluminium undergoes both elasticity and plasticity deformations. As the objective was to determine only the plastic deformation of the aluminium structure (workpiece), the rate of plasticity was specified for the aluminium structure from the pre-defined aluminium strain rate (for rate of plasticity) available in the MSC software. The plasticity had piecewise linear strain rate and an isotropic hardening rule (discussed in section 2.2). It was also defined that the material thickness should be updated after plastic strain in order to measure the thickness after each impact.

### 5.3 FEA modelling of the hammer

After the material properties were defined as aluminium, the next step was to make a structure similar to the hammer, to impact the aluminium structure. As the impact material used in manual experiments had curvature towards the impacting side, the hammer was assumed to be a spherical structure for the purpose of FEA. Hence, a sphere with the same radius of curvature as the instrumented hammer's head was created. As the hammer was a non-deformable structure, the sphere was considered to be a rigid body in the FEA model.

Then, the rigid sphere (hammer) was placed 0.80 m above the aluminium structure (shown in Fig 49) similar to the manual process.

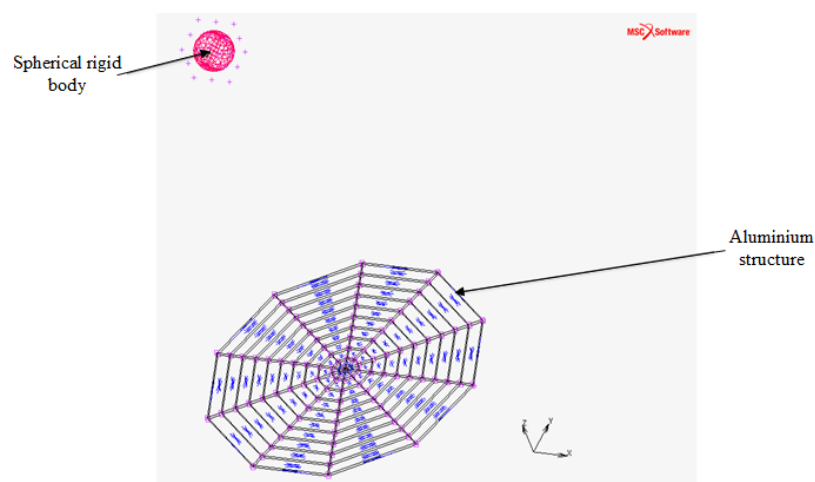


**Fig 49 - Rigid body placed 0.8 m above the aluminium structure**

## 5.4 Applying constraints

Once the sphere was placed at a height, it was important to have a support similar to the manual process. Hence, constraints are used to define support similar to the one used in manual process. The aluminium structure was constrained at 135 mm in a circular manner (shown in Fig 50 and Fig 51) to create a similar set up as in reality. In the experimental methods, the support restricts the flow of workpiece in X, Y and Z axis at the edge where the workpiece meets the support. Therefore, in FEA, constraints were made at the nodes where the radius was 67.5 mm in the aluminium structure. The constraints were made to restrict displacement in the X, Y and Z axes at those nodes.

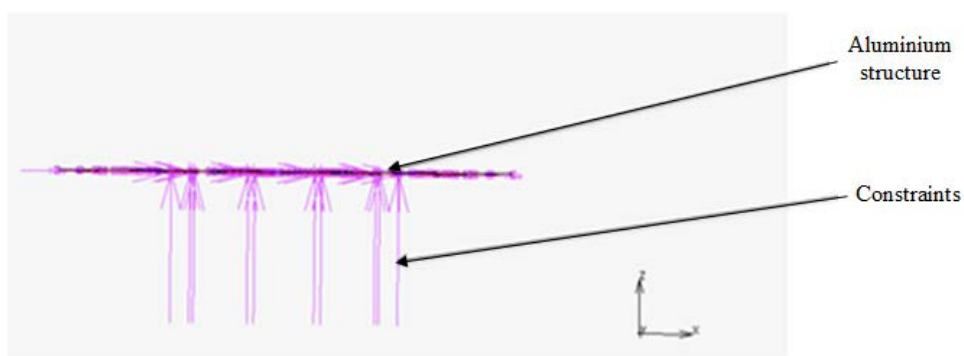


**Fig 50 - Constraints - front view**

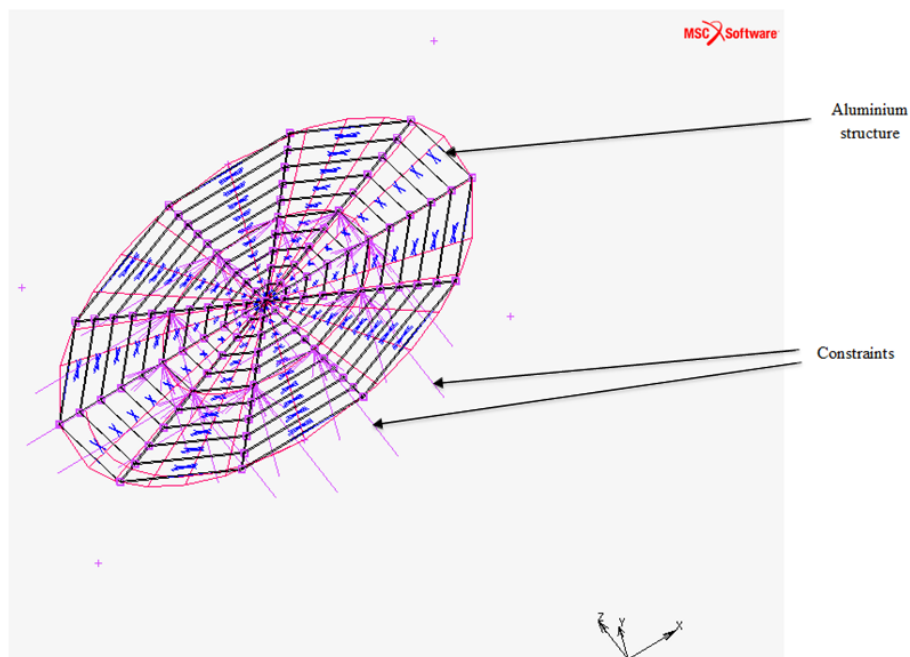


**Fig 51 - Constraints - orthogonal view**

## 5.5 Formulating the contact (impact) between rigid body and the aluminium structure

Once the initial properties were specified, the next step was to define the contact motion between the rigid body and aluminium structure. As the objective was to find out the impact force from a relative deformation similar to the manual process, the deformation of sheet metal in manual process was defined as the deformation of the aluminium structure in FEA. The rigid body was defined to move the distance  $D$  (0.8 m) and an additional distance,  $d$  (shown in Fig 37). Providing the movement of distance “ $d$ ” the rigid body into the aluminium structure meant that the aluminium structure will be deformed to a distance “ $d$ ” with which the relative impact force could be calculated in FEA.

The contact (impact) was specified using the time and distance. The time of hammer motion was inferred from the real process and the distance of hammer motion (as calculated) in manual process. A table was made for the impact to be made with time as “ $X$ ” function and distance as “ $Y$ ” function (shown in Fig 52). The peak of the table is the total distance to be travelled by the rigid body.

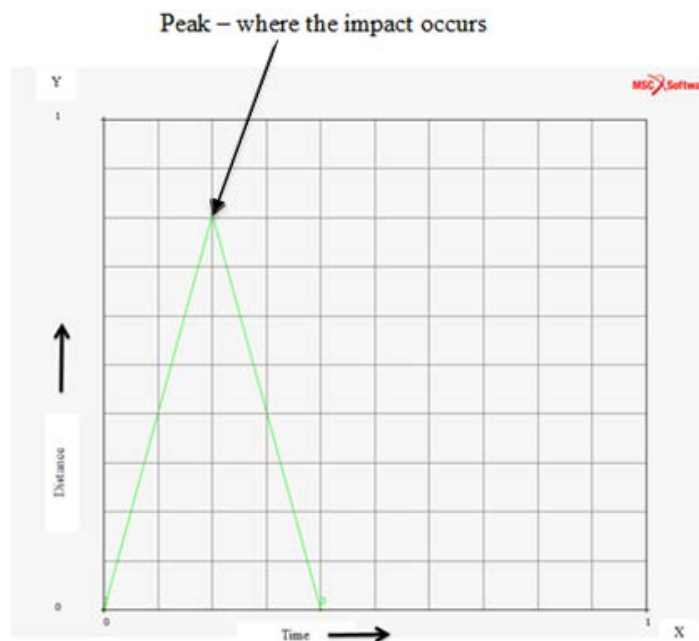
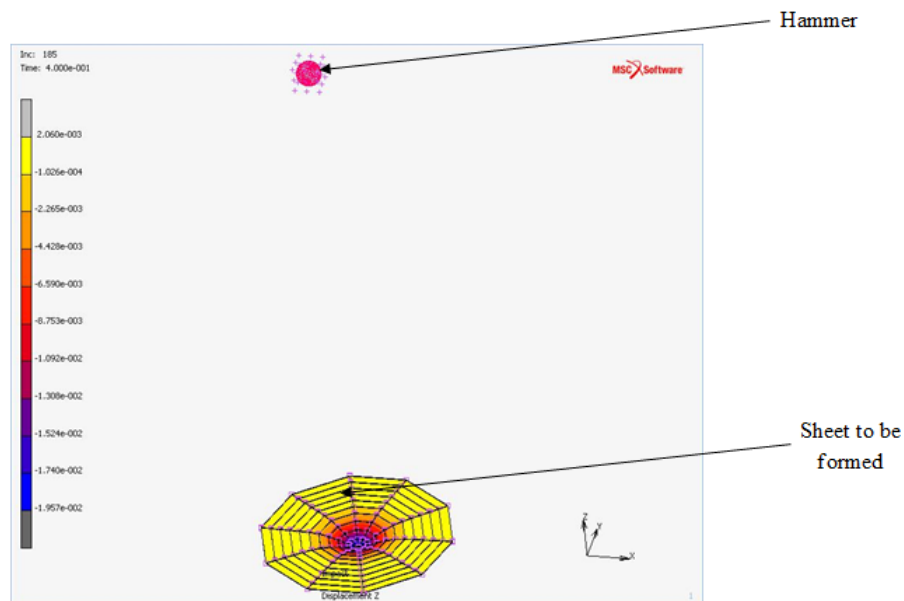


Fig 52 - Contact table – example

Subsequently, the load case condition was defined as “impact” in the FEA as it was an impact in the manual process. As a static force calculation technique was used in the

high speed camera, the analysis in FEA was based on static analysis. The MSC Marc is also capable of achieving dynamic analysis when repetitive impacts are made. Checking for job errors, the FEA job was then run in the MSC Marc environment and the results of impact force were observed (shown in Fig 53). The simulation could be saved in animation and used for later analysis.



**Fig 53 - Finite element analysis of deformation**

### **5.6 FEA modelling results**

FEA modelling was used to find the impact force involved in deforming the sheet metal as discussed in sections 4.6.1 and 4.6.2.

### **Experimental Analysis 1**

Applying the hammering data of experiment 1 discussed in section 4.6.1 (hammer travelling for a distance of 0.8065 m (D+d) to produce a deformation of 0.0065 m (d) in 0.212 s) in FEA simulation, performing numerical analysis, an impact velocity of  $7 \text{ ms}^{-1}$  was calculated for deforming the sheet metal to 0.0065 m. The impact force was calculated as 3783 N.

## Experimental Analysis 2

Applying the hammering data of experiment 2 discussed in Section 4.6.2 (hammer travelling for a distance of 0.8037 m (D+d) to produce a deformation of 0.0037 m (d) in 0.210 s) in FEA simulation, performing numerical analysis, an impact velocity of 5.91 ms<sup>-1</sup> was calculated for deforming the sheet metal to 0.0037 m. The impact force was calculated as 4721 N.

### 5.7 Discussion and comparison of experimental results and FEA results

The results obtained using the two experimental data are tabulated below.

Experiment No.	Time travelled by hammer (s)	Distance travelled by hammer (D+d) (m)	Deformation achieved (d) (m)	Instrumented impact hammer results	High speed camera results		FEA results	
				Impact Force** (N)	Impact Velocity* (ms <sup>-1</sup> )	Impact Force* (N)	Impact Velocity* (ms <sup>-1</sup> )	Impact Force* (N)
1	0.212	0.8065	0.0065	4168	7.17	3954.5	7	3783
2	0.210	0.8037	0.0037	5290.5	6.02	4897.35	5.91	4721

**Table 3 - Experimental and FEA results**

On comparing the FEA results with experimental results (discussed in section 4.6), it could be observed that the impact force results obtained using an instrumented impact hammer and the finite element analysis are different. Therefore, further investigations were carried out to detect the fault.

#### 5.7.1 FEA material input problem

Investigating FEA results, it was found that the plasticity properties of the aluminium structure defined in the FEA were based on the numerical parameters of the material used in manual process and also the plasticity rate for the aluminium was defined using the pre-defined aluminium material in MSC Marc software. It was understood that if the plasticity rate that is undergone by the aluminium in manual process is given to the aluminium structure in FEA, it might give more appropriate results.

To ensure the properties of the aluminium used in experimental methods is given as input to the aluminium structure used in FEA, the actual plasticity rate of a material is

found using the stress-strain curve. For calculating the stress-strain curve, the material will have to be tested for its tensile strength using dog bone samples.

These tensile tests were performed for the aluminium used in manual experiments. For the tensile results to be more accurate the tests were done along the grain, across the grain, at 45° to grain and at 135° to grain (the importance of grain distribution is explained in Section 2.2). The dog bone samples are shown in Fig 54.



**Fig 54 - Dog bone samples**

The tensile tests were carried out in Instron material testing machines (tensile). The dog bone samples were clamped between the holders (shown in Fig 55) and a standard load of 100 N was applied to find the stress/ strain curve (as illustrated in Fig 56).

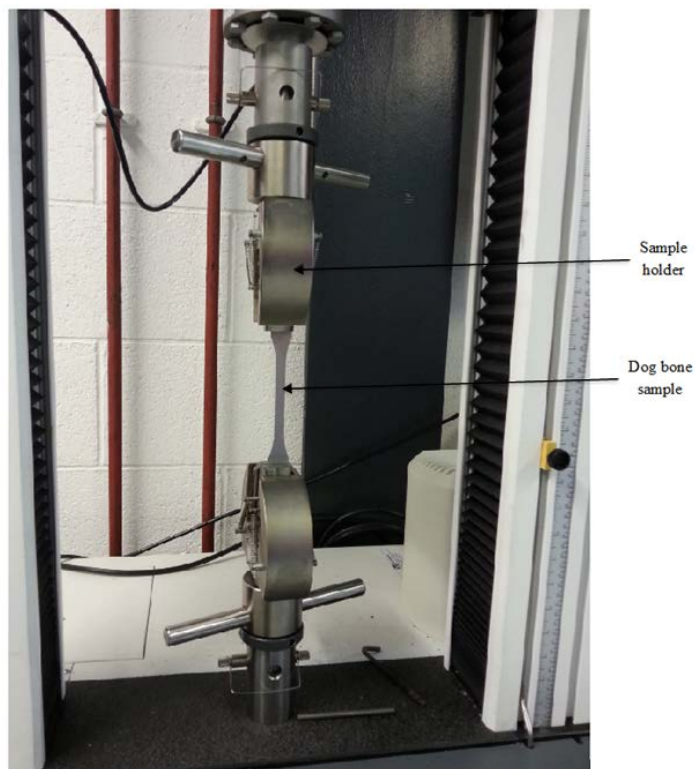


**Fig 55 - Instron tensile testing machine**

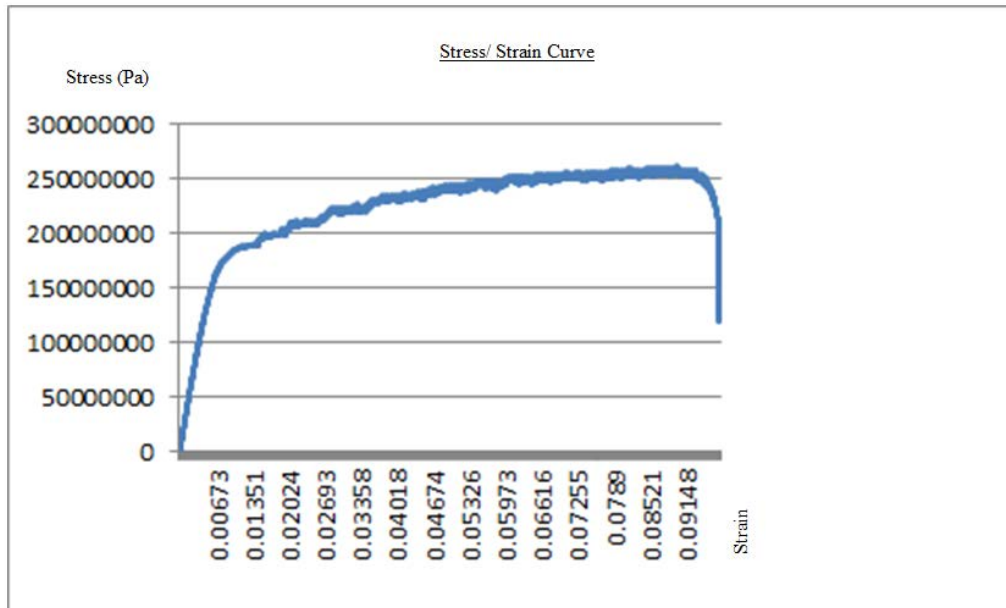


**Fig 56 - Stress/ strain curve obtained based on tensile test**

Applying the stress/ strain curve in the FEA for the plasticity rate of aluminium, improved the FEA results and were found to coincide closely with the results of the instrumented hammer. The results obtained in this analysis was 4033 N (for experimental analysis 1) and 5183 N (for experimental analysis 2).

Comparing the results, it could be observed that the impact force found using three methods (i.e. impact hammer, high speed video and FEA) are similar with an acceptable margin of error.

Therefore, both experiments provide proof of concept on predicting the magnitude of the impact force required for incremental deformation of the part used in these experiments. Such prediction is to be used to specify a pattern of part movement and related impact forces required to achieve the final deformation of parts.

## **6. Development of automated solution based on captured human skills**

---

### **6.1 Introduction**

The control system developed, experimental analysis performed (as discussed in Chapters 4 and 5) lead to the envisioned automated panel forming process, which is discussed in this chapter. Based on the traditional panel forming observations (as discussed in Section 2.3.1), human skills for forming a sheet metal contour were determined. The human skills captured were analysed and deployed as a basis for the target automated process.

These tacit skills of a panel beater in forming a sheet metal contour were interpreted within an engineering framework. The human skills were analysed and transformed into parametric solutions to be provided as input to the automated panel forming process. The observed human skills, variability involved in those skills, significance of that variability, and how the human skills were transformed into a parametric solution overcoming the variability are discussed in this chapter.

It was necessary to understand the underlying problems and challenges in automating the process discussed in section 3.4. Experimental analysis on a specific artefact was carried out to help narrow down the research and focus on understanding the challenges involved in automating. The chosen target artefact is discussed in this chapter.

A novel method of capturing the manual panel forming skills using the motion capture system Vicon [78] is also discussed in this chapter. The manipulation skills of a skilled operator forming a sheet metal using a repetitive impact hammering machine (deployed hammering machine is discussed in Section 2.8.1) were analysed using the Vicon system. Experimental analyses of the data obtained from the captured human skills, their results and contribution in developing the automated process is also discussed in this chapter.

### **6.2 Envisaged automated system**

An automated system was designed and developed constructing on the proposed research methodology and perceiving the process requirements from experimental analysis performed using instrumented hammer and FEA modelling. Based on the



traditional forming process, it was hypothesised that a robot could replace a human for manipulating the sheet metal, and an impact hammering machine could be used to form the sheet metal by repetitive vertical impact. The process flow diagram of the proposed automated system is illustrated by Fig 57.

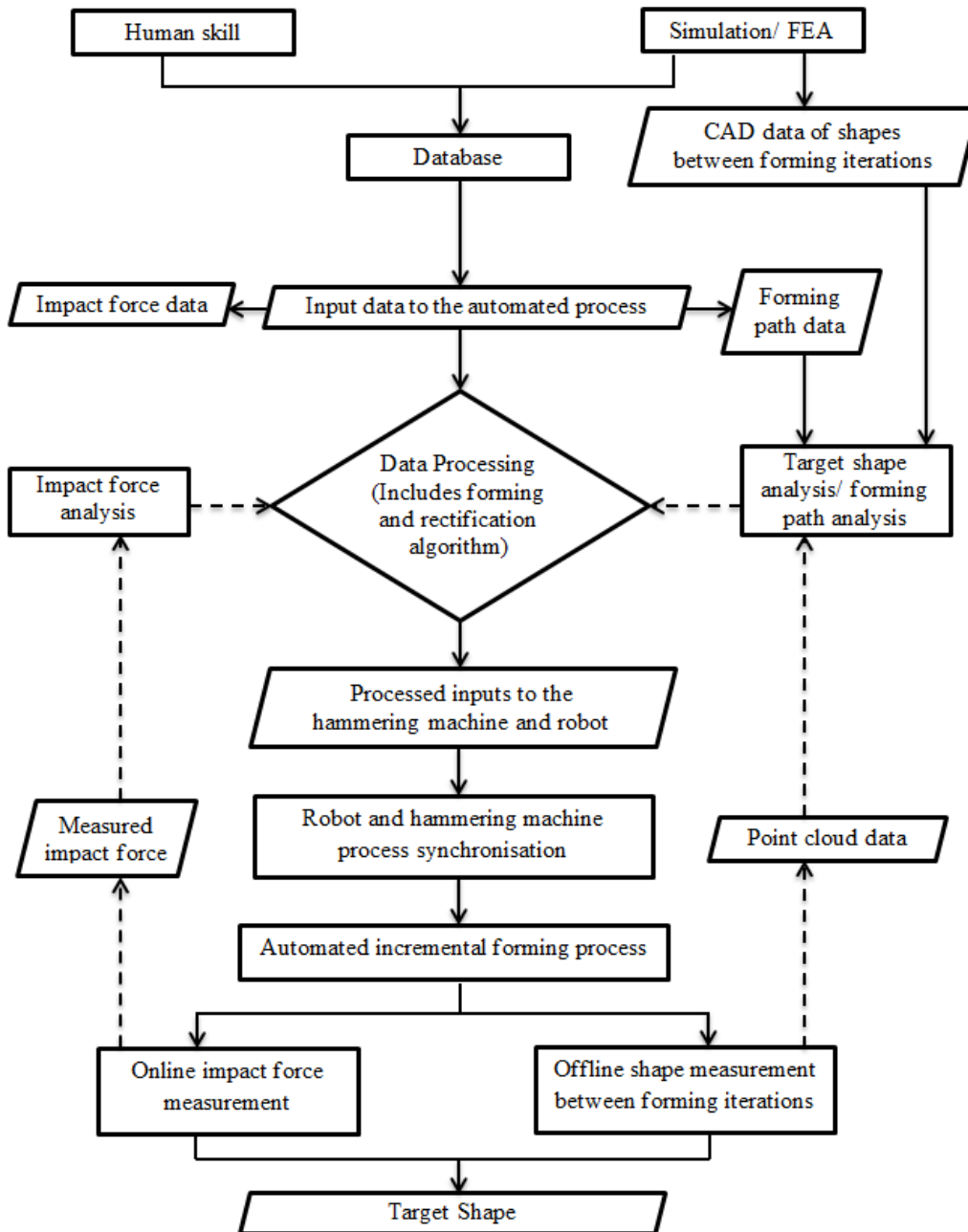


**Fig 57 - Process flow diagram**

As represented, human skills (e.g. force and the angle of beating) captured and FEA analyses performed would form a knowledge-based system (indicated as database). The human skills captured are transformed into parametric solutions to be included in the

database. Based on the shape required, input data are provided to the automated process. The data are processed to provide inputs to the hammering machine and robot, for forming the required shape. The robot and the hammering machine are synchronised to perform the automated incremental sheet metal forming process.

A feedback system was developed to monitor and optimise the forming process. The feedback system was envisioned to include an online force measurement using a force transducer and an off-process shape measurement using a 3D machine vision system.

In between iterations, a 3D vision measurement system is used to perform the shape measurement on the formed sheet metal. For the corresponding iterations, a CAD model is envisaged to be generated using the FE analysis. The point cloud data obtained from the 3D vision system and the CAD model are anticipated to be compared to find the deviation from a target shape. Any deviation to the target shape is envisaged to be compensated in the following iteration by modifying the forming path as a result of the forming path analysis.

Based on the 3D vision measurement feedback, necessary rectifications are anticipated to be performed through data processing to provide modified inputs to achieve the target shape. This is further discussed in Chapter 9.

The ideal forming strategy in Section 3.2 was further enhanced based on the envisaged automated system. Fig 58 illustrates the complete control system with the proposed processing sequence and feedback. As illustrated in the control system diagram, a pre-defined impact and pre-defined path are provided as input to the processing unit. The processing unit receives feedback from the force sensor and 3D shape measurement system. Comparing the pre-defined inputs and feedback data, the processing unit performs data analyses. Based on the results of data analyses, the next impact force and modified path are given as input to the integrated force controller<sup>3</sup> (hammering machine) and robot controller (robot) respectively. The robot and hammering machine are synchronised to perform the forming process. The feedback systems will also monitor the process to increase accuracy, but may increase the cycle time of the forming process.

---

<sup>3</sup> Impact force was envisaged to be controlled using an integrated force controller. However, integrated force control was not implemented as a part of this research and the impact force was set to a constant of 5 KN as observed from manual hammering process.

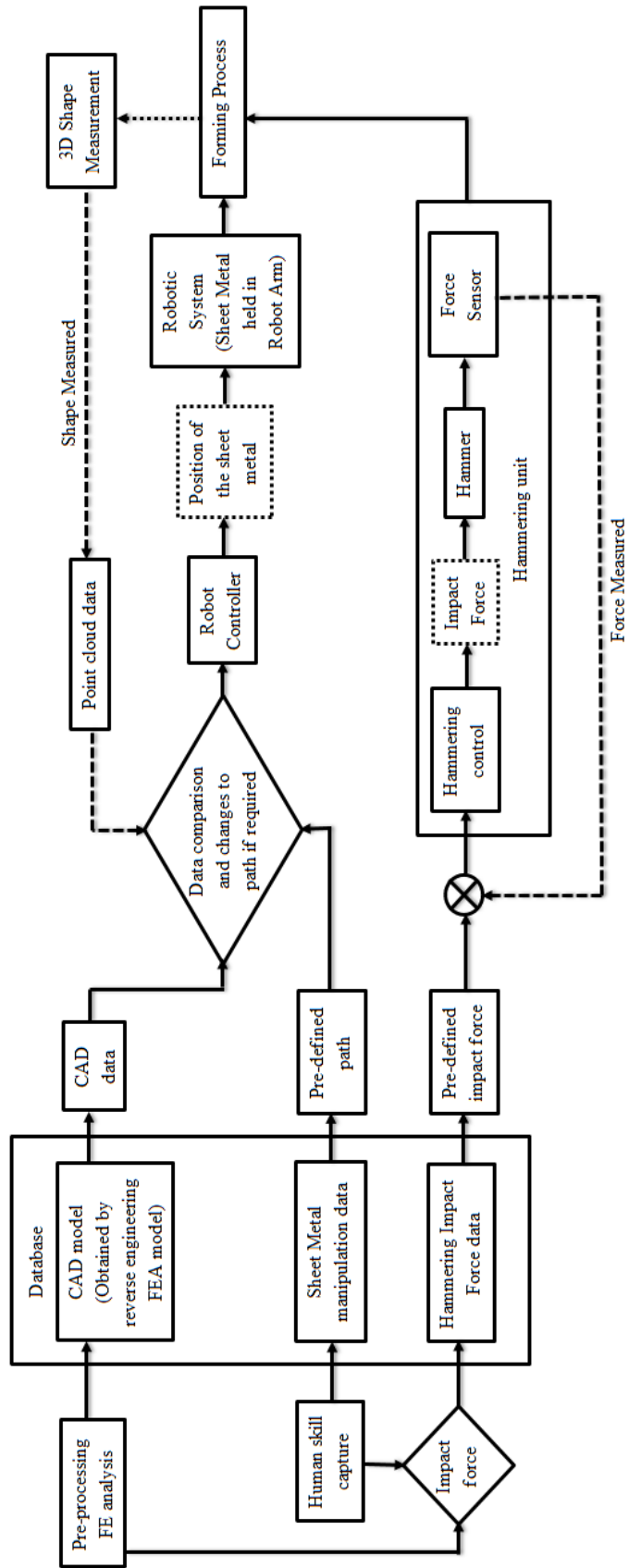


Fig 58 - Enhanced control system (ideal)

### **6.3 Manual panel forming skills**

By observing the manual forming closely and analysing the tacit knowledge used by manual panel beaters, skills and techniques used to form the sheet metal were identified. The theoretical reasoning behind each and every technique used was perceived on interviewing the panel beaters, in addition to studying the literature available on sheet metal forming.

There are many tools and processes involved in sheet metal forming, as described in Section 2.3. The human skills determined were based on using a wooden mallet and wooden support (anvil) to form a sheet metal contour. The observed human skills have been categorised into 10 different human skills which are:

1. Position of the hammer
2. Stroke length of the hammer
3. Impact force of the hammer
4. Angle of the hammer
5. Compliant gripping of the sheet metal
6. Position of the sheet metal
7. Skewing (angular rotation) of the sheet metal
8. Pattern of hammering
9. Path of hammering
10. Spacing between the consecutive impacts

These human skills have been discussed in detail and summarised below.

#### ***Human Skills 1 to 4***

Panel beaters are skilled in achieving the precise position of the hammer and stroke length of the hammer - with respect to the support - to apply the required impact force. As illustrated in Fig 59, the human skills are necessary to analyse the anticipated deformation. Panel beaters are also experts in predicting the impact force necessary to produce the required depth whilst deforming the sheet metal. These three human skills form the basis of how a deformation of required depth is achieved. The angle of the hammer as illustrated in Fig 59, determines the geometric definition (shape) of the deformation achieved. It is the most difficult human skill to gain due to a wide range of variability involved, and can differ from material to material. However, it is an essential

human skill to achieve the required shape with accuracy. Similarly, there are human skills (or techniques) related to handling the sheet metal and also human skills based on the forming strategy of the sheet metal.

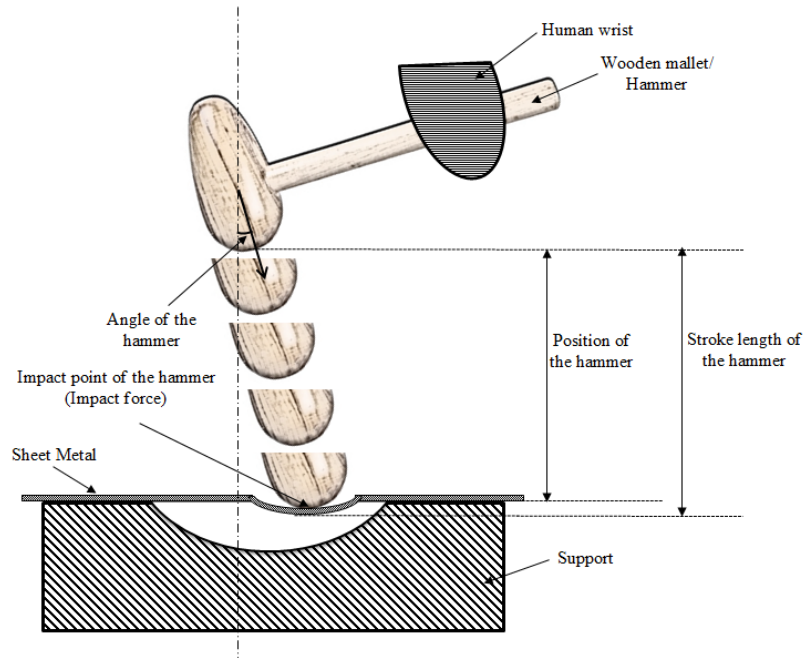


**Fig 59 - Illustration of human skills related to hammer (skills 1 – 4)**

### ***Human Skill 5***

As shown in Fig 60, compliant (i.e. adjustable) gripping of the sheet metal is essential in producing an unconstrained material flow which ensures the forming is smooth. Also, constraining the sheet metal will be equivalent to using fixtures which reduces the thickness of the sheet metal being formed.

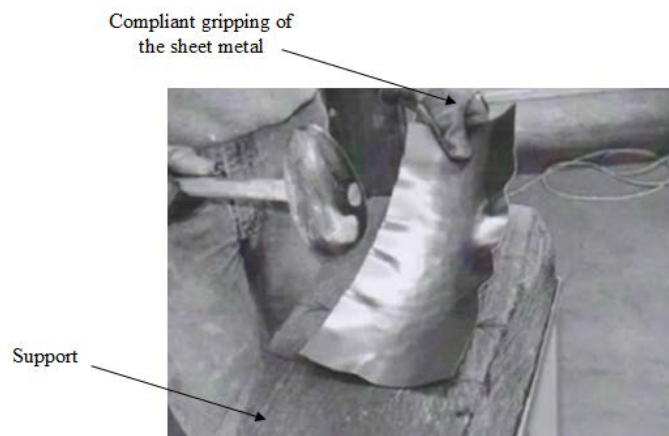


**Fig 60 - Compliant gripping of the sheet metal (human skill 5)**

### ***Human Skills 6 and 7***

The position and skewing of the sheet metal, as illustrated in Fig 61, are significant in determining the final shape of the sheet metal. A fault positioning or skewing of sheet metal could yield an irrelevant shape compared to what is required. Thus, it has a significant contribution towards the ease of forming the sheet metal.

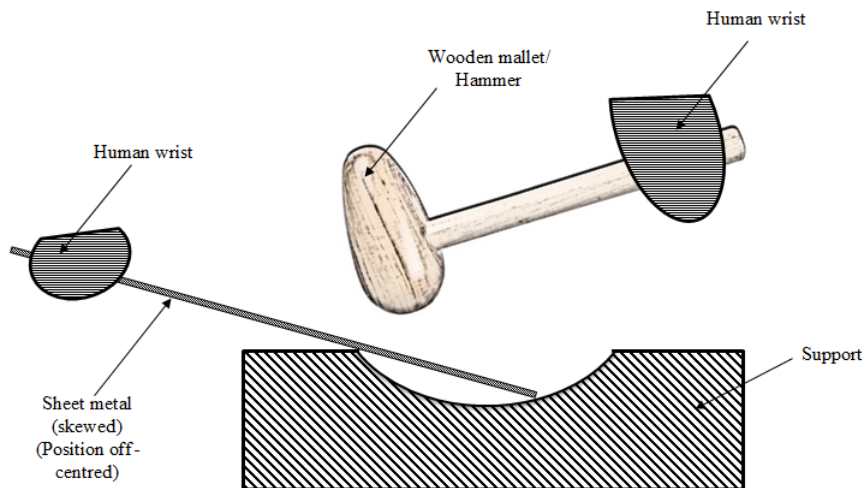


**Fig 61 - Position and Skewing of the sheet metal (human skills 6 and 7)**

### ***Human Skills 8 to 10***

Based on the shape required, different patterns are used by a panel beater to achieve the final shape. It was observed that based on the final shape and depending on the accuracy required, a selection of patterns and paths are executed. Fig 62 illustrates the zig-zag patterns used by the skilled labour in achieving a double curvature from a rectangular contour (shown in Fig 60).

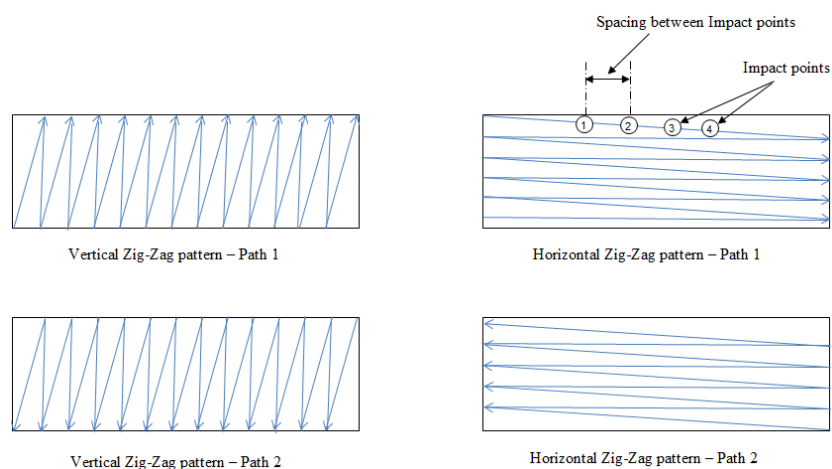


**Fig 62 – Human Skills based on forming strategy of the sheet metal (skills 8 - 10)**

Patterns and paths differ from shape to shape. However, the fundamental theory involved in sheet metal forming is the same as discussed in Section 2.3.1. In addition, the impacts are carefully spaced (as shown in Fig 62) to overcome the effects of overlapping and wrinkling. The spacing between impacts is important as this influences the effect of residual stresses, as discussed in Section 3.4. The human skills identified and their theoretical reasoning are summarised in Table 4:

<b>S.No</b>	<b>Human Skill identified</b>	<b>Theoretical reasoning</b>
<b>1</b>	<b>Position of the hammer</b> with respect to support (or) distance between hammer and support	The position of hammer with respect to support is a factor determining the impact force applied to form the sheet metal
<b>2</b>	<b>Stroke length of the hammer</b> with respect to the support	Stroke length of the hammer is another factor determining the impact force applied to form the sheet metal
<b>3</b>	<b>Impact force of the hammer</b> applied on to the sheet metal	Impact force determines the deformation of the sheet metal contour to the required depth
<b>4</b>	<b>Angle of the hammer</b> with respect to the sheet metal	Angle of the hammer has a deterministic effect on shape of the sheet metal being formed
<b>5</b>	<b>Compliant gripping of the sheet metal</b>	Compliance is necessary to allow the sheet metal form without constraining its flow and also to introduce dampening of reaction force/vibration
<b>6</b>	<b>Position of the sheet metal</b> with respect to the hammer and the support	The Cartesian co-ordinate (X,Y,Z) positioning of the determines the area of sheet metal contour being formed
<b>7</b>	<b>Skewing</b> (angular rotation) <b>of the sheet metal</b> with respect to the hammer and the support	The Polar co-ordinate (roll, pitch, yaw) positioning of the sheet metal is necessary to form the sheet metal to the required three dimensional shape
<b>8</b>	<b>Pattern of hammering</b>	The hammering sequence of the contour being developed is important to increase the ease of sheet metal forming and to reduce the effect of residual stress
<b>9</b>	<b>Path of hammering</b>	The hammering path influences the material flow, hence, influencing the shape of sheet metal being formed
<b>10</b>	<b>Spacing between the consecutive impacts</b> (ref. Fig 62)	The spacing is necessary to avoid an overlap between impacts to produce the shape accurately and reduce the effects of residual stress

**Table 4 – Human Skills determined**

#### 6.4 Target artefact

The categories of the observed human skills appear to be common for forming many different contours. However, to analyse the elementary techniques of sheet metal forming and to transform them to parametric inputs for an automated system, a bowl shape workpiece was determined as the experimental artefact. The rationales for selecting this shape initially were simplification and practicability, according to the available equipment. Such symmetrical shapes allow an equal flow of material in all directions, minimising deformation due to residual stresses (by avoiding sharp corners) and enables access by the robotic system to a reasonable depth, sufficient to prove the concept.

An aluminium sheet, thickness of one millimetre (mm), cut in a circular shape, was prepared as the raw material to be transformed into a bowl shape, as illustrated by Fig 63. The diameter and the depth of the final bowl shape were targeted to be 130 and 15 mm.

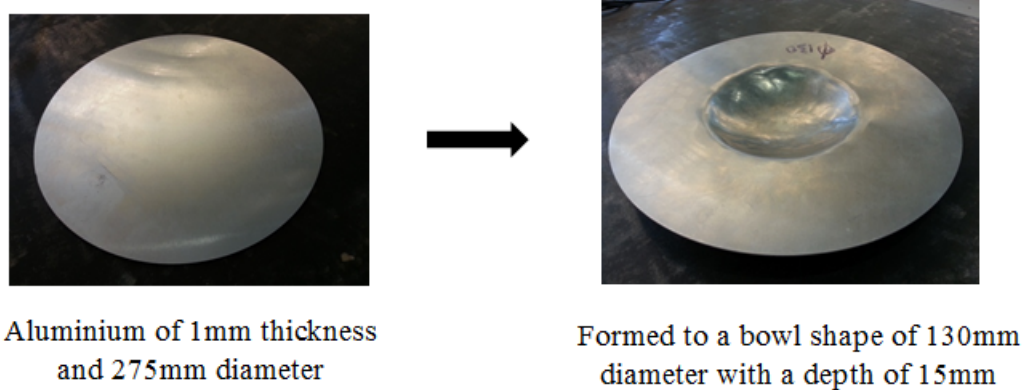


**Fig 63 - Target artefact**

Inclusion of integrated force controller and generation of CAD models from FE analysis were considered to be out of the scope of this research. Therefore, they were not implemented as a part of the process control illustrated in Fig 57.

#### 6.5 Transfer of human skills to the human operated hammering machine

The first step in human skill transfer was transforming the human skills related to the hammer as parametric inputs to the automated system. The hammering machine, Eckold Kraftformer 170PD was selected and procured due to its configurability of the



hammering stroke, the impact force and frequency, and the ability to integrate with the automation control system by minor modifications. The reconfiguration settings of the hammering machine are as illustrated in Fig 64.

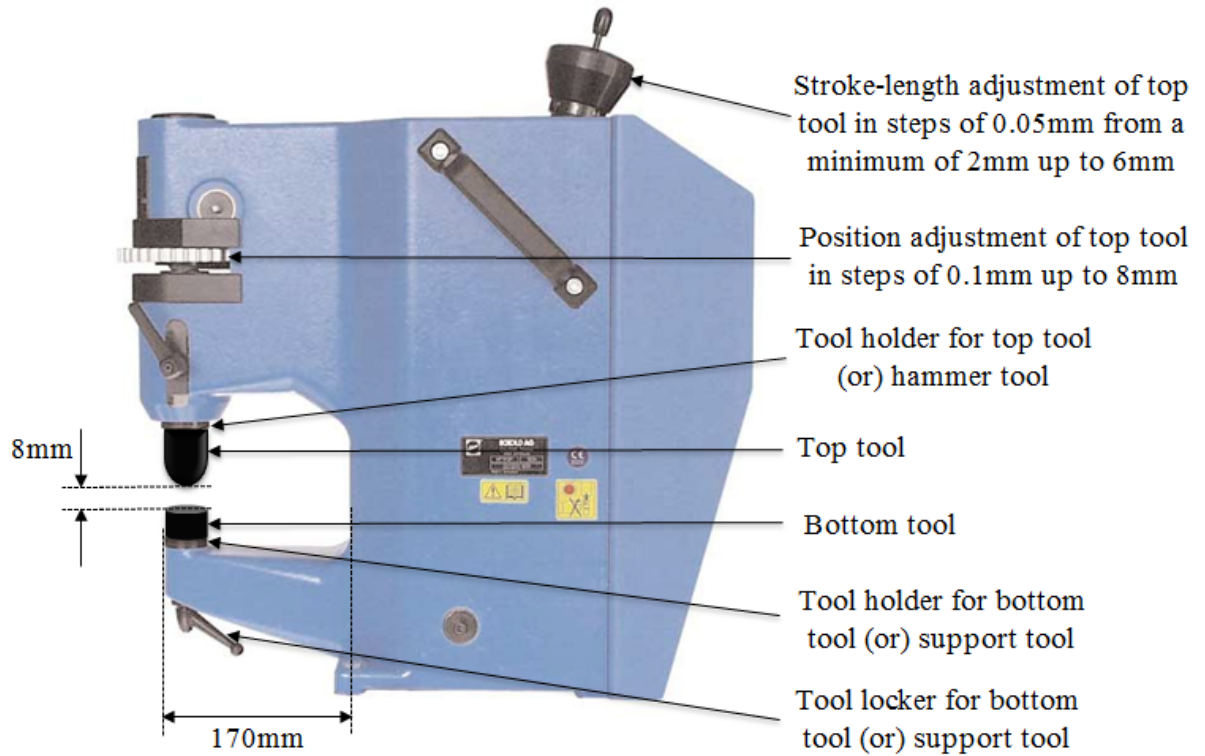


**Fig 64 - Hammering machine reconfigurable settings**

The maximum clearance between the top tool and the bottom support is 8mm, as indicated in Fig 64. Adjusting the position and stroke-length of the top tool determines the impact force of the hammer. A foot pedal control (human-operated) actuates the hammer tool, producing the required impact force. This hammer meets the requirements for human skills 1, 2 and 3 in Table 4.

The angular orientation (human skill 4 in Table 4) of the hammer is eliminated to simplify the computational complexity and development of the automation system. The required angle between the sheet and the hammer is provided by manipulating the part by the robot wrist to the required orientation (human skill 7 in Table 4).

The hammering machine is capable of using different tools. However, a universal doming tool was used for the experiments in this research. The doming tool, illustrated in Fig 65, replaces the manual hammer (a wooden mallet) and the anvil in the

automated system. The doming tool consists of a positive and a negative die made of steel with a hardness factor of 45-50 HRC. The tool weighs 0.85 kg in total; with the top tool weighing 0.58 kg and the bottom tool weighing 0.27 kg, which is comparable with a small manual hammer. The doming tool locks on to the tool holder of the hammering machine.

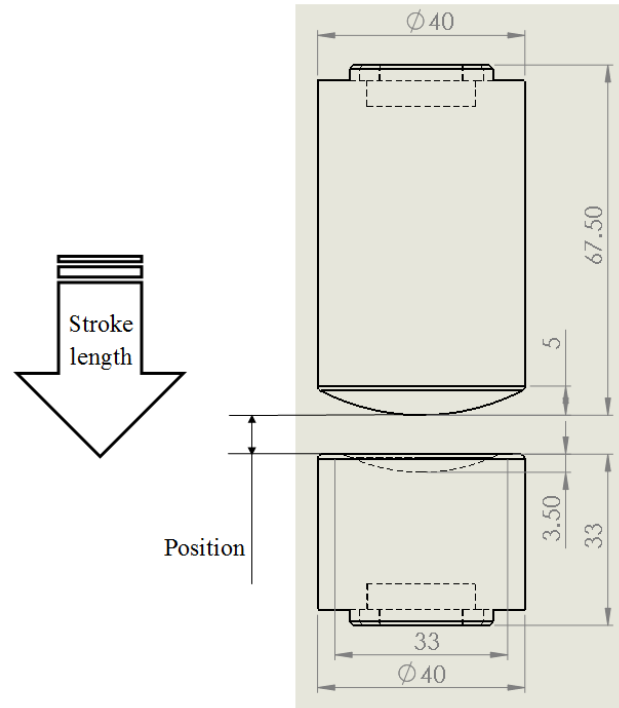


**Fig 65 - Doming tool (dimensions are in mm)**

### 6.5.1 Parameter settings of the hammering machine

To streamline the analysis process, the stroke length and position of the top tool (or hammer) was adjusted to be constant in order to achieve consistent impact force throughout the process of forming. Experiments were performed focussing on determining the optimum stroke length and position in the hammering machine for forming the aluminium of 1mm thickness. Various combinations of stroke length and position were tested. The optimum combination was determined based on the following factors,

- Depth on first impact
- Total depth of the aluminium sheet formed
- Cycle time

- Friction created by the hammer during sheet metal manipulation

The results obtained based on performing experiments with different stroke length-position combinations are shown in Table 5.

Exp No.	Stroke length (mm)	Position (mm)	First hit deformation (mm)	Total depth of bowl (mm)	Cycle time (Minutes)	Friction (1 – worst 10 – perfect)	Significance
1	4	4	3.35	21.55	3.59	6.5	Good
2	4	6	No deformation in first hit				
3	4	2	Clearance between top and bottom tool not enough				
4	4	3	3.40	25.20	4.02	4	Acceptable
5	4	5	No significant depth formed				
6	6	4	3.52	24.02	3.35	5	
			No continuous stroke possible – though deformation can be achieved manually				
7	6	3	No continuous stroke possible				
8	2	4	No significant deformation				
9	3	4	No significant deformation				
10	5	4	3.58	22.05	3.16	8	Better
11	5	3	No continuous stroke possible				
12	5	5	3.45	20.50	3.07	9	Best
13	5	6	No significant forming				
14	2	3	No significant forming				
15	2	2	Sheet cannot be inserted				
16	6	5	3.33	21.91	2.48	3.5	
17	3	3	3.20	18.53	2.40	8	Vibrating more

**Table 5 - Optimum position and stroke length (for optimum impact force)**

The experiments involved a human operator forming the sheet metal into a bowl shape (target artefact) by actuating the hammering tool using a foot pedal. Some combinations

were not tested and rejected based on the knowledge of results obtained in earlier combinations. The forming was found to be particularly significant when the top tool was positioned at 5mm from the bottom tool, and the stroke length of top tool set to 5mm. This optimum combination is used throughout the experimentation (including the robotic system). Therefore, the impact force produced will always be consistent.

### **6.6 Human motion capture using Vicon system**

Motion capture technology was used to perceive the forming strategy used by the panel beater. As the hammer-related motions were eliminated by vertical hammering on the machine, the movement of the part under the hammer was captured using a vision system.

The initial experiments included a semi-automated system utilising the Eckold Kraftformer and manual manipulation of the sheet metal blank between the hammer and the anvil during automatically repetitive hammering. During the action of forming a Vicon 3D motion capture system [78] was used to capture and analyse the movement of the sheet metal blank. The experiments were aimed at understanding the manual motion of the part and therefore finding the most suitable pattern and path for achieving the target artefact. The experiments were also aimed at obtaining the information related to spacing between impacts.

The technique executed by human operator to form the sheet metal is shown in Fig 66. The human operator used two hands to manipulate the aluminium test piece to form the bowl shape while controlling the sequential hammering action by foot pedal control. The workpiece motion was tracked using the Vicon system, also shown in Fig 66.

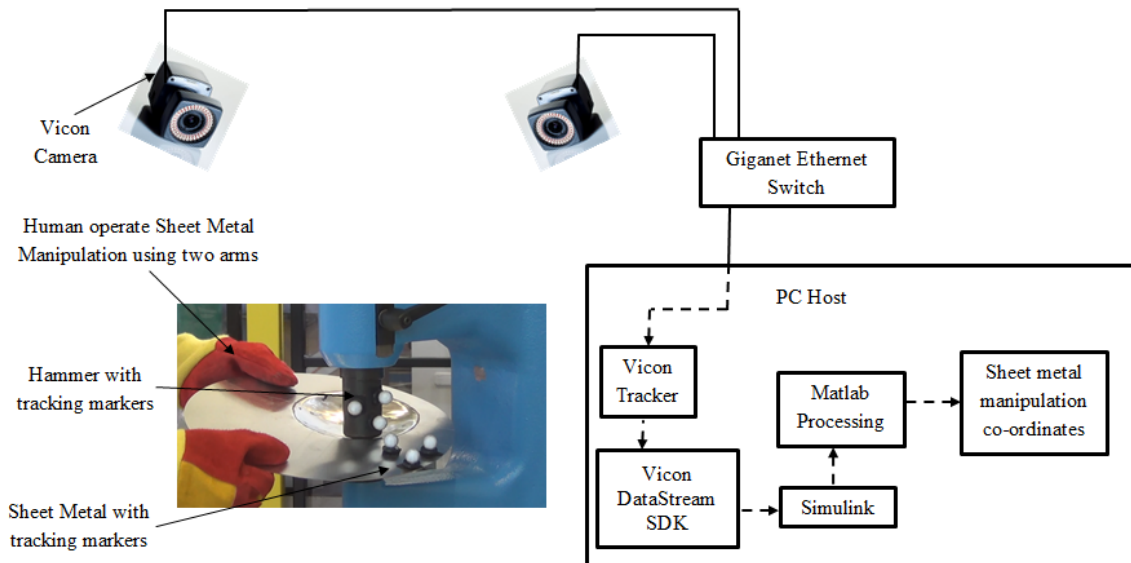


**Fig 66 – The Vicon system**

The bowl shape was formed towards the edge of the aluminium sheet as show in the figure, considering 170mm throat depth limit of the hammering machine (refer Fig 64). Two Vicon T-series 2 [79] megapixel cameras were used to capture and interpret the human motion. The Vicon cameras were connected to a PC host through Gigaset-Ethernet switch for fast data transfer. The cameras were calibrated for the experimental environment using the Vicon active wand [86]. Hence, the universal position of hammer and the position of sheet metal relative to the hammer were identifiable.

As shown in Fig 66, tracking markers were affixed on the hammer and sheet metal to recognise the objects in the Vicon environment using the tracker analyser (Vicon tracker software). The motion of the hammer and sheet metal manipulation data were streamed out into Simulink [87], by using the Vicon data stream software development (for Matlab Simulink) available from the Vicon system. Simulink was used to retrieve the manipulation data relative to the simulation pace set. The Simulink model shown in Fig 67 was used to export the data into the Matlab for processing.

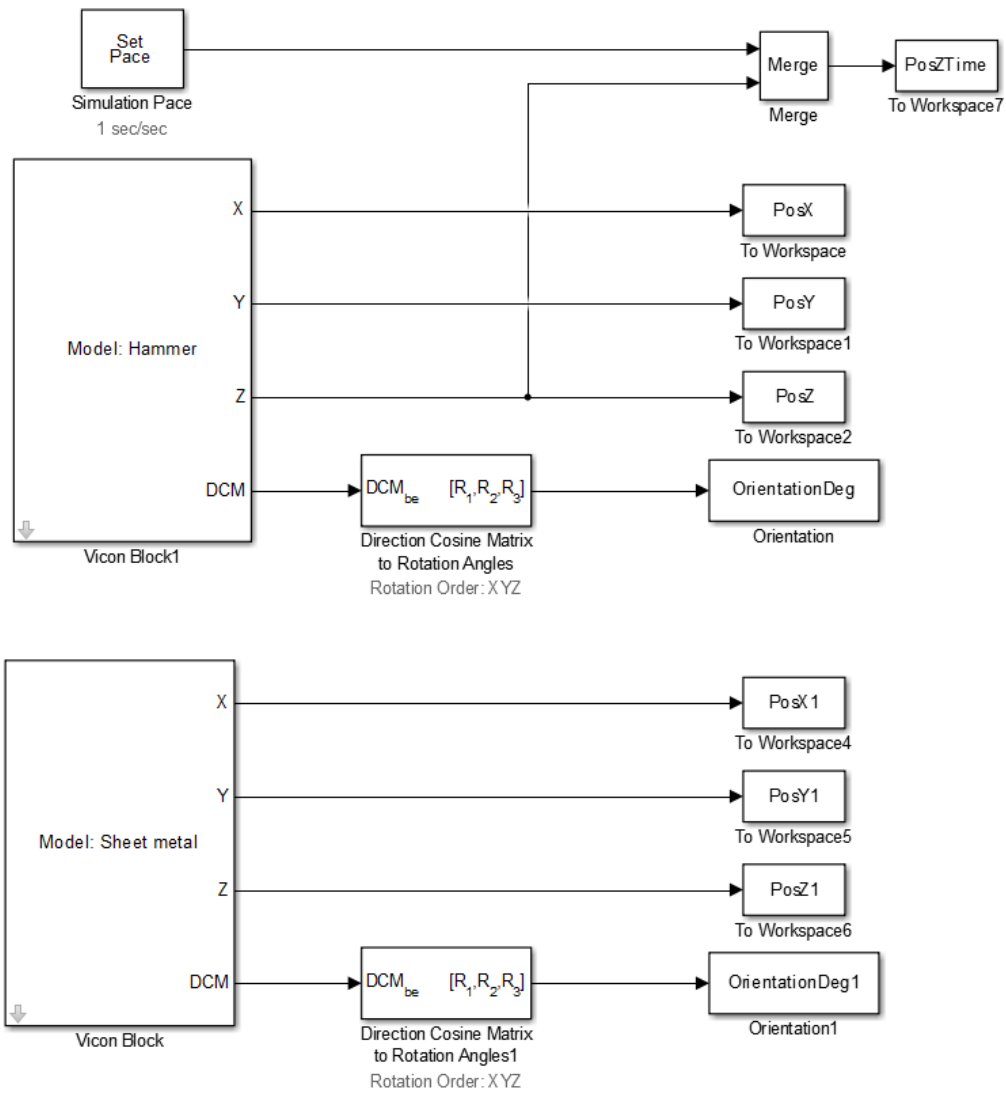


**Fig 67 - Simulink model**

The simulation pace of the motion tracking was set at 0.01 sec as frame rate of 100Hz was used in the Vicon cameras to capture the motion of hammer and the sheet metal. All the 6 DOF (position and orientation) were obtained from the Simulink model. Hammer impact time corresponding to Z-axis position of the hammer was also acquired. The data was processed in Matlab to obtain significant information to analyse the best pattern and path for forming the bowl shape.

The captured data was used in determining the impact frequency, impact cycle time and the impact duration. For the set hammering parameters (as discussed in Section 6.5), the hammering machine produced approximately 4 impacts/sec. The impact cycle time (one reciprocating action of the hammering tool) was determined as 0.25 sec. The impact duration was calculated to be approximately 0.04 sec per impact. These values

are used to develop a parametric automation system when integrating and synchronising the hammer strokes with the robotic manipulator motion.

An algorithm was developed in Matlab to analyse the sheet metal manipulation in relation to the hammering impact point. The algorithm developed also determined the impact points and the corresponding impact time. The 3D manipulation path information acquired using Matlab processing is shown in Fig 68. The coloured dots in Fig 68 represent the hammering impact points relative to the manipulation path. The corresponding hammering frequency (impact time) is shown in Fig 69.

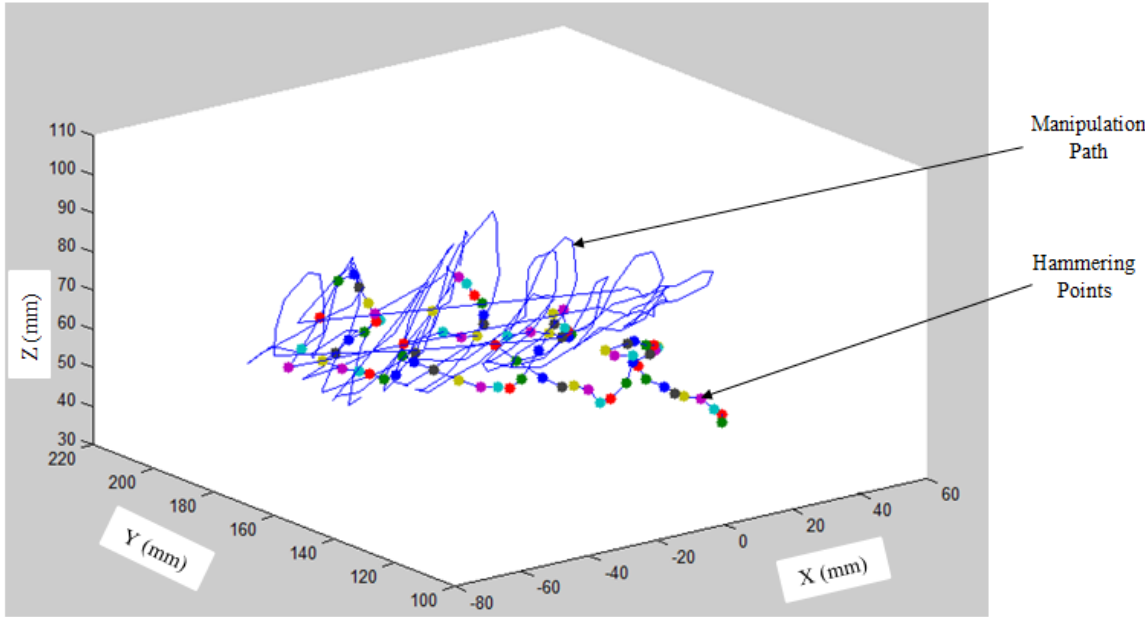


**Fig 68 - Manipulation path (data from Matlab processing)**

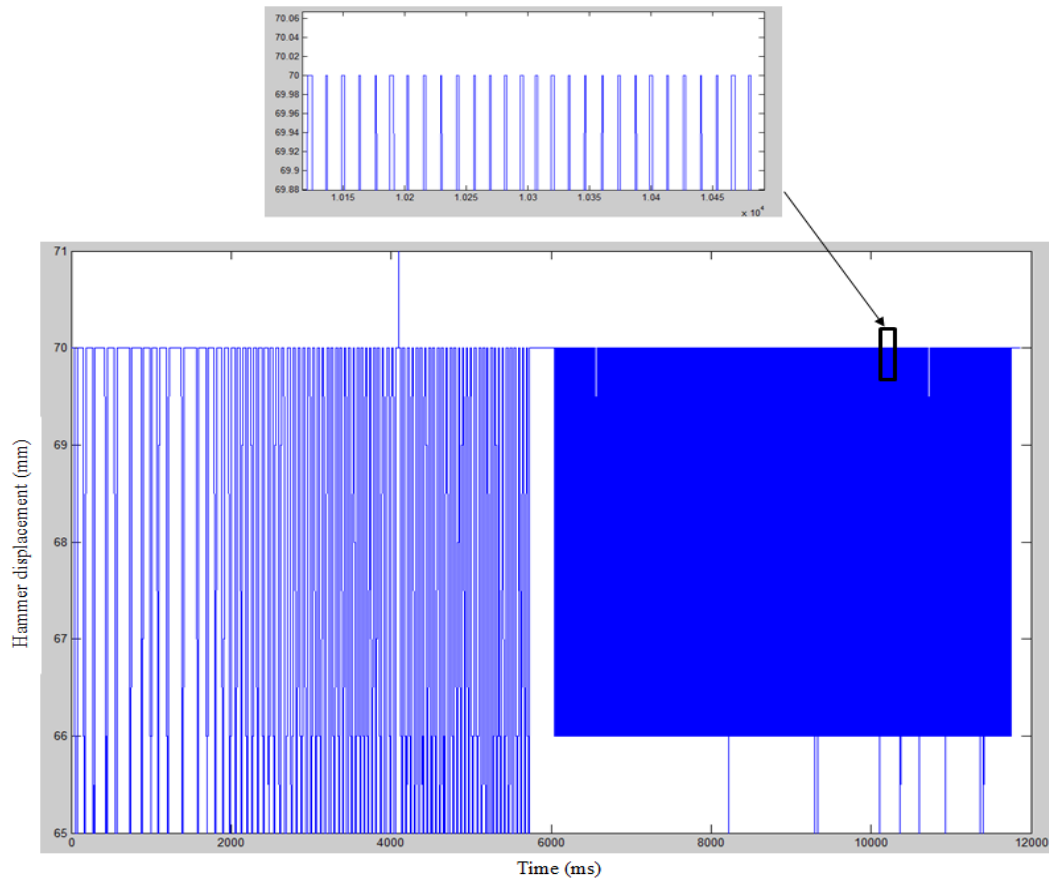


**Fig 69 - Hammering frequency**

The 3D manipulation of the sheet metal was tracked at an accuracy of 0.5 mm which provided with sufficient data to analyse the sheet metal forming pattern and path used by a skilled operator.

In the initial phase of forming, it could be noticed from Fig 69 that the hammering frequency is low. This is due to the human operator forming tucks in the sheet metal (similar to the manual forming – refer to Section 2.3.1) by applying impacts at the required region. The operator used single stroke action and applied the impact when required by using the foot pedal. In the later phase, the hammering action was set to continuous mode and the operator formed the sheet metal utilising the repetitive hammering action. The hammering frequency is quite high in the continuous stroke, as shown in Fig 69.

Based on the manipulation path analysis, it was determined that the spacing between impacts was about 4 - 5 mm during initial tucks. On some occasions, there were also overlaps between impacts. During the continuous strokes, the operator used minimal



distance between impacts. The spacing between impacts was only about 1 - 2 mm. However, the small spacing between impacts, and the occasional overlaps had a significant effect on the forming. This action improved the quality of forming and it was determined the closer impacts will enhance the sheet metal forming considering the flow of the material.

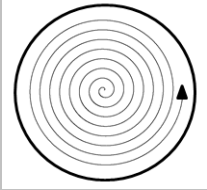
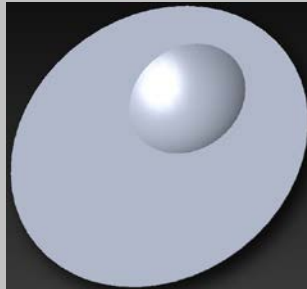
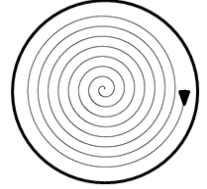
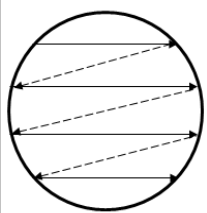
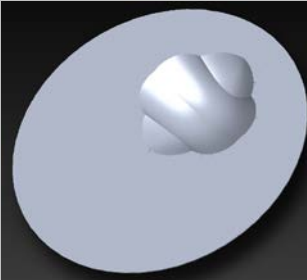
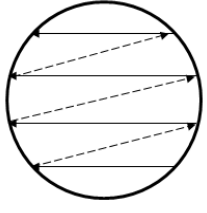
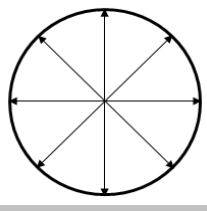
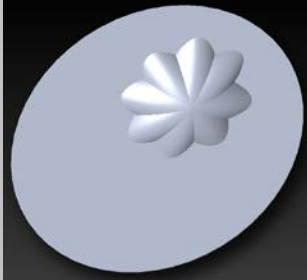
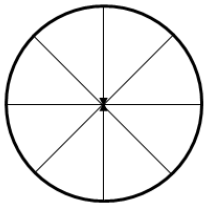
As a result of this experiment, it was realised that the unidirectional hammer can remove the effects that might have been caused due to angular hammering (such as wrinkling). Nevertheless, it was also recognised that the quality and ease of sheet metal forming is now excessively dependant on sheet metal manipulation. Experimental results provided an insight into the effect of spacing impacts in forming a bowl shape. Therefore, human skill 10 (in Table 4) is now transferrable to the automated system.

### **6.7 Determination of the best pattern and path**

From the human skill analysis using the Vicon system, it was observed that the sheet metal manipulation (i.e. artefact 3D positioning in relation to the hammer's axis) has a significant influence on the sheet metal being formed. Therefore, experiments were carried out to determine the best pattern and path for forming the target artefact using vertical hammering.

Based on the literature review; spiral, diagonal and zig-zag patterns were recognised to be ideal for sheet metal forming. The human operator used these patterns to form the aluminium sheet into a bowl shape. However, the patterns can be performed using different paths. While using spiral and zig-zag, the operator can perform in-out or out-in patterns. The Zig-zag pattern is also used from top to bottom, or vice-versa. Therefore all the patterns were used in all possible paths to analyse the best possible pattern and path for forming the target artefact. The experiments were also captured and analysed using the Vicon system to determine the ease of formation and the effect of patterns on forming the bowl shape.

The human operator used the method of forming initial tucks followed by progressively forming the desired bowl shape. The same method was used for all the patterns and paths. The results obtained based on using different patterns and paths for forming a bowl shape are illustrated in Table 6.

Parameters Pattern & Path name	Input pattern and path	Depth (mm)	Finish Quality (%) & Ease of Forming (%)	Output
Spiral in - out		15.97	95% & 95%	
Spiral out - in		16.05	95% & 90%	
Zig-Zag top - bottom		18.53	65% & 50%	
Zig-Zag bottom - top		18.80	65% & 50%	
Diagonal in - out		17.05	50% & 30%	
Diagonal out - in		15.02	45% & 20%	

**Table 6 - Patterns and paths tested\***

(\*Note: the output illustration is only for guidance and is similar to the output achieved)

As shown in the Table 6, the diagonal pattern was identified as the most difficult to implement due to excessive friction created from a multi-directional material flow, and therefore was identified as the least suitable technique to form a bowl shape. Thus, for the ease of forming, this was least suitable, and the quality of the sheet metal was less than 50% to the target shape.

A deeper contour was achievable using zig-zag pattern but with low finish quality. The circumferential edges were not completely formed and the forming lacked geometric definition. It was identified that the flow of material was easier. However, this influenced the inaccuracy in forming as there was less motion control using the zig-zag pattern. Though 'spiral out-in' was found to be adequate (labelled as good in the table), it had impression marks from the hammer, which was realised to be the effect of material flow. While forming a bowl shape from the outside-in, the material flow is constrained from its natural flow direction and this affects the grain distribution. This leads to the residual stresses due to which patches of hammering may occur, as shown in the Table 6.

The spiral in-out had a better formation in comparison with other patterns and had a better quality of finish, especially towards the edges of the bowl shape. The material flows easier and there was good motion control to form the sheet metal to the required contour. The effect of residual stresses was found to be at their least. Therefore, spiral was determined to be a better pattern and in-out was identified to be the better path for forming a bowl shape using the hammering machine. Hence, the robotic manipulation system will also use a spiral in-out pattern to form the aluminium sheet into a bowl.

Based on the experimental analysis performed for determining the best pattern and path, human skill number 8 and 9 (in Table 4) are now transferrable to the automated system.

### **6.8 Summary of human skills transferable to the automated system**

On analysing the manual panel forming, hammering related human skills, workpiece manipulation human skills and forming strategy-related human skills were identified. The hammer-related human skills are transformed as parametric inputs to the hammering machine including the stroke length, position, impact force (skills 1, 2 & 3). Human skill 4 (angular hammering) was determined to be compensated by ensuring

human skill 7 (sheet metal skewing) is also transformed to the automated system by the use of robotic manipulator. The forming strategy related skills, the best pattern and path (human skills 8 & 9) was also identified based on experimental analysis. The significance of spacing between impacts (human skill 10) was also determined using the Vicon system.

Consequently, human skills 1 to 4 and 8 to 10 were transformed to be parametric inputs to the automated system. Therefore, the tacit knowledge of a highly skilled panel beater has been transformed into quantifiable parameters to incrementally form the sheet metal.

The human skills 5 to 7 are the most crucial and challenging sheet metal motion-related human skills, with a multitude of human variability. These human skills are to be transferred into a robotic system to perform the sheet metal manipulation. The challenges involved in transforming the sheet metal related human skills and integrating the process are discussed in Chapter 7.

# **7. Automation approach and system integration**

---

## **7.1 Introduction**

The design and development of a robotic automated system to transform the sheet metal manipulation technique - used by skilled operators - into a parametric automated solution is described in this chapter.

A gripping unit was essential to replace the human grip of the sheet metal. The significance of selecting an appropriate gripping unit is discussed in this chapter. Experimental results of gripping performed using standard gripper, and the design of new gripper fingers based on the experimental results are discussed in this chapter.

Mechanical integration of the gripping unit to the end of robot's arm and the transformation of sheet metal-related human skills into the robotic system (robot with gripping unit) is discussed in this chapter. The conversion of the foot pedal-operated hammering machine to a solenoid-operated hammering machine and sourcing its trigger from the robot controller is also discussed in this chapter. The integration of the hammering machine to the robotic system and the user co-ordinate set-up is also discussed in this chapter.

Initial experiments performed on the integrated system and their results are explained. The need for compliance in the gripping unit is also discussed in this chapter.

## **7.2 Robot manipulation of the sheet metal**

The manual panel beaters typically use one arm for sheet metal manipulation and the other for hammering. However, both his arms are used for sheet metal manipulation when forming the sheet metal using a hammering machine. The use of two arms provides a better control over sheet metal manipulation and an improved precision in the final form.

However, it was envisaged that one arm's robotic manipulation could also provide sufficient dexterity if an adequately firm grip is applied, to avoid part slippage during hammering. Yaskawa Motoman SDA10 [88] shown in Fig 70 was chosen for the sheet metal manipulation as it met all the required specifications in terms of dexterity, the required force and reachability. In addition, this robot was available for this research, but any other robot with the similar specifications could have been used.



**Fig 70 - Yaskawa Motoman SDA10**

### **7.3 Development of the gripping unit for the automated system**

As discussed in Section 6.3, a compliant gripping of the sheet metal (human skill 5 in Table 4) was required to have a non-constrained flow of material on the sheet metal being formed. Determining a compliant gripping unit was significant as a highly constrained gripping unit would produce effect similar to a fixture and a completely non-constrained gripping unit would result in inaccuracies in forming. Therefore, a gripping unit with optimum force and compliance was developed for the automated system.

#### **7.3.1 Experiments using a standard gripper and standard finger design**

Potential damage to electrical grippers due to the impact force ruled out the use of this type of grippers. Therefore, pneumatic grippers were considered. Initially, a pneumatic gripper from Schunk (PGN plus 80-1 – 6 bar [89] ) was used along with the standard gripping finger (as shown in Fig 71) to determine the quality of gripping during the hammering process.

The standard finger, made 80mm x 40mm x 20mm of a steel block was made sure to be under permissible finger extension and load limits of the gripper. The fingers were mounted onto the gripper using threaded fasteners. This gripper had a closing force of 415N for gripping the sheet metal of 1mm thick, using the standard fingers with a stroke length of 8mm per finger. The gripping unit was tested for its quality of grip - by determining the sheet metal slippage during the hammering process. It was determined

that the sheet metal slipped axially (perpendicular to the direction of gripping force) in the direction as shown in Fig 71.

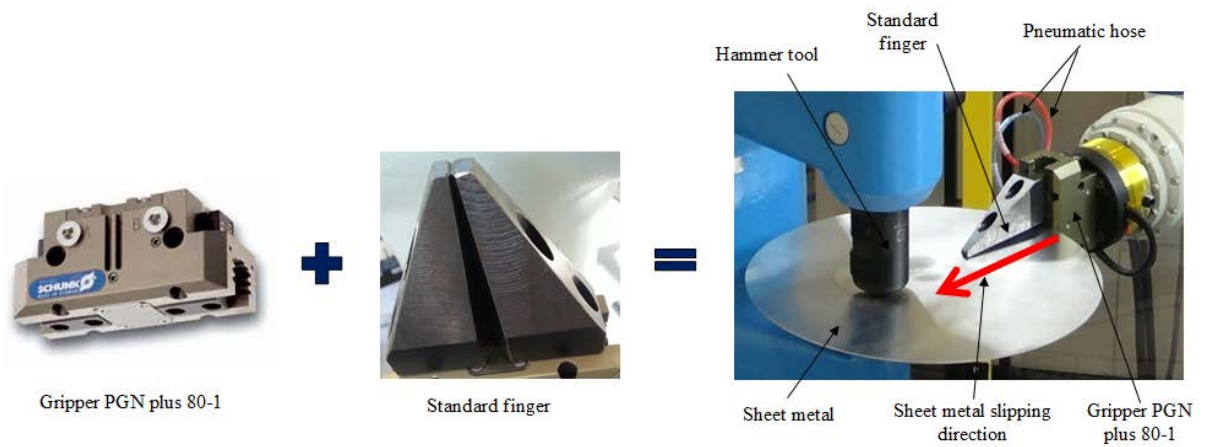


**Fig 71 - Experiments using a standard gripper**

Based on the experimental analysis it was identified that the gripping force was not enough to grip the sheet metal and it was also determined that a larger surface of grip is required to grip the sheet metal firmly at a particular position.

### **7.3.2 Gripper with the required force and modified finger design**

On careful analysis of the gripping force required and by liaising with the gripper manufacturer, the Schunk gripper PGN plus 80-2 [90] was determined as the suitable gripper for gripping the sheet metal. The gripper was an enhanced version of the PGN plus 80-1, with a shorter stroke length producing a higher closing force. The gripper produced a closing force of 860N, with a stroke length of 4mm per finger. The working pressure was similar to PGN plus 80-1 gripper but the gripper had a different permissible finger extension limits. The recommended workpiece weight that could be mounted on the gripper was twice as high as the one recommended for the PGN plus 80-1 gripper. This ensured that PGN plus 80-2 gripper will be capable of producing a firm grip as required. A complete data sheet of the grippers is provided in Appendix 7.

Analysing the requirements of the gripping surface and based on the surface area of the grip used by the skilled operator in the semi-automated system, the finger design was modified as shown in Fig 72.

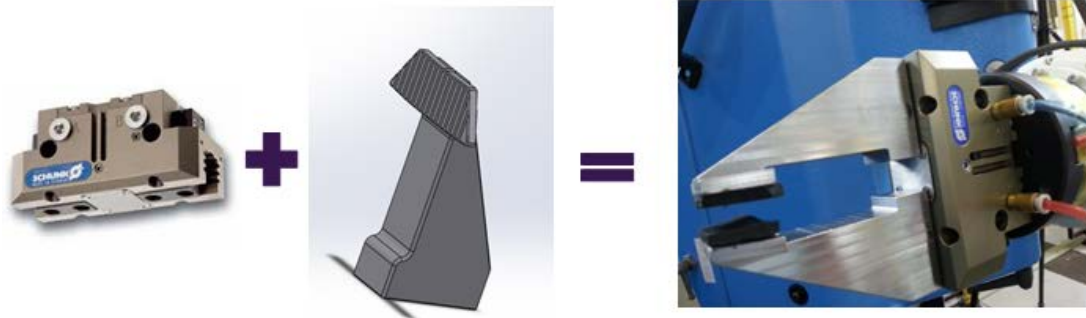


**Fig 72 - Gripper with modified finger design**

The human skill involved in gripping the sheet metal had significant influence in designing the finger. It was determined that the skilled operator uses only his thumb finger to grip the sheet metal (refer Fig 66). The grip provided significant compliance allowing the sheet metal flow without any constraints. On close observation, it was observed only the distal portion of the thumb applies a high pressure to hold the sheet metal and the proximal part of the thumb does not typically have contact with the sheet metal. To reproduce the same effect in the automated system, the gripper's head was designed similar to the surface area of the thumb and had a gradual curvature. To reproduce the same frictional effect, the head portion had a ridged surface on its gripping side. To make sure only the gripper head had contact with the sheet metal, portion beneath the gripper head was designed to be hollow.

The gripper was tested using finite element analysis for its failure under different loading conditions. Experimental analysis proved that the design's structural capabilities are adequately strong while maintaining a light weight. The finger design had a dimension of 80mm x 40mm x 20 mm with the gripping head surface of 17mm x 52mm. The groove beneath the gripping head had a dimension of 48mm x 4mm. A complete specification of the finger design is provided in Appendix 8. The finger design was fabricated using a block of steel and mounted on the gripper unit onto the end of robot's arm. Pneumatic connections were established and the gripper was tested successfully for gripping the sheet metal of 1 mm thickness. It was determined that there was a firm grip, as no slips were detected. This ensured the suitability of gripper and the finger design for the automated system. Rubber pads were added onto the gripping heads to provide the necessary dampening of vibrations. This is discussed in detail in Section 7.6.2.



#### **7.4 Transfer of human skills to the robot-operated hammering machine**

As the gripping unit was mounted on to the robot using adapter plates, the robotic arm completely replaced the human operator's arm involved in sheet metal forming. Subsequently, the position and skewing human skills related to the sheet metal (human skills 6 and 7 in Table 4) were transferred to the robotic system.

To transfer human skills 6 and 7, a user co-ordinate system was set-up between the robot and the hammering machine to ensure transformation of data between robot co-ordinates and hammer co-ordinates. The angular skewing actions required to be fed into the robot were also analysed.

During the forming of the sheet metal by skilled operator, it was also observed that the sheet metal must always be touching the anvil for the hammer to be able to apply a maximum impact force. Any clearance between the support and the sheet metal will cause unpredicted effects. Therefore, the position of the hammering machine was fixed and the top centre of the support tool (or bottom tool) was set as the origin of the user frame, to ensure that the aluminium sheet always touches the support tool. The robot's origin relative to the hammer's origin was defined to the robot. To define the robot's origin/ sheet metal's origin, it was essential to specify the tool centre point of the robot. Therefore, the tool centre point was defined by using a sharp edged calibration tool with the height of the support tool. The height difference that is likely to be caused by the bottom collar locking mechanism was also considered when positioning the sharp edged calibration tool. The top centre point of the calibration tool (shown in Fig 73) represents the top centre of the support tool.

As a firm grip was required, it was adjudicated that the gripping head of the gripping unit will grip the sheet metal 120mm away from the centre of the support tool (which will also be the centre of the bowl shape formed in the sheet metal or sheet metal's origin). Therefore, the tool centre point was defined to the robot at 120mm away from the hammer's origin in the Y-axis, by using a tough piece of metal held at the centre of the gripping finger (as shown in Fig 74). Thus, the tool centre point was successfully defined to the robot's arm with an error of 0.05mm. The origin of the robot was the same as the tool centre point. It was necessary to calculate the distance of gripping head from the hammer's origin before defining the tool centre point of the robot, to ensure the rotational motion of the robot will be about the sheet metal's origin.

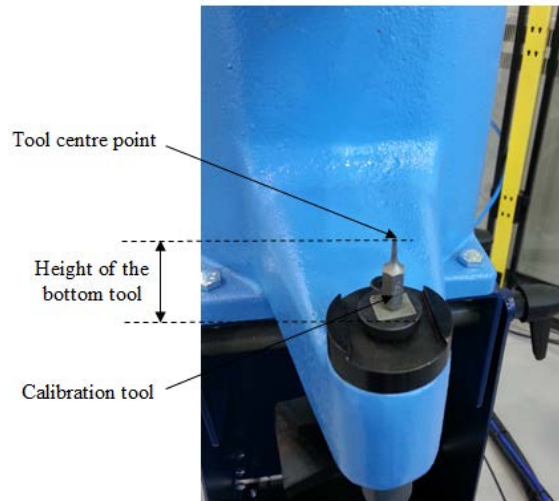


**Fig 73 - Tool centre point**

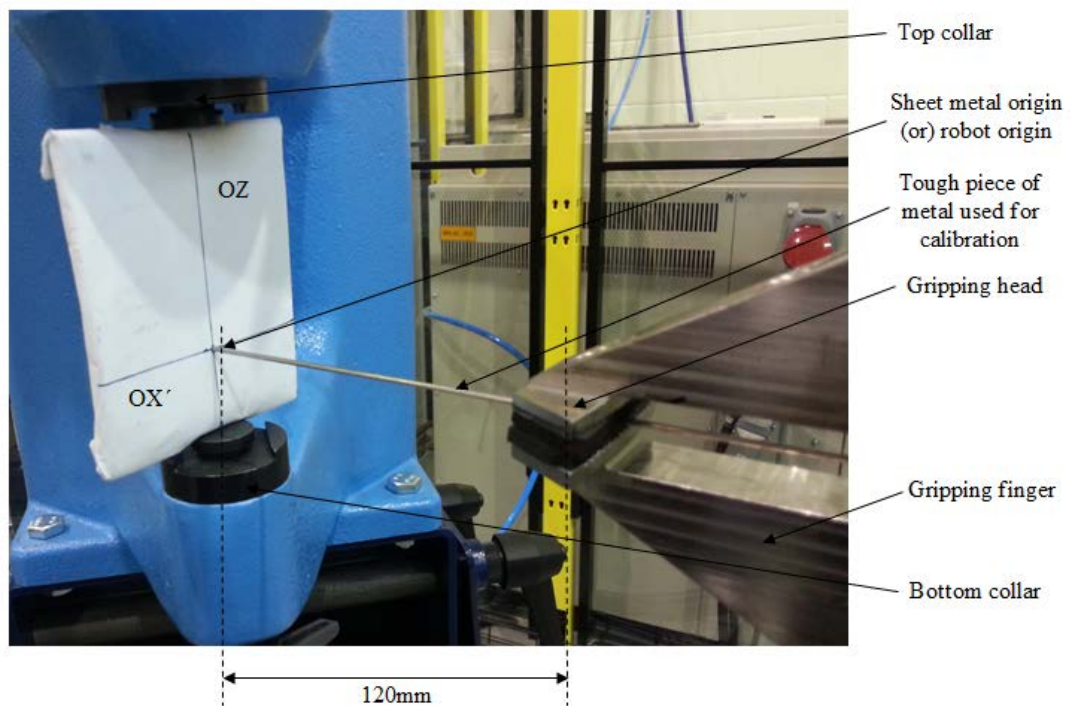


**Fig 74 - Translational directions of the robot**

The subsequent step was to define the robot's translation in the X, Y and Z axes. A calibration board was prepared to define the translation and was fixed in between the top and bottom collar of the hammering machine, as shown in Fig 74. The centre point in the calibration board where the two lines meet represents the sheet metal's origin. A tough piece of metal was held at the centre of the gripping finger at a distance of

120mm away from the sheet metal's origin to define the translational directions. The edge of the metal was moved to a point in the OX direction to define the X-axis translation and was moved in the OZ direction to define the Z-axis translation. The OY direction was identified by the robot on defining the OX and OZ direction. 'O' represents the origin. The translational directions of the robot gripping the sheet metal were tested successfully for its accuracy. The user co-ordinate was then set-up, as described in Fig 75.

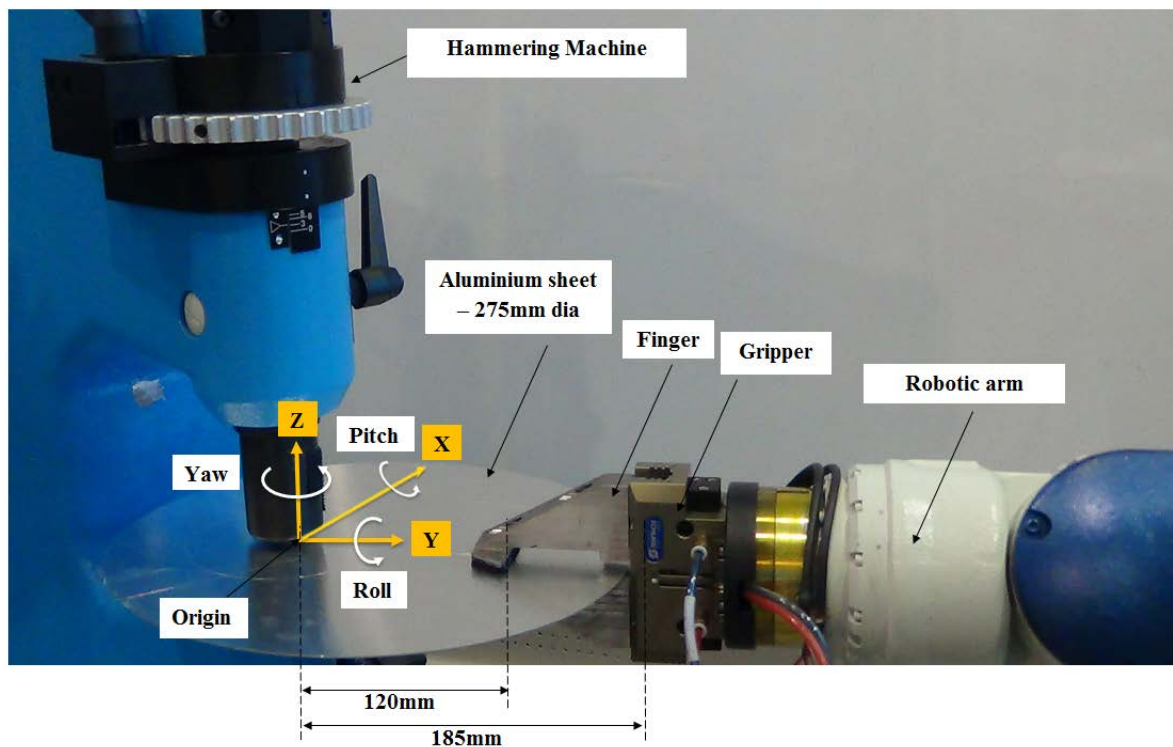


**Fig 75 - User co-ordinate set up for transfer of human skills 6 and 7**

On setting these parameters, it was ensured that the sheet metal's origin is exactly coinciding with the origin of the hammer. Therefore any translational motion of the robotic arm (along X, Y or Z axis) will now result in a positional transformation of the sheet metal. Thus, ensuring human skill 6 in Table 4 is now transferrable to the automated system.

As previously mentioned, the skewing action is important in determining the shape of the sheet metal. As it could be inferred from the Fig 75, only rolling (rotation about Y) and pitching (rotation about X) are required to perform the skewing action. Therefore any rotational motion of the robotic arm (about X or Y axis) will now result in skewing

of the sheet metal. Thus, ensuring human skill 7 in Table 4 is now transferrable to the automated system.

As the positional translation origin and skewing was set to the robot relative to the centre of hammering tool, it was also essential to programme the robot in the axial translations and skewing angles about the origin. The subsequent step was to teach the tool centre point to the robot.

### **7.5 Integration of hammering machine to the robotic system**

It was essential that a common control platform integrates systems together. The robot's controller was chosen for integrating systems as it provided the feasibility for connecting many external systems with its I/O configuration. Intending to operate hammering machine through robot controller, studies were carried out to understand the working principle of hammering machine and how it could be controlled using robot's I/O ports.

It was studied that the hammering machine uses a large spring return pneumatic cylinder to achieve the forward and reverse stroke of the hammering tool (or the top tool). It was understood that the forward/ reverse action of the hammering tool was controlled via a 5/2 way double-pilot pneumatic valve which is connected to the foot pedal. The continuous and single strokes were possible using a 3-way ball valve which is turn-key operated.

During the single stroke, the press of foot pedal produces a forward stroke in the hammering tool and retains it due to the action of spring. When the pressure is released of the foot pedal, the hammering tool reaches back to its original position. During the continuous stroke, the press of foot pedal produces a forward-reverse reciprocating action in the hammering tool due to the action of spring return in the pneumatic cylinder. The reciprocating action stops when the pressure is released from the foot pedal. It was understood that foot pedal operation has to be replaced to operate the hammering machine via the robot controller. Having investigated on the type of foot pedal and electronically controlling the hammer, it was then replaced by a 2-way normally closed solenoid valve [91] as shown in Fig 76.

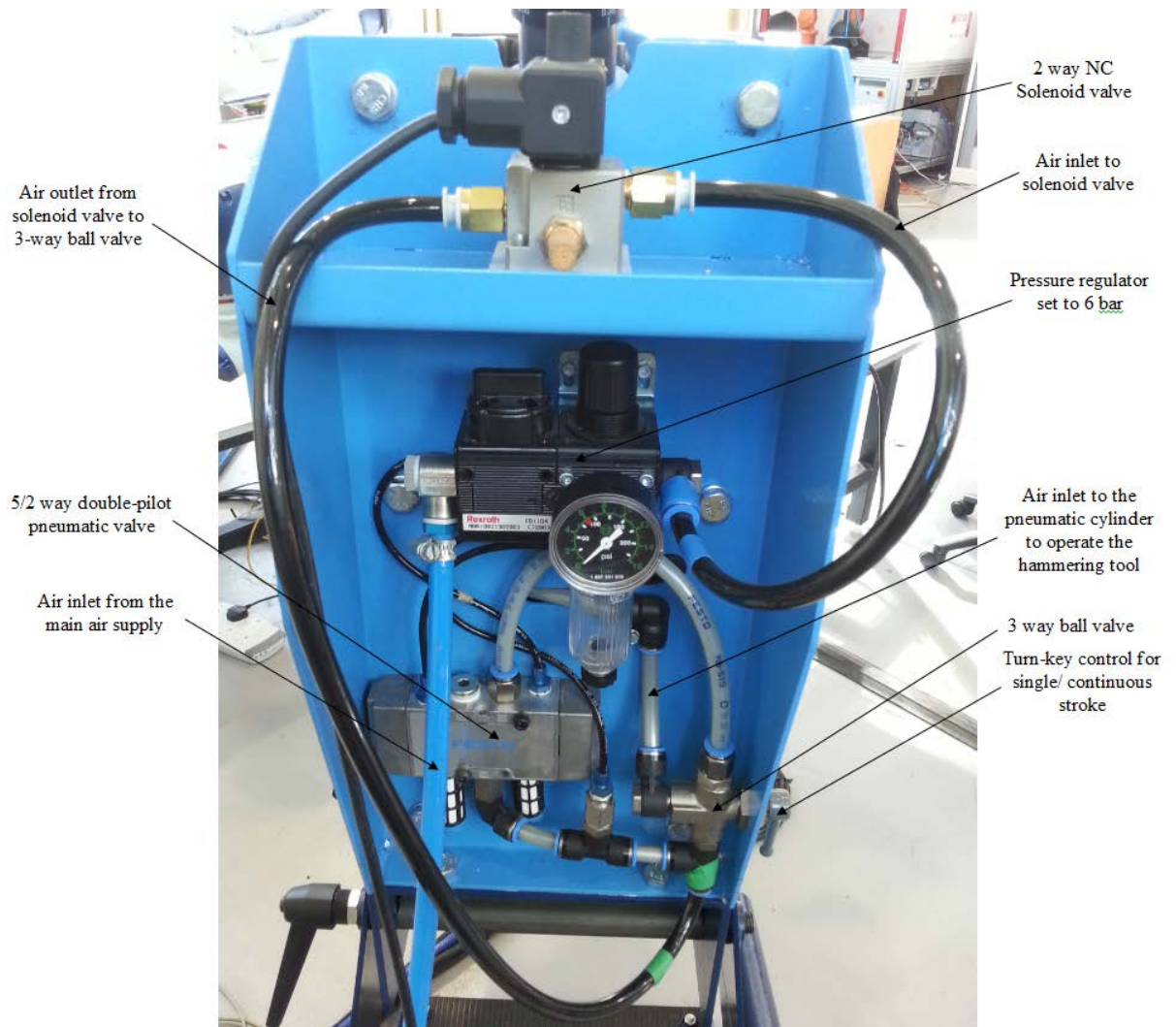


**Fig 76 - Solenoid valve replacing foot pedal in the hammering machine**

Subsequently controlling the trigger of the hammering tool was made feasible by connecting the solenoid valve to the I/O ports of the robot controller. The solenoid was connected to the two output ports, one for actuation and the other for de-actuation. An output port must be active to actuate or de-actuate the solenoid. The solenoid, normally closed, does not provide any supply of air when it is not actuated. Therefore, there is no hammering action. When the solenoid is actuated, air is supplied to the hammering machine. This produces the hammering tool impact. The action of the hammer is determined to be single or continuous by the 3-way ball valve setting. The actuation of the solenoid valve is illustrated in Fig 77.

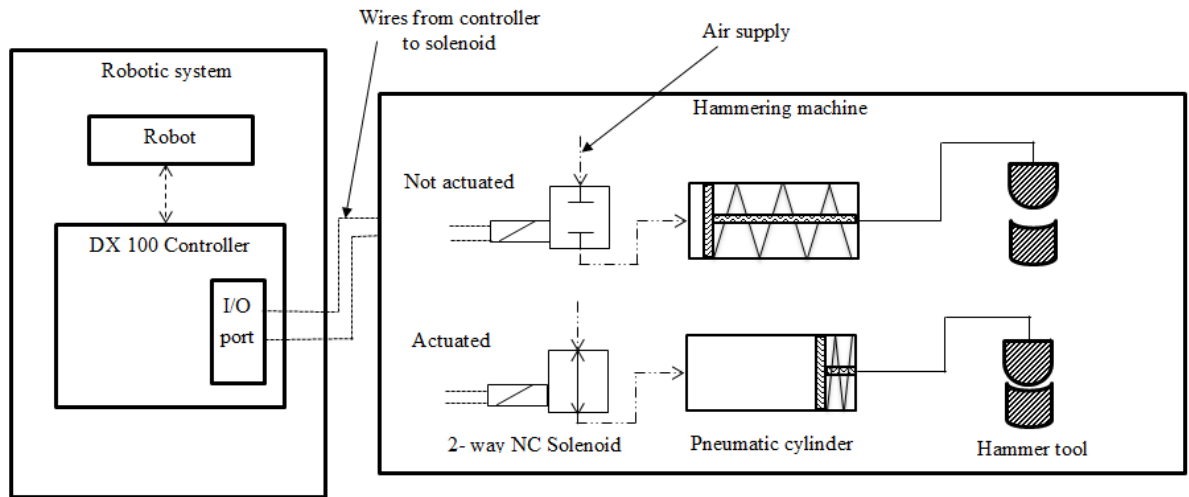


**Fig 77 - Solenoid actuation through robot controller**

Thus, the trigger control of the hammering tool via robot controller was established and the hammering tool was now programmable using the robot programming. Therefore, the hammering tool could be triggered when required for the duration as necessary.

## **7.6 Assembly and experiments on the integrated system**

As the integration of system was complete, the automated system was ready for the preliminary tests. The origin position of the robot/ sheet metal relative to the hammering tool's origin was known (refer Fig 75). Therefore, a programming algorithm was created in the robot to test the accuracy of integrated system and the capability of the gripping unit.

### **7.6.1 Findings from the preliminary tests**

The experiments included a single stroke and continuous hammering while the sheet metal is moved by the robot arm. Initially, in a single stroke hammering, the robot was programmed to actuate the gripper to position and hold the sheet metal in the predefined co-ordinates. Following this, the sheet metal was moved to its origin and the hammering tool was triggered to make an impact. The hammer was triggered for 0.25 sec based on the results from the Vicon system (refer section 6.6). In the next step, the sheet metal was moved in the positive X-direction for 5mm (point A in figure 23) and an impact was applied. Subsequently, the sheet metal was returned back to the origin and then moved for 5mm in the positive Y-direction (point B) to apply an impact at that position. The robot was moved on a linear move sequence. The sheet metal was moved to the origin and then in the Y-direction to make sure the robot does not take the



shortest route from point A to point B moving across (see Fig 78). The algorithm used is represented as a flowchart in Fig 79.

The same algorithm was used to roll the sheet metal 2° about the origin (angle obtained from the manual skewing data interpreted using the Vicon system) and then apply an impact. Reaching back to the origin, the sheet metal was pitched 2° about the origin and an impact was applied. The skewing action of the sheet metal was tested through this sequence for its accuracy.

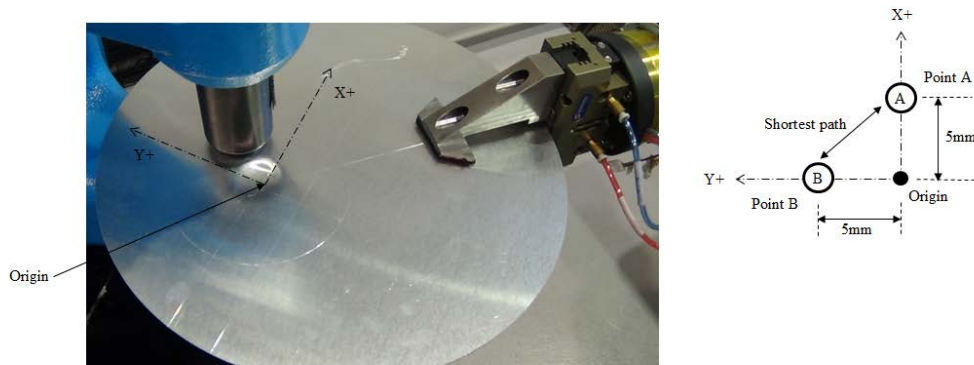


**Fig 78 - Path taken by the robot**

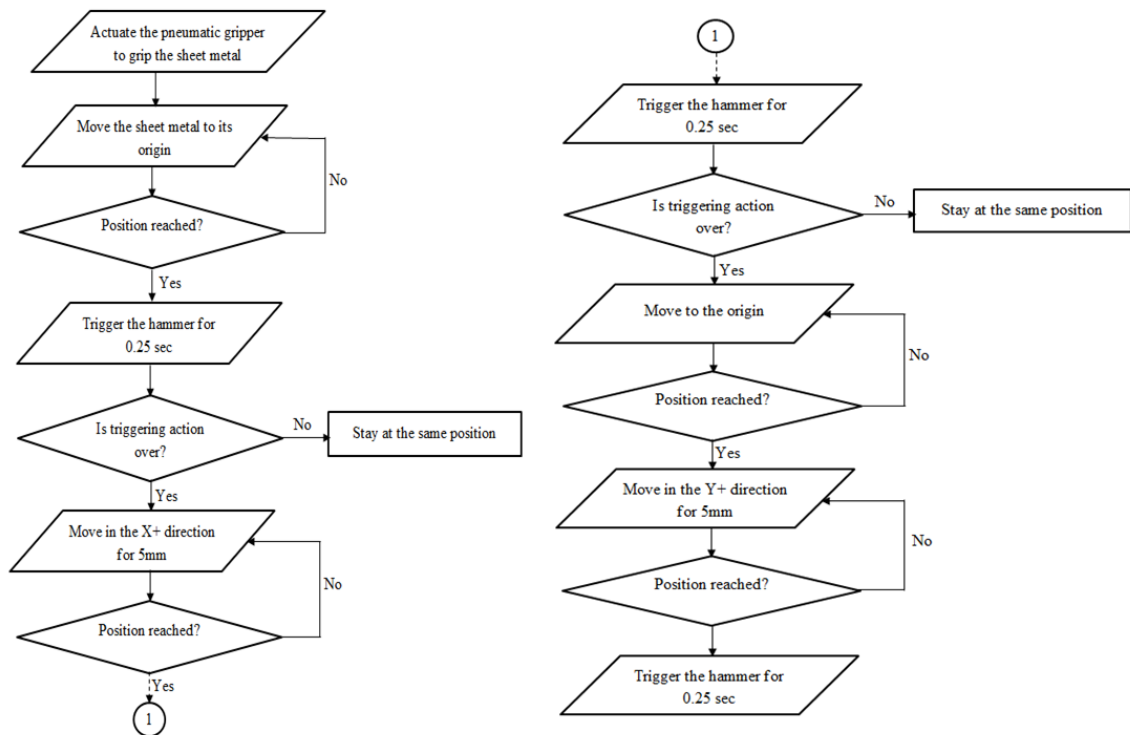


**Fig 79 - Preliminary test strategy (flowchart)**

The positional translation and skewing action were tested successfully for their accuracy with a translation error of 0.05mm and an angular orientation error of 0.1°. However, on closer inspection, it was determined that the depth 'D' of deformation at the origin is larger than the clearance 'C' between the tools (as shown in Fig 80). This caused reaction forces and resulted in the sheet metal slipping from its point of grip.

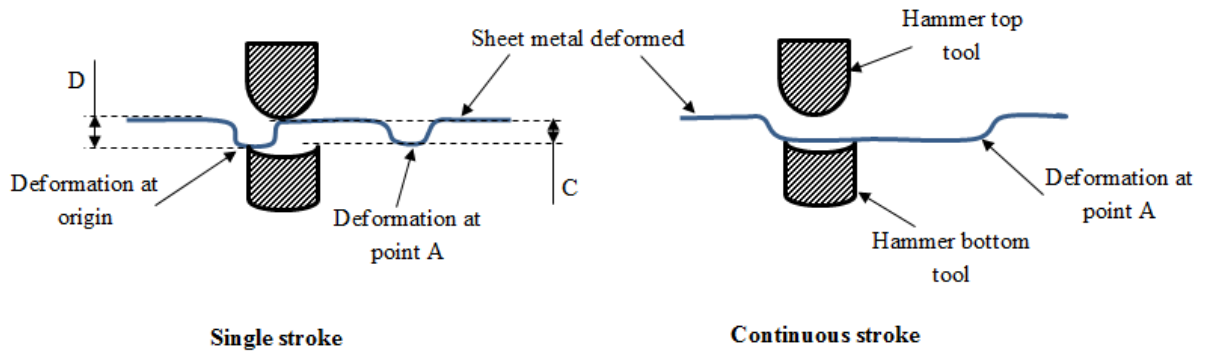


**Fig 80 - Smooth path transition in continuous stroke**

The same algorithms were used to test the sheet metal motion in a continuous stroke action. It was observed that transition from point A to the origin was very smooth, producing a good quality surface. Though observing the same problem of passing between the tools, it was insignificant compared to the motion during single stroke action.

During the single stroke, several peaks and troughs (non-deformed and deformed region) are produced in the sheet metal due to the impact at located points. Therefore, while reaching back to the origin, the sheet metal's irregular/ wavy contour will need to pass in between the hammer tools (as shown in Fig 80) which cause a significant disturbance at the region of grip. During a continuous stroke, unlike the single stroke, the deformation produced is consistent from point A to the origin. Therefore, when returning back to the origin, the transition is smooth as it passes through a consistent deformation (as shown in Fig 80). However, the clearance is not enough to pass between the hammer tools. Hence, it was adjudicated so that the continuous stroke would be used in the automated process to ensure smooth transition and a gradual flow of material.

On closely observing the gripping finger, it was realised that significant vibration is caused due to the impact forces of the hammer. Also, it was observed during the



skewing that the firm grip of the sheet metal at the gripping head caused a slight bend in the sheet metal. Thus, the mechanism required additional dampening and compliance.

### 7.6.2 Improving the compliance of the gripping unit

Based on the observation from preliminary tests, investigations were carried out to provide a dampening effect on the gripping and improve its compliance. Tests were performed using materials of different shore hardness.

Shore hardness materials, ranging from extra soft to hard, were tested to perform the previously mentioned translational and skewing motion (discussed in Section 7.6.1) during a continuous stroke action. A set of experiments were performed to determine the sufficient friction and gripping force required to grip the sheet metal. The results obtained from the shore hardness tests, measured in terms of accuracy of grip and compliance to forming motion, are shown in Fig 81.

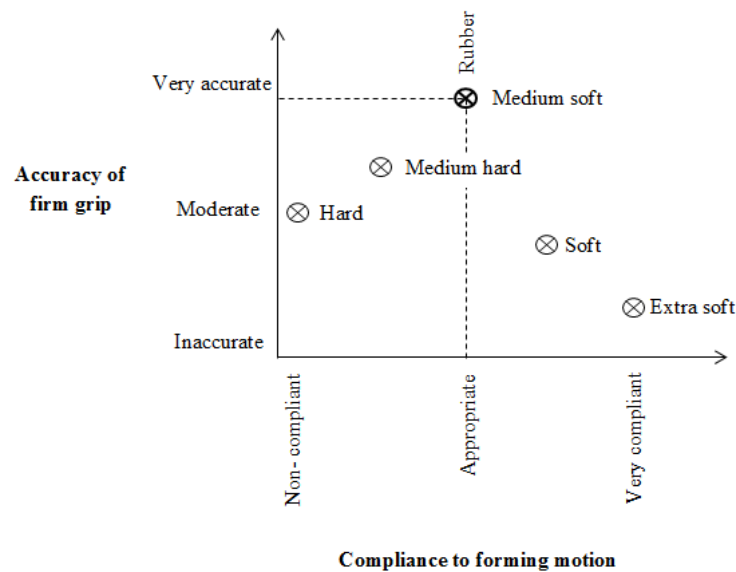


**Fig 81 - Shore hardness test**

As illustrated, the extra soft and soft materials provided a higher compliance but as a result there was lot of inaccuracy in the path. Though hard and medium hard materials provided accuracy at the beginning of the process, the accuracy dropped to moderate due to the bending effect caused by the stiff grip. Therefore, a material that could produce optimum compliance with higher accuracy was required.

When a medium soft rubber pad of shore hardness ( $\approx 80$ ) was tested, it provided the required compliance without loss in accuracy. On careful analysis, a rubber pad of 4mm thickness with the gripping side grooved (to provide necessary friction) was added to the gripping head. This provided the required compliance and damped the vibrations to an extent. However, it was anticipated that the bending effect would still persist at higher angular orientation causing inaccuracies.

Providing compliance to the gripping unit ensured that it is now possible to transfer human skill 5 in Table 4 to the automated system.

### **7.7 Summary of the integrated system and initial test results**

Based on experimental analysis, Yaskawa Motoman SDA10 robot was chosen to be used in the proposed automated system, however only one arm was used. Experiments were made on standard gripper and standard finger to analyse the requirements for replacing the human grip. Based on the analysis results, an enhanced gripper and modified finger design were used in the automated system.

The gripper was mounted onto the robot arm to replace the gripping of the sheet metal by a skilled operator. The hammering origin and sheet metal's origin/ robot's origin were defined. The position and skewing skills of a skilled operator (human skills 6 and 7 in Table 4) were transformed into quantifiable parameters to be transferred to the automated system.

The foot pedal operation of the hammering machine was replaced by a solenoid actuation. Subsequently, the hammering machine was integrated to the robot's controller to be triggered via the robot. Thus, the robot and hammering machine were both completely integrated and controllable using the robot controller.

Initial tests were performed on the integrated system to analyse the path of sheet metal manipulation by the robot and the capability of gripping unit to be used in the automated system. Initial test results proved the accuracy of the integrated system. However, there were inaccuracies in the single stroke action due to the rough/ irregular contour produced. As the continuous stroke provided a smooth path transition with insignificant disturbances, it was adjudicated that continuous stroke shall be used in the automated system.

The tests also provided an insight of non-compliant gripping. Therefore, investigations were carried out on using materials with different shore hardness for acquiring the required compliance without loss of accuracy. A rubber pad of medium soft shore hardness was determined to provide the required compliance without loss of accuracy. Therefore, rubber was added to the gripping head to provide the necessary friction and compliance.

Thus, completing the system integration and performing initial tests to enhance the system, the platform for automated panel forming was delivered. The integrated system was determined to be capable of producing a bowl shape and further tests were carried out to analyse the forming of bowl shape.

# 8. Synchronisation and path planning for the robotic automation system

---

## 8.1 Introduction

It was determined that the continuous stroke method is more suitable approach for the proposed automated system. The initial result based on guiding the robot to form a bowl shape using a continuous stroke has been discussed in this chapter, in addition to the accumulation of errors and the requirement for the synchronisation of the system components.

The initial algorithm developed, based on Archimedean Spiral [92] for forming a bowl shape has been presented in this chapter with further discussions on the final developed algorithm that led to successful forming of a bowl shape without geometrical errors.

Test results based on the successful algorithm for forming the target artefact and testing the system - to achieve a deeper profile - are discussed in this chapter, as well as the repeatability of the automated system to produce the bowl shape and the limitations of the proposed automated process.

## 8.2 Initial tests using robotic manipulation

Primary tests were performed to investigate robotic path planning when producing a bowl shape part.

Configuring the hammering machine on continuous stroke, the robot was guided to the required impact points using the robot teach pendant. The sequence of impact points were defined to the robot in teach mode (as opposed to programming) and the triggering signal was sent to the hammer through the robot. The robot positioned the sheet metal part to the required sequential impact points while the hammer was impacting the part continuously. In this simple experiment, the impact frequency was not synchronised by the motion of the robot. This test results in undesirable parts being formed, as illustrated in Fig 82.

Using a part with 275mm diameter and gripping the part as indicated earlier in Fig 75, the shape achieved deviated from the target boundary. Significant geometrical errors

and a bending at the edges were observed. There were also many geometrical patches (tool marks and lack of smoothness) in the path.



**Fig 82 - Initial test results on forming a bowl shape**

Investigating further and examining the high quality video of the process, the following significant factors were found:

- It was determined that the motion of the sheet metal part was not synchronised with the hammering frequency. This was the major reason for deviation from the target boundary and for the occurrence of impact patches on the sheet metal part.
- It is essential to analyse the geometrical path executed by the robot as it influences the shape of the sheet metal formed.
- It was also determined that the error caused due to the deviation at one impact point will accumulate as it will cause deviation to the future impact points. This would result in a faulty shape being formed.

It was found to be essential to synchronise the robotic sheet metal manipulation with the hammering frequency. Based on analysis, linear motion was set as the geometrical path to be executed by the robot.

It was also concluded as a result of this experiment that a monitoring mechanism is required to observe the forming of the part as it occurs and feedback to the robot manipulation program for optimisation through trajectory adjustments. A 3D vision measurement system was installed to measure the shape and geometrical deviation to

provide feedback for optimising the process further. The 3D vision measurement system is discussed in Chapter 9.

### **8.3 Synchronising part motions with the impact frequency**

It was understood that the incremental movement of the part using the robot should be in relation to the hammering impacts. According to the observation and the lesson learned from the manual operation captured using the Vicon system, it was identified that the hammer produces approximately 4 impacts per second. It was also determined that the skilled operator manipulates the sheet metal at the frequency of 5mm/sec during a translational motion and 2mm/sec during a skewing/ translation action (which involves translation and angular orientation). Therefore, the incremental movement of the part had to be synchronised with the frequency used by a skilled operator to achieve smooth manipulation.

A hardware linkage between the incremental movement of the robot and each hammer impact was investigated through modular programming and IO based event conditioning. This was proved to be very inefficient due to the need for high frequency hammering impacts. An alternative approach was designed and experimented based on empirical observation and evidence.

In the earlier experiment discussed in Section 8.2, the robot was operated at a speed of 1mm/sec, which resulted in the occurrence of impact patches and hammer marks. Tests were performed to observe the forming at a speed of 8mm/sec (near the maximum speed allowed to be used safely in an unprotected robotic system). It was observed that, at such high speeds, there was not enough time to develop the geometrical forms as the robot moved too quickly without complying with the hammering frequency or the material flow. On the other hand, low speed movements of the robot results in excessive overlapping of the impact points, thinning the material, and causing unpredictable forms. The part motion speed was gradually increased during a series of experiments and the forming of the part was monitored. It was found that the motion speed of 4 mm/sec would provide an optimum surface quality, geometrical accuracy, and an acceptable cycle time. Synchronising the hammering frequency with robot manipulation frequency, an essential impact was applied at the required time interval to produce the expected deformation.

Furthermore, the angular manipulation of the sheet metal part is an essential factor in the process of forming the part. Thus, speed synchronisation during angular manipulation was also essential to be optimised at the required rate. Based on the observation from the skilled operator, this was determined to be  $2^\circ/\text{sec}$ , which resulted in appropriate quality of the final part. Hence, the angular manipulations were defined at a speed of  $2^\circ/\text{sec}$  to achieve the required shape. This was embedded into the programme that defined the robot trajectory in relation with the pattern and path planning as discussed in the following sections.

#### 8.4 Path planning algorithm

An algorithm was developed based on the progressive forming methodology (refer to Section 2.3.1) used by manual panel former. However, few modifications were made to the manual forming approach to adapt to the automated environment. Considering the robot's accuracy and precision, the adaptation made the process simple and easy.

The manual panel former had a lot of spacing between the impacts while using an anvil and hammer to form the sheet metal. This practise was followed during the semi-automated approach and the frequency of hammering was initially less to accommodate the time taken to manipulate the sheet metal from one position to another. Based on analysis, it was found the same approach is not required in the automated system as more accurate solution could be achieved repeatedly. In the automated system, the impacts were very close and overlapping as shown in Fig 83 to produce a continuous and smooth forming of the sheet metal. The methodology towards applying closer and overlapping impacts is explained further in the forthcoming sections.

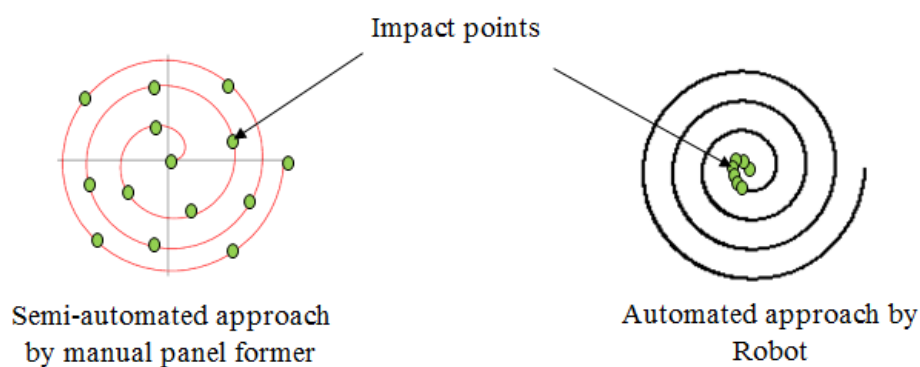


**Fig 83 - Significance of automation over manual forming**

To form the sheet metal to the required circumference, a hammer positioning algorithm was developed using the Archimedean spiral formulation with constant step sizes. Use of spiral path along with the conical helix formulation with constant step height ensured that the depth and the curvature required are formed. The Archimedean spiral is illustrated in Fig 84.

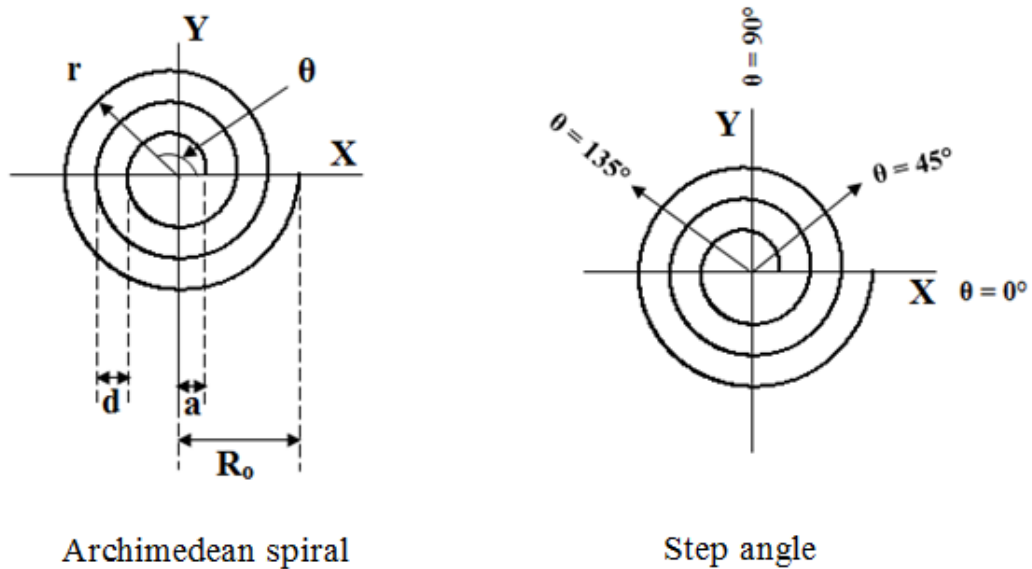


**Fig 84 - Archimedean spiral and initial increase of step angle**

If the inner radius 'a', outer radius 'R<sub>o</sub>' and the number of turns required 'n' is known, the step size (or) increasing distance between the each turn can be determined using the formula,

$$\text{Step size, } d = \frac{(R_o - a)}{n}$$

the total angle turned by the spiral is given by  $2\pi b$  (i.e., from starting point to the end) and is equivalent to the step size 'd'. From this the step size determinant 'b' could be calculated.

$$b = \frac{d}{2\pi}$$

As shown in Fig 84, the position on the spiral motion graph is determined by calculating the radius of motion 'r' to the required angle of spiral motion 'θ'. Knowing



the inner radius 'a', step size determinant 'b' and the required angle 'θ', the radius of motion can be calculated.

$$r = a + b\theta$$

Knowing the 'r' and 'θ', the position is determined in polar co-ordinates. The robot requires the Cartesian co-ordinates 'X' and 'Y' to position the sheet metal part accurately to perform the required spiral motion. So, the Cartesian co-ordinates are determined by using:

$$X = r \cos\theta$$

$$Y = r \sin\theta$$

The robot was able to perform the spiral motion after the 'X' and 'Y' co-ordinate positions were determined relatively to the increasing radius 'r' and required angle 'θ'. The spiral motion was achievable from the set inner radius 'a' to the required outer 'R<sub>o</sub>' to various step sizes 'd' by varying the determinant 'b'. This ensured the robot was capable of producing the bowl shape to the required circumference, as shown in Fig 85. The 'Z' position was not altered to make sure the aluminium sheet always touched the support tool as discussed in Section 7.4.

As shown in Fig 84, the increase of step angle 'θ' was initially set to be 45° for simplicity. It was envisaged that the step angle of 45° would produce the required bowl shape, however, the results produced led to a conclusion that 45° step angle was not appropriate as explained later in this section. By varying the step size between turns 'd' and step angle 'θ', the spacing between impacts could be changed which ensures that human skill 10 (in Table 4) could be varied according to the requirement of the contour to be formed.

The developed algorithm was used to programme the robot trajectory based on the Archimedean spiral. To test the algorithm, the robot was used to draw a graph on the surface of a sheet metal part, by locating a pen instead of the supporting tool. The programme parameters were set for producing a 130mm diameter bowl on the sheet metal part. The drawn graph was then measured and analysed, which indicated 99% precision on the drawn graph.

The consequent step in developing the path planning algorithm was to identify a strategy for forming the depth of the bowl shape required. The depth of bowl ‘D’ required along ‘Z’ axis as shown in Fig 85 was formed by applying conical helix formulation on an Archimedean spiral. The robot was required to skew the plate about X (pitch) and Y (Roll) to achieve the required depth ‘D’ and curvature of the bowl shape. To achieve this, the spiral path was segmented into four quadrants, each specifying a different skewing direction as shown in the figure, to achieve the required depth and curvature.

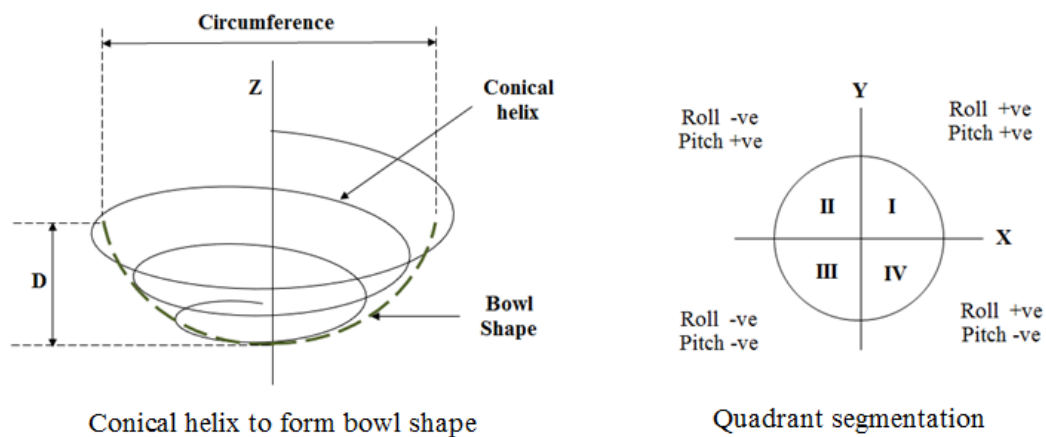


**Fig 85 - Conical helix to form bowl shape and the quadrant segmentation**

The segmented quadrants I, II, III & IV are shown in Fig 85. The rolling and pitching were incremented or decremented about the point of impact based on the criteria assigned for each quadrant.

The algorithm to form the bowl shape was executed iteratively. A single iteration consists of  $4 \times 360^\circ$  turns of the Archimedean spiral and includes an equal skewing angle in each quadrant throughout the iteration. The depth ‘D’ was achieved through progressive forming based on iteration. In the first iteration (completion of total angle turned by the spiral,  $2\pi b$ ), the skewing angle was in short increments which formed a shallower shape. In the consecutive iterations, the skewing angle was in large increments which resulted in a deeper contour with larger curvature.

A series of experiments carried out to test the algorithm. An analysis of results achieved in each experiment and a step by step improvement of the algorithm to achieve the desired bowl shape has also been explained in the following section.

### 8.4.1 45 degree step angle resulting in hexagonal shape

The initial tests were implemented using a 45° step angle (see Fig 84). Aiming at producing a circumference of 130mm diameter, 3 iterations were executed with increasing skewing angles of 3.5°, 7° and 11° from the first to third iteration respectively. The skewing angles were decided based on the bowl shape formed by a skilled operator. The input parameters to the algorithm and the results achieved using the 45° step angle is shown in Table 7 and illustrated in Fig 86.

Serial. No	Input/ Output	Input/ Output parameter	Represented by	Dimensions
1	Input	Inner radius	a	5mm
2		Outer radius	R <sub>o</sub>	65mm
3		Step size	d	15mm
4		Step angle	θ	45°
5		Skewing angle	Roll and Pitch	3.5°, 7°, 11°
6	Output	Circumferential edge	Circumference	Hexagon with diameter of 136mm along X axis and 141mm along Y axis
7		Depth	D	9.50mm
8		Thickness	T	Irregular

**Table 7 - Inputs for forming the target artefact with 45 deg step angle**

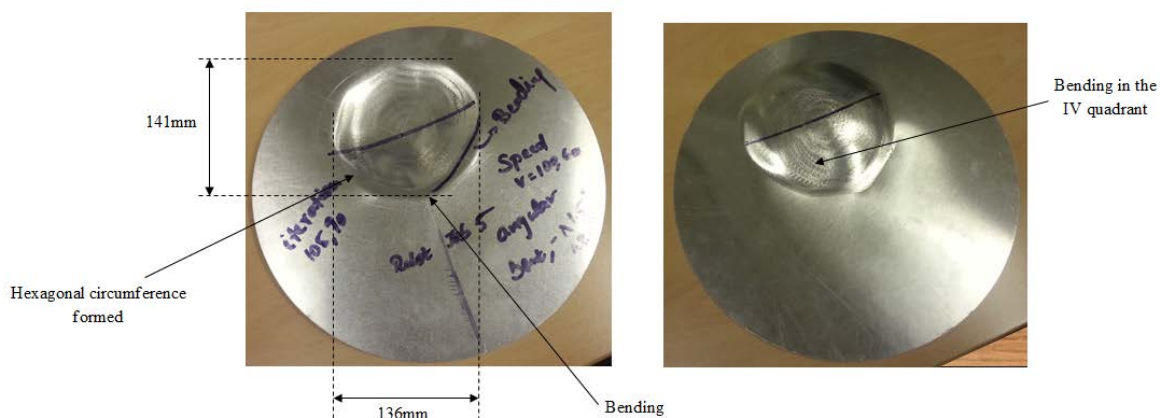


**Fig 86 - Results obtained with 45 deg step angle**

As it was noted, a hexagonal circumference was produced instead of a circular shape, as it could be expected from the 45 degree angular increments. Nevertheless, there was a good depth formed at the centre. By moving the impact points towards the outer edge of the bowl shape, the incremental movement had to be increased to cover the area, and therefore more curvature irregularities appeared on the outer side of the formed part. A significant bend was also identified in the IV quadrant and along the axis of gripping at the edge of the circumference formed. Through frame-by-frame examining of the process, the cause was determined to be the lack of gripping compliance. The experiment was repeated for 5 trials by attaching rubber pads to the gripping surfaces, which led to improvement of the results as summarised in Table 8.

<b>Exp. No</b>	<b>Diameter along X axis (mm)</b>	<b>Diameter along Y axis (mm)</b>	<b>Depth (mm)</b>	<b>Bending along the axis of grip</b>	<b>Bending in the IV quadrant</b>
<b>1</b>	136	141	9.50	8°	Yes
<b>2</b>	134.5	140	9.60	9°	Yes
<b>3</b>	138	140.5	9.30	7°	Yes
<b>4</b>	133.7	139	10	11°	Yes
<b>5</b>	135	142	9.20	11°	Yes

**Table 8 - Experimental trails with 45 deg step angle**

The hexagonal circumference formed in the sheet metal was off-centred by 10mm due to the effect of bending along the axis of grip. As shown in Table 8, the errors were consistent and required a modification to the path planning algorithm as described in the following section.

#### **8.4.2 Modifications to the algorithm**

Targeting at eliminating the bend in the IV quadrant, analyses were made by disseminating the video of automated panel forming executed with a 45° step angle algorithm. It was determined that during transitions between quadrants there was a motion ambiguity and the angular transition was not gradual. It was identified that in-between each quadrant transition there is an additional state where either only rolling or pitching occurs when it is along the axis. Therefore, four new segmentations were introduced into the algorithm as shown in Fig 87.

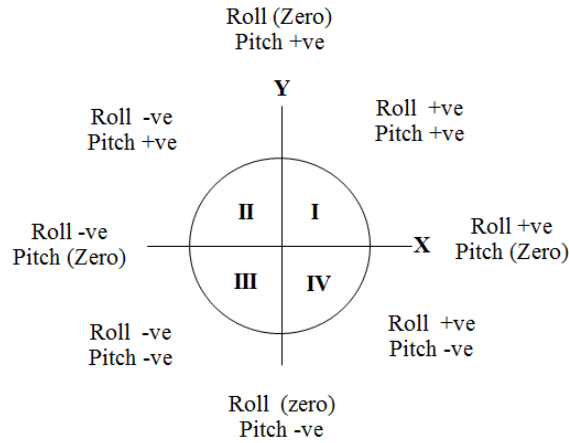


**Fig 87 - Additional segmentations for skewing**

After running the new 8 segment algorithm, the more successful forming was achieved as shown in Fig 88. The inputs were given to produce a bowl shape of 100mm diameter. Therefore, only 3 x 360° turns were executed per iteration. Introducing 8 segmentations eliminated the bend in IV quadrant and provided a gradual transition between quadrants. This also improved the geometrical shape produced. However, the bending along the axis of grip was still occurring due to which the shape produced was off-centred from the target by 10mm. Also, a hexagonal circumference was still being produced instead of a circular circumference.



**Fig 88 - Results based on 8 segments**

Investigations were made to analyse the cause of producing a hexagonal circumference. It was determined that the step angle of 45° was a reason due to which a hexagonal circumference was produced. Therefore, the step angle was reduced to 10° as shown in

Fig 89. This increased the precision of spiral being formed and resulted in producing a regular circular shape as required.

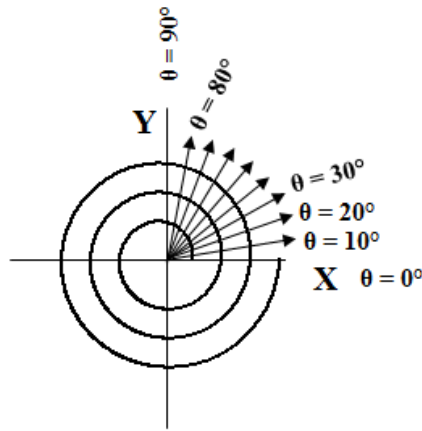


**Fig 89 - Minimising the step angle to 10 deg**

Aiming at producing a similar 130mm bowl shape, a single iteration had 4 x 360° turns. Only 2 iterations were executed at increasing skewing angle of 3.5° and 7°. This resulted in a depth of 6.50mm. Though a complete circle was formed, as shown in Fig 90, the bend in IV quadrant re-occurred. It was identified that the bend along the axis of grip is also causing the bend in IV quadrant which was not as significant compared to the earlier IV quadrant bend discussed in Section 8.4.1. The bend along the axis of grip also caused the bowl shape formed to be off-centred by 10mm. Therefore investigations were focused on understanding the cause and resolving the part bend along the axis of grip.



**Fig 90 - Results of minimising the step angle to 10 degrees**

### 8.4.3 Perpendicular positioning of the sheet metal relative to the hammer's origin

As mentioned earlier, the angular skewing of the sheet metal is about the point of impact. Examining the video of earlier experiments confirmed that skewing was made around the point of impact. However, analysing the video of skilled operator determined that the angular skewing of the sheet will have to be relative to the origin of the hammer's support tool. Investigating further, it was determined that the impact point on the sheet metal part should always be perpendicular to the hammer's centre or origin. This will avoid lateral forces and will ensure that the impact causes maximum deformation and provides the required shape definition to the impact point.

Fig 91 illustrates that if the point of impact is at angle to the hammer's centre, there will be a bending effect along the axis of grip. This is due to the hammer's impact force trying to form the material but the gripper restraining the movement of part and try to maintain the position of the sheet metal part relative to the hammer's centre. This issue was resolved by locating the sheet metal's impact point to always be perpendicular to the hammer's centre. As a result, a maximum deformation and a high shape definition will be achieved.

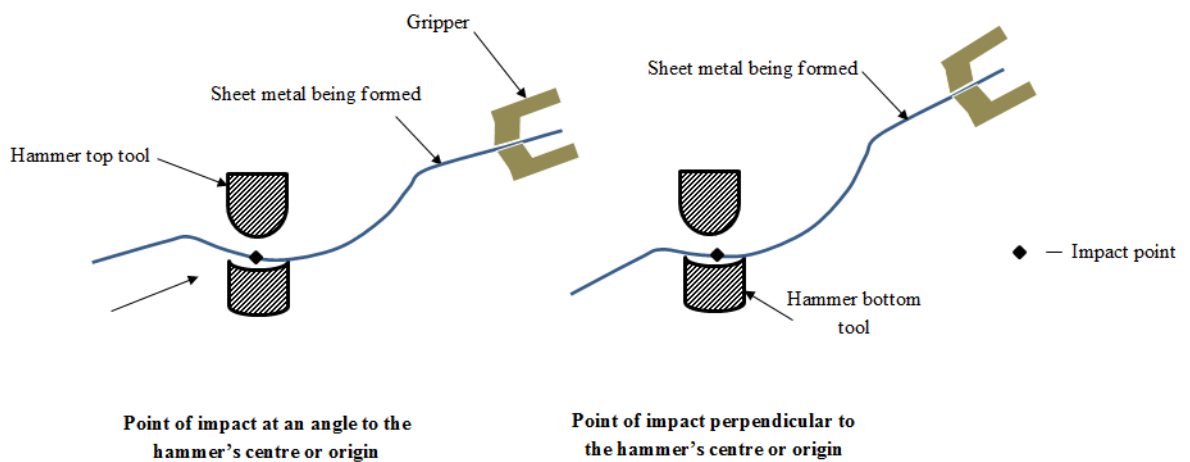


**Fig 91 - Sheet metal's point of impact always perpendicular to the centre of hammer**

Accordingly, the algorithm was modified to provide the skewing relative to origin which made the sheet metal's impact point perpendicular to the hammer's centre. Thus,

the bend along the axis of grip was eliminated, as shown by Fig 92 (part shown on the right side).



**Fig 92 - Results based on skewing sheet metal perpendicular to the hammer's centre**

Targeted at producing a bowl shape of 100mm, a single iteration executed 3 x 360° turns. The angle of skewing was increased at a rate of 3.5°, 7° and 11° to acquire the desired depth and curvature. Applying the skew relative to the hammer's origin eliminated the bending in IV quadrant and also the bowl shape was formed in the target circumference. A complete bowl shape was formed with a diameter of 105mm and a depth of 10.20mm. The diameter was slightly more than expected as the finish of the hammering sequence was not shortened within the bowl shape's circumference. This is explained further in the next section.

#### **8.4.4 Further enhancement of the algorithm**

As explained in the experiments performed, the skewing was applied from the beginning of the process. However this is not the case with the bowl shape formed by the skilled operator. As observed from the bowl shaped formed by the skilled operator, the centre of the bowl is almost planar and then it gradually curves to become a circular bowl as illustrated in Fig 93.





**Fig 93 - Planar surface of the bowl**

To accommodate this scenario, the first 360° turn in all the iterations the skewing angle was set to zero. Therefore, a planar surface was formed initially and then it gradually curved into a bowl.

As mentioned in Section 8.4.3, the diameter of the bowl shape formed elapsed slightly due to the error in finishing the spiral. As a constant step size determinant 'b' was used in the Archimedean spiral to achieve a constant size 'd', the circumference of the spiral was ever increasing. This caused the occurrence of extra impacts in the bowl shape being formed as shown in the Fig 94.

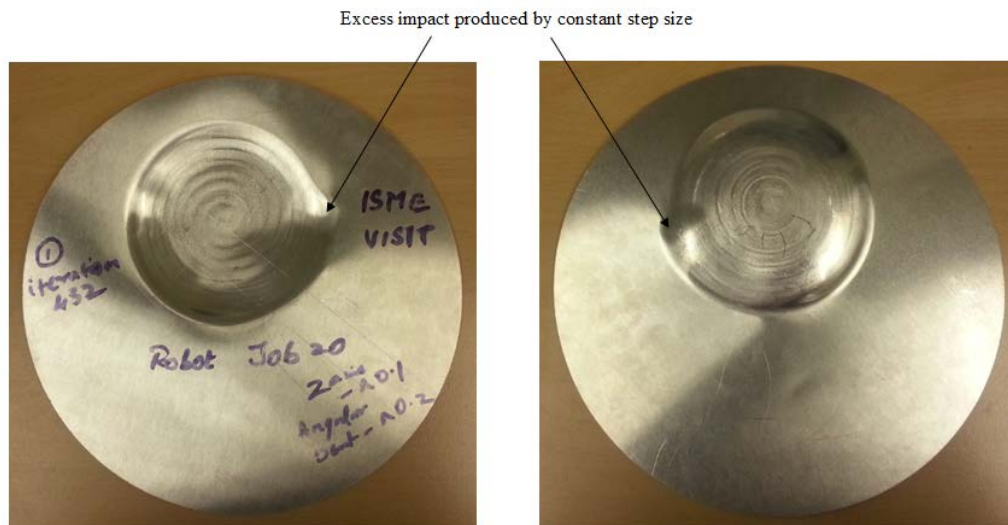


**Fig 94 - Excess impact due to constant step size determinant**

Therefore, it was necessary to decrease the value of step size determinant 'b' gradually to achieve a complete circular shape without an excess impact. Hence, the algorithm was modified to have gradual decrement in the step size in the last 360° turn. This decrement started from 180° to end at 0° (starting axial direction X+) as shown in Fig 95. This gradually finished the bowl into a perfect circular shape.

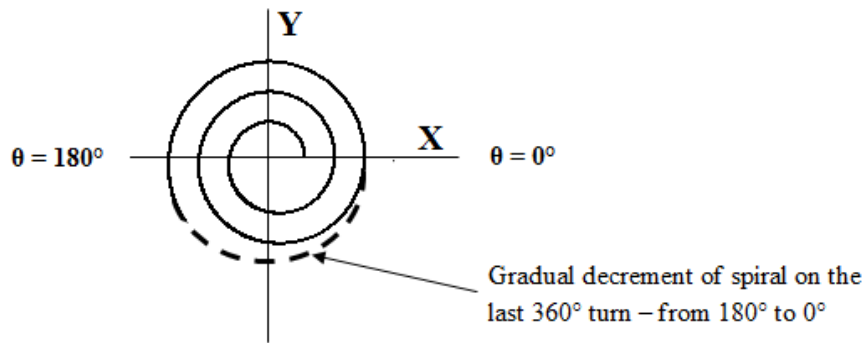


**Fig 95 - Gradual decrement of step size**

The finish achieved based on decrementing the step size is shown in Fig 96. Based on the successful achievement of the target artefact, further tests were performed to analyse the consistency of forming and robustness of the system.



**Fig 96 - Improved finish**

### 8.5 Results based on the successful manipulation algorithm

Following several rounds of tests, observations, and refinement of the manipulation algorithm, the final path planning sequence of processes that tested successfully to form the bowl shape of any circumference and depth is shown in Fig 97.

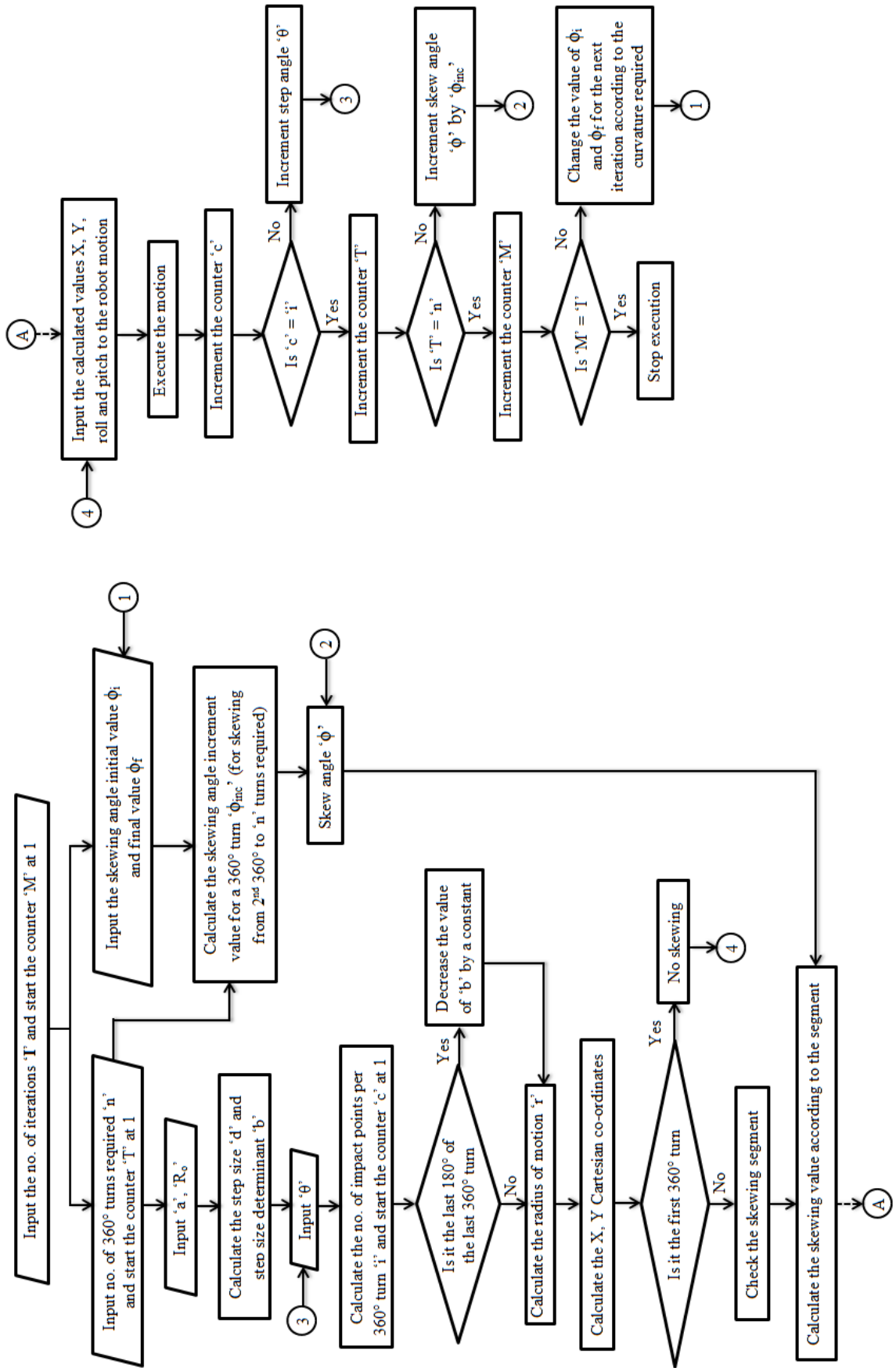


Fig 97 - Successful algorithm for forming a bowl shape

As demonstrated, the initial number of iterations and full 360° turns required per iteration were provided as inputs. Also, the values required for calculating the radius of the spiral motion were also given as input. In addition, the initial and final skewing angle required to be gradually incremented to form a bowl shape is also given as input. For each impact, the X, Y, roll and pitch values were calculated based on the user inputs and were provided as inputs to the robot parametric program to manipulate the sheet metal. Once the motion was executed (by locating the part at predefined impact point), the step angle was increased to move to the next impact point. For the first 360° turn there was no skewing to obtain a planar surface at the centre of bowl shape.

For the other 360° turns, the skewing angle was calculated according to the segments and fed to the program to define the robot trajectory. Conditions were applied to the programme to ensure that if a 360° turn were over, the skew angle would be incremented according to the calculated value and provided as input to the next 360° turn. However, if the execution was in the last 180° of the last 360° turn, then the step size would be decremented to achieve a circular finish. Once the iteration was over, the initial skew angle and the final skew angle values were changed for the consecutive iteration to obtain a deeper bowl shape and increased curvature. The process continues to form a bowl shape until all the iterations are completed. The hammering tool was set to trigger at the beginning of the process in the continuous stroke action and was stopped only when the process execution was completed.

Using the above algorithm, two sets of experiments were performed. The experiments were aimed at producing a shallower bowl with larger circumference and a deeper bowl with smaller circumference. The results of the experiments are discussed below.

### **8.5.1 Experiment 1**

The first experiment was aimed at producing a bowl shape of 130mm diameter with a depth of 15mm. 10 trials were performed to assess the consistency of the bowl shape formed. The inputs and outputs of the first trials are given in Table 9.

S. No	Input	Input parameter	Represented by	Dimensions
1		Iteration	I	2
2		No. of 360° turns	n	4
3		Inner radius	a	5mm
4		Outer radius	R <sub>o</sub>	65mm
5		Step size	d	15mm
6		Step angle	θ	10°
7	Skewing angle	φ for first 360° turn	0°	
		φ <sub>i</sub> and φ <sub>f</sub> (for I = 1)	0° and 3.5°	
		φ <sub>i</sub> and φ <sub>f</sub> (for I = 2)	3.5° and 7°	
S. No	Output	Output parameter	Represented by	Result
8		Circumferential edge	Circumference	132.5mm
9		Depth	D	6.60mm
10		Thickness	T	0.98mm
11		Execution time	t	205 sec

**Table 9 - Experiment 1 - 1st trial**

In this experiment, the spiral had 4 x 360° turns to produce a bowl shape with 130mm circumference. For the first 360° turn, the skewing angle was set to zero to make sure the centre surface of the bowl is planar and not curved. For the following consecutive turns, the skewing angle was incremented to obtain a gradual curvature according to the calculated value based on φ<sub>i</sub> and φ<sub>f</sub>. The initial and final skewing angles for the two iterations were defined as shown in Table 9. Accordingly, the skew angle was calculated to produce the required curvature and depth values. Iterations were performed to a total of a 7° skew angle, producing a depth of 6.60mm. It took 205 sec for the robot to produce a bowl shape with a circumference of 132.5mm and depth 6.60mm.

As it could be inferred from the results, the part from the first trial has significant deviation from the target shape due to the inappropriate constant value used to decrement the step size determinant 'b' in the last 180° of the spiral shape formed. The accuracy of the diameter of bowl shape formed in the 10 trials is shown in Fig 98. The forming had a geometrical error of +1mm as shown in Fig 99. The cycle time was almost nominal for all the 10 trials as shown in Fig 100.

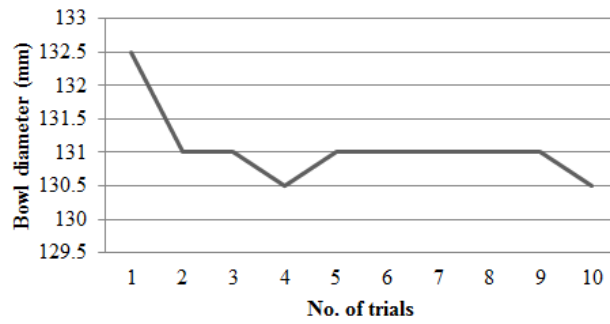


**Fig 98 - Accuracy of the bowl diameter formed (Exp 1 - trials)**

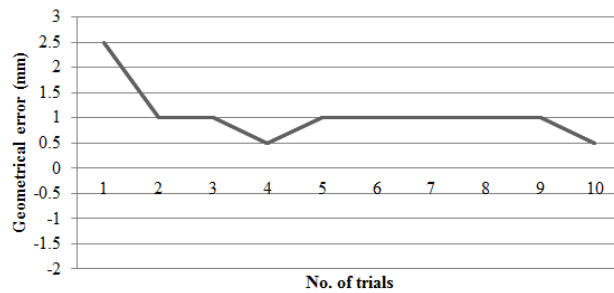


**Fig 99 - Geometrical error of the final bowl shape formed (Exp 1 – trials)**

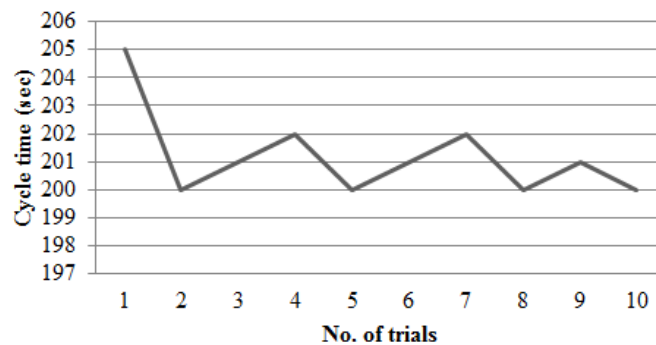


**Fig 100 - Cycle time for forming a bowl shape (Exp 1 – trials)**

As shown in Fig 98, the diameter of the bowl shape formed, only had a deviation of 1 mm (on an average) to the target bowl diameter required. Also, the diameter of the bowl shape formed was always in excess, representing a consistent positive geometrical error, as shown in Fig 99. Based on these results, it was determined that the dimensions of the bowl shape formed are almost 95% repeatable with a deviation of only 1% in the shape formed compared to the target form.

The bowl shape had a uniform thickness of 0.98mm, almost unchanged from the initial aluminium sheet thickness of 1mm, as shown in Fig 101. This ensured the quality of material formed enhanced by using the automated process.

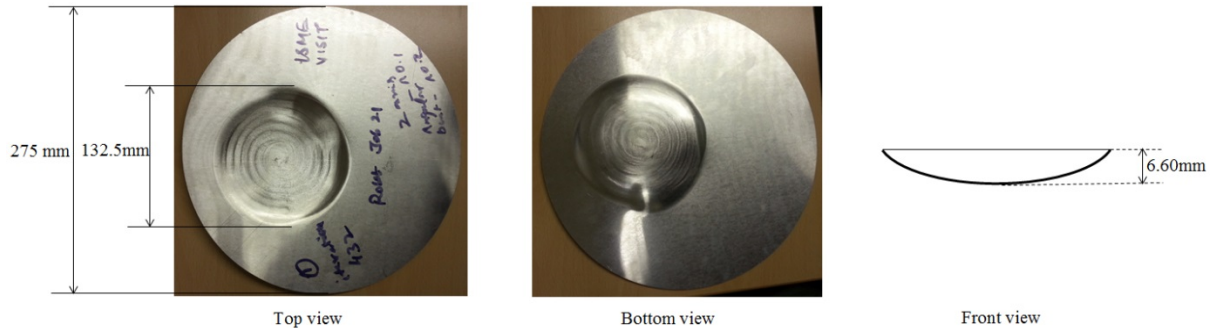


**Fig 101 - Result of Experiment 1 - 1st Trial**

### 8.5.2 Experiment 2

The next test was aimed at reducing the diameter of the bowl shape to 100mm and increasing the depth of forming. The inputs and outputs of the first trial of this experiment is given in the Table 10.

A 3 x 360° turn spiral was calculated to produce a bowl shape with 100 mm diameter. As discussed earlier in experiment 1, the skewing angle for the first 360° turn was zero and then the skewing angle was gradually incremented to obtain the curvature required. The skewing angle was incremented until 15°, as mentioned in Table 10. Though 18° skewing was possible in the fifth iteration, there was ambiguity in the forming due to the aluminium sheet skewing being limited by the vertical and horizontal throat depth limit of the hammering machine. This is discussed later in Section 8.6. Hence, the execution was completed with four iterations forming the aluminium sheet to depth of 10.60mm and 100.4mm in circumference. It took the robot 235 sec to produce a deeper bowl shape.

S. No		Input parameter	Represented by	Dimensions
1	<b>Input</b>	Iteration	I	4
2		No. of 360° turns	n	3
3		Inner radius	a	5mm
4		Outer radius	R <sub>o</sub>	50mm
5		Step size	d	15mm
6		Step angle	θ	10°

7		Skewing angle	$\phi$ for first 360° turn	0°
			$\phi_i$ and $\phi_f$ (for I = 1)	0° and 3.5°
			$\phi_i$ and $\phi_f$ (for I = 2)	3.5° and 7°
			$\phi_i$ and $\phi_f$ (for I = 3)	7° and 11°
			$\phi_i$ and $\phi_f$ (for I = 4)	11° and 15°
<b>S. No</b>	<b>Output</b>	<b>Output parameter</b>	<b>Represented by</b>	<b>Result</b>
8		Circumferential edge	Circumference	100.4mm
9		Depth	D	10.60mm
10		Thickness	T	0.95mm
11		Execution time	t	235 sec

**Table 10 - Experiment 2 - 1st trial**

The diameter of the bowl shape formed was only 0.5 mm in excess to the target bowl diameter required as shown in Fig 102. As observed from the results, the accuracy of bowl diameter formed is very high with a geometrical error of +0.5mm as shown in Fig 103 and consistently positive. From the results, it was concluded that dimensions formed were 98% repeatable and had a deviation of less than 1% to the target form.

The cycle time was almost consistent except for one trial where it was quicker by 4 sec as shown in Fig 104.

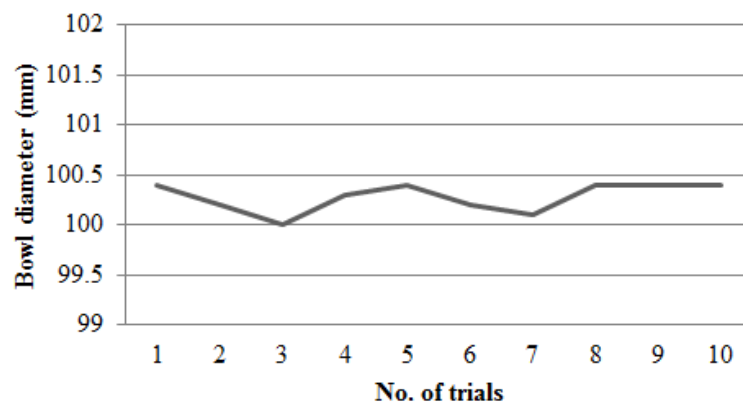


**Fig 102 - Accuracy of the bowl diameter formed (Exp 2 - trials)**



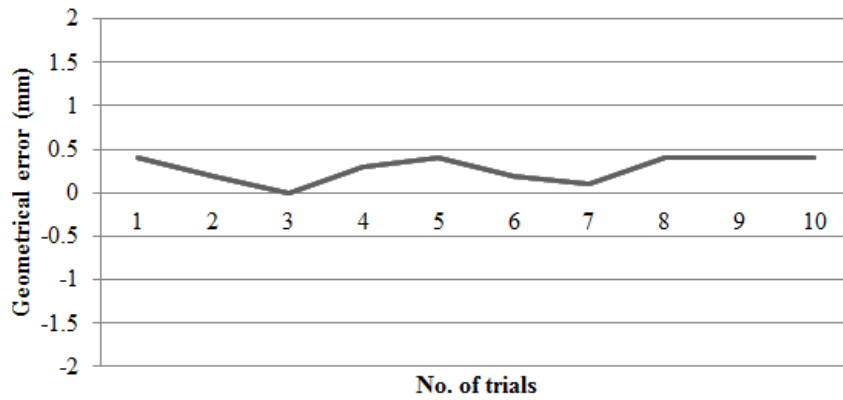


**Fig 103 - Geometrical error of the final bowl shape formed (Exp 2 – trials)**

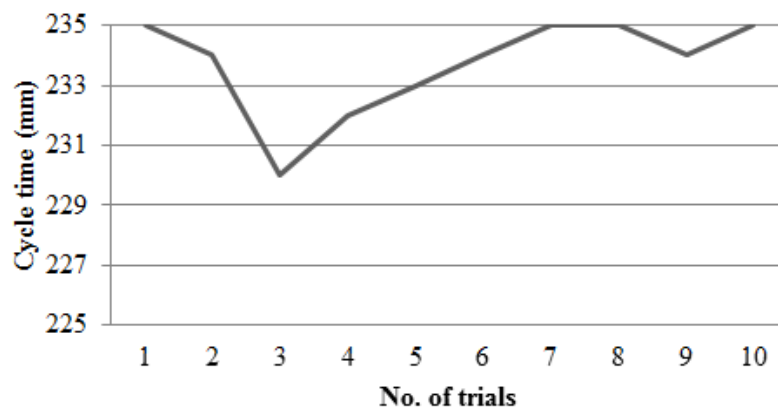


**Fig 104 - Cycle time for forming a bowl shape (Exp 2 – trials)**

The bowl shape formed had a uniform thickness of 0.95mm ash shown in Fig 105. The finish quality of the bowl shape formed was good and smooth. The thickness distribution was uniform and a nearly perfect bowl shape was formed with the required diameter and depth.

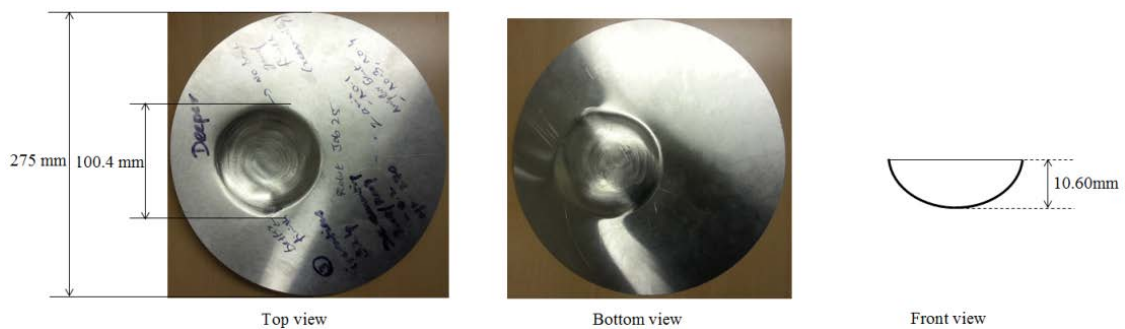


**Fig 105 - Results of Experiment 2 – 1st trial**

## 8.6 Limitations of the automated system

The results achieved were limited to forming a bowl shape of maximum 130mm diameter and 10.60mm depth at a 15° curvature. Although higher skewing angles were possible, there was a limitation in the size of the hammering machine as shown in Fig 106.

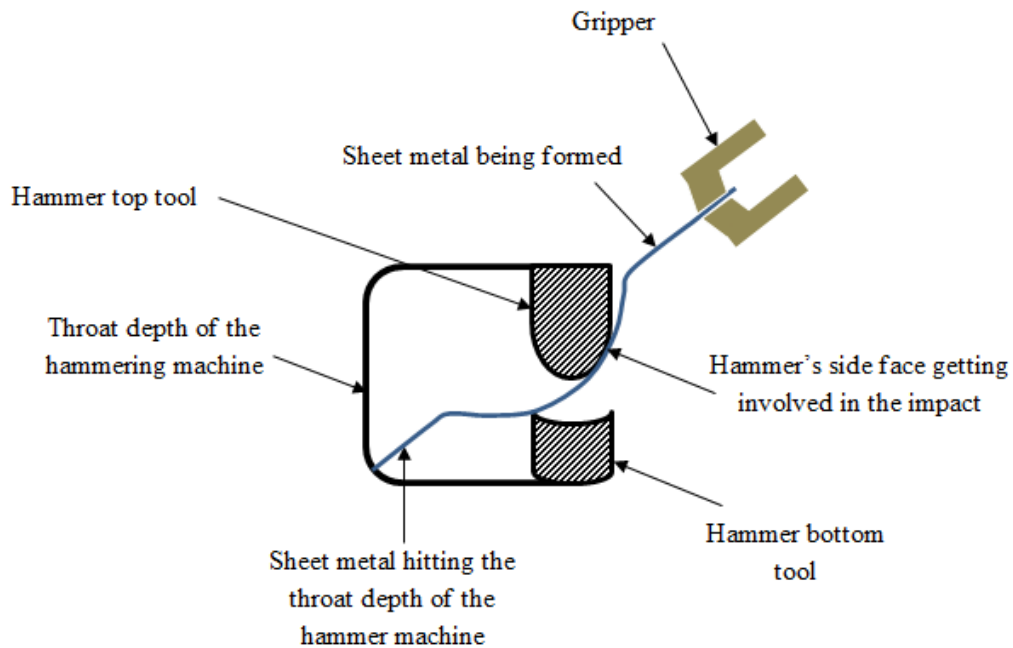


**Fig 106 - Limitations of the automated system**

The throat depth of the hammering machine is 146mm high and 170mm wide. However, the sheet metal being formed hits the throat depth of the machine at extreme skewing angle as shown in Fig 106. This causes concerns to the system as the sheet metal may either get bent or slip from the region of grip. Also, during such extreme skewing angles (such as 21°), the hammer's side face comes into contact with the sheet metal being formed. This results in a faulty shape being formed. These are the two major physical factors that limit the forming to the circumference of 130mm and a depth of less than 11mm.

Nevertheless, this could be overcome by using a hammering machine of larger throat depth available in the market. The problem caused by the hammer tool could be resolved by using a hammer tool of reduced impact surface. The impact face of the hammering tool which is currently 40mm wide could be reduced to 10mm to increase the accuracy of forming.

## **8.7 Summary of the results achieved**

Initial tests were carried out to analyse the challenges in forming a bowl shape using the automated system. Based on the analysis, it was determined that the geometrical path taken by the robot's arm, accumulation of errors and synchronisation between the hammering frequency, and sheet metal manipulation frequency are significant factors to produce the bowl shape successfully.

Therefore, based on analysis, the geometrical path was set to a linear motion. The hammering frequency and the sheet metal manipulation frequency were synchronised. The accumulation of errors is envisaged to be solved by using a 3D measurement system which is discussed in Chapter 9.

A path planning algorithm with Archimedean spiral to obtain the circular circumference and a conical helix to obtain the depth was used. Using the algorithm developed, initial tests were performed. Based on the results achieved, several modifications were made on the path planning algorithm and the significance of manipulating the sheet metal perpendicular to the centre of hammer was recognized. A final algorithm to form a bowl shape of any required circumference and depth of curvature was generated. The inputs to the automated system were defined.

Based on the final algorithm, two sets of experiments were performed and their results have been discussed. Based on the results achieved, it was determined that the automated system forms the bowl shape consistently and is 98% repeatable with a deviation of less than 1% from the target shape. However, this is the ideal case of the automated system and errors may be possible due to the deviated position of grip of the sheet metal and several other factors.

## **9. In-process measurement of forming**

---

### **9.1 Introduction**

In the manual forming process, it was observed that operators inspect the part formed frequently during the process. These inspections are carried out visually or by using simple gauges and templates, and then the forming process is readjusted accordingly.

The developed automated system successfully forms sheet metal parts to the required shape with 1% deviation from the target form. However, there are possibilities where accumulation of errors could result in a more significant deviation from the target shape and the predicted forming process. Therefore, monitoring the forming process through an in-process measurement of the shape being formed was considered to be essential to address inspection and rectification methods that human operators use.

Following investigations and a review of the literatures, the 3D vision measurement approach was determined to be the most appropriate solution as it provided the required measurement resolution. Subsequently, further investigations were carried out to identify the suitable 3D vision measurement system that could be used to scan a smooth and reflective surface such as aluminium. On careful analysis, 3D vision measurement using laser triangulation was identified as a suitable system to measure the sheet metal being formed and to monitor the automated panel forming.

The principle of laser triangulation is explained in this chapter. The green laser scanner and the experimental set-up for obtaining the point cloud data is also explained in detail. Furthermore, image processing of the acquired point cloud data to measure the depth and area of the sheet metal being formed is discussed in this chapter, along with the description of the experimental tests carried out.

Based on the results obtained, an error rectification methodology is proposed based on the in-process measurement approach.

### **9.2 Laser scanner set-up**

A laser scanner setup consists of two main components, a camera and a laser source. Usually the laser unit is a low power source, such as compact laser diode, which provides a line illumination on the object surface. The image of the illuminated object contour is captured by the camera. A structured relative movement between the object

and scanner allows a sequence of object contour images to be captured. This sequence of light line contours represents the 3D surface profile of the object and later can be processed and converted into a 3D point cloud.

The illumination laser can be of various patterns. It can vary from a very simple single dot to more complex patterns. In a single dot illumination, the laser only illuminates a spot on the object surface. More complex patterns such as a single line, cross hair, parallel lines or dot matrix are also used for illumination. Also, complex geometries such as square, circle and concentric circles, can also be used to increase the illuminated area of the surface in a single camera acquisition [93]. A single laser line used to illuminate the surface of the sheet metal formed is discussed in Section 9.2.1.

To ensure only the surface contour is detected in every image acquisition, an optical band pass filter is usually attached in front of the camera lens. Typically, the peak transmittance of the filter matches the wavelength of the illuminating laser. As a result, the acquired image is of high contrast with a high intensity object profile on a low intensity background.

The object under investigation, the camera and the laser geometrically form a triangle. From this geometry, the distance of every point on the object surface to the camera can be determined using a triangulation method which is a well-established technique [94, 95].

One of the significant parameters of the laser triangulation setup geometry is the triangulation angle,  $\psi$ . This angle is formed between the optical axis of the camera and the illuminating laser, as shown in Fig 107. The intensity of laser light received by the camera is significantly influenced by the test sample's optical properties, its orientation and the triangulation angle. Therefore, varying the triangulation angle  $\psi$  (radians) has an effect on the data acquired. The theoretical limit of vertical resolution can be determined using the triangulation angle [96] and is given by:

$$\Delta h = \frac{P_h}{\sin \psi}$$

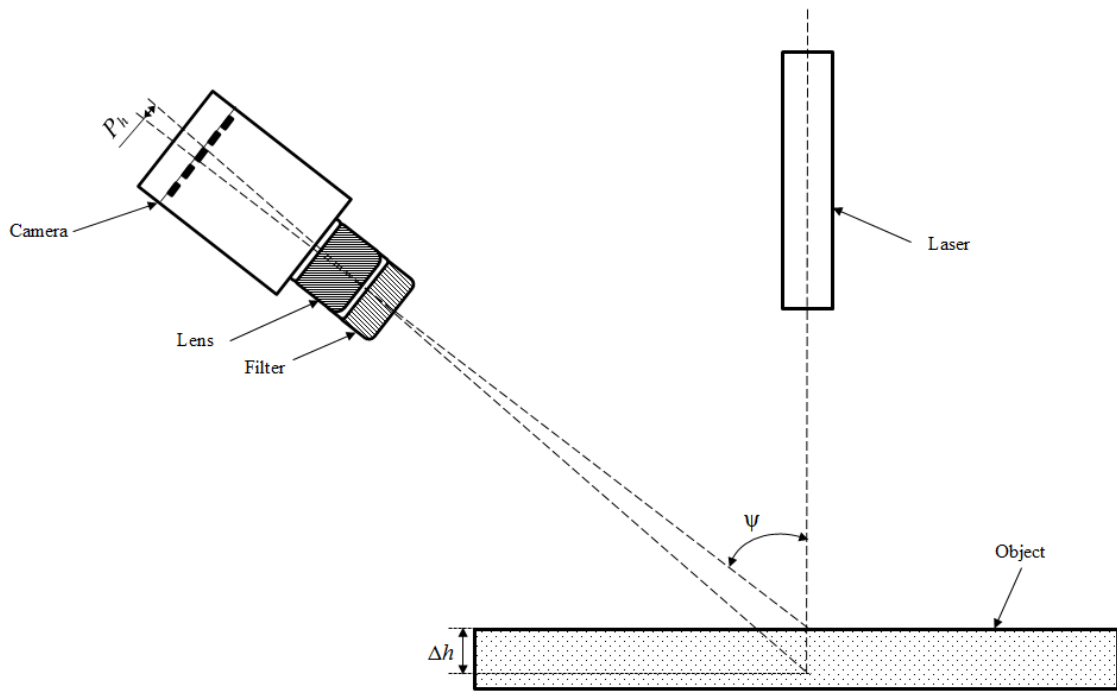


**Fig 107 - Triangulation angle**

where  $\Delta h$  and  $P_h$  are the target vertical resolution (height in  $\mu$ ) and camera pixel size ( $\mu$ ) in the vertical direction. The scanner therefore cannot resolve any surface feature with the height less than this theoretical limit. However, the vertical resolution is usually very high and the requirements vary for different applications. Therefore, the triangulation angle is set-up according to experimental requirements. Upon setting up the triangulation angle, a typical camera view of laser stripe with and without filter is shown in Fig 108.

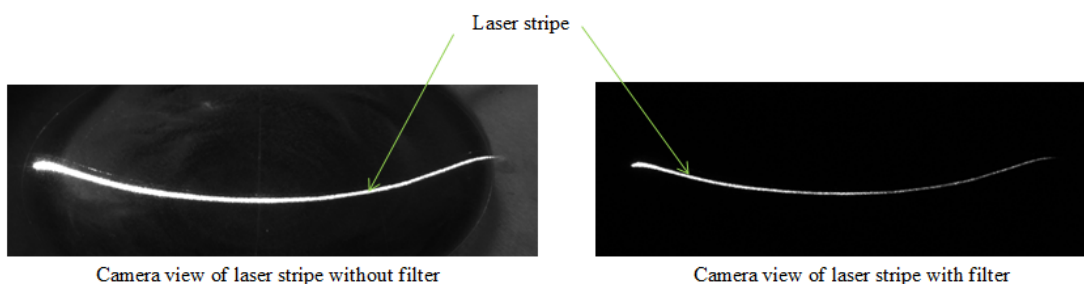


**Fig 108 - Camera view of laser stripe with and without filter**

### 9.2.1 Experimental set-up

The first step in the set-up was to identify the best laser source for the automated panel forming application which involves aluminium as the object to be scanned. There are

various commercial laser scanners available in the market. Most of the laser scanners use red laser light as illumination source. However, based on analysis, it was identified that red laser was not suitable for the intended application because of the longer wavelength of red-laser light (660 nm). Longer wavelengths cause a larger spot diameter [97] which reduces the spatial resolution of the scanner. Also, longer wavelengths may cause more speckle (a granular pattern observed when coherent and monochromatic laser light hits a rough surface [98]) which will cause uncertainty in determining the laser spot position and amplitude [94]. This degrades the quality of measurements.

On careful analysis, a green-laser light source was determined to have the optimum wavelength (520 nm) required for measuring the aluminium samples. Therefore, a Coherent-Stingray green-laser light with 4.96 mW (class 2) optical power and 45° beam fan angle was used as the laser illumination source in the experimental set-up. Subsequently, the best-suited camera and filter were determined.

Basler monochrome Gigabit Ethernet acA 1600-20gm [99] was chosen as the camera for the laser triangulation set-up. The camera includes a Sony Charge-Coupled Device (CCD) ICX274 sensor array with 1628 pixels (horizontal) × 1236 pixels (vertical). Each pixel has a size of 4.4 μm × 4.4 μm. The camera has a frame rate of 20 frames per second. A Tamron f/1.4 C- mount lens [100] with focal length of 8 mm was mounted on the camera to focus the objects under investigation. A full specification of camera is provided in Appendix 9. The camera set-up was also mounted with a green band pass filter with a centre frequency of 520 nm to transmit only the green light into the camera for object identification as green-laser light was used as the illumination source.

Depending on the application requirement, the geometry of the laser triangulation required was determined and the structure was set-up as shown in Fig 109. A mounting structure was built using aluminium frame on an aluminium table to locate the vision system in position for measuring sheet metal parts. It was ensured that enough clearance was provided for the workpiece to be brought in by the robot to be scanned under the laser scanner set-up.

The error monitoring for the sheet metal being formed required a resolution of 0.5 mm at a minimum, for measuring the errors. Therefore, depending on application

requirements, the triangulation angle was set-up which determined the vertical resolution. The triangulation angle; vertical height, ' $h$ ' between the laser source and the object; slant height, ' $l$ ' between the camera and the object; and the line-length of the laser were calculated to meet the resolution requirements, as illustrated in Fig 109.

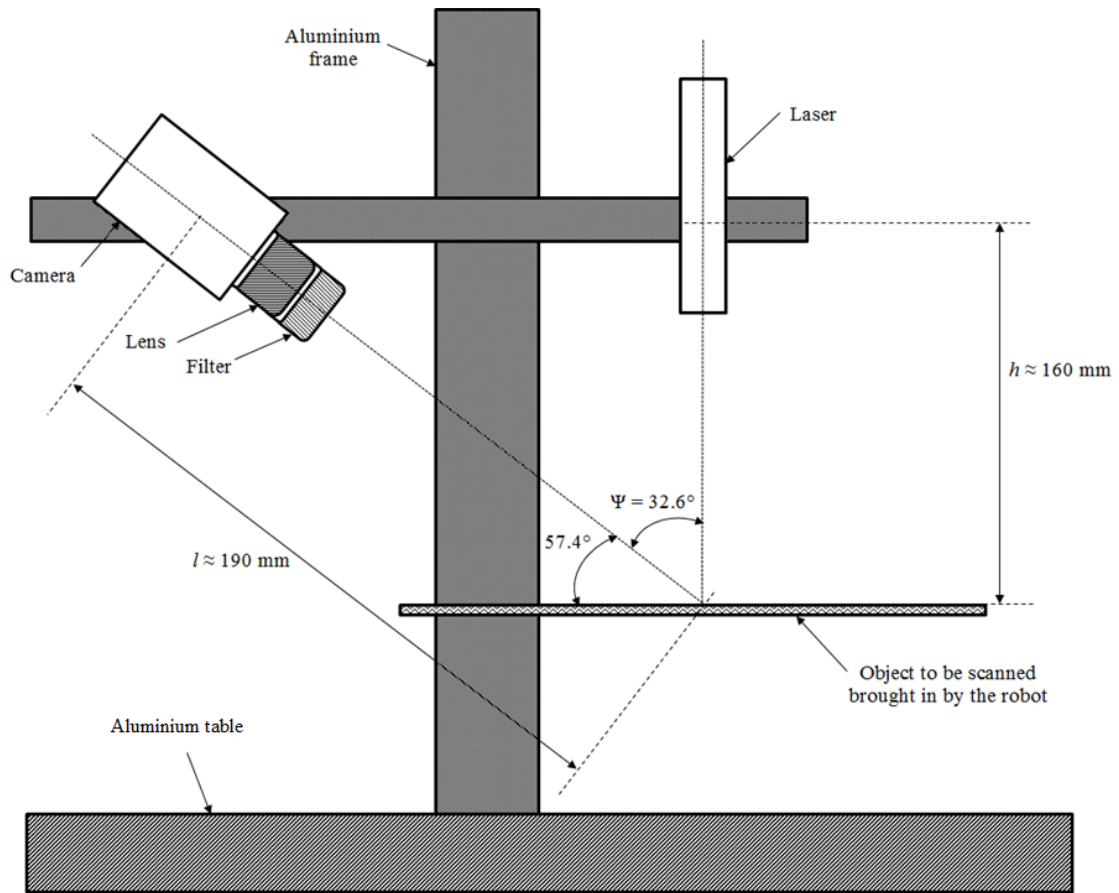


**Fig 109 - Laser scanner set-up illustration**

Intending to get a target vertical resolution of 0.1 mm, the set-up was made using a trial and error method to obtain a triangulation angle between  $30^\circ$  and  $60^\circ$  (based on Halcon's recommendation for triangulation angle). As the camera's CCD (charge-coupled device) position and the laser's light source could not be identified to the exact starting point, slant height ' $l$ ' and vertical height ' $h$ ' were set to 190 mm and 160 mm respectively to produce a single line of length 144 mm on the object at a triangulation angle of  $32.6^\circ$ . This ensured that the bowl shape of 100 mm diameter can be scanned to recognise its features.

Set at a slant height of 190 mm, the camera field of view of 210 mm ensured the bowl shape diameter of 100 mm is covered. It is necessary to strike a balance between



camera's field of view and resolution, which is essential to enhance the data acquired and eliminate the computational and processing requirements of the unwanted data points. The camera's field of view also determined the horizontal resolution of the laser scanner. The experimental set-up is shown in Fig 110.

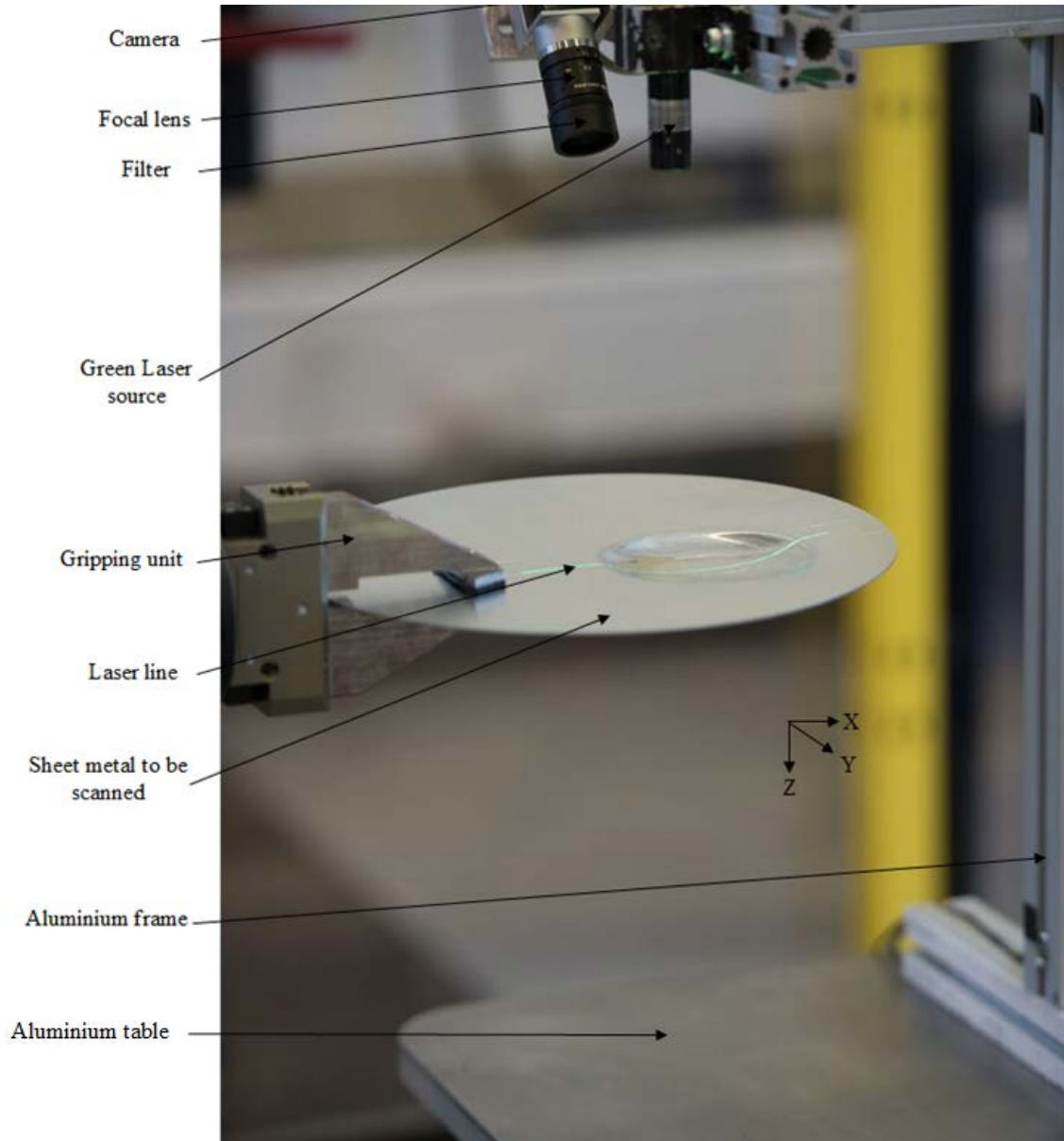


**Fig 110 - Laser scanner experimental set-up**

The vertical resolution of the scanner was calculated as  $8 \mu\text{m}/\text{pixel}$ ,

$$\Delta h = \frac{P_h}{\sin\psi} = \frac{4.4 \mu\text{m}}{\sin(32.6^\circ)} = 8 \mu\text{m}/\text{pix}$$

The horizontal resolution of the scanner was calculated as 129  $\mu\text{m}$ / pixel,

$$\text{Horizontal resolution} = \frac{\text{Field of view of the camera}}{\text{Total no. of horizontal pixels}} = \frac{210}{1628} = 129 \mu\text{m}/\text{pix}$$

The resolution achieved based on the laser scanner set-up explained above provided a higher resolution than required.

### 9.2.2 Calibration

The laser scanner was calibrated for the measurement area and volume (100 mm diameter of the bowl shape formed and 15 mm depth of the bowl shape formed). Based on Halcon's recommendations, the calibration grid should occupy at least quarter of the intended field of view. Therefore, a standard calibration grid of 80 mm x 80 mm was used to calibrate the laser scanner as shown in Fig 111. The calibration grid was created using the Halcon software and the description file (see Appendix 10) of the same was uploaded into calibration set-up. Therefore, the inaccuracy is minimal.

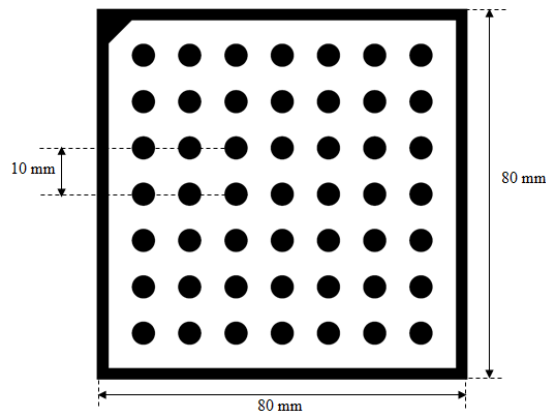


**Fig 111 - Calibration grid**

The calibration grid had 7 rows and 7 columns with a total height and width of 80 mm x 80 mm. The calibration dots of 5 mm diameter were separated by a distance of 10 mm along the height and the width to obtain a diameter ratio of 0.5. The calibration grid was affixed to a plate to be used for defining the measurement area and volume. The focal length of the camera is 8 mm and its aperture was set to obtain the optimal exposure of the laser line before commencing the calibration.

The calibration was carried out in Halcon software (version 12) [81] as Halcon was used for image acquisition and point cloud data generation. Initially, the intrinsic

parameters of the camera such as cell width (4.4  $\mu\text{m}$ ), cell height (4.4  $\mu\text{m}$ ) and focal length (8 mm) were given as inputs to the calibration set-up. The thickness of the calibration plate (calibration grid mounted onto a plate) was also given as input (in this case it is 4 mm – based on micrometer measurements). Subsequently, the camera was made live in the calibration set-up (in Halcon) to grab the live images of calibration grid. The calibration grid would be detected immediately upon identifying the live image (as the description file of same calibration grid was uploaded into Halcon calibration set-up) if it is within the depth of field and field of view of the camera.

In order to re-construct the 3D point cloud data of a scanned object, the data points of the acquired laser profiles needs to be mapped to the co-ordinates of the laser line relative to a selected reference. This is performed using the sheet of light method which is illustrated in Fig 112. When the laser stripe falls on the object, it creates a light plane. A triangle is formed between the light plane, object and the camera. If the light plane pose, world co-ordinates, camera co-ordinates and triangulation angle are known, the rows (y) and columns (x) of the image co-ordinates could be obtained. The height (z) shall be obtained if the camera's sensor location with respect to the object is known. As the camera's sensor location is unknown, calibration is done is two reference planes to identify the camera's sensor location with respect to the triangulation angle and where the laser hits the object. Usually, this lowest reference plane where the camera's vision and light plane interferes is selected as the datum to define the measurement volume above it. The calibration method and defining measurement volume is explained in Fig 115.

On scanning the object at a known distance in the 'y' direction, several profiles of the object are obtained. The point 'P' in the object is re-constructed as point 'P' in the image. A row (y) x column (x) matrix could be obtained for each profile to know its location in the world co-ordinates. Upon calibration, the number of points (dots) per pixel information shall be obtained to calculate the height (z). Therefore, the x, y, z co-ordinates of the object could be obtained.

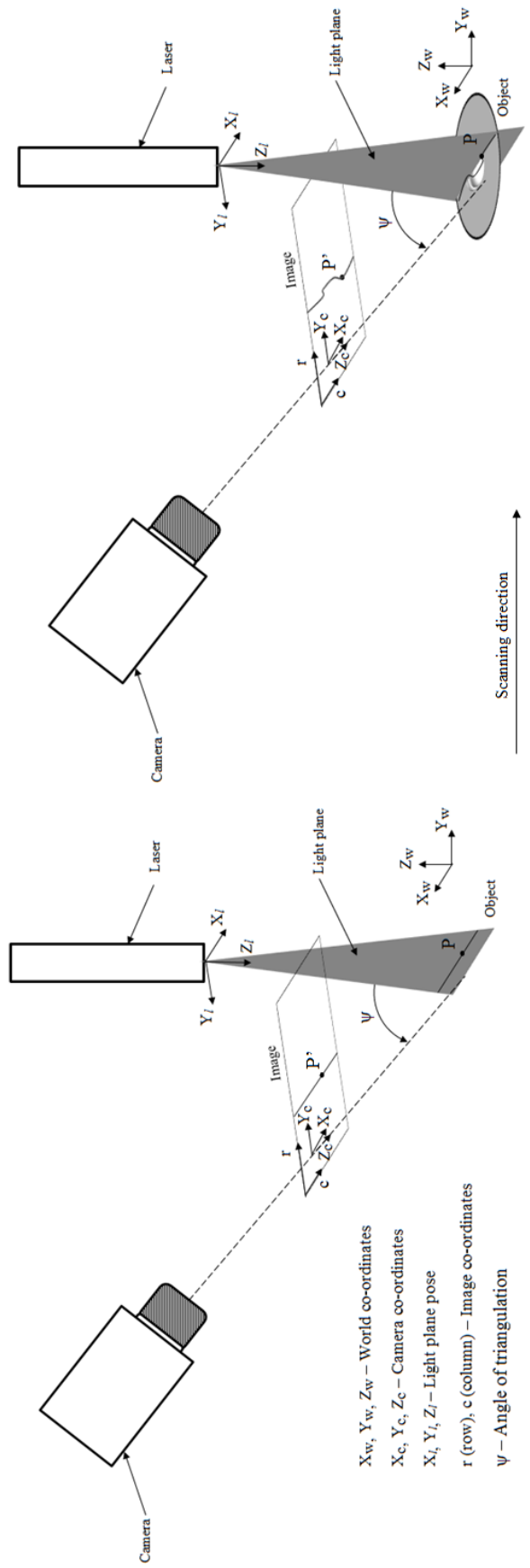


**Fig 112 - Principle of sheet of light**

A total of 18 images are captured of the calibration plate held at different orientations covering the measurement area and field of view of the camera. This ensured that object could be detected at different orientations. Successively, two images were captured at the lowest measurement volume (with the calibration plate held flat on the lowest reference plane), one image without laser line and other with the laser line, as shown in Fig 113.

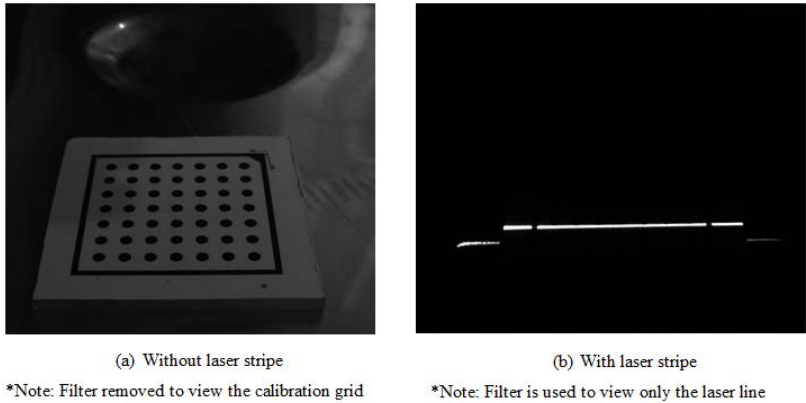


**Fig 113 – Calibration images at lowest reference plane**

Finally, two images were captured at the highest measurement volume (in this case, the highest measurement plane was set to 30 mm to detect a bowl of depth up to 30 mm). The calibration plate was raised by 30 mm and images were taken, one without laser line and one with laser line as shown in Fig 114

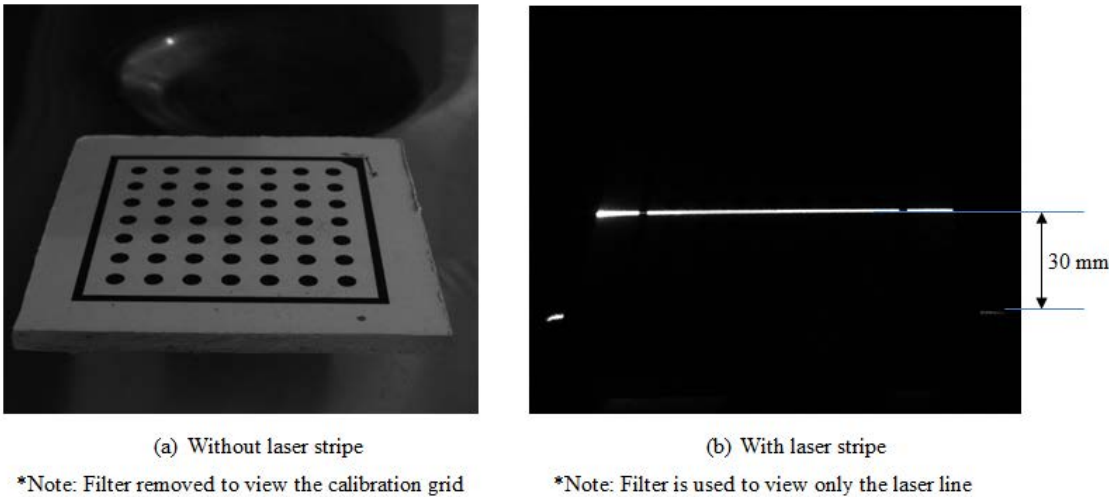
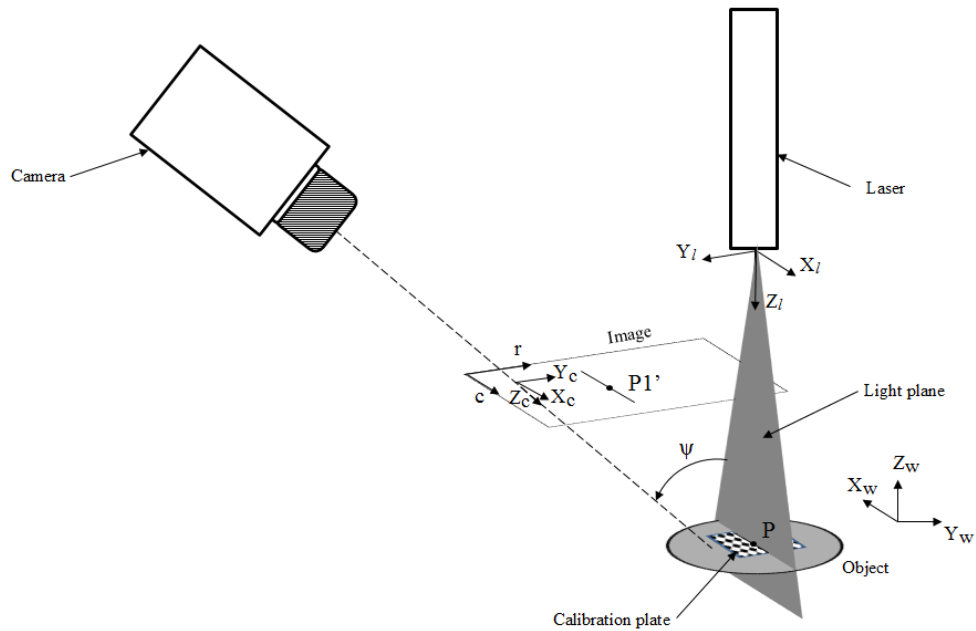
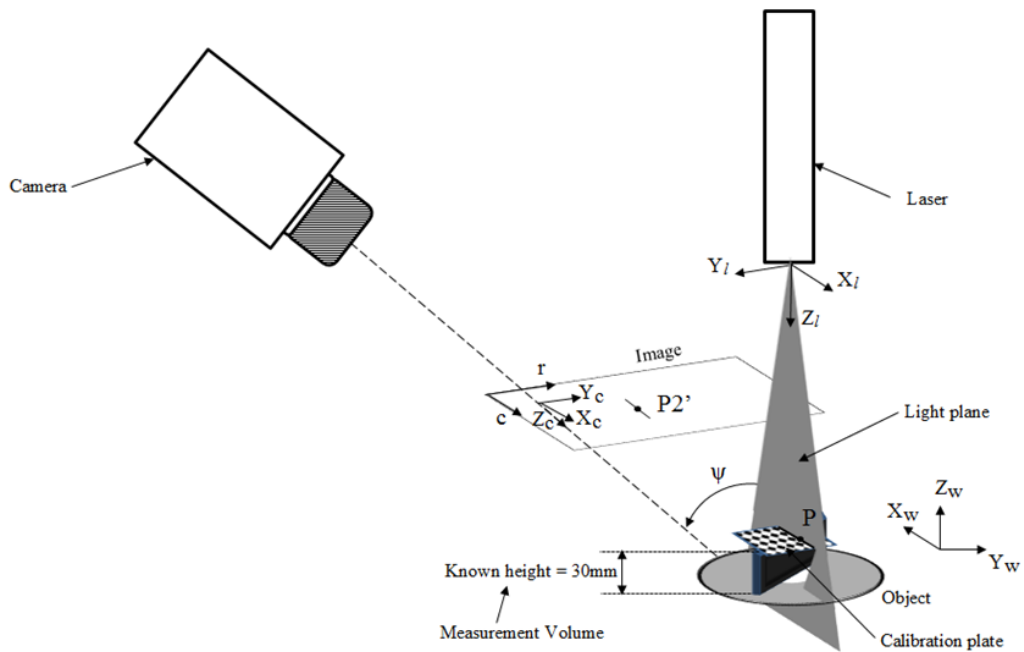


**Fig 114 - Calibration images at highest reference plane**

The Fig 113 and Fig 114 were required to be captured to define the measurement volume of the object (to be measured) as illustrated in Fig 115.



(a) World Co-ordinate System (WCS) definition



(b) Temporary Co-ordinate System (TCS) definition

**Fig 115 - Defining measurement volume**

Therefore, the extrinsic parameters of the camera and the position were defined based on the captured images. Image Fig 113(a) was set as the reference for world co-ordinate system (WCS) based on which the image profiles would be re-constructed as the 3D point cloud data. Image Fig 114(a) was set as the reference for temporary co-ordinate system (TCS).

Based on setting these references, using Halcon's process-numeriser built-in function, an error of 0.13 per pixel was obtained as a calibration result which indicated that only an error of  $0.57 \mu\text{m}$  ( $4.4 \mu\text{m}$  pixel size \* 0.13) is expected per pixel.

The images Fig 113(b) and Fig 114(b) were defined as bottom and top images respectively to fit a plane for the acquired laser profile based on the defined measuring volume.

### **9.3 Image acquisition and point cloud data generation**

The image profiles of the bowl shape panels to be measured were acquired by scanning the formed panel in the defined measurement volume (refer Fig 115). The panel to be measured was moved at a set speed of 2mm/sec to match the frequency of the camera trigger at every 2mm. It is essential that both motion frequency of the panel to be measured and triggering frequency of the camera matched, to obtain accurate image profiles of the panel being scanned. This was ensured by having a control loop to trigger the camera from the robot controller after every 2mm of robot's movement. Any delay in trigger or motion will result in an ambiguous image profile (bad image – distorted, ellipse; good image – circle, since a bowl shape is being scanned) being acquired.

On acquiring the image profiles, an algorithm in Halcon software is used to retrieve the point cloud data. The algorithm requires a number of image profiles and triggering sequence as an input. The algorithm acquires the image profiles and converts them into point cloud data using the conversion factor based on the calibration results. The point cloud data is stored in a text file and could be retrieved later for processing. A cross-section of the bowl shape formed at its maximum depth and diameter is shown in Fig 116.

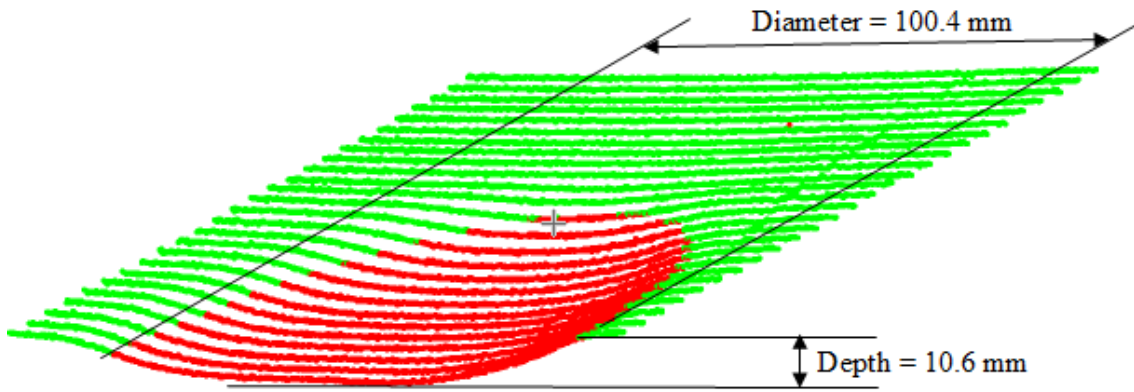


**Fig 116 - Cross section of the bowl shape formed**

### 9.3.1 Image acquisition

In order to acquire the image of the sheet metal to be measured using laser scanner, the laser scanner was interfaced with the robot controller as shown in Fig 117. The interface facilitated the camera to be triggered from the robot controller using the algorithm as shown in Fig 118.

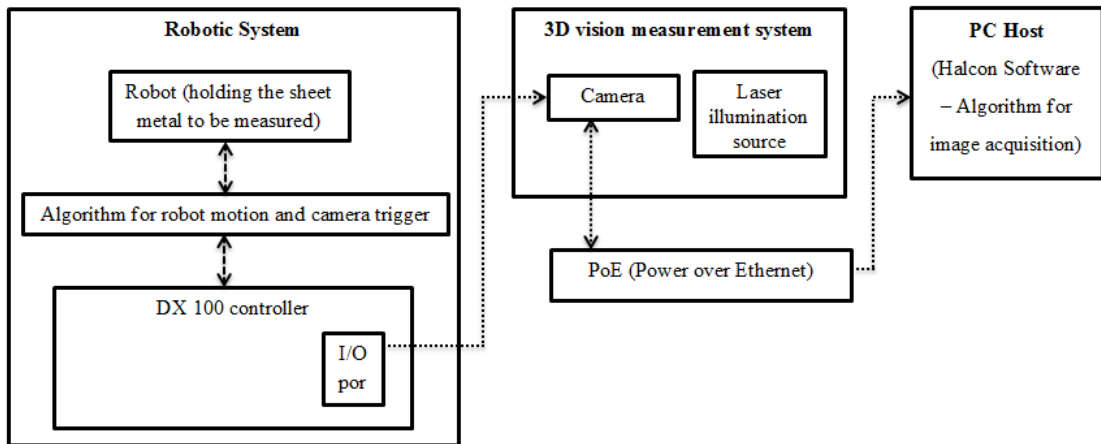


**Fig 117 - Camera interface with robot controller**



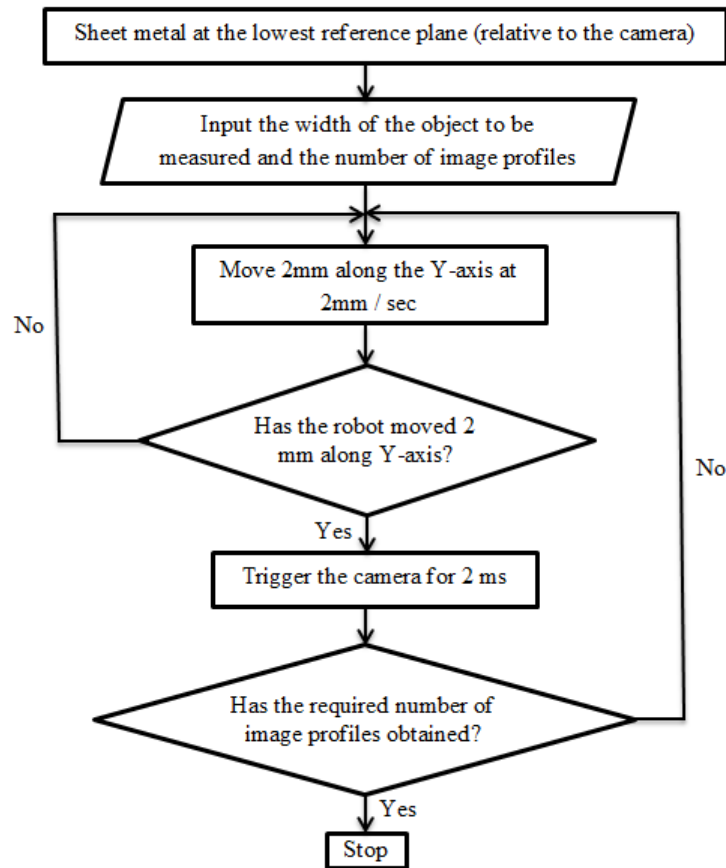


**Fig 118 - Algorithm for camera trigger sequence**

It was determined that 2 mm/ sec is an optimum frequency for image acquisition (1mm/ sec was too slow but had same result as 2mm/ sec; 3mm/ sec was fast and did not provide the required resolution). Therefore, the algorithm was generated in the robot to move the panel at 2 mm/ sec and trigger the camera for every 2mm movement of the panel while it is moving continuously. The sheet metal to be measured was moved along the Y-axis (refer Fig 110 – the sheet metal translational/ rotational motions were referenced relative to the laser scanner set-up) at 2 mm/ sec to obtain the image profiles of the formed shape. Based on the spectral relative response of Sony CCD ICX274, the camera was triggered at an exposure time of 2 ms which was recognised as the best exposure time to acquire the image profiles (since the set-up was in open space might affect exposing too much of light – defining exposure will limit the effect due to light)

The algorithm for image acquisition was developed in Halcon software. Based on the bottom image and top image (refer Fig 113 and Fig 114), the profile region for image acquisition was defined. It is essential to define an optimum region for image

acquisition to obtain only the image profile of the object to be measured and eliminate other images being acquired.

The algorithms (refer Fig 117 and Fig 118) developed in the robot and the Halcon software are run simultaneously to acquire the images without time delays.

### 9.3.2 Point cloud data generation

It is vital to obtain good data points from the image profile acquired. Using the Halcon software, a threshold limit can be defined to identify the good data points acquired from a single laser line profile. The image profile acquired might have pixels of lower intensity or higher intensity. At a lower intensity, the pixel is very dim and is referred to as non-measured data point. At a higher intensity (255), the pixel is saturated and is referred to as saturated data point. The pixel between lower intensity and higher intensity is referred to as a good data point. To ensure good data points are acquired, a dynamic threshold value was defined using the centre of gravity approach. Based on the centre of gravity of pixel intensity, only the good data points were used to generate the 3D point cloud data of the acquired image profile.

The image profiles were acquired for every 2 mm and were converted into 3D point cloud data. The algorithm in Halcon included an iteration to generate the X and Z data points for the image profile acquired for every 2 mm on Y-axis. The 3D point cloud was generated based on the lowest reference plane defined relative to the camera (refer 9.2.2). The co-ordinate system conversions were based on the set reference plane. Based on the 3D point cloud data generated for the obtained image profiles, the model of object scanned was re-constructed in Halcon as shown in Fig 119.

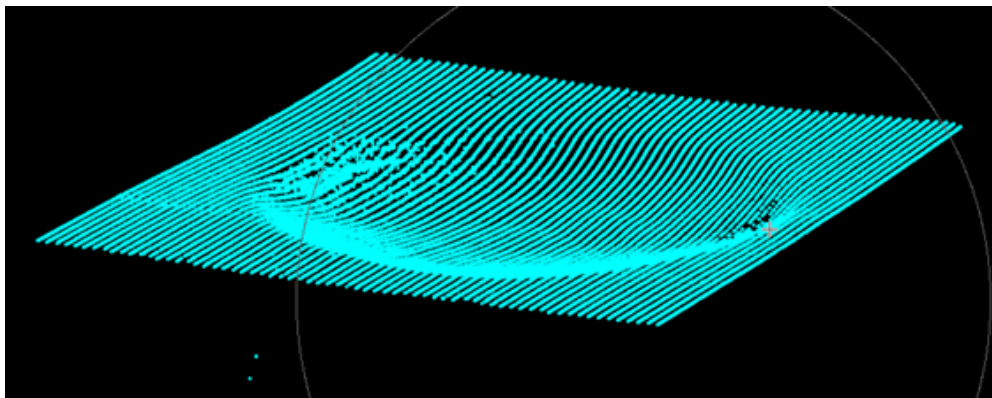


**Fig 119 - Re-constructed model in Halcon**

As it can be inferred from Fig 119, there are only a few non-measured data points and almost negligible data points due to noise (saturation or no data – pixel value is below threshold). The 3D point cloud data were stored in a text file in X, Y, Z format to be retrieved for processing.

#### **9.4 Image processing for depth/ area measurement and experimental validation**

The 3D point cloud data stored in a text file was retrieved to be processed in Matlab. The 3D point cloud data was plotted in Matlab to analyse the data. Initially, a deformation made on the sheet metal upon single impact was measured using the laser scanner as shown in Fig 120.

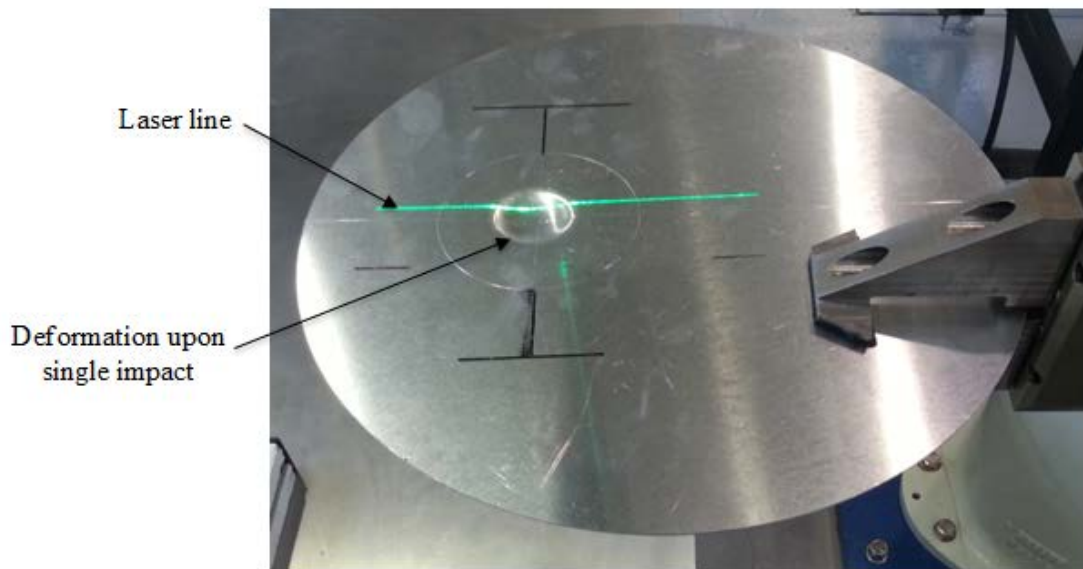


**Fig 120 - Deformation on single impact measured under laser scanner**

The 3D point cloud data generated was retrieved in Matlab to analyse the data. As shown in Fig 121, it could be observed that the reference plane of the sheet metal is not planar and is curved. It was observed that a measurement plane has to be defined (by calculation) to accurately measure the depth of the deformation achieved. The same is illustrated in Fig 122.

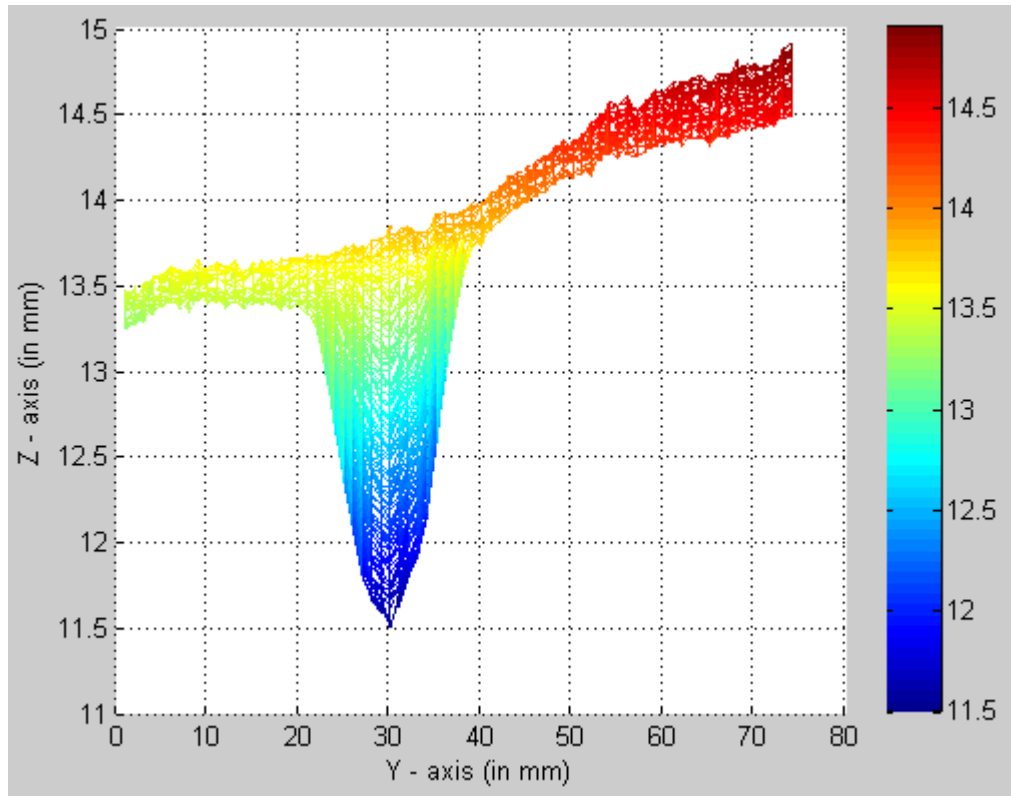


**Fig 121 - Reference plane ambiguity in depth measurement**

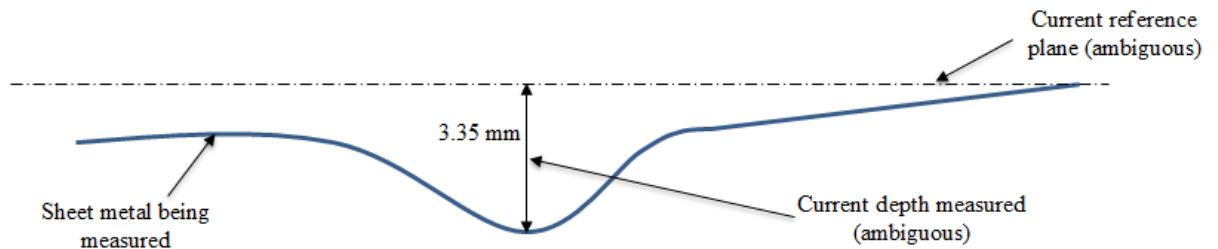


**Fig 122 - Reference plane ambiguity - illustration**

As it could be inferred from the Fig 121, the difference between the highest point (14.85 mm) and the lowest point (11.5 mm) is 3.35 mm. The results were compared with the depth map generated in Matlab using the same 3D point cloud data. It was observed that the depth of spherical depression was about 2 mm as shown in Fig 123. It was determined that the ambiguous measurement in depth was due to the ambiguity in reference plane set for measurement as shown in Fig 122.

In order to solve the ambiguity in reference plane, automated surface defect quantification developed by Tailor, M. [101] was used. Using the algorithm based on polynomial fitting technique, an optimum planar reference could be fitted to measure

the depth accurately. The algorithm was also used to calculate the depth and the area of the deformation in the sheet metal being measured. On fitting the reference plane, the depth could be calculated accurately as the distance between lowest measured data point and the fitted reference plane. The area was calculated by determining the circumference of the deformation. The circumference was identified by a sudden descent in gradient between the data points as shown in Fig 124.

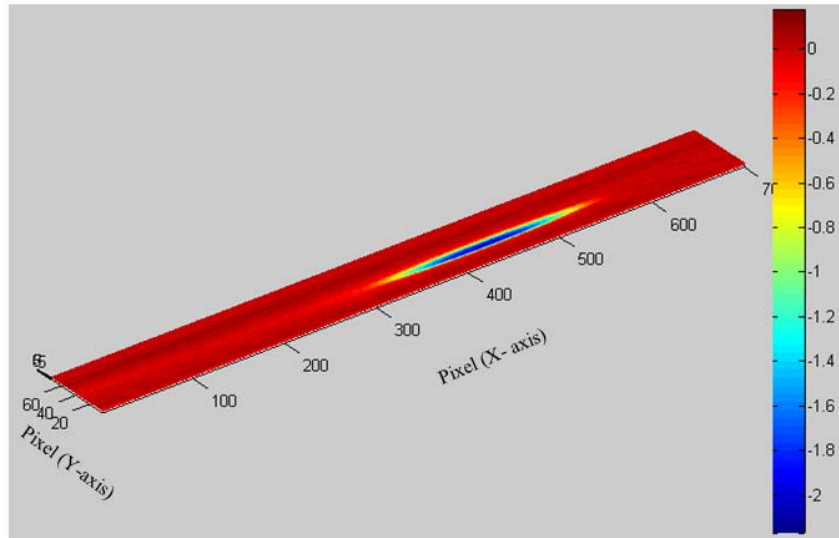


**Fig 123 - Depth map of spherical depression**

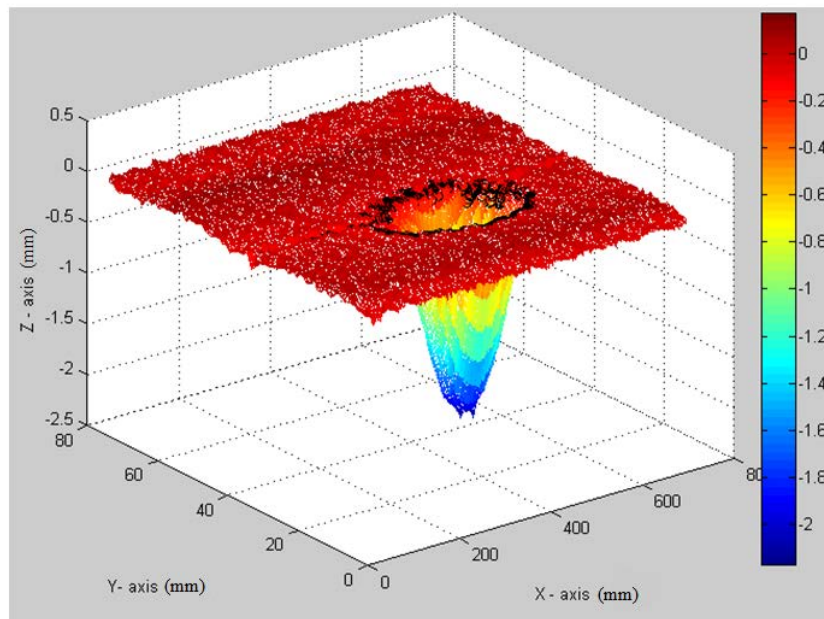


**Fig 124 - Circumference and depth of the deformation determined**

The black dots in Fig 124 represent the circumferential edge determined by the sudden descent in gradient. The planar surface (in red) represents the fitted reference plane. Based on this, the depth and area of the deformation were calculated as 2.030 mm and  $1.408e+03 \text{ mm}^2$  respectively (The final vertical resolution of the laser scanner was  $50 \text{ }\mu\text{m}$  based on the slip gauge measurements).

#### 9.4.1 Validation of results on comparison with CMM measurement

The accuracy of the laser scanner results were validated by measuring the same deformed sheet metal panel using a Nikon Metrology CMM ultra (measurement resolution of  $0.5 \text{ }\mu\text{m}$ ). The result obtained is shown in Fig 125.

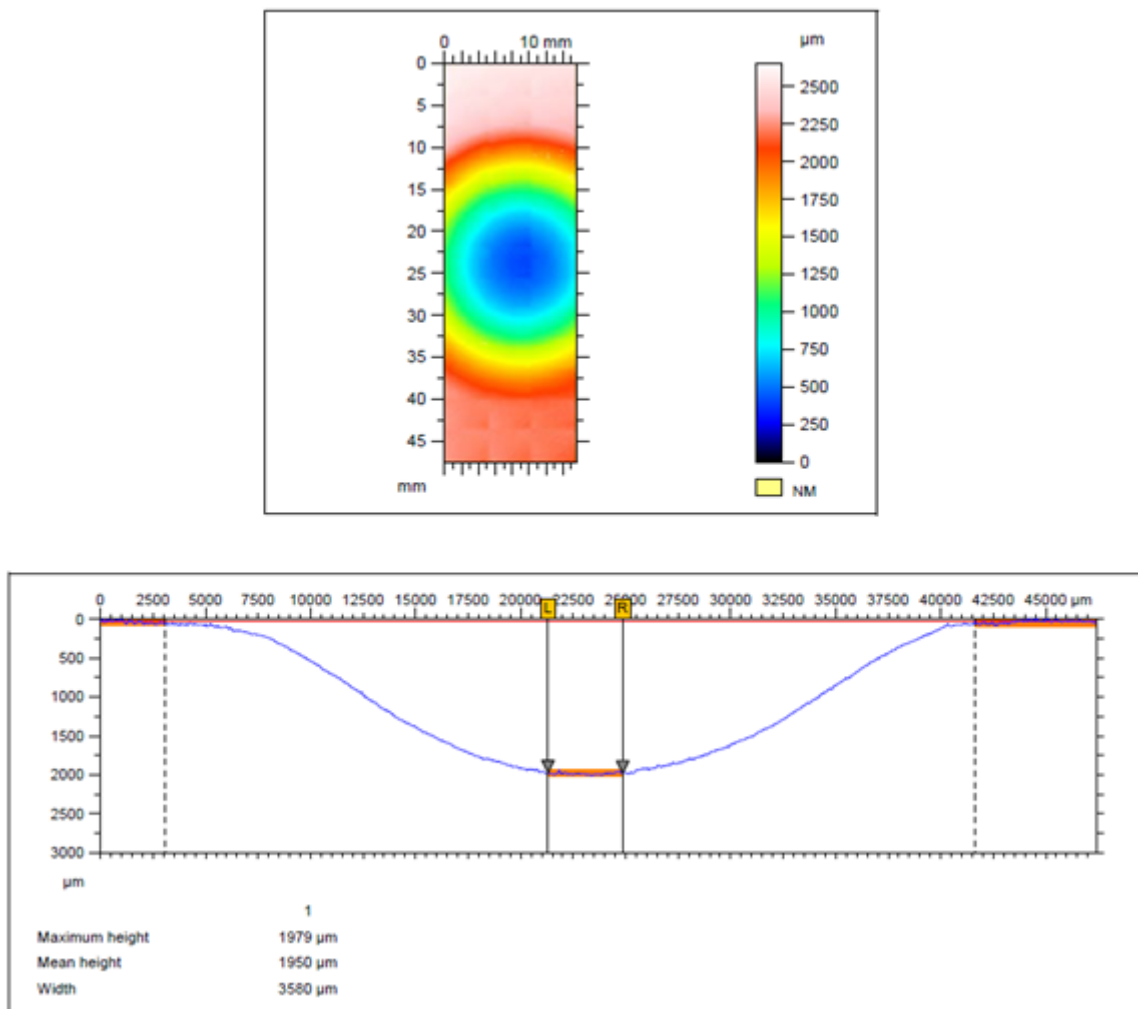


**Fig 125 - CMM measurement of the deformation**

The depth of the deformation was measured as 1950  $\mu\text{m}$  using the CMM. 3 trials were carried out using similar deformed sheet metal plate. The results were compared with the results of the laser scanner as tabulated below in Table 11.

Experiment No.	Sheet metal sample used	Laser scanner measurement	CMM measurement
		Depth** ( $\mu\text{m}$ )	Depth* ( $\mu\text{m}$ )
1	Single impact deformation	2030	1950
2		2010	1960
3		2025	1965

Note: \*denotes measured values, \*\*denotes calculated values

**Table 11 - Laser scanner and CMM measurement comparison**

On comparing the results, it was identified that the laser scanner measurements are at their most inaccurate by 70  $\mu\text{m}$ . The obtained results were within the measurement requirements for the sheet metal forming application. Therefore, the laser scanner set-up and calibration were used for performing further experiments.

### 9.5 Shape and feature detection experiments

Based on the initial experimental validation, the shape and feature detection were performed on a particular shape throughout the experiments. The experiments were carried out on a sheet metal formed for 2 x 360° turns in the second iteration which had a final skewing angle,  $\phi_f$  of 7° (refer section 8.5.2). The shape to be measured is shown in Fig 126.

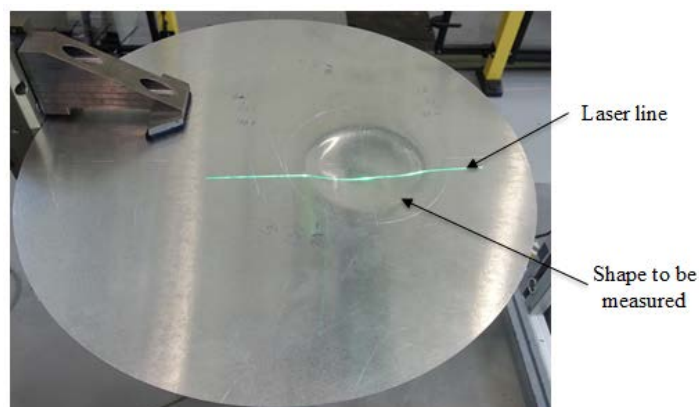


**Fig 126 - Shape to be measured**



The shape to be measured was scanned under the laser scanner to acquire the image profiles and generate them into 3D point cloud data. The point cloud data was retrieved to be processed in Matlab which produced the result as shown in Fig 127.

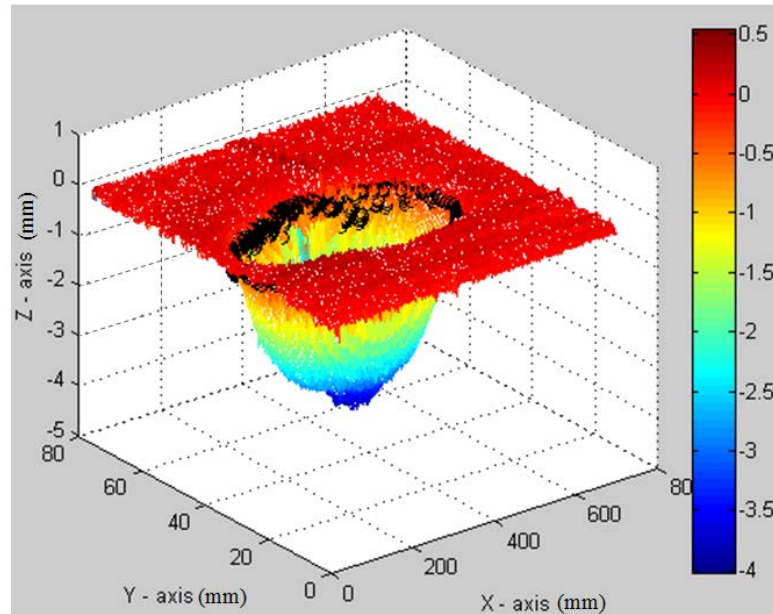


**Fig 127 - Shape measurement results**

The depth of the shape formed was determined to be 4.052 mm and the area was determined as  $3.296 \times 10^3 \text{ mm}^2$ . Calculating the diameter of the circumferential edge, it was determined as 64.80 mm. As the radius, 'r' and depth, 'D' of the bowl shape formed were known, angle of the gradient between the bottom centre and edge of the bowl shape formed could be calculated as shown in Fig 128. The middle image profile passing nearest to the centre of the bowl shape formed was chosen to calculate the angle of the gradient.

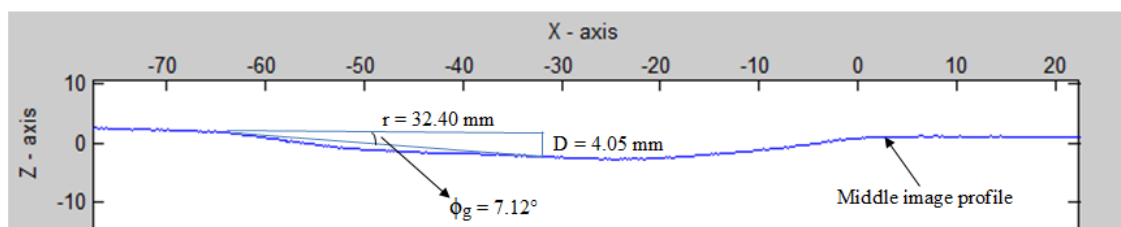


**Fig 128 - Angle of the gradient**



The angle of the gradient, ' $\phi_g$ ' was calculated using the Pythagoras theorem and was determined to be  $7.12^\circ$ . The gradient angle was determined using the formula:

$$\phi_g = \arctan\left(\frac{D}{r}\right)$$

The result obtained was closer to the  $7^\circ$  skewing angle given as input to the automated system to form the bowl shape. Thus, indicating that the errors were minor in the bowl shape formed. Ideally, the angle of curvature should be determined to analyse the bowl shape formed. However, as shown in Fig 128, the gradient was almost closer to the curvature formed as it was a very gradual curvature. Therefore, angle of the gradient was used instead of angle of curvature.

The experiments were carried out for 5 trials using a similar shape with  $7^\circ$  provided as skewing input to the automated system. The results are tabulated below in Table 12

Experiment No.	Sheet metal sample used	Laser scanner measurement			
		Depth (D)** (mm)	Area** (mm <sup>2</sup> )	Radius (r)** (mm)	Angle of the gradient ( $\phi_g$ )** (degrees)
1	Sheet metal formed from 2 x 360° turns for 2 iterations	4.05	3.296e+03	32.40	7.12°
2		4.15	3.224e+03	32.03	7.38°
3		4.07	3.248e+03	32.15	7.21°
4		4.12	3.120e+03	31.51	7.45°
5		4.06	3.412e+03	32.95	7.02°

Note: \*\*denotes calculated values

**Table 12 - Shape and feature detection experimental results**

Based on the results obtained, it could be inferred that a skewing angle of  $7^\circ$  is expected to produce a depth of about 4 mm and circumferential diameter between 64 – 66 mm. This data could be compared with the intermediate CAD models to determine

the potential error. Based on the error, the path could be modified to achieve the target shape.

## **9.6 Discussion of results and proposed method for error rectification**

The laser scanner set-up using the green laser was determined to produce accurate results based on the initial experiments carried out. The laser scanner results were only 70  $\mu\text{m}$  inaccurate in comparison with the CMM measurement results. The inaccuracy was well within the acceptable margin of error for the sheet metal forming measurements.

The shape and feature detections experiments were limited to a shape formed by providing an input of 2 x 360° turns for 2 iterations with the skewing angle of 7°. The bowl shape formed was measured to have a depth of 4 mm and diameter of 65 mm. The experiments were limited to particular shape due to the algorithm used for determining the depth and the area. The algorithm required an excess non-formed boundary (flat surface) along with the bowl shape formed to fit a planar surface as measurement reference. As the laser line was only 144 mm long, when a bowl shape of 100 mm was scanned for measurement, the algorithm could not fit a reference plane for measurement. Therefore, the shape being formed was limited to an input of 2 x 360° turns. It is anticipated that a longer laser line with a similar spatial resolution will increase the excess boundary which shall facilitate the measurement of a bowl shape with a larger diameter.

On performing the experiment for 5 trials, using a similar shape, the angle of gradient was determined. The results indicated that the angle of gradient was closer to the skewing angle provided as the input. Thus, the expected results of the automated system were validated using the laser scanner measurement and calculated results. However, the minor error determined by the 3D vision measurement system is vital to monitor the shape being formed and modify the forming path relatively. A method that could be used for identifying the error and rectifying the forming path has been proposed.

### **9.6.1 Method proposed for error identification and rectification**

As discussed in Section 9.5, the shape and feature detection experiments were performed by selecting the middle image profile for determining the angle of gradient.

However, the image obtained could be sliced at step angles of every 15° (refer section 8.4) and the angle of the gradient could be determined. Also, as mentioned earlier, it is better to calculate the angle of curvature for large curvatures of the bowl shape formed. As a result, enhanced precision in error identification could be achieved.

In order to increase the precision in measuring the angle of curvature, the angles could be measured between two selected data points. The data points could be selected relative to the number of 360° turns involved in the bowl shape formed. The angle of curvature could be measured at the particular data point to narrow down the path modification criteria. This is illustrated in Fig 129

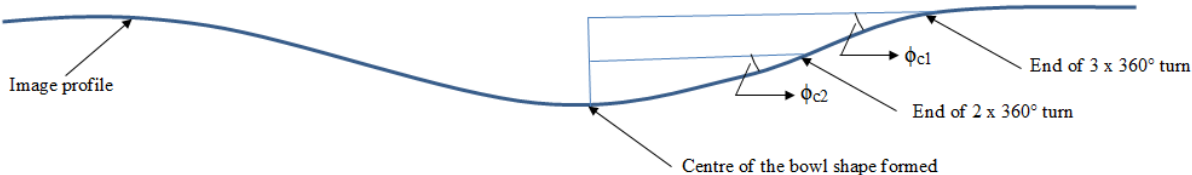


**Fig 129 - Increasing the precision of measurement**

As shown in Fig 129, the angle of curvature,  $\phi_c$  can be determined at the end of 2<sup>nd</sup> and 3<sup>rd</sup> 360° turns in the case of bowl shape formed to a diameter of 100 mm. The angle of the curvature results obtained could be compared with the skewing angle (refer section 8.4) given as input to determine the error. Depending on the angle variation, the input for skewing angle in the next iteration could be changed.

Using the automated system proposed in this thesis, it is very unlikely for buckles to occur in the sheet metal being formed. In order to check for the buckles, checking the difference between gradients is an approach that could be used. Since 3D data points are available for every 130 μm, the gradient could be determined between neighbouring data points as shown in Fig 130 (The gradients 1 – 5 indicated in the figure is only for reference. In reality, this will be in micrometre level).

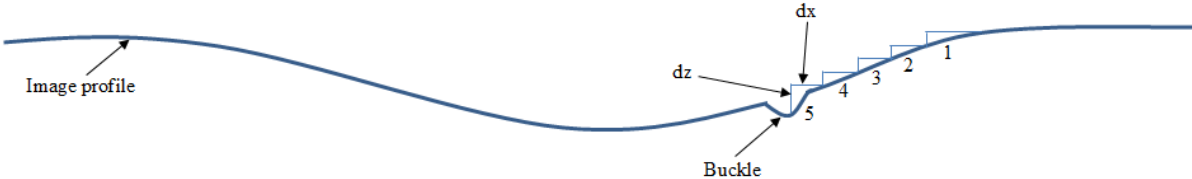


**Fig 130 - Buckle identification**

As shown in Fig 130, the gradients are found using the  $dz/dx$  methodology. The gradients 1 – 4 will have a gradual descent. The gradient 5 will have an unusual descent due to the occurrence of buckle. The buckle could be identified when an uncertain gradient descent occurs. A more detailed calculation could be performed on the neighbouring data points to identify the buckle's height and width. On identifying the region of the buckle, the path planning algorithm could be modified to rectify the buckle. The angle of skewing could be changed at the identified region to rectify the buckle.

The above proposed error identification and rectification could be used to enhance the monitoring process and feedback rectification information to the automated system which is currently done manually. However, the time taken to measure and analyse the shape and its features should be considered. An optimum measurement and analysis strategy has to be employed to optimise the processing time.

### **9.7 Summary**

One of the observed manual panel beating skills is the ability to measure the semi-finished sheet metal part formed during the process and adjust the forming process accordingly.

An in-process measurement system was designed and deployed to measure the curvature of semi-finished parts using a 3D vision system, and compare them with the dimension of the part at that stage of forming. Accepting a margin of error of 70  $\mu\text{m}$ , any excessive deviation from the intermediate shapes would be identified and the forming algorithm (i.e. the robotic motion of the part under the hammer) would be corrected.

The in-process measurement approach was developed and tested as part of this research as a proof-of-concept approach. However, further investigation is required to integrate such a monitoring system with the proposed automated panel forming (please see Chapter 10 - further research).

# 10. Conclusions

---

## 10.1 Research overview

A need for research was identified in developing a fixtureless automated solution for sheet metal forming to increase the flexibility in forming and to provide a uniform thickness distribution. A need for an automated solution was identified amongst the industries that deploy manual panel beaters for forming one-off/ low volume products.

On comparison with the existing methodologies, panel beating process provides better consistency on the material thickness and offers the required flexibility in the forming process. Therefore, the research was focused on forming the sheet metal by replicating the skill of a manual panel beater.

Based on the research objectives discussed in Section 1.3, the Mechatroforming® approach was proposed and the research methodology was developed in three stages. These consist of capturing human skill, developing a semi-automated system, and a fully automated system incremental sheet metal forming system. Initially, experienced panel beaters were closely observed and their tacit human skill was analysed. Based on the human skills identified and impact force determined for forming the sheet metal, a hammering machine capable of operating at the required impact force and frequency was identified.

The semi-automated system utilises the hammering machine and manual manipulation of the sheet metal blank between the hammer and the supporting tool (i.e. the anvil) during repetitive hammering to progressively form the desired 3D shape. During the action of forming the shape, a motion capture system was used to capture and analyse the movement of the sheet metal blank. The human skills observed were formulated into mechatronic / robotic mechanisms to be provided as parametric inputs to the automated system.

The proposed automated system includes an electrical hammering machine and a robotic arm to replicate the combination of human manipulation of the part and the hammer. It also comprises of a gripping unit which acts similar to a human grip (i.e. panel beater hand) that holds and positions part under the hammer. The robot and the hammering machine were integrated into one automation unit. The robotic motion of

the sheet metal was synchronised with the frequency of sequential hammering to form a required 3D shape. A control algorithm was developed to form a simple sheet metal part: a bowl shape. On forming a bowl shape, experiments proved that the automated process is successful with 98% forming repeatability and less than 1% deviation from the original shape required. The automation process developed is believed to make a significant contribution to the sheet metal forming industry, especially in rapid prototyping and maintenance.

Further enhancement to the proposed automated system was made by addition of an error monitoring mechanism using a 3D vision measurement system. Using this system, the geometry of the semi-finished parts are measured and analysed, and corresponding modifications to the forming path is proposed.

## **10.2 Research achievements**

With the development of the fixtureless automated forming solution for simple sheet metal parts, the following was achieved in this research- which also meets the research objectives discussed in Section 1.3:

- The developed automated solution was able to form 3D sheet metal shapes using a fixtureless forming approach based on human panel beating skills.
- A series of bowl shape parts were formed automatically without human interference, which are considered as proof-of-concept developed in this research. Based on experimental analysis, the best path and pattern for forming bowl shape parts were both investigated and selected. The automated solution was focused on producing a bowl shape measured at 100 mm diameter, 10.60 mm depth, and a thickness of 0.95 mm.
- The need for a fixture was eliminated, allowing the free flow of material during the forming process. This resulted in minimising the stress in finished parts and therefore, a higher dimensional accuracy by reducing part deformation due to the release of residual stresses.
- A sequential vertical hammering process was deployed, eliminating need for angular hammering (a technique used by skilled operators). This significantly

facilitated the development of the automation system by embedding the required angular impacts into the positioning of parts (carried out by the robot wrist).

- By adopting an incremental forming approach, it was proved that one size tool set (i.e. a hammer and an anvil) should be able to produce various shapes. This was achieved through the gradual forming of a desired shape through incremental impact forming.
- The impact force and energy involved in the sheet metal forming were measured and calculated using the instrumented hammer and high speed camera. The results were essential to: a) develop a FEA model of the forming process, and b) determine the hardware specification for the automation system. The experimented measurement approach was proved to also be effective for other parts with various material and sizes.
- A 3D vision measurement system was implemented to measure the geometry and features of completed or semi-finished parts. Through this measurement system, it was proved that the developed automation solution is able to produce bowl shape parts at high dimensional accuracy with a maximum deviation of 0.15 mm to its circumference and  $0.45^\circ$  to its skewing angle. The proposed vision system was also investigated and tested as part of an in-process measurement mechanism that should allow rectification of forming process based on intermediate measurement feedback.
- FEA modelling was used to predict the forming process and the influence of various impact patterns used by individual panel beaters.
- This research has been published by multiple sources, including: a) International Journal of Advanced Manufacturing Technology, b) Industrial Journal of Institution of Sheet Metal Engineers, c) Industrial magazine of Confederation of British Metal Forming, and d) 2<sup>nd</sup> Annual EPSRC Manufacturing the Future Conference 2013. (See “Appendix 11” and “LIST OF PUBLICATIONS” for details)

### **10.3 Contribution to the knowledge**

The concept of automated sheet metal forming has been previously investigated by other research groups. Nonetheless, none of the available research results meet the aims

and objectives of this research. The proposed solution developed as a part of this research contributes considerably to the state of the art by introducing novel approaches, and improving the existing methods as outlined below:

#### ***Development of fixtureless automated system based on human skills***

The existing researches in sheet metal forming do not consider the skills of a manual panel beater to develop an automated system. A novel idea of interpreting the skills of a panel beater into robotic skills has been introduced by this research. For example, to the best knowledge of the author, this is the first instance of using a motion capture technology to analyse the sheet metal forming skills of a panel beater and understand the beating patterns.

#### ***Application of FEA to support incremental forming***

Finite element analyses of sheet metal forming are available in the research domain. However, finite element analysis related to impact force to support incremental impact forming has not been investigated prior to this research. Modelling and simulation of the manual panel beating and non-linear dynamic analysis of the impact force involved are new approach proposed and tested by this research.

#### ***Use of a simple hammer to form the 3D shapes***

Research in impact forming has contributed to the forming of 2D shapes, using a sheet metal through a specific stretching or shrinking tool. However, research has not been carried out on forming a 3D shape of a metal sheet using a simple hammer. A novel approach of forming a 3D shape using a simple hammer has been proposed in this research.

#### ***Design of the Mechatroforming System***

The design and development of the Mechatroforming system is one of the significant contributions providing a new dimension to sheet metal forming by using a robot and a hammering machine. The integration of the robot and the machine and synchronising their motion to achieve the desired shape of the sheet metal is a notable contribution.

#### ***Design of the gripping fingers***

The gripping fingers were designed and developed learning from the sheet metal grasping strategy practised by human. The design of gripping fingers was vital to make sure the sheet metal was not bent during the automated process.



### *In-process measurement of semi-finished parts*

A proof-of-concept, in-process 3D vision measurement system has been implemented and tested to measure the 3D shape of semi-finished parts (refer Section 2.6). This method was proved to be highly accurate in comparison with the gauging and template measurement techniques used by panel beaters. It was proposed, and partially tested, that intermediate measurement information can be used to reconfigure the robot trajectory in order to correct any potential deviations from the required forming process. Further research could be carried out to integrate monitoring and corrective mechanisms to the proposed solution.

### **10.4 Further discussions**

During this research, the author realised the true extent of complexity of human operations in manual panel beating and the level of dexterity required to replicate manual processes.

It was understood that an automated system may not be able to fully support the flexibility that a skilled operator offers. However, such systems can improve the repeatability and consistency of the processes, reducing the human skill level required, and the need for long term training.

Furthermore, the developed automated system could prove to be costly for industries. A full cost analysis would be necessary to enable the estimation of potential financial advantages of the proposed automated system in long term. However, it is envisaged that repeatability of products and reliability of processes can develop considerable opportunities in high-value industries, such as aerospace.

On a technical perspective, restrictions in equipment availability to this research have limited the domain of the experiments. For example, aluminium test pieces with a bowl depth of only 10.60 mm could be produced due to the throat depth limitations of the hammering machine. In similar comparison, a human skilled operator is able to form the same aluminium test piece to a depth of 20 mm due to the higher degree of flexibility in his wrist and his ability to use his flexion, extension, pronation and supination motions. A similar degree of flexibility could not be delivered by a robot.

## 10.5 Recommended Future work

This research could be continued further in a number of directions as recommended below:

The proposed proof-of-concept automated system is focused initially on forming a bowl shape artefact. Clearly, the next research stage could be investigations of applicability of the proposed approach to various 3D contours, such as pyramids, cubes, or any other non-uniform 3D contour. To form such shapes, the robot motion algorithm should be enhanced based on the geometrical model of the required parts. However, it is expected that the basis of the forming and path planning could be supported by the results of this research.

The use of finite element analysis was proved beneficial to the forming prediction by determining the best forming path and pattern for a particular geometry. Further research is required to facilitate the development of intermediate CAD models of semi-finished parts. Such models could be integrated to the in-process measurement system.

It is anticipated that non-sequential hammering could be used to eliminate the stress involved in sheet metal forming. If the FEA prediction and intermediate check between iterations are accurate, the non-sequential hammering could be implemented.

The change of material properties upon impact forming could be significant in thicker ductile or in thinner brittle material. Theoretically, the FEA models could be further enhanced by including the material properties of the sheet metal (mainly stress and strain curve) to improve the accuracy in the simulation. However in this case, the FEA model should be regenerated upon every impact to provide input variables for the consecutive impacts. It is expected that this type of analysis and prediction will minimise the number of impacts required to produce the complex contours. However currently, a real-time integration of FEA is not feasible as a higher computational time is required for processing.

Further integration between in-process measurement, the FEA model, and the real-time robot trajectory modification could be investigated further in the future. The 3D vision measurement has a significant benefit in in-line, off-process error monitoring and path optimisation. The intermediate CAD models generated from FEA could be compared with the corresponding 3D point cloud data of the shape formed between iterations. In

comparison, the deviation in the forming path could be identified. Subsequently, the forming path could be modified to optimise the forming process, increase the precision of forming and achieve the target shape with the required accuracy.

Research could be carried out to investigate the influence of variable-controlled impact force on the accuracy of part formation. Such mechanisms could operate closely with the FEA model to optimise the impact force required for forming various features of the part.

## REFERENCES

1. Nicklin A., 2015. *Confederation of British Metal Forming*. 09.05.2015, Available from: <http://www.britishmetalforming.com/>.
2. Young D and Jeswiet J., 2004. Wall thickness variations in single-point incremental forming. *Proceedings of the Institution of Mechanical Engineers, Part B: Journal of Engineering Manufacture*, vol. 218 (Issue 11), pp. 1453-1459. ISSN 0954-4054.
3. Mallieswaran K, Anjum SA and Pradeep A., 2012. Case Study on Manufacturing of Light Weight Component by Metal Forming. *Journal of Advanced Technology in Engineering*, vol. 1 (Issue 1), pp. 63-70.
4. Hagan E and Jeswiet J., 2003. A review of conventional and modern single-point sheet metal forming methods. *Proceedings of the Institution of Mechanical Engineers, Part B: Journal of Engineering Manufacture*, vol. 217 (Issue 2), pp. 213-225.
5. Allwood J, King G and Duflou J., 2005. A structured search for applications of the incremental sheet-forming process by product segmentation. *Proceedings of the Institution of Mechanical Engineers, Part B: Journal of Engineering Manufacture*, vol. 219 (Issue 2), pp. 239-244.
6. Okoye CN, Jiang JH and Hu ZD. Application of electromagnetic-assisted stamping (EMAS) technique in incremental sheet metal forming. *International Journal of Machine Tools and Manufacture*, vol. 46 (Issue 11), pp. 1248-1252. ISSN 0890-6955.
7. Leacock AG., 2012. The Future of Sheet Metal Forming Research. *Materials and Manufacturing Processes*, vol. 27 (Issue 4), pp. 366-369.
8. An Y, Vegter H, Melzer S and Triguero PR., 2013. Evolution of the plastic anisotropy with straining and its implication on formability for sheet metals. *Journal of Materials Processing Technology*, vol. 213 (Issue 8), pp. 1419-1425.
9. Kubli, W and Krainer, A. *Method and Computing System for Designing a Formed Sheet Metal Part*. 2013. US: EP Patent 2,463,793. OCT 15, 2013. ISBN US8560103 B2.
10. Ben Hmida R, Thibaud S, Gilbin A and Richard F., 2013. Influence of the initial grain size in single point incremental forming process for thin sheets metal and microparts: Experimental investigations. *Materials & Design*, vol. 45, pp. 155-165. ISSN 0261-3069. DOI <http://dx.doi.org/10.1016/j.matdes.2012.08.077>.
11. Groche P and Christiany M., 2013. Evaluation of the potential of tool materials for the cold forming of advanced high strength steels. *Wear*, vol. 302 (Issue 1-2), pp. 1279-1285. ISSN 0041-1648. DOI <http://dx.doi.org/10.1016/j.wear.2013.01.001>.

12. Bouchard P and Bay F., Damage and Crack Propagation Theories Applied to Sheet Metal Cutting. EMAS. *ECF 14: 14th Biennial Conference on Fracture : Fracture Mechanics Beyond 2000*, 8 - 13 September, Cracow, Poland, 2002.
13. Yang ZR, Scherer D, Golle M and Hoffmann H., 2011. Geometrical Modeling of the sheet metal parts in the incremental shrinking process. *Key Engineering Materials*, vol. 473, pp. 509-515. DOI 10.4028/www.scientific.net/KEM.473.509.
14. Behera AK, Lauwers B and Dufloy JR., 2012. Advanced feature detection algorithms for incrementally formed sheet metal parts. *Transactions of Nonferrous Metals Society of China*, vol. 22 (Issue 12), pp. s315-s322. ISSN 1003-6326. DOI [http://dx.doi.org/10.1016/S1003-6326\(12\)61725-7](http://dx.doi.org/10.1016/S1003-6326(12)61725-7).
15. Jeswiet J, Hagan E and Szekeres A. Forming parameters for incremental forming of aluminium alloy sheet metal. *Proceedings of the Institution of Mechanical Engineers, Part B: Journal of Engineering Manufacture*, vol. 216 (Issue 10), pp. 1367-1371. ISSN 0954-4054.
16. Lamminen L., 2005. Incremental Sheet Forming with an Industrial Robot—Forming Limits and Their Effect on Component Design. *Advanced Materials Research*, vol. 6, pp. 457-464.
17. Stoughton TB and Yoon JW., 2005. Sheet metal formability analysis for anisotropic materials under non-proportional loading. *International Journal of Mechanical Sciences*, vol. 47 (Issue 12), pp. 1972-2002. DOI <http://dx.doi.org/10.1016/j.ijmecsci.2005.06.005>.
18. Silva M and Martins P., 2013. Two-Point Incremental Forming with Partial Die: Theory and Experimentation. *Journal of Materials Engineering and Performance*, vol. 22 (Issue 4), pp. 1018-1027.
19. Kim H, Kim C, Barlat F, Pavlina E and Lee M., 2012. Nonlinear elastic behaviors of low and high strength steels in unloading and reloading. *Materials Science and Engineering: A*.
20. RADU C., Analysis of the Correlation Accuracy-Distribution of Residual Stresses in the Case of Parts Processed by SPIF. *14th Mathematical models and methods in modern science*, July 1 - 3, Portugal, 2012.
21. Nguyen D, Park J, Lee H and Kim Y., 2010. Finite element method study of incremental sheet forming for complex shape and its improvement. *Proceedings of the Institution of Mechanical Engineers, Part B: Journal of Engineering Manufacture*, vol. 224 (Issue 6), pp. 913-924.
22. Taherizadeh A, Green DE, Ghaei A and Yoon J. A non-associated constitutive model with mixed iso-kinematic hardening for finite element simulation of sheet metal forming. *International Journal of Plasticity*, vol. 26 (Issue 2), pp. 288-309. ISSN 0749-6419.

23. de Souza T and Rolfe B., 2013. Understanding Robustness of Springback in High Strength Steels. *International Journal of Mechanical Sciences*, vol. 68, pp. 236-245. ISSN 0020-7403. DOI <http://dx.doi.org/10.1016/j.ijmecsci.2013.01.021>.
24. Khan MS, Coenen F, Dixon C and El-Salhi S., 2012. Classification based 3-D surface analysis: predicting springback in sheet metal forming. *Journal of Theoretical and Applied Computer Science Vol*, vol. 6 (Issue 2), pp. 45-59.
25. Chung W, Cho J and Belytschko T., 1998. On the dynamic effects of explicit FEM in sheet metal forming analysis. *Engineering Computations*, vol. 15 (Issue 6), pp. 750-776. ISSN 0264-4401.
26. Yavuz MM., 2013. INVESTIGATION OF THE EFFECT OF PLATE DIMENSIONS AND THICKNESSES ON THE IMPACT EFFECT OF A STEEL BALL. *International Journal of Engineering*, vol. 2 (Issue 1), pp. 2305-8269.
27. Singh R and Sekhon GS. An intelligent system for optimal selection of dies and tools for sheet metal operations. *Proceedings of the Institution of Mechanical Engineers, Part B: Journal of Engineering Manufacture*, vol. 216 (Issue 5), pp. 821-828. ISSN 0954-4054.
28. Fratini L, Lo Casto S and Lo Valvo E., 2006. A technical note on an experimental device to measure friction coefficient in sheet metal forming. *Journal of Materials Processing Technology*, vol. 172 (Issue 1), pp. 16-21.
29. Meier H, Brüninghaus J, Buff B, Hypki A, Schyja A and Smukala V., 2009. Tool path generation for free form surfaces in robot-based incremental sheet metal forming. *Key Engineering Materials*, vol. 410, pp. 143-150.
30. Lu B, Chen J, Ou H and Cao J., 2013. Feature-Based Tool Path Generation Approach for Incremental Sheet Forming Process. *Journal of Materials Processing Technology*.
31. Xu D, Malhotra R, Reddy NV, Chen J and Cao J., 2012. Analytical prediction of stepped feature generation in multi-pass single point incremental forming. *Journal of Manufacturing Processes*.
32. Schafer T and Schraft RD., 2005. Incremental sheet metal forming by industrial robots. *Rapid Prototyping Journal*, vol. 11 (Issue 5), pp. 278-286.
33. Tanaka H, Naka S and Asakawa N., 2012. Development of CAM System Using Linear Servo Motor to Automate Metal Hammering—A Study on Forging-Type Rapid Prototyping System—. *Journal Ref: International Journal of Automation Technology*, vol. 6 (Issue 5), pp. 604-610.
34. Yuan X, Zhenrong X and Haibin W. Research on integrated reverse engineering technology for forming sheet metal with a freeform surface. *Journal of Materials Processing Tech.*, vol. 112 (Issue 2), pp. 153-156. ISSN 0924-0136.

35. Meier H, Buff B and Smukala V., 2009. Robot-Based Incremental Sheet Metal Forming—Increasing the Part Accuracy in an Automated, Industrial Forming Cell. *Key Engineering Materials*, vol. 410 - 411, pp. 159-166. DOI 10.4028/www.scientific.net/KEM.410-411.159.
36. Hirt G, Ames J, Bambach M and Kopp R., 2004. Forming strategies and process modelling for CNC incremental sheet forming. *CIRP Annals-Manufacturing Technology*, vol. 53 (Issue 1), pp. 203-206.
37. Świllo S, Czyzewski P, Lisok J and Chamera M., Advanced Computer Based Techniques and Methods in Process Design for Large Car-Body Parts. *The 3rd International Lower Silesia - Saxony Conference: Advanced Metal Forming Processes in Automotive Industry*, 13 - 16 May, Wrocław, Poland, 2012.
38. Ambrogio G, Filice L, De Napoli L and Muzzupappa M., 2005. A simple approach for reducing profile diverting in a single point incremental forming process. *Proceedings of the Institution of Mechanical Engineers, Part B: Journal of Engineering Manufacture*, vol. 219 (Issue 11), pp. 823-830.
39. Fu Z, Mo J, Han F and Gong P. Tool path correction algorithm for single-point incremental forming of sheet metal. *The International Journal of Advanced Manufacturing Technology*, vol. 64 (Issue 9), pp. 1239-1248. ISSN 0268-3768.
40. Meier H, Laurischkat R, Bertsch C and Reese S., 2009. Prediction of Path Deviation in Robot Based Incremental Sheet Metal Forming by Means of an Integrated Finite Element–Multi Body System Model. *Key Engineering Materials*, vol. 410, pp. 365-372.
41. Meier H, Buff B, Laurischkat R and Smukala V. Increasing the part accuracy in dieless robot-based incremental sheet metal forming. *CIRP Annals - Manufacturing Technology*, vol. 58 (Issue 1), pp. 233-238. ISSN 0007-8506.
42. Belchior J, Guillo M, Courteille E, Maurine P, Leotoing L and Guines D., 2012. Off-line compensation of the tool path deviations on robotic machining: Application to incremental sheet forming. *Robotics and Computer-Integrated Manufacturing*.
43. Echrif SBM and Hrairi M., 2011. Research and Progress in Incremental Sheet Forming Processes. *Materials and Manufacturing Processes*, vol. 26 (Issue 11), pp. 1404-1414. ISSN 1042-6914.
44. Emmens WC and Van den Boogaard A., 2007. Strain in shear, and material behaviour in incremental forming. *Key Engineering Materials*, vol. 344, pp. 519-526.
45. Jurisevic B, Kuzman K and Junkar M., 2006. Water jetting technology: an alternative in incremental sheet metal forming. *The International Journal of Advanced Manufacturing Technology*, vol. 31 (Issue 1), pp. 18-23.
46. Göttmann A, Diettrich J, Bergweiler G, Bambach M, Hirt G, Loosen P and Poprawe R., 2011. Laser-assisted asymmetric incremental sheet forming of titanium sheet metal parts. *Production Engineering*, vol. 5 (Issue 3), pp. 263-271.

47. Jeswiet J, Micari F, Hirt G, Bramley A, Duflou J and Allwood J. Asymmetric Single Point Incremental Forming of Sheet Metal. *CIRP Annals - Manufacturing Technology*, vol. 54 (Issue 2), pp. 88-114. ISSN 0007-8506.
48. *Dieless NC Forming*. AMINO North America Corporation, United States. [viewed 20.02.2014]. Available from: [http://www.aminonac.ca/technology\\_dnc.asp](http://www.aminonac.ca/technology_dnc.asp).
49. *Sheet Metal Fast Prototyping*. OCAS BV, Belgium. [viewed 20.02.2014]. Available from: <http://www.ocas.be/>.
50. *Asymmetrical Incremental Plate Forming Technology and Tool-less Forming Processes*. ASCAMM TECHNOLOGY CENTRE, SPAIN. [viewed 20.02.2014]. Available from: <http://www.ascamm.com/en/recerca/materials-i-processos/processat-metal%C2%B7lic/>.
51. *Freeform Fabrication Technology*. FORD, United States. [viewed 20.02.2014]. Available from: <https://media.ford.com/content/fordmedia/fna/us/en/news/2013/07/03/ford-develops-advanced-technology-to-revolutionize-prototyping--.html>.
52. Oscoz MP, Zettler J and Papadopoulos MP., 2011. Innovative Manufacturing of Complex Ti Sheet Components (INMA). *International Journal of Structural Integrity*, vol. 2 (Issue 4) ISSN 1757-9864.
53. Kreimeier D, Zhu JH and Laurischkat R., 2012. Integrated Process Design for Two Robots Based Incremental Sheet Metal Forming. *Key Engineering Materials*, vol. 504, pp. 877-882.
54. Kreimeier D, Buff B, Magnus C, Smukala V and Zhu J., 2011. Robot-Based Incremental Sheet Metal Forming—Increasing the Geometrical Accuracy of Complex Parts. *Key Engineering Materials*, vol. 473, pp. 853-860.
55. *Incremental Sheetmetal Forming: a die-less rapid prototyping process for sheet metal* . IMRC, Bath University, UK. [viewed 21.02.2014]. Available from: <http://www.bath.ac.uk/idmrc/themes/projects/amps/MPS-Project-ISF.pdf>.
56. *Incremental Sheet Forming*. AFRC, University of Strathclyde Engineering, UK. [viewed 21.02.2014]. Available from: <http://www.strath.ac.uk/afrc/research/sheet-forming/>.
57. *Sheet Metal Forming Processes*. RWTH (IBF), Aachen University, Germany. [viewed 21.02.2014]. Available from: <http://www.ibf.rwth-aachen.de/en/research-development/sheet-metal-forming/>.
58. *Dieless Sheet Metal Part Production Technique*. Ku Leuven University, Germany. [viewed 21.02.2014]. Available from: <https://www.mech.kuleuven.be/pp/research/spif>.
59. *Incremental Sheet Forming (ISF) of Metal sheets with a FANUC Robot*. CIM Robotics Laboratory, MTA, SZTAKI, Computer and Automation Research Institute



Hungary Academy of Sciences, Hungary. [viewed 21.02.2014]. Available from: <http://archive.is/BqKc>.

60. Callegari M, Gabrielli A, Palpacelli M and Principi M., 2008. Incremental Forming of Sheet Metal by Means of Parallel Kinematics Machines. *Journal of Manufacturing Science and Engineering*, vol. 130 (Issue 5), pp. 054501-054501. DOI 10.1115/1.2823064.
61. Agote D and Penalva ML. *Incremental Sheet Forming (ISF): A flexible, cost-effective alternative for small series and prototypes in sheet metal forming (The Sculptor Project)*. Fatronik, Spain. [viewed 21.02.2014]. Available from: [http://www.interempresas.net/MetalWorking/Articles/19430-Incremental-sheet-forming-\(ISF\)-A-flexible-cost-effective-alternative-for-small-series.html](http://www.interempresas.net/MetalWorking/Articles/19430-Incremental-sheet-forming-(ISF)-A-flexible-cost-effective-alternative-for-small-series.html).
62. *Incremental Forming at Multi-Scales*. AMPL, Northwestern University, United States. [viewed 21.02.2014]. Available from: [http://cao.mech.northwestern.edu/incremental\\_forming.html](http://cao.mech.northwestern.edu/incremental_forming.html).
63. Matsubara S., 2001. A computer numerically controlled dieless incremental forming of a sheet metal. *Proceedings of the Institution of Mechanical Engineers, Part B: Journal of Engineering Manufacture*, vol. 215 (Issue 7), pp. 959-966.
64. Meier H, Magnus C and Smukala V. Impact of superimposed pressure on dieless incremental sheet metal forming with two moving tools. *CIRP Annals - Manufacturing Technology*, vol. 60 (Issue 1), pp. 327-330. ISSN 0007-8506.
65. Hagan E and Jeswiet J., 2004. Analysis of surface roughness for parts formed by computer numerical controlled incremental forming. *Proceedings of the Institution of Mechanical Engineers, Part B: Journal of Engineering Manufacture*, vol. 218 (Issue 10), pp. 1307-1312.
66. Hussain G, Hayat N and Lin G., 2012. Pyramid as test geometry to evaluate formability in incremental forming: Recent results. *Journal of Mechanical Science and Technology*, vol. 26 (Issue 8), pp. 2337-2345.
67. Kopac J and Kampus Z. Incremental sheet metal forming on CNC milling machine-tool. *Journal of Materials Processing Tech.*, vol. 162, pp. 622-628. ISSN 0924-0136.
68. Ma L and Mo J. Three-dimensional finite element method simulation of sheet metal single-point incremental forming and the deformation pattern analysis. *Proceedings of the Institution of Mechanical Engineers, Part B: Journal of Engineering Manufacture*, vol. 222 (Issue 3), pp. 373-380. ISSN 0954-4054.
69. *Innovative Sheet Forming Processes*. University of Cambridge, UK. [viewed 21.02.2014]. Available from: <http://www.lcmp.eng.cam.ac.uk/wellformed/innovative-sheet-forming-processes>.

70. Tanaka H, Asakawa N and Hirao M., 2005. Development of a Forging Type Rapid Prototyping System; Automation of a Free Forging and Metal Hammering Working. *JOURNAL OF ROBOTICS AND MECHATRONICS*, vol. 17 (Issue 5), pp. 523.
71. Asakawa N, Tanaka H, Takasugi K, Yamamoto K and Okada M., Development of a Forging Type Rapid Prototyping System (the Recent Summary). *Proceedings of the International Conference on Mechatronics Technology*, Oct 2014, Japan, 2014.
72. Yamamoto K, Asakawa N, Okada M, Takasugi K and Tanaka H., Development of a Forging Type Rapid Prototyping System - Influence of Local Heating by Gas Burner and Tool Path on Formability. *Proceedings of the International Conference on Mechatronics Technology*, Oct 2014, Japan, 2014.
73. Luo Y, He K and Du R., 2010. A new sheet metal forming system based on incremental punching, part 2: machine building and experiment results. *The International Journal of Advanced Manufacturing Technology*, vol. 51 (Issue 5), pp. 493-506.
74. Opritescu D, Sachnik P, Yang Z, Golle R, Volk W, Hoffmann H, Schmiedl F, Ritter M and Gritzmann P., 2012. Automated Driving by Standardizing and Scaling the Manufacturing Strategy. *Procedia CIRP*, vol. 3, pp. 138-143.
75. *CoDrive*. Costesys, Germany. [viewed 21.02.2014]. Available from: <http://cotesys-v2.in.tum.de/research/list-of-projects.html?projectid=33&cHash=e8aa83dcdf>.
76. Scherer D, Yang Z and Hoffmann H., 2010. Driving - A flexible manufacturing method for individualized sheet metal products. *International Journal of Material Forming*, vol. 3, pp. 955-958. ISSN 1960-6206. DOI 10.1007/s12289-010-0927-5.
77. Eckold., 2015. *Kraftformer KF 170 PD*. 05.02.2015, Available from: <http://www.eckold.com/en-us/productsforsheetmetalworking/kraftformer/kraftformerkf170pd.aspx>.
78. Vicon., 2015. *Vicon System*. 14.04.2015, Available from: <http://www.vicon.com/>.
79. Vicon., 2015. *Vicon T-Series*. 10.04.2015, Available from: <http://www.vicon.com/System/TSeries>.
80. Mathworks. *MATLAB*. R2012a ed.
81. Halcon., 2015. *Halcon 12*. 04.06.2015, Available from: <http://www.halcon.com/>.
82. Nave CR., 2014. *HyperPhysics (Mechanics)*. [viewed 17.04.2014]. Available from: <http://hyperphysics.phy-astr.gsu.edu/hbase/avari.html>.
83. Goldsmith W., 2001. *Impact: The Theory and Physical Behaviour of Colliding Solids*. Mineola, NY: Dover Publications ISBN 9780486420042.
84. DJB Instruments. *IEPE IH-10 Impact Hammer*. [viewed 26.03.2014]. Available from: <http://www.djbinstruments.com/en/products/instrumentation/impact-hammers>.

85. MSC Software. *MARC and MENTAT*. 2012th ed.
86. Vicon., 2015. *Vicon active wand*. 10.04.2015, Available from: <http://www.vicon.com/System/Calibration>.
87. Matlab., 2015. *Simulink*. 14.04.2015, Available from: <http://uk.mathworks.com/products/simulink/>.
88. Yaskawa., 2015. *Motoman SDA10D*. 05.02.15, Available from: <http://www.motoman.com/products/robots/assembly-robots.php>.
89. Schunk., 2015. *2 finger paraller gripper PGN plus 80 - 1*. 25.5.2015, Available from: [http://www.us.schunk.com/schunk/schunk\\_websites/products/products\\_level\\_3/product\\_level3.html?product\\_level\\_3=289&product\\_level\\_2=250&product\\_level\\_1=244&country=USA&r=1#](http://www.us.schunk.com/schunk/schunk_websites/products/products_level_3/product_level3.html?product_level_3=289&product_level_2=250&product_level_1=244&country=USA&r=1#).
90. Schunk., 2015. *2 finger parallel gripper PGN plus 80-2*. 25.05.15, Available from: [http://www.us.schunk.com/schunk/schunk\\_websites/products/products\\_level\\_3/product\\_level3.html?product\\_level\\_3=289&product\\_level\\_2=250&product\\_level\\_1=244&country=USA&r=1#](http://www.us.schunk.com/schunk/schunk_websites/products/products_level_3/product_level3.html?product_level_3=289&product_level_2=250&product_level_1=244&country=USA&r=1#).
91. SMC., 2015. *2-way normally closed solenoid valve VXD 2130-03F-5D1*. 25.05.2015, [viewed 25.05.2015]. Available from: <http://www.smc pneumatics.com/VXD2130-03F-5D1.html>.
92. Archimedes., 2015. *Archimedean Spiral*. 26.06.2015, Available from: [https://en.wikipedia.org/wiki/Archimedean\\_spiral](https://en.wikipedia.org/wiki/Archimedean_spiral).
93. Fofi D, Sliwa T and Voisin Y., 2004. A comparative survey on invisible structured light, Machine Vision Applications in Industrial Inspection XII. *Proceedings of SPIE*, vol. 5303, pp. 90. DOI 10.1117/12.525369.
94. Amann M-, Bosch T, Lescure M, Myllylä R and Rioux M., 2001. Laser ranging: A critical review of usual techniques for distance measurement. *Optical Engineering*, vol. 40 (Issue 1), pp. 10-19. ISSN 00913286. DOI 10.1117/1.1330700.
95. Franca JGDM, Gazziro MA, Ide AN and Saito JH., 2005. *A 3D scanning system based on laser triangulation and variable field of view*. USA: .
96. Dorsch RG, Hausler G and Herrmann JM., 1994. Laser triangulation: fundamental uncertainty in distance measurement. *Applied Optics*, vol. 33 (Issue 7), pp. 1306. ISSN 0003-6935.
97. Smith WJ., 2008. *Modern optical engineering : the design of optical systems*. 4th ed.. ed. New York ; London: McGraw-Hill.
98. Fricke-Begemann T and Hinsch K., 2004. Measurement of random processes at rough surfaces with digital speckle correlation. *Journal of the Optical Society of America A-Optics Image Science and Vision; J.Opt.Soc.Am.A-Opt.Image Sci.Vis.*, vol. 21 (Issue 2), pp. 252-262. ISSN 1084-7529.

99. Basler., 2015. *Basler ace acA1600-20gm*. 13.06.2015, Available from:  
<http://www.baslerweb.com/en/products/area-scan-cameras/ace/aca1600-20gm>.
100. Tamron., 2015. *Tamron focal lens*. 13.06.2015, Available  
from: <http://ccddirect.com/tamron-23fm08-1-2-3-8mm-f-1.4-high-resolution-c-mount-lens-with-lock.html>.
101. Tailor M., 2014. *Automatic surface defect quantification in 3D*. PhD ed.  
Loughborough University.

## **LIST OF APPENDICES**

**Appendix 1** - Technical Report on Panel Beating Training underwent at Peterborough

**Appendix 2** – Power hammer investigation

**Appendix 3** – Eckold Kraftformer KF 170 PD – Specification

**Appendix 4** - Experiment using wooden hammer and High Speed Camera (400 fps)

**Appendix 5** – Instrumented impact hammer – Specification

**Appendix 6** – Yaskawa Motoman SDA10 – Specification

**Appendix 7** – PGN Plus 80-2 Schunk Gripper – Specification

**Appendix 8** – Finger design – Specification

**Appendix 9** – Basler acA 1600 20gm Camera – Specification

**Appendix 10** – Calibration description file

**Appendix 11** – List of published work

## **LIST OF PUBLICATIONS**

**Publication 1** – International Journal of Advanced Manufacturing Technology

**Publication 2** – Industrial Journal of Institution of Sheet Metal Engineers

**Publication 3** – Industrial magazine of Confederation of British Metal Forming

**Publication 4** - 2<sup>nd</sup> Annual EPSRC Manufacturing the Future Conference 2013

## An automated solution for fixtureless sheet metal forming

Balaji Ilangoan<sup>1,2</sup> · Radmehr P. Monfared<sup>1,2</sup> ·  
Michael Jackson<sup>1,2</sup>

Received: 15 December 2014 / Accepted: 21 May 2015  
© The Author(s) 2015. This article is published with open access at Springerlink.com

**Abstract** Manual forming of sheet metal parts through traditional panel beating is a highly skilled profession used in many industries, particularly for sample manufacturing or repair and maintenance. However, this skill is becoming gradually isolated mainly due to the high cost and lack of expertise. Nonetheless, a cost-effective and flexible approach to forming sheet metal parts could significantly assist various industries by providing a method for fast prototyping sheet metal parts. The development of a new fixtureless sheet metal forming approach is discussed in this article. The proposed approach, named Mechatroforming<sup>®</sup>, consists of integrated mechanisms to manipulate sheet metal parts by a robotic arm under a controlled hammering tool. The method includes mechatronics-based monitoring and control systems for (near) real-time prediction and control of incremental deformations of parts. This article includes description of the proposed approach, the theoretical and modelling backgrounds used to predict the forming, skills learned from manual operations, and proposed automation system being built.

**Keywords** Automation · Flexible manufacturing · Rapid prototyping · Incremental forming

✉ Balaji Ilangoan  
B.ilangoan@lboro.ac.uk

<sup>1</sup> EPSRC Centre for Innovative Manufacturing in Intelligent Automation, Loughborough University, Loughborough, UK

<sup>2</sup> Wolfson School of Mechanical and Manufacturing Engineering, Loughborough University, Loughborough, UK LE11 3TU

### 1 Introduction

In many industries, dies are used for forming sheet metals but they typically lack flexibility and cost-effectiveness when low-volume production or prototyping are considered. For these cases, the traditional manual panel beating is still used. However, manual panel beating is a highly skilled process and unfortunately, due to the lack of interest (by new trainees), high cost, and sporadic industrial applications, is becoming isolated and gradually being lost.

There is not enough research carried out to fully understand and capture the skills of experienced panel beaters and its links with the formal sheet metal forming theories.

Analysing the conventional manual practises has led to an ongoing research work in robotic sheet metal forming which has been discussed in this article. The proposed research methodology could potentially be used by many industries, especially for maintenance and rapid prototyping of sheet metal parts.

There has been some research in die-less incremental forming of sheet metals [1]. Most proposed methods use either stretching or drawing techniques with or without an anvil support. The sheet metal is formed by using a round headed tool which moves down vertically (i.e. in Z axis). The sheet metal is typically held by fixtures along the edges to avoid movement caused by tool. Either the sheet metal or the tool is moved along XY axes (i.e. the horizontal plane) to achieve the required contour. The forming is often computer controlled. Employing this technique achieves a smooth finish but may result in fractures due to excessive stretching and often fails while forming complex contours (e.g. having more than 55° wall angle [2]). These methods use fixtures to hold the sheet and typically result in non-uniform thickness of the formed sheet metal, hence, affecting the quality.

## Die-less Automated Sheet Metal Forming



Die-less forming is one of the emerging techniques in the sheet metal forming industry. Research is being carried out to develop a new automated method for sheet metal forming, based on human technique captured from studies of highly skilled panel beaters.

The methodology developed uses a sequential hammering mechanism, the Eckold Kraftformer KF 170 PD. The mechanism incrementally forms the sheet metal which is held and manipulated by a robot to form the required shape. The developed approach includes an in-process monitoring system using machine vision. The vision system feedback is used to accurately control the formation of the material to the three dimensional shape required.

In many industries, dies are used to form sheet metal panels of different contours. Dies lack flexibility and cost effectiveness when low volume production, repair or prototyping is required. In such cases, manual panel beating is typically undertaken for incremental forming of metal panels. This is a highly skilled operation with very little documentation. Unfortunately, due to recruitment issues, high cost and



**By Balaji Ilangovan**  
MISME MIET AMIMECHE  
BEng, MSc.,

**PhD Researcher**  
**in Automated Sheet Metal Forming**  
EPSRC Centre for Innovative  
Manufacturing in Intelligent  
Automation, Loughborough  
University, UK

**Treasurer**  
IMechE, Leicestershire  
Young Members Panel

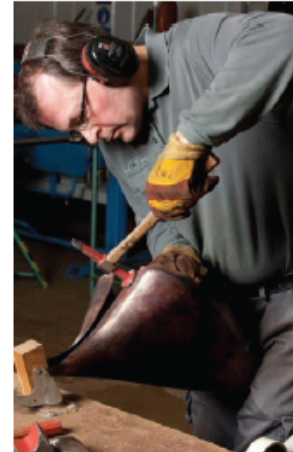
**Email:** B.ilangovan@lboro.ac.uk,  
B.ilangovan88@gmail.com

**Linkedin:** [uk.linkedin.com/pub/  
balaji-ilangovan/40/b82/70a/](https://uk.linkedin.com/pub/balaji-ilangovan/40/b82/70a/)



# Die-less Automated Sheet Metal Forming

Die-less forming is one of the emerging techniques in sheet metal forming. Research is being carried out to develop a new automated method for sheet metal forming based on human skill captured from highly skilled panel beaters. The methodology developed uses a sequential hammering mechanism, the Eckold Krafftormer KF 170 PD. The mechanism incrementally forms the sheet metal which is held and manipulated by a robot to form the required shape. The developed approach includes an in-process monitoring system using machine vision. The vision system feedback is used to control the formation of sheet metal accurately to the three dimensional shape required.



In many industries, dies are used to form sheet metal panels of different contours. Dies lack flexibility and cost effectiveness when low volume production, repair or prototyping is required. In such cases, manual panel beating is typically undertaken for incremental forming of metal panels. This is a highly skilled operation with very little documentation. Unfortunately, due to recruitment issues, high cost and sporadic industrial applications, manual panel beating is being isolated and gradually forgotten. It is essential to capture the highly skilled process and preserve the knowledge of metal forming practise.

The EPSRC Centre for Innovative Manufacturing in Intelligent Automation launched a PhD in July 2012 to develop an automated panel forming process. Primarily, the research aimed at understanding and analysing the skills of a manual panel beater. A comprehensive literature review was carried out to understand the industrial and research work in this area. Though there has been a significant research in automated incremental forming processes, the current technology for die-less forming typically uses either stretching or drawing of sheets, usually by pushing the material. This causes a thinning effect on the panel and almost all the current methods require substantial fixtures to hold the panel.

Based on the literature review, the research was focused on forming the sheet metal without using dies and fixtures allowing free formation of sheet metal replicating the skill of a panel beater. The research methodology was developed in three stages, consisting of capturing human skill, semi-automated system and fully automated system. This work included several modelling and experimental process analyses.



Initially, experienced panel beaters were closely observed and their tacit human skill was analysed. It was identified that consecutive shrinking and stretching (through hammering) of sheet metal produces a sheet with uniform thickness. It was also determined that imposing repetitive kinetic energy through hammering allows better control over producing shapes incrementally by consecutive stretching and shrinking without fixtures. This method is also believed to improve release of residual stresses during the forming process. The constructive methodology used by the panel beater improves the quality of the sheet metal by maintaining the uniform distribution of material.

Measurement of the impact force and kinetic energy involved in panel beating of sheet metal was carried out using an instrumented mallet and high speed video to capture data during manual hammering tests conducted in a structured laboratory environment. Based on the impact force determined and corresponding kinetic energy, a hammering machine capable of producing the required force and able to operate at the required frequency was investigated. The Eckold Krafftormer KF 170 PD was purchased as this met the requirements for the automated panel beating test cell.

The semi-automated system utilises the Eckold Krafftormer and manual manipulation of the sheet metal blank between the hammer and the anvil during automatically repetitive hammering to progressively form the desired 3D shape. During the action of forming the shape a Vicon 3D imaging system was used to capture and analyse the movement of the sheet metal blank. Based on several experimental trials, the most suitable movement pattern and path was determined to be used as an input to the robotic manipulation.

The development of an automated system included the integration of an Eckold Krafftormer and Motoman SDA10D on a common control platform. This approach synchronised the sequential hammering of the Eckold Krafftormer with the forming manipulation pattern executed by the robot. A gripper was designed similar to the holding-area of a human grip in manual forming process. The gripper was installed on the robotic arm to be able to hold the sheet metal and provide the required manipulation.

Based on this set-up, experimental trials were performed in developing an automated sheet metal forming process. The trials based on forming a bowl shape were successful and repeatable after several analyses and modifications. The human skills studied and decomposing the video of trials to examine the formation contributed towards performance enhancement.

continued on page 20 ---->

## MANUFACTURING THE FUTURE CONFERENCE 2013

Free- Form Automated Incremental Panel Forming

Balaji Ilangoan, Radmehr P. Monfared, Michael Jackson

EPSRC Centre for Innovative Manufacturing in Intelligent Automation, Wolfson School of Mechanical & Manufacturing Engineering, Loughborough University, Loughborough, B. Ilangoan@lboro.ac.uk

Dies are used in many industries to form metal panels of different contours but they lack flexibility and cost effectiveness when low volume production, repair or prototyping is considered. In such cases, manual panel beating is typically undertaken for incremental forming of metal panels. Manual panel forming is a highly skilled operation with very little documentation and the skill is disappearing due to non-observance and lack of training. There has been a significant amount of research in automated incremental forming processes. However, the current technology for die-less forming typically uses either stretching or drawing of sheets, usually by pushing the material. This causes a thinning effect on the panel which requires substantial fixtures.

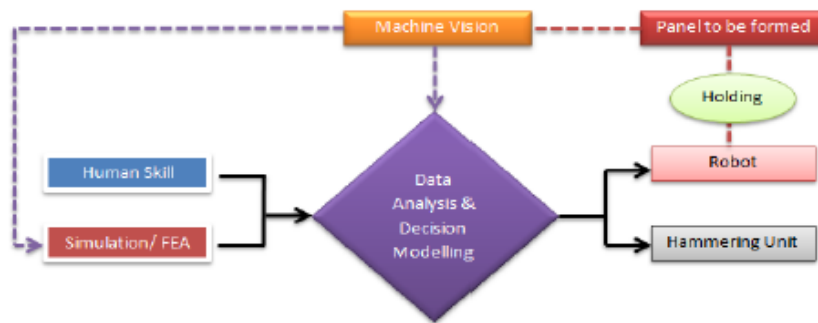


Figure 1

This research is aimed at developing a new automated method for panel formation based on human skill captured from manual operators. The methodology being developed, incrementally forms the material through impacting with continuous control and modification through a fixtureless integrated process. The proposed approach includes automating panel forming with a near real time monitoring system using machine vision. This process is targeted at producing nearly uniform panel thickness by introducing a higher degree of freedom in formation with continuous stress analysis. This research has the potential to optimise the panel formation and reduce reworks in forming irregular shapes. The process model based on human skill capture is illustrated in Figure 1. The scope of this research is limited to 1mm thick aluminium and steel which covers standard industry applications. The formation is carried out by an impact energy delivery unit causing deformation in the panel, which is held by a robot controlling the movement of the panel, adhering to the formation. The distance of deformation is obtained by using point-cloud data, which is generated by using machine vision and analysed through finite elements.

**Significance Statement:** This research will provide a proof of principle for automated one off, flexible production of irregular panels. Highly accurate production will be achieved based on the panel formation skills captured from human operators.

# APPENDIX 1

## A Technical Report on Panel Beating Training underwent at Peterborough

(24<sup>th</sup> – 28<sup>th</sup> September 2012)

### Contents

PREFACE.....	1
INTRODUCTION .....	2
CHAPTER 1 – STEPS INVOLVED IN FORMING THE SHEET METAL .....	5
1.1 Choice of Material .....	5
1.2 Uncoiling.....	5
1.3 Snipping .....	7
1.4 Panel Beating using Mallet and Wooden Block .....	9
1.5 Panel Beating using Hammer & Dollies.....	16
1.6 Wheeling.....	18
1.7 Shrinking/ Stretching .....	20
1.8 Flanging .....	22
CHAPTER 2 – FACTORS THAT AFFECT SHEET METAL FORMATION.....	27
2.1 Tooling.....	27
2.2 Types of Wheels .....	30
2.3 Measuring & Marking Techniques .....	32
2.4 Filing Techniques.....	36

CHAPTER 3 – ENGINEERING FACTORS .....	37
3.1 Velocity of the Tool .....	37
3.2 Motion of the Work Piece.....	37
3.3 Relative motion of Tool to Work Piece .....	37
3.4 Ductility, Malleability and Rigidity of the Material .....	38
3.5 Involute Curves .....	38
3.6 Designing/ Drafting .....	38
CONCLUSION.....	39

## **PREFACE**

This document provides the basic panel beating methods being followed by the traditional panel beaters. These traditional methodologies evolve to be the basis and fundamental of sheet metal forming. The sheet metal are formed using cold rolling/ forming technologies to ensure that the quality of the material is not lost and the material remains durable for years. There are several factors involved in sheet metal forming starting from uncoiling the non-formed sheet to final finish of the formed sheet metal. Each and every step of the sheet metal forming technology has got a design consideration. Considering sheet metal forming as an incremental forming technology, each step has got its own importance. If the steps are not designed/ worked out properly or eluded, final shape attained will not be of perfect dimensions and desired shape. These steps of manufacturing/ forming process will be discussed in detail in this document.

Tooling plays an important role in sheet metal forming. Whether it is traditional forming method or it is a large die, the shape of the tool will determine the shape of the sheet metal formed. These include wheeling techniques as well. This document focusses on discussing the traditional, semi- automatic and automatic tooling methodologies that exist in the sheet metal forming industry.

There are several engineering factors involved in forming a sheet metal. These vary from material science to finite element mechanics. The traditional art of sheet metal forming related to current engineering technologies will be discussed in this document.

The basic aim to introduce incremental sheet forming involving traditional hammering methodology will be overviewed. Its benefit over existing technologies will be discussed in this document.



## INTRODUCTION

The knowledge of this document is based on learning the traditional sheet metal forming process at CONTOUR AUTOCRAFT, Peterborough, United Kingdom. The small workshop has got traditional sheet metal craftsman working on the body of XK JAGUAR. Training was undergone to understand the behaviour of sheet metal under different forming methodologies. The characteristics of sheet metal during its formation stages were studied and their design engineering/ finite elemental aspects were analysed during the training course.

The figure (i) below shows the Jig of XK Jaguar body which was used as a template in forming the sheet metal for XK Jaguar Body.



Figure i – Jig of XK Jaguar Body

The initial part formed was a double curvature that would fit the top curvature of the bonnet in the XK Jaguar. The next part formed was slight wave curved sheet metal to fit the top curvature of the bonnet alongside the earlier made part. Figure (ii) below shows the parts.





Figure ii – Parts formed to fit the top curvature of Bonnet

There were several aspects involved in crafting these two parts. The steps involved are as follows:

1. Choice of material
2. Uncoiling
3. Snipping
4. Panel Beating using Mallet & Wooden Block
5. Panel Beating using Hammer & Dollies
6. Wheeling
7. Shrinking/ Stretching
8. Flanging

Each step listed above is of paramount importance to attain the required shape of the sheet metal. There are several factors related to geometry and shaping affecting this successive methodology. The factors that affect the sheet metal formation are:

1. Tooling (while involving Hammer & Dolly, Flanging)
2. Types of Wheels (during Wheeling)
3. Measuring & Marking Techniques
4. Filing Techniques

The methodologies and parameters affecting them are related based on basic engineering terminologies. To term some:

1. Velocity of the Tool

2. Motion of the Work Piece
3. Relative motion of Tool to Work Piece
4. Ductility of the Material
5. Malleability of the Material
6. Rigidity of the Material
7. Involute Curves
8. Designing/ Drafting

Listed above are some engineering factors which affect the sheet metal forming. These factors need to be studied relatively to form the sheet metal to perfection. This documentation will discuss on how to combine the factors and analyse the results produced based on advanced engineering methodologies. The traditional analyses will be considered in relating the factors as it forms the basis for modern technology.



## **CHAPTER 1 – STEPS INVOLVED IN FORMING THE SHEET METAL**

### **1.1 Choice of Material**

Choosing the right material according to the purpose of use is of much importance. There are two types of sheet metal generally used in the industry. They are Cold Reduced/ Rolled (CR) and Hot Reduced/ Rolled (HR). The commonly used sheet metal in car/ aerospace industry is Cold Reduced as it has got a better strength/ durability compared to Hot Reduced.

There are several material types available in Cold Reduced sheet metal such as CR sheet metal – high temperature atmospheric resistant, CR sheet metal – corrosion resistant, CR sheet metal – for galvanizing, CR sheet metal – without annealing, CR sheet metal – for porcelain enamelling, etc. These cold rolled sheet metal types are used for varied purposes and have got varied material properties.

The commonly used Cold Reduced sheet metal in Car industries are low carbon, ferrous and annealed. This CR sheet metal type is of higher strength and has got higher forming capabilities. The CR sheet metal comes with a suffix number which is for material identification (e.g. CR4 – Good Malleability, CR8 – Highly Rigid). CR4 is the sheet metal usually used by car manufacturers.

The thickness of the sheet metal also plays an important role in deformation of the material. The sheet metals are of 1mm, 1.2mm, 1.5mm thickness. The most commonly used sheet metal in car industries is of 1mm thickness.

The manufacturing/ forming capability of a sheet metal gets varied relevant to the properties of sheet metal being used. So choosing the right material should be given a higher priority before moving on to manufacturing processes.

### **1.2 Uncoiling**

Uncoiling is the foremost step in preparing the sheet metal for its manufacturing/ forming phase. The distortions in the sheet metal surface are likely to cause effects during the forming process.

The Cold Reduced sheet metal is rolled into a coil and delivered to the manufacturer. The manufacturer uses the necessary wheeling process to uncoil the sheet according to the need

and later snip it to required sizes. This process usually involves sliding the sheet to be uncoiled between two rollers. The final sheet quality depends on the alignment of the rollers. Figure (1.2.1) shows how the process is being done.

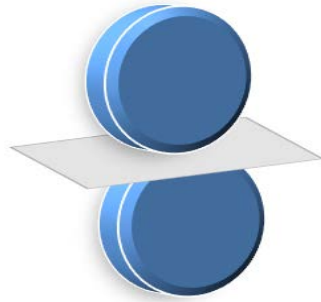


Figure 1.2.1 – Sheet being slide between two rollers.

For a perfect flat sheet to yield out of rolling, the rolling wheels should be concentric. If the rollers are not concentric they are likely to produce wavy distortions in the yielded sheet. The figure (1.2.2) shows the rolling of a sheet metal using concentric rollers and the sheet it yields. As it could be seen, the sheet doesn't have any distortions since the rollers are concentric. The figure (1.2.3) shows the rollers which are non- concentric. The sheet it yields has got wavy distortions as illustrated in the diagram. These distortion though they are of millimetre/ micrometre range, they cause lot of problems in precision manufacturing of the sheet metal. It should be noted that either this distortion should be kept very minimal or to compensate for the distorted sheet metal.



Figure 1.2.2 – Concentric Rollers and the Sheet yield caused by the process

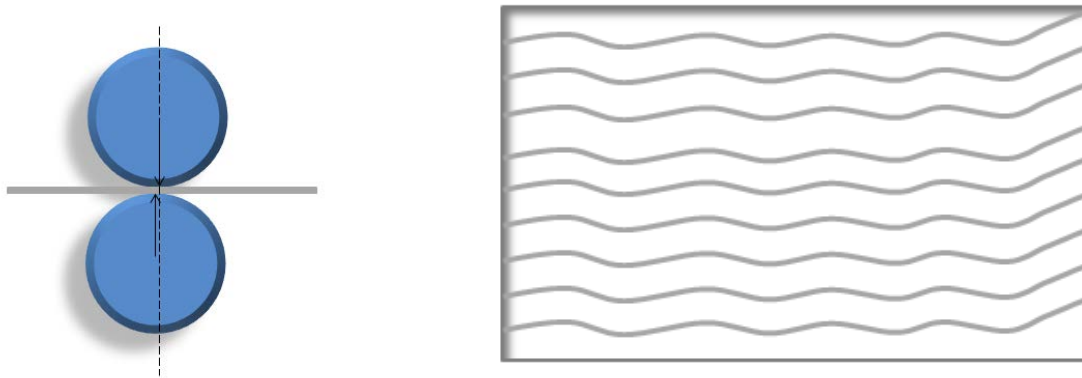


Figure 1.2.3 – Non- Concentric Rollers and the Sheet yield by the process

### 1.3 Snipping

It is important to cut the sheet metal before forming. It is better to cut the non- formed sheet metal than to cut out of the formed sheet metal to maintain the strength of the sheet metal at the edge where material is snipped off. The figures below shows the types of snips/ hand shearing tool used to cut off the material.



Figure 1.3.1 – Straight Snip

Figure (1.3.1) shows the Straight snip that is used to cut along a straight line or very gentle curvature.



Figure 1.3.2 – Right Hand Snip

Figure (1.3.2) shows the Right Hand snip which is used to cut from right to left with waste material on left hand side of cut.



Figure 1.3.3 – Left Hand Snip

Figure (1.3.3) shows the Left Hand snip which is used to cut from left to right with waste of material on right hand side of cut.

All these snips have got a basic method of handling. It is always good to use the middle third of the blade to cut. Bottom blade is to be flat always when using the left hand snip and the vice- versa is followed for right hand snip. If the blade is not held properly as stated, it makes the shearing harder and causes lots of burrs. The figure (1.3.4) below shows the usage of right hand and left hand snip.

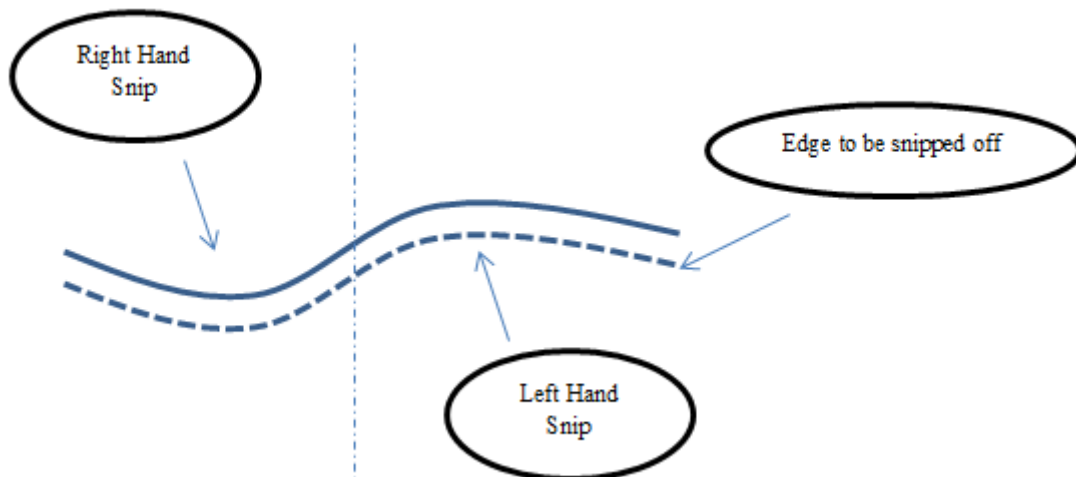


Figure 1.3.4 Usage of Right Hand & Left Hand snips

It is always good to maintain the snips for a better shearing. The snip blades are to be filed using diamond files. It is good to oil the bolt and nut which are usually held loose but without any slack to make the shearing easier. Oil should not be applied on the blades.

There is a considerable cutting aspect that could be inferred from traditional process to get the best out of snipping. The considerable factor is the source of light which might cause a shadow and hence angle of snip may be lost. The figure (1.3.5) illustrates the light source effect on snipping.

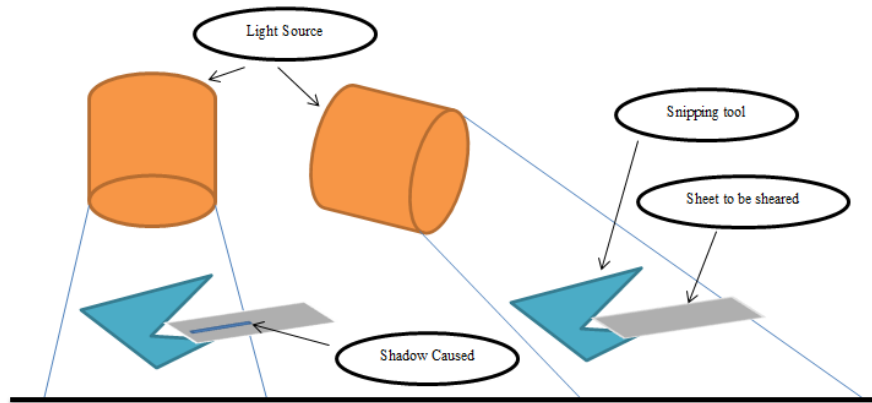


Figure 1.3.5 Light source effect on snipping

As illustrated in the figure (1.3.5), it is good to have the light source at angle appropriate to the angle at which the snipping tool is being held. Otherwise shadows may be caused which may lead to angular disparity.

There are several new engineering technologies which could easily cut off the unwanted/ excess material in seconds. Laser cutting is the most precise technology being used in the industry currently.

#### 1.4 Panel Beating using Mallet and Wooden Block

The basic shape required is acquired using the Mallet and Wooden Block which is shaped according to the required shape of the sheet metal. Ideally the shape of the Mallet and shape of the Wooden Block will be of shape that is required to be formed. In the figure (1.4.1) below, the wooden block is curved since the final sheet metal to be produced is curved. The mallet has a curved edge as well to complement the wooden block's curvature.

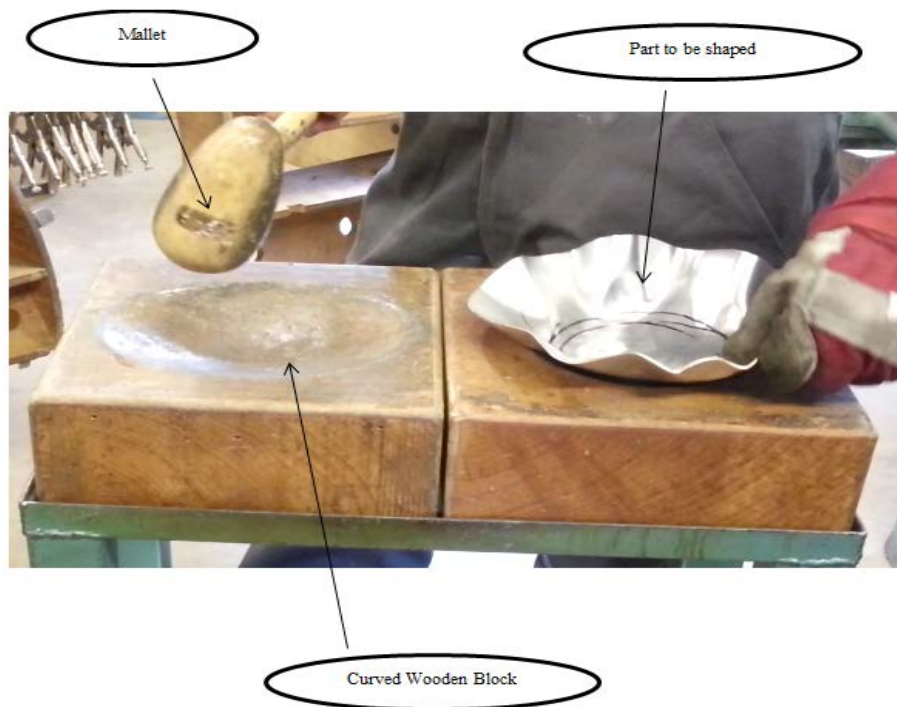


Figure 1.4.1 – Curved wooden block to form a curved sheet metal

In the example considered, it is required to form a double curvature for the body of XK Jaguar. So, the shape of the wooden block and the mallet are required to be similar to a double curvature. Figures (1.4.2 & 1.4.3) show the wooden block and mallet that has been used to form a double curvature of sheet metal.



Figure 1.4.2 – Wooden Block with Double Curvature



Figure 1.4.3 – Mallet and the Wooden Block

The final shape to be produced is shown below in the figure (1.4.4). The sheet metal has got differing curvatures and hollowness which are marked in the figure to illustrate the mechanism required to produce the shape.

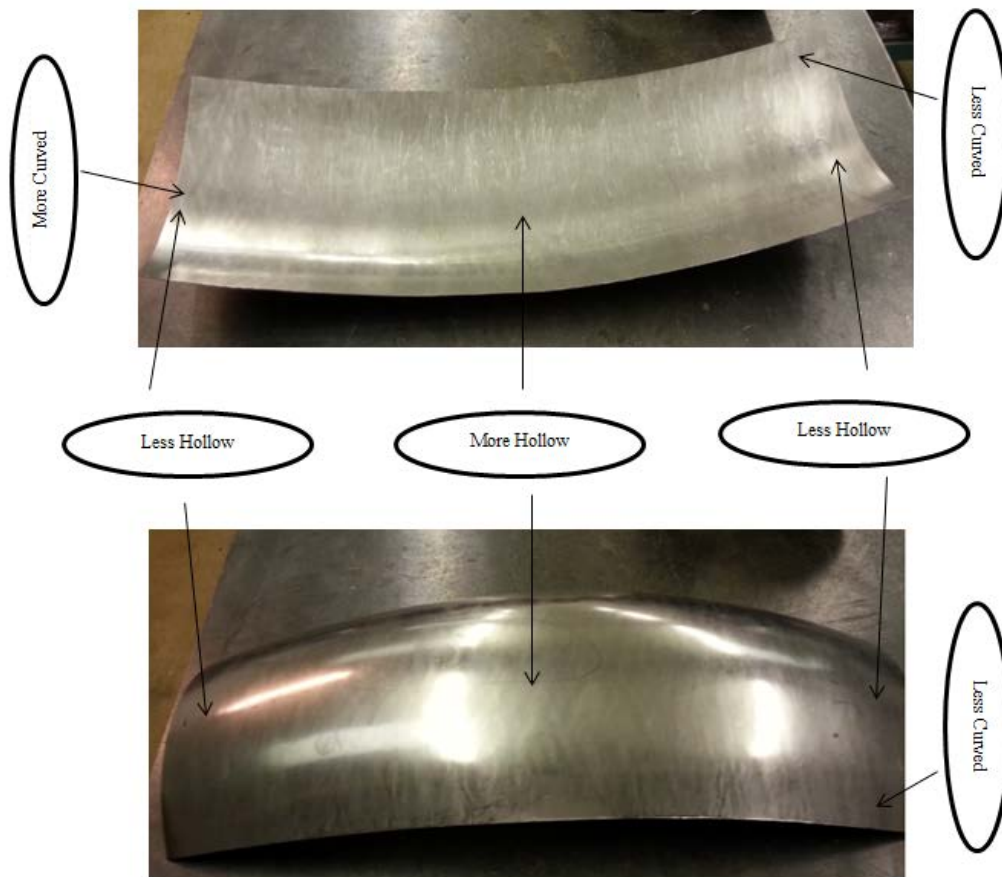


Figure 1.4.4 – Final shape to be produced with illustration on curvature and hollowness

For the portion to be hollow, it needs a greater impact/ force. For the portion to be less hollow, it needs a much controlled force with lesser impact/ force. This hammering/ mallet blows are determined by defining the fulcrum position of the hammer being held by the user. If the hammer is held farther away from hammer head, it produces a greater impact/ force. If the hammer is held closer to the hammer head, it produces a lesser but much controlled force. This is illustrated in figure (1.4.5). The resultant deformations caused by both these methods are illustrated in figures (1.4.6 & 1.4.7).

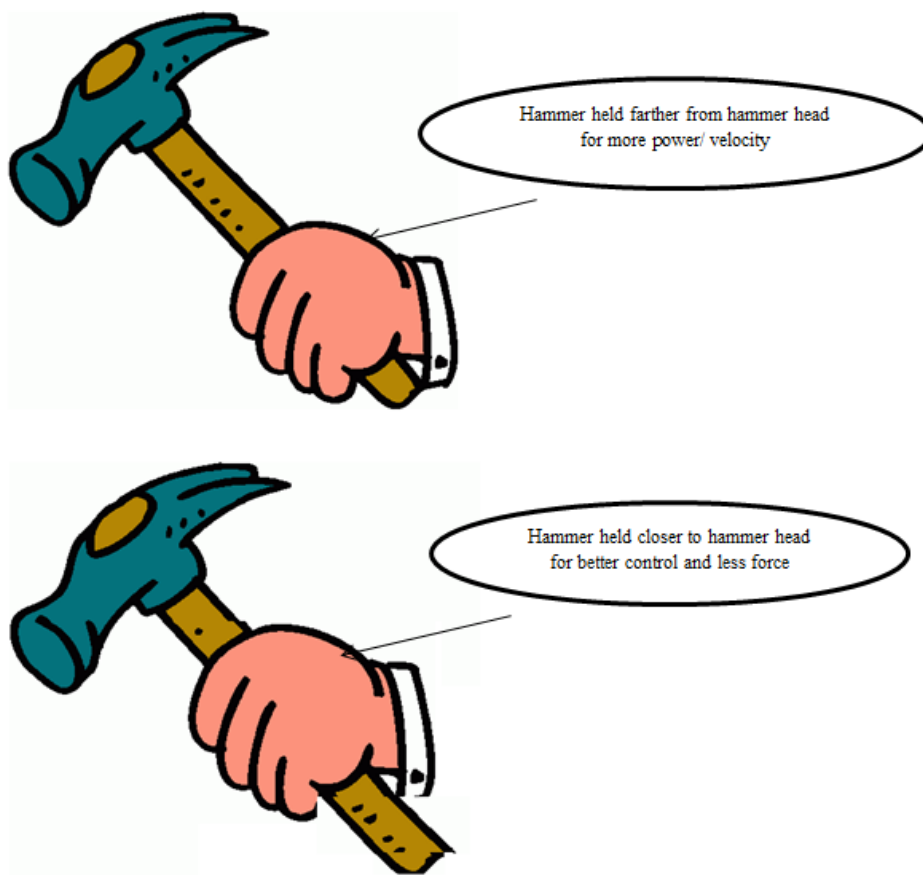


Figure 1.4.5 – Illustration of Hammer holding mechanism



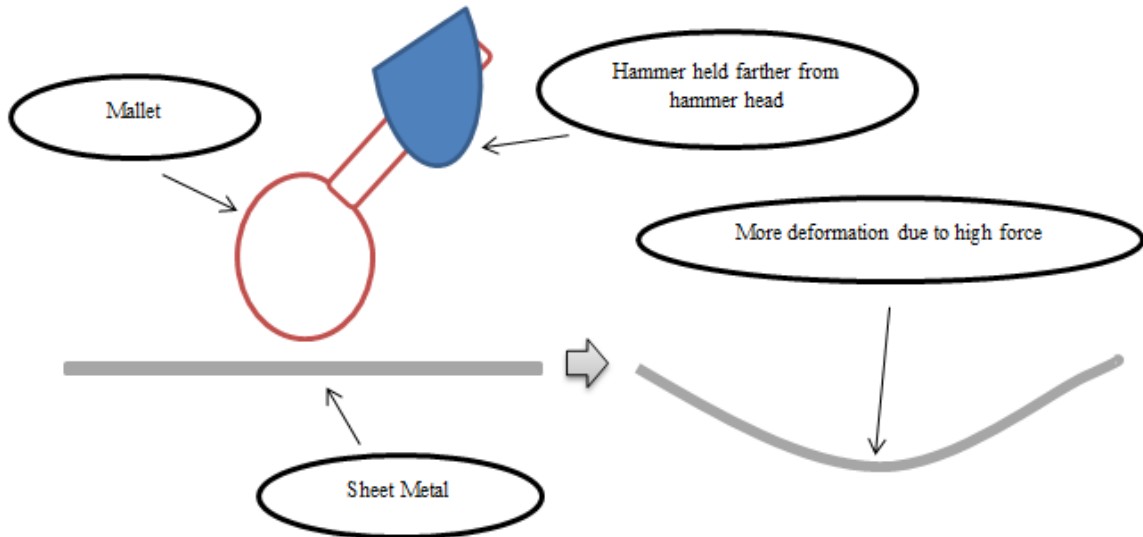


Figure 1.4.6 – Deformation caused when the hammer is held farther away from hammer head

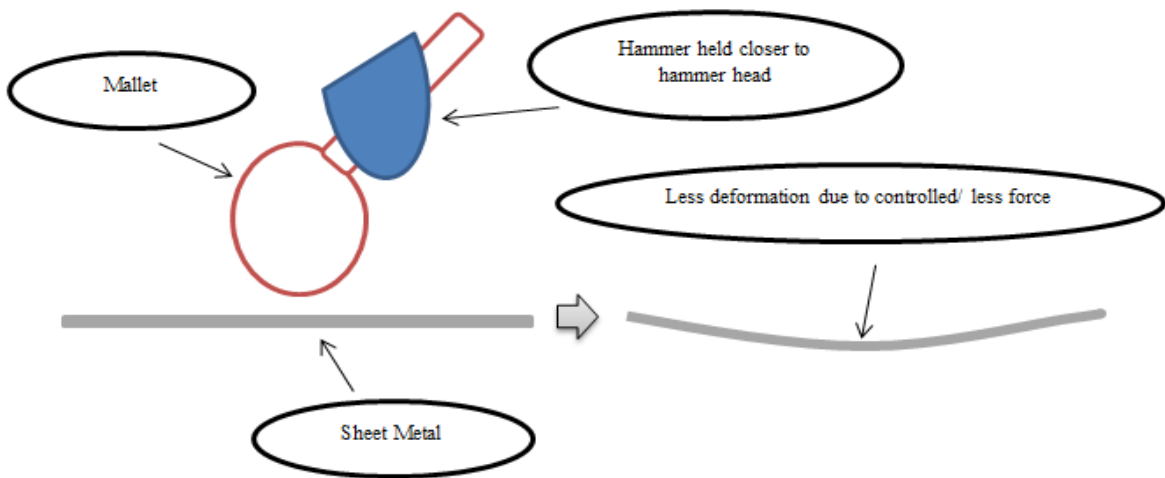


Figure 1.4.7 – Deformation caused when the hammer is held closer to hammer head

In order to produce the required deformations as illustrated, it is necessary to know the point of hammering blows with the information on force required to produce the deformation at each point. These are usually determined in crafting using tucks drawn on the before starting to deform them. The tucks define the amount of force required to deform each point. Larger the tuck, larger is the force of impact and hence, higher the deformation. It is necessary to

have tucks which are equally spaced. It is also good to have less number of tucks as possible to produce the shape appropriately. If too many tucks are introduced, it is very hard to have control over the shaping as the neighbouring loci (or point) will have a consequence deformation due to earlier blow given to its neighbour (actual point of impact). This consequence deformation caused will affect the shape of the sheet metal as to when that point or loci (Neighbouring Loci) is deformed. This is illustrated in figure (1.4.8).

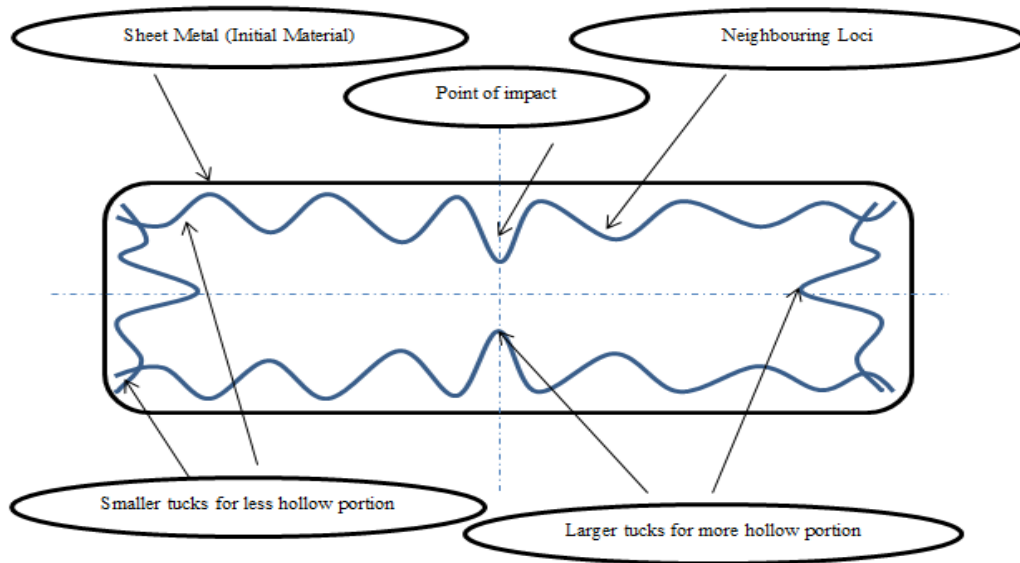


Figure 1.4.8 – Tucks Illustrated

In order to produce the required shape, the sheet metal has to be stretched and shrunk simultaneously. It is not advisable to stretch it completely and shrunk it later or the vice-versa. The complete stretching or shrinking will not incrementally shape the material to required dimensions. So it is important that both shrinking and stretching are carried out simultaneously according to the requirement. As the mechanism is known, it is now required to find the order of deformation (where to start and where to finish). It is always good to start at the portion which requires shrinking (these are the portion which requires less curvature). Later the material should be stretched at the portions which need larger curvature. This should be simultaneously carried out according to the tucks layout. In producing the double curvature, the edges are shrunk and the middle portion is stretched simultaneously.

The art of impacting the wooden block using the mallet with the sheet held between them is much necessary to be understood. It is very important to have an impact bearing anvil (such as wooden block) shaped to the required shape of the sheet metal. This anvil helps in forming

the shape gradually. The hammering mallet should impact only at middle of the wooden block as shown in figure (1.4.9). It is not necessary to move the mallet/ hammer over the wooden block to produce the required shape. The point of impact should always be the same. The impact force and impact angle might differ according to the shape needed. To get the necessary shape, the sheet metal has to be moved over the wooden block. Figure (1.4.10) shows the sheet metal edge being moved over to the middle and held at an angle to get a minor deformation. According to the curvature required, the angle of impact will differ. Figure (1.4.11) shows on how to get a larger deformation for hollow shape.

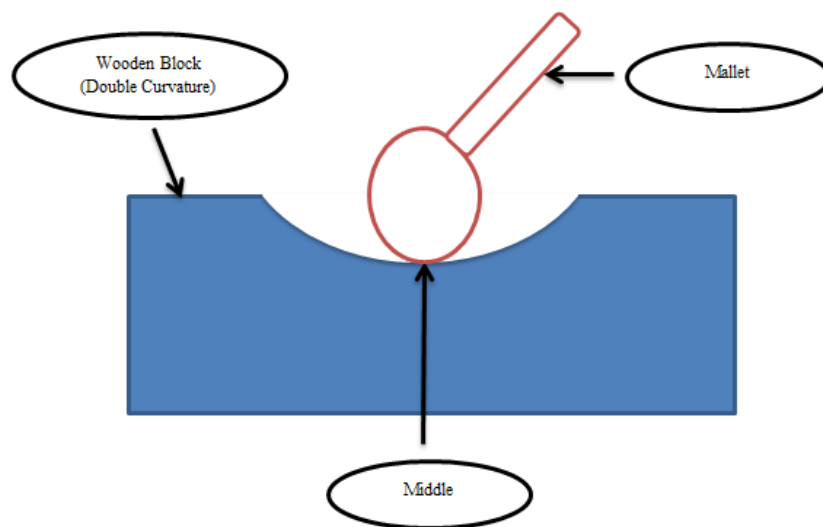


Figure 1.4.9 – Mallet impacting the middle of Wooden Block

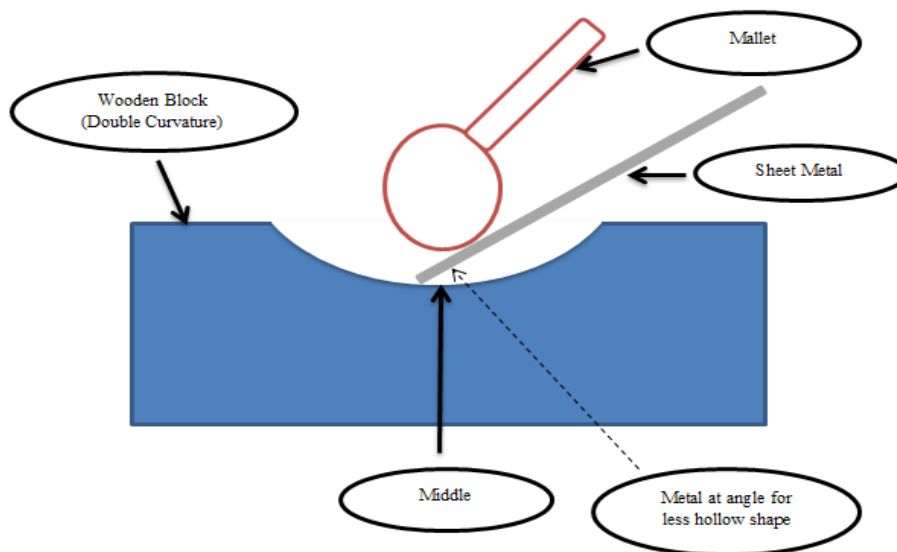


Figure 1.4.10 – Sheet Metal held in the middle at an angle to produce minor deformation

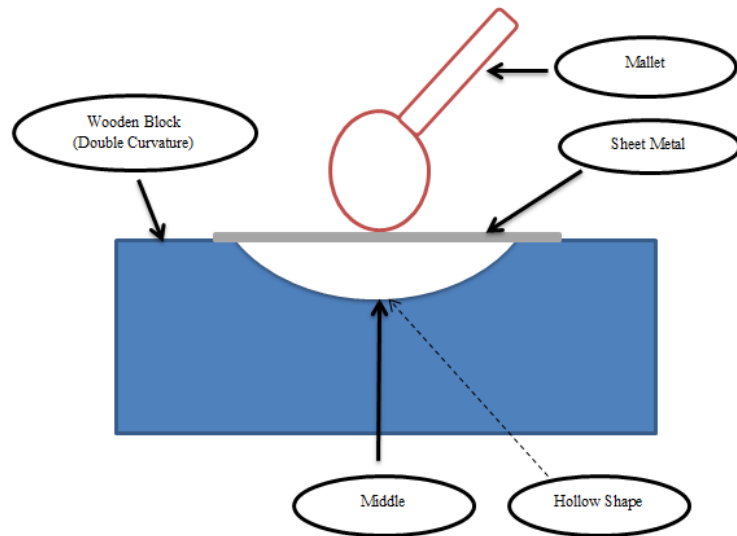


Figure 1.4.11 – Sheet Metal held to get a hollow deformation

It is necessary to have the tucks until the required shape (appropriate) is acquired. If the sheet metal is smoothed/ finished before getting the required shape, it will remove the tucks. If the tucks are not present, it is very hard to alter the shape of the sheet metal as it loses all its shaping capabilities (this is due to material flow being constrained due to smoothing). Figure (1.4.12) shows the steps involved with the right hand bottom box showing the sheet metal with tucks shaped appropriately to double curvature.

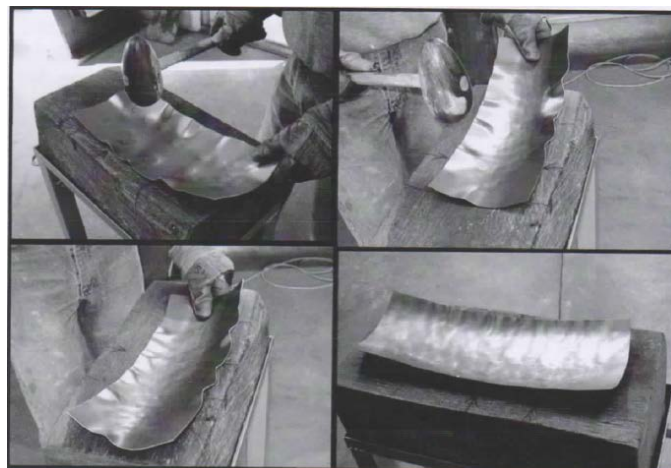


Figure 1.4.12 – Double curvature produced in sheet metal using tucks

### 1.5 Panel Beating using Hammer & Dollies

The hammer and dollies are usually used to smoothen and finish the shape formed using mallet and wooden block. The hammer & dollies are not used in first phase of deformation as

they are of higher accuracy. It is hard to compensate and get a balance between rigidity, malleability and deformability when using hammer & dollies. Thus, mallet & wooden block are being used in the first phase. There are different types of hammers & dollies that could be used to attain different shapes. These are discussed later in the document in chapter 2 under tooling.

The behaviour of sheet metal is to be understood when using the hammer & dollies. Hammer and dollies are usually used to correct the hammering tucks and finish them to a good curvature. In this process, it is required to use a flat faced square hammer with a utility dolly underneath. Using this will stretch the material more at the top surface than at the bottom surface causing the curvature. This is illustrated in figure (1.5.1).

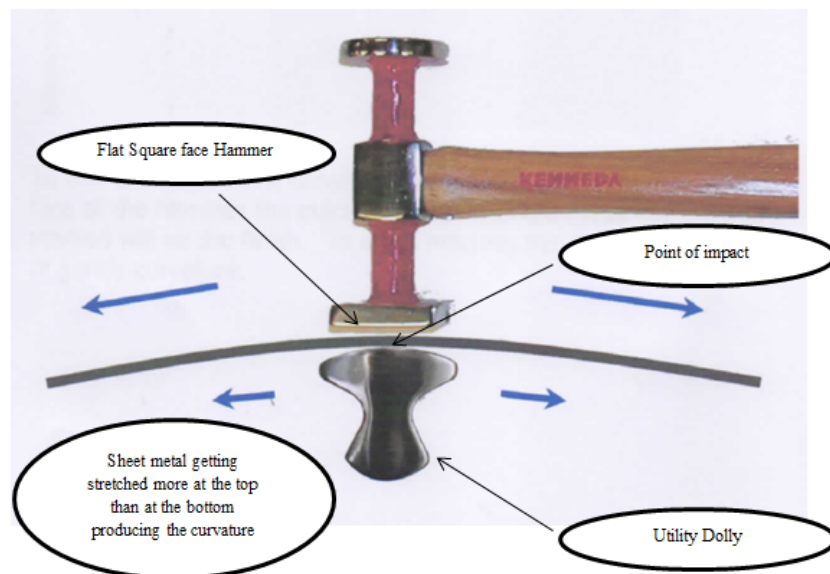


Figure 1.5.1 – Using flat faced square hammer with utility dolly for finishing the curvature (Stretching)

As discussed earlier, sheet metal forming involved simultaneous shrinking and stretching. Finishing also involves both. The sheet metal will have highs at certain areas which have to be shrunk back to surface to flow along the curvature. This is also done using the flat faced square hammer with utility dolly. The only difference between stretching and shrinking being point of impact. For the shrinking purpose, the metal has to be hit at the highs with the curvature surface of utility dolly underneath. This is shown in figure (1.5.2).

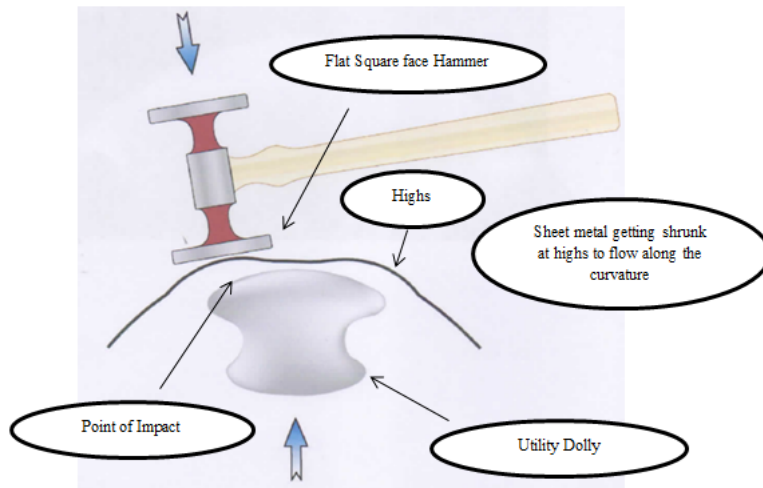


Figure 1.5.2 – Using flat faced square hammer with utility dolly for finishing the curvature (Shrinking)

Hammer & Dollies are sometimes used for thinning the material. In case of thinning the material, a utility dolly is to be used along with a curved round hammer as shown in figure (1.5.3). When the impact is made, the metal will stretch out thinning at the point of impact.

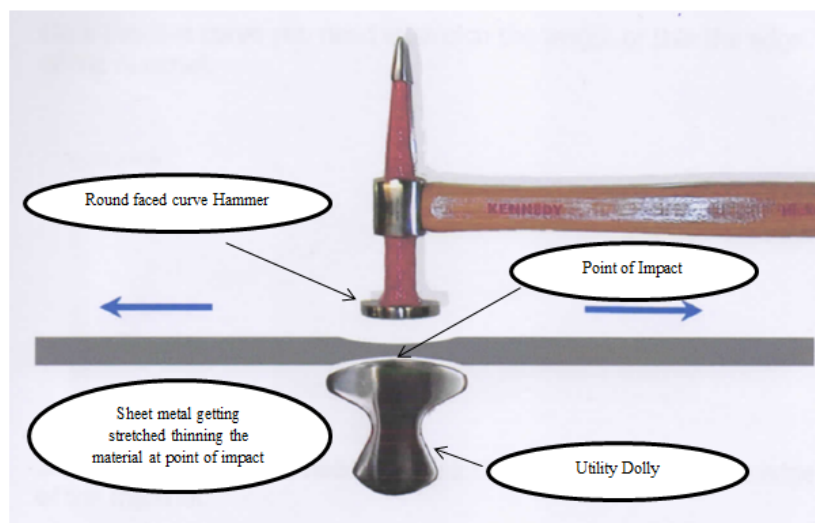


Figure 1.5.3 – Using round faced curve hammer with utility dolly to thin the metal

## 1.6 Wheeling

Wheeling is the process of smoothing the metal to give it a final finish removing all the lines, tucks, high/ low spots in the panel. Wheeling is also used to acquire flat sheets as well as sheets with single curvatures. For acquiring flat sheets or single curvature sheets, flat wheels

are used with the difference in diameter of the wheels causing curvature. This is illustrated in figure (1.6.1).

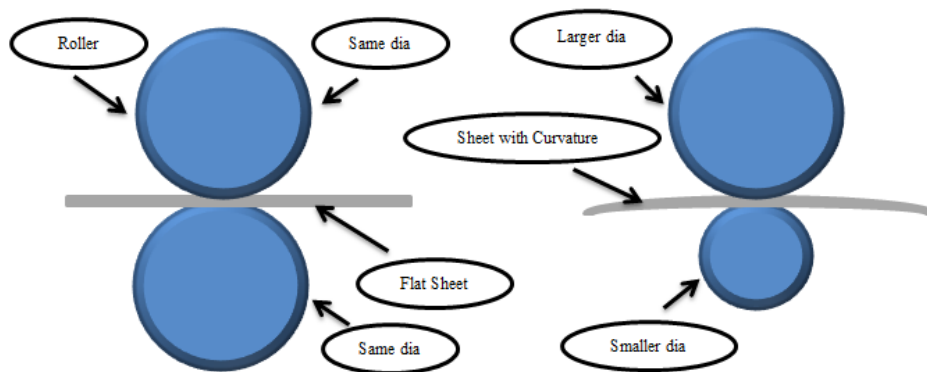


Figure 1.6.1 – Flat wheels used to yield flat sheet and single curvature sheet

English Wheels are used by sheet metal manufacturers to produce the double curvature. The English Wheel has usually got a top flat wheel coinciding with curved wheel underneath. The difference in radii of the curved wheel at the curvature edges gives rise to different curvatures. This is illustrated in figure (1.6.2). Figure (1.6.3) shows the English Wheel in action.

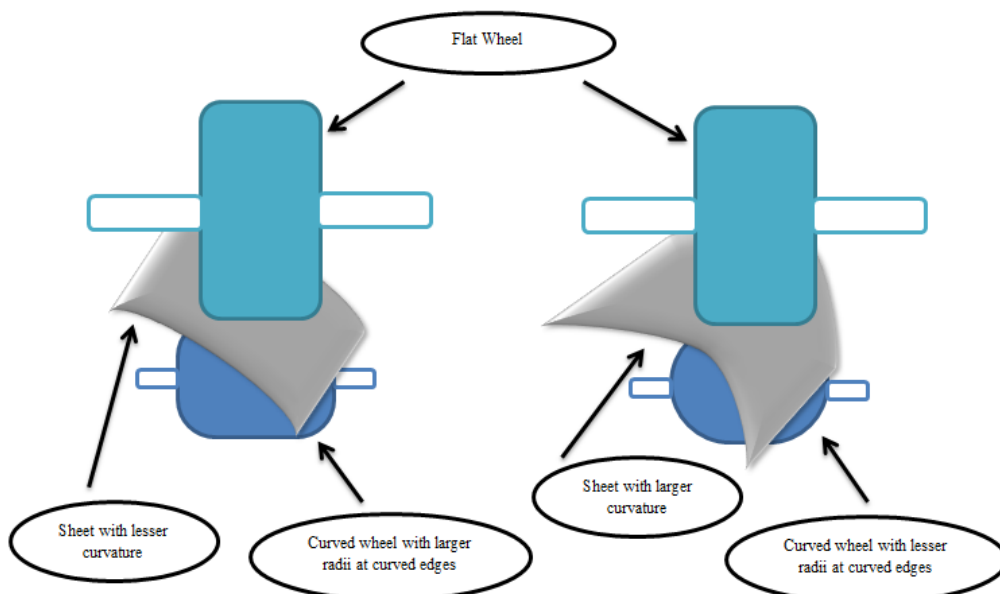


Figure 1.6.2 – English Wheel working mechanism

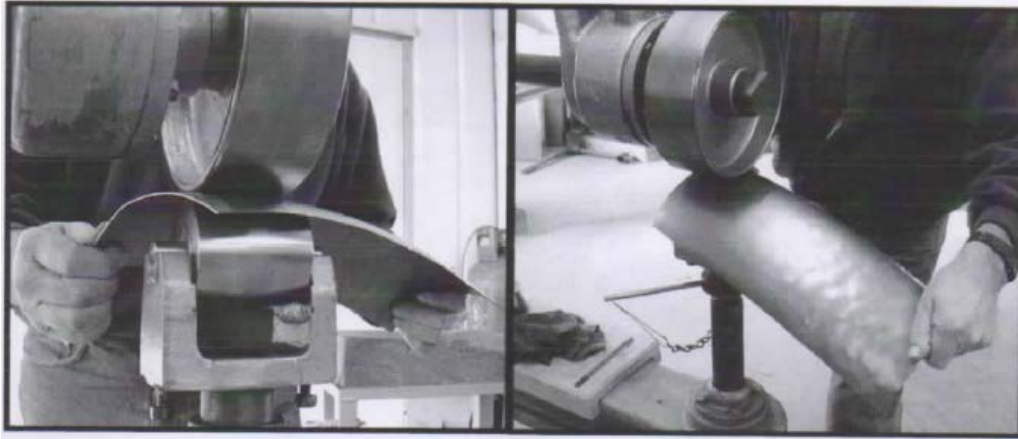


Figure 1.6.3 – English Wheel in action

Wheeling seems to be an easy task but it needs high skill as the patterns involved in wheeling are highly sensitive. Figure (1.6.4) below shows the stepwise pattern involved in wheeling a double curvature sheet metal. The pressure between the wheels could be increased according to the curvature required to be produced.

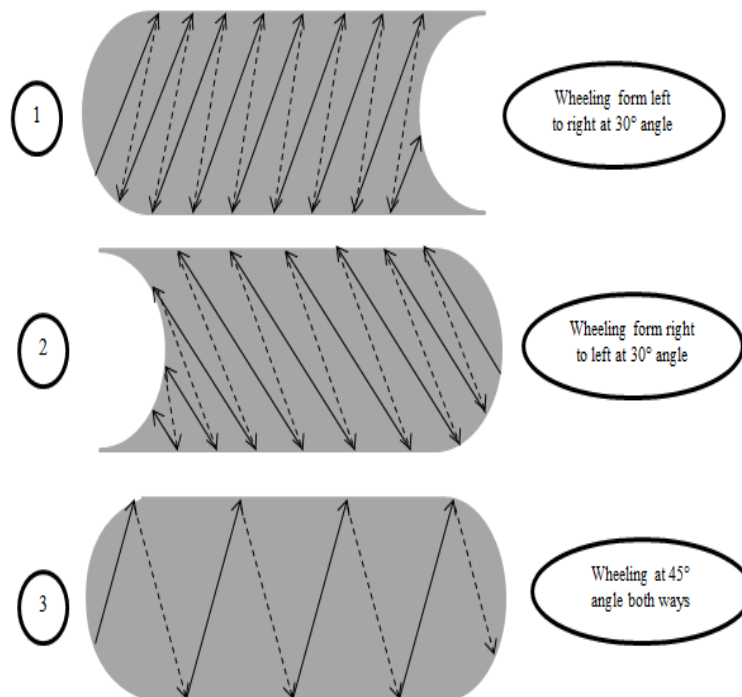


Figure 1.6.4 – Wheeling pattern

### 1.7 Shrinking/ Stretching

There are mechanical machines for shrinking and stretching the sheet metal. It makes it easier for the angled sheet metal portion to be shrunk or stretched easily. The figure (1.7.1) below shows the four blocks used in the Shrinker/ Stretcher Mechanism to provide the necessary



output. The sheet is held across the horizontal plane (across the vertical plane in the picture) between the upper two blocks and lower two blocks. The Shrinker and Stretcher use same mechanical elements to produce the shape with the mechanism being different. Figure (1.7.2) shows the Shrinker with mechanical handle to deliver the mechanism.

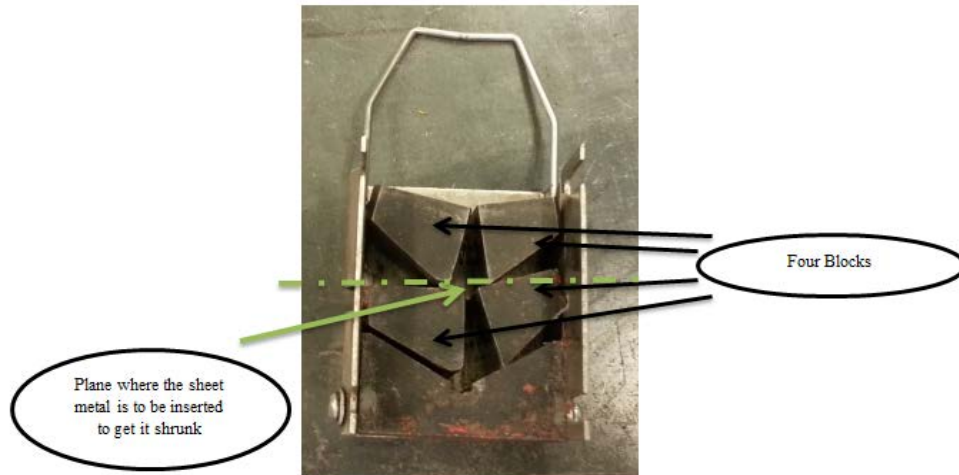


Figure 7.1 – Shrinker/ Stretcher mechanical elements

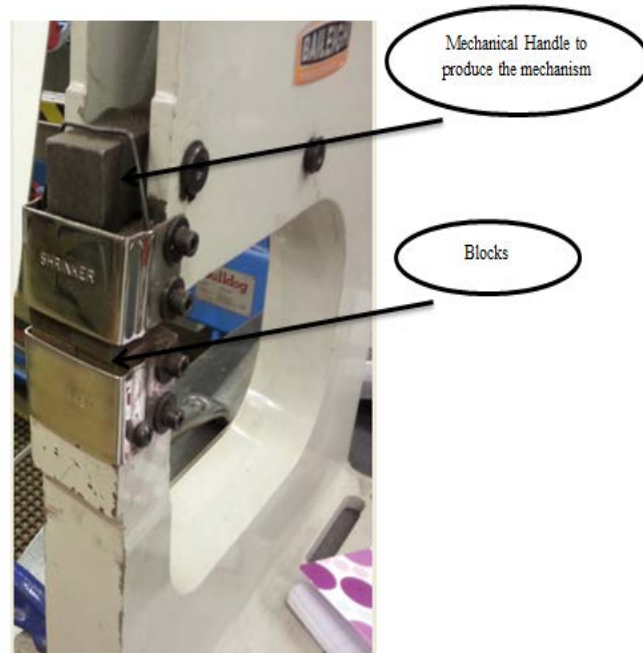


Figure 1.7.2 – Shrinker with mechanical handle

The mechanism involved in shrinking is pushing in the sheet metal to give the shrinking properties to the sheet metal. This is illustrated in the figure (1.7.3) with the action of blocks. The arrows define the motion of blocks to produce the shrinking action.

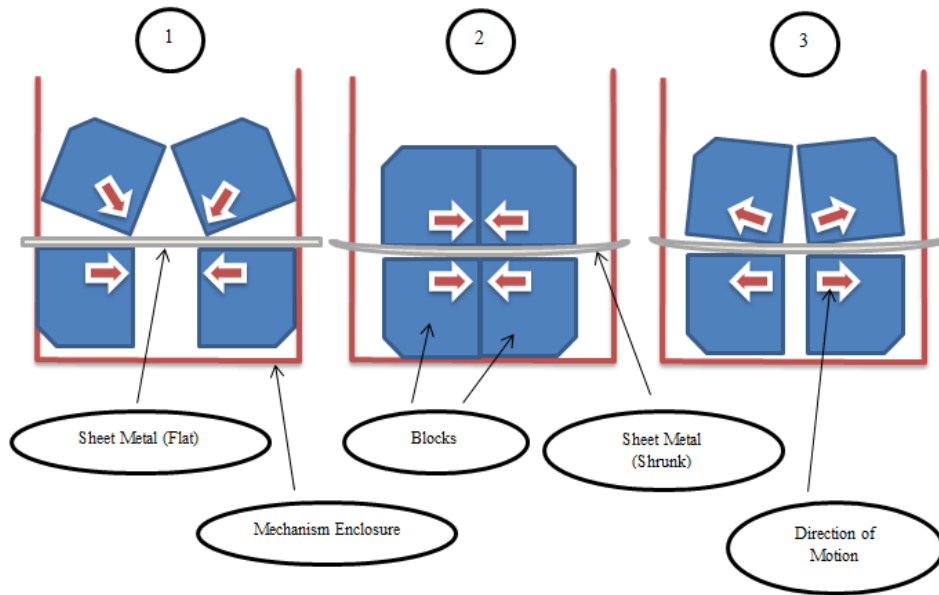


Figure 1.7.3 – Shrinking action

Stretching involves the mechanism of pulling out the sheet to stretch it. Figure (1.7.4) below illustrates the step wise stretching action.

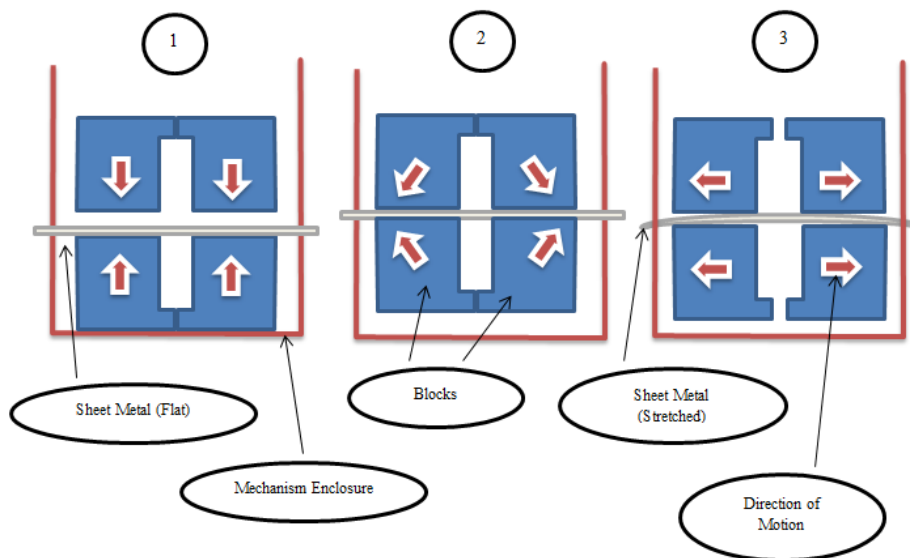


Figure 1.7.4 – Stretching action

### 1.8 Flanging

Flanges are made on the edge of the panels to make them strong and also to make them corrosive resistant. It also gives a better finish to the sheet metal and makes it more complete. Flanges could be made on flat surface, convex or concave surface. Figure (1.8.1) illustrates

the mechanism that has to be followed to flange a sheet metal according when it is concave surface.

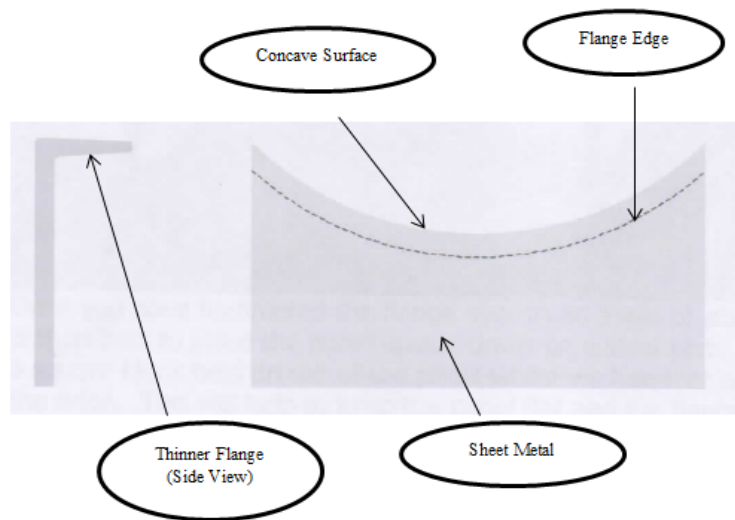


Figure 1.8.1 – Flanging Concave Surface

When it is a concave surface, it is required to stretch the edge or in other words, thin the edge of the sheet metal as shown in the figure above. For this purpose, a Cross pein hammer which has got a sharp edge is to be used. As shown in the fig (1.8.2) below, the sheet metal is held over the edge of a steel block or stake with the flange edge (inner edge) over the corner of the block underneath. The flange is produced by hammering the outer edge of the flange, thinning it between hammer and the block. This methodology is used produced about 80° of the flange.

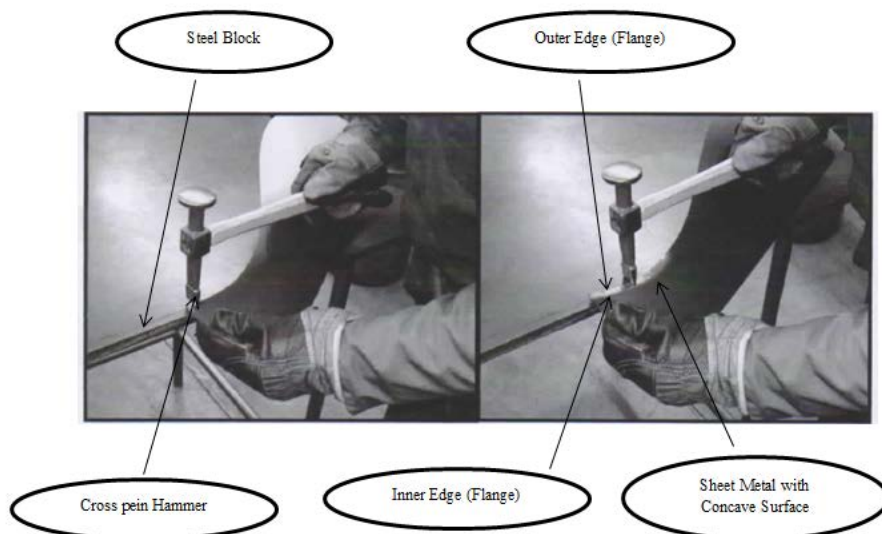


Figure 1.8.2 – Cross pein hammer to thin the concave surface

Once the 80° flange has been produced, it is better to have the panel flat and the flange edge over the square block which is held above the panel. This is shown in figure (1.8.3). Then the edge of the flange is hammered over the square block. This will help to keep the panel flat and the flange square. This final method improves the accuracy of flanging.

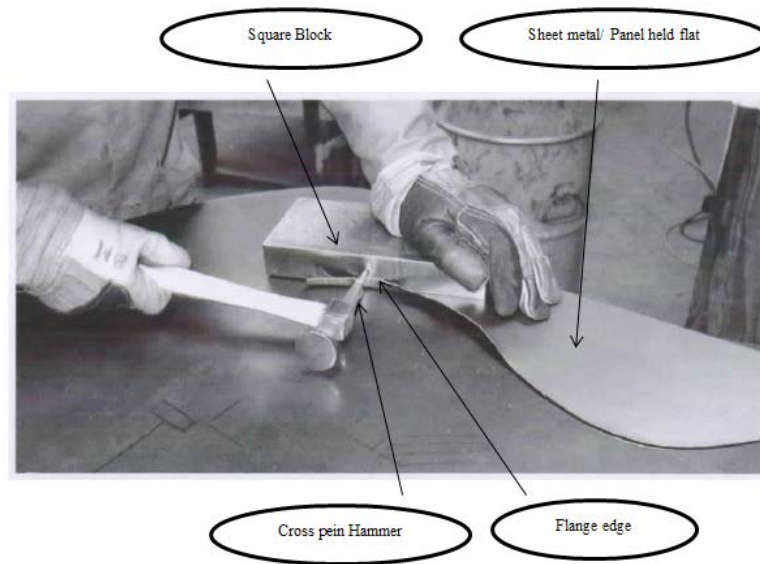


Figure 1.8.3 – Final flanging using square block

Flanging a convex surface needs thickening the edge or in other words, shrinking the edge of the panel. Figure (1.8.4) shows the flanging of convex surface.

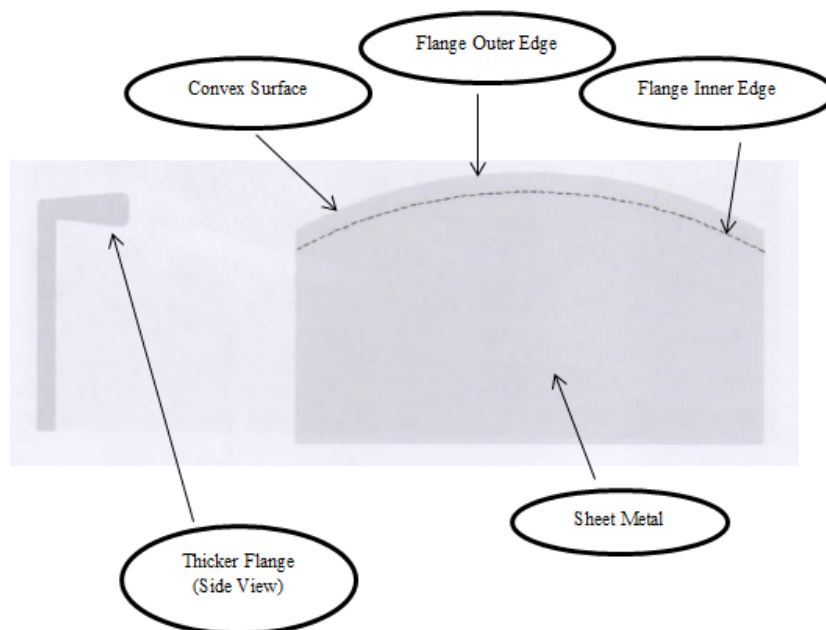


Figure 1.8.4 – Flanging Convex Surface

Flanging the convex surface requires flat faced hammer and a curved plate. As shown in figure (1.8.5), the inner edge of the flange is held over the corner of the curved block underneath. As the panel is being shrunk, hammer the inner edge of the flange to produce the perfect flange.

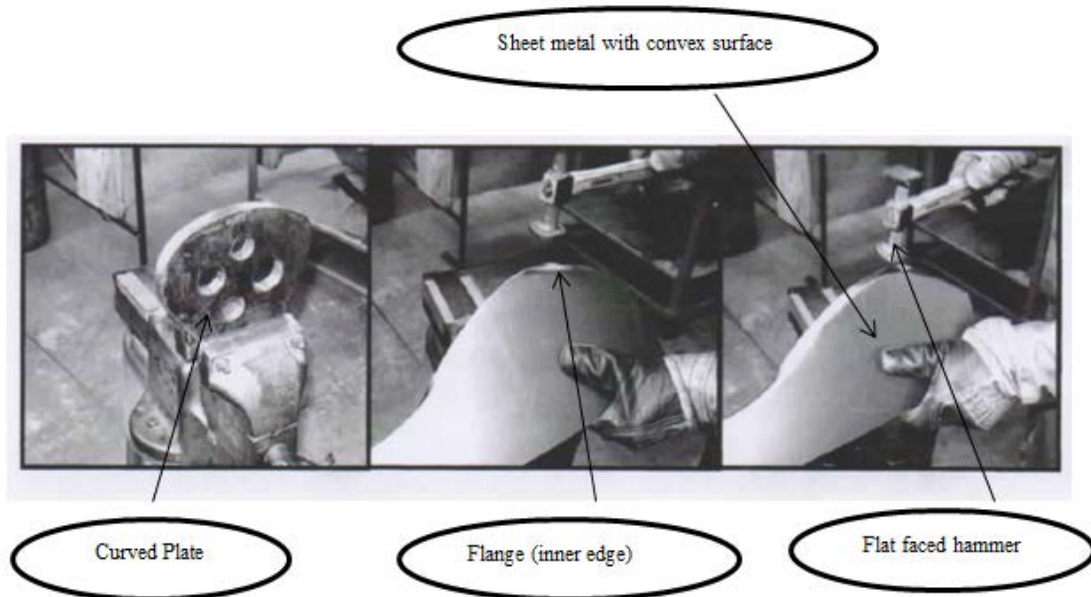


Figure 1.8.5 – Flat faced hammer to thicken the convex surface

Once 80° flange has been done, panel is held flat and the flange outer edge is hammered at a right angle to shrink the panel edge. This is illustrated in the figure (1.8.6). Then the flange edge is hammered over the curved plate to get a square flange.

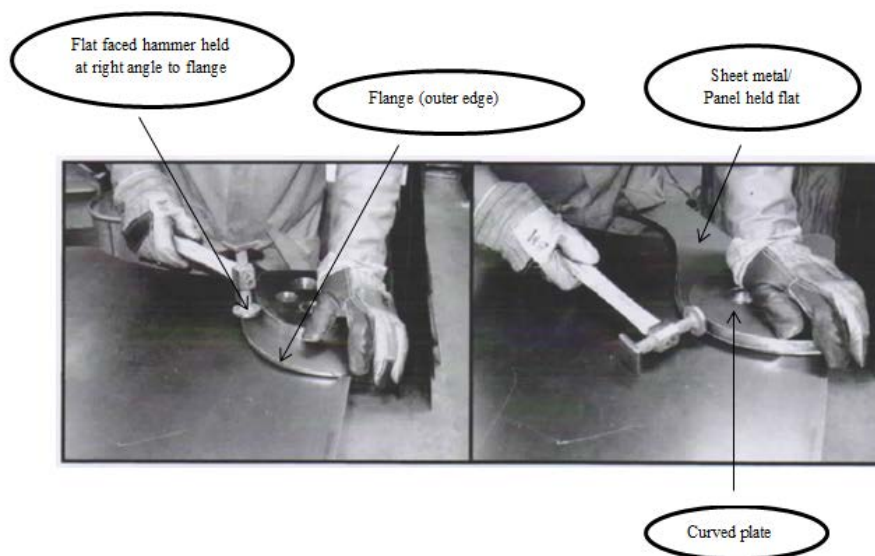


Figure 1.8.6 – Final flanging using curved plate

Figure (1.8.7) shows the finished panel after flanging both the convex and concave surfaces.



Figure 1.8.7 – Finished flange

The flanges which are usually  $90^\circ$  can also be angled at certain degrees. The flange can also be overturned to  $180^\circ$  with a galvanized wire underneath the flange as shown in figure (1.8.8). This method of flanging with a galvanized wire will reduce the corrosion of the panel.

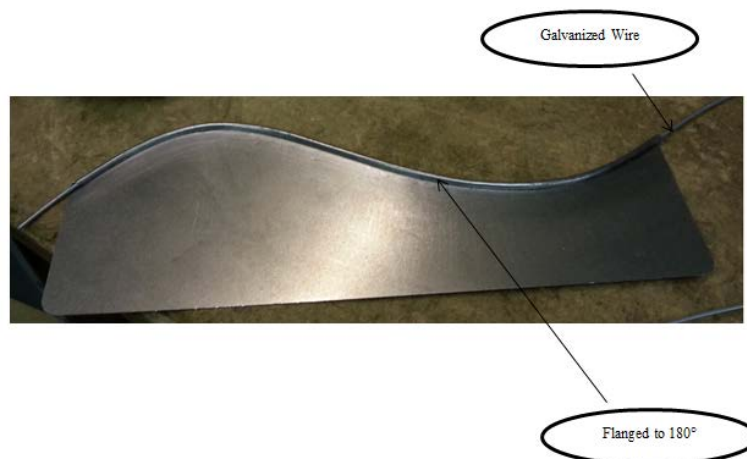


Figure 1.8.8 – Flanging with galvanized wire

The eight steps that have been discussed define the sheet metal forming from its initial stage of uncoiling to final stage of finishing. The different type of tooling that could be used for these purposes will be discussed in the next chapter.



## CHAPTER 2 – FACTORS THAT AFFECT SHEET METAL FORMATION

### 2.1 Tooling

Tooling plays an important role in determining the shape of the sheet metal while forming. The difference in tooling arises according to different sheet metal shapes required. As discussed earlier, the shape of the wooden block and the mallet differs according to the shape of the sheet metal required to be formed. There are no defined shapes of wooden blocks or mallet existing as sheet metal shapes vary largely.

Though the same applies for the hammer and dolly mechanism, there are defined hammers and dollies available industrially. The different types of hammers used are shown in figure (2.1.1). The Cross pein hammer is usually used to hammer sharp edges such as flanges. The Curve face hammer is usually used to thin the sheet metal. The Flat face hammer is usually used to smooth the sheet metal.

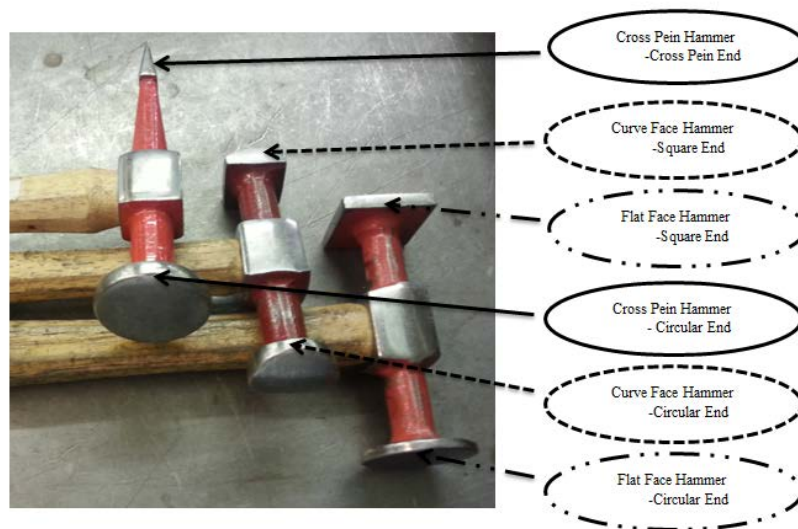


Figure 2.1.1 – Different types of hammers

The figure (2.1.2) below show the different types of dollies being used to complement the hammers seen above. Same dolly with different hammers will produce a different flow of material. The most commonly used dolly is Utility Dolly. This dolly has got a curvature at both its ends. The utility dolly when used with flat face hammer will smooth the metal. The utility dolly when used with a curve face hammer will thin the metal. The Heel dolly and Toe dolly are usually used along with the Cross pein hammer to produce flanges as they have got

sharp corners. The Curved dolly has got a similar usage as utility dolly with a single curvature definition only.

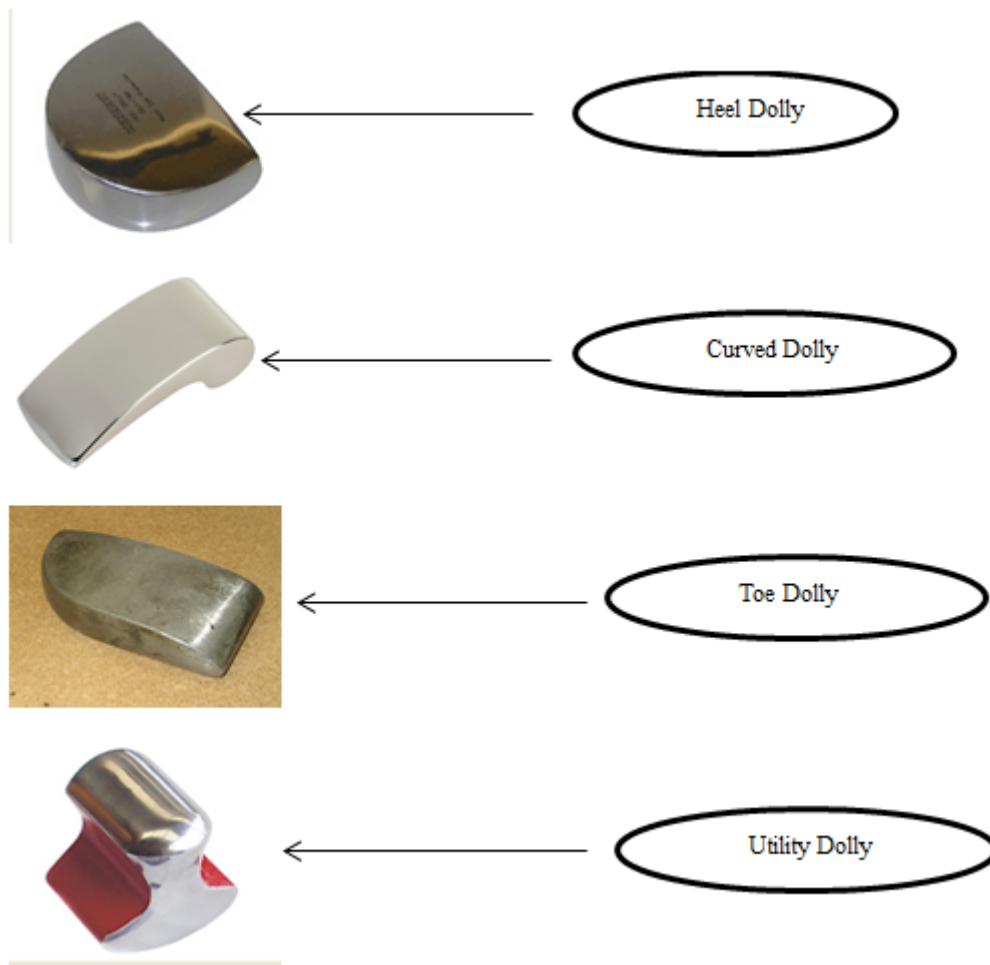


Figure 2.1.2 – Different types of Dollies

During the forming process, several clamping mechanisms are to be considered especially while flanging. The clamps and grips used in the process of forming are illustrated below in figure (2.1.3). The clamps and grips give the firm hold to the material/ panel allowing required formability of the material/ panel.



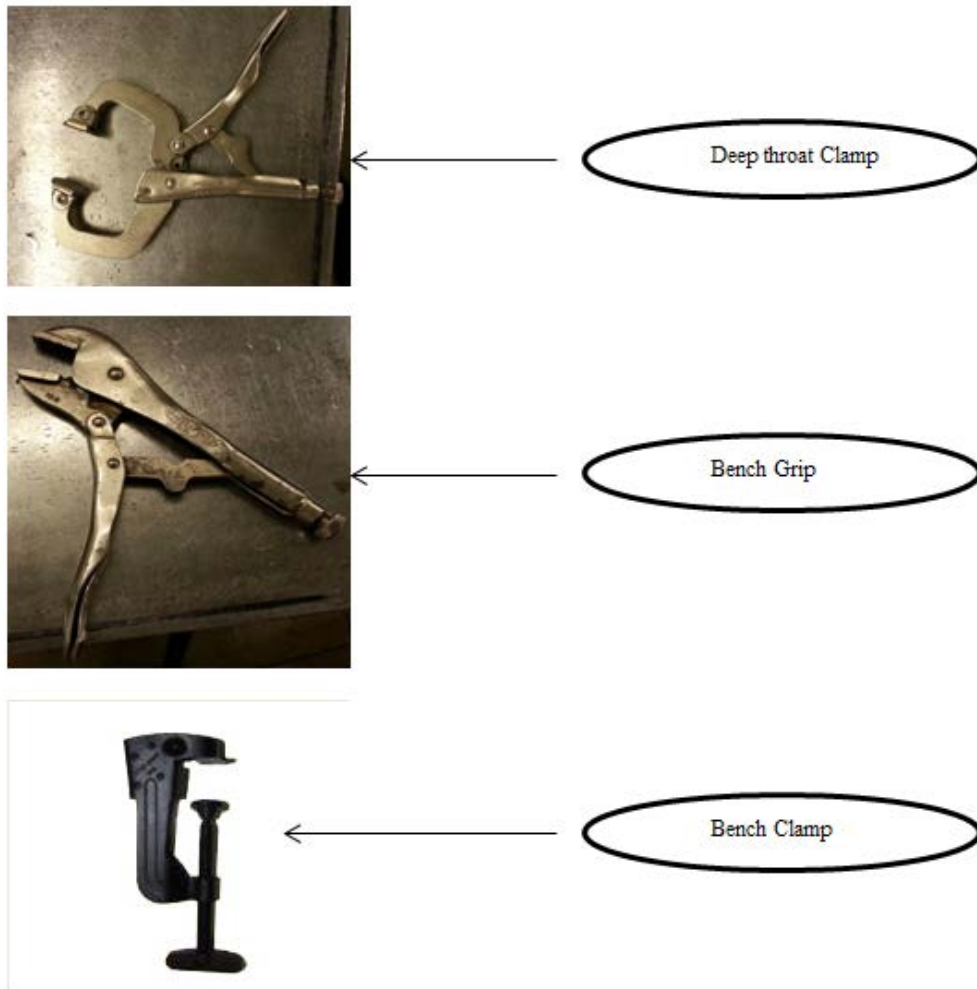


Figure 2.1.3 – Clamps & Grips

Flanging can be done using various mechanical devices. These vary from being mechanical to semi- automatic. As discussed earlier, hammer, curve plate or square block is the traditional mechanism used. Later, the use of chaser came into existence. Chaser is usually used to chase down the flanging surface. To finish the chased surface, flipper or slapper is used to slap down the flange flat to a right angle. Later, the use of vibrators was introduced. The vibrators are similar to chaser but semi- automated since they are electrically driven by a linear drive. Using the vibrator might make things faster but it leaves patches on the surface of the flange. All these equipment are shown below in the figure (2.1.4).

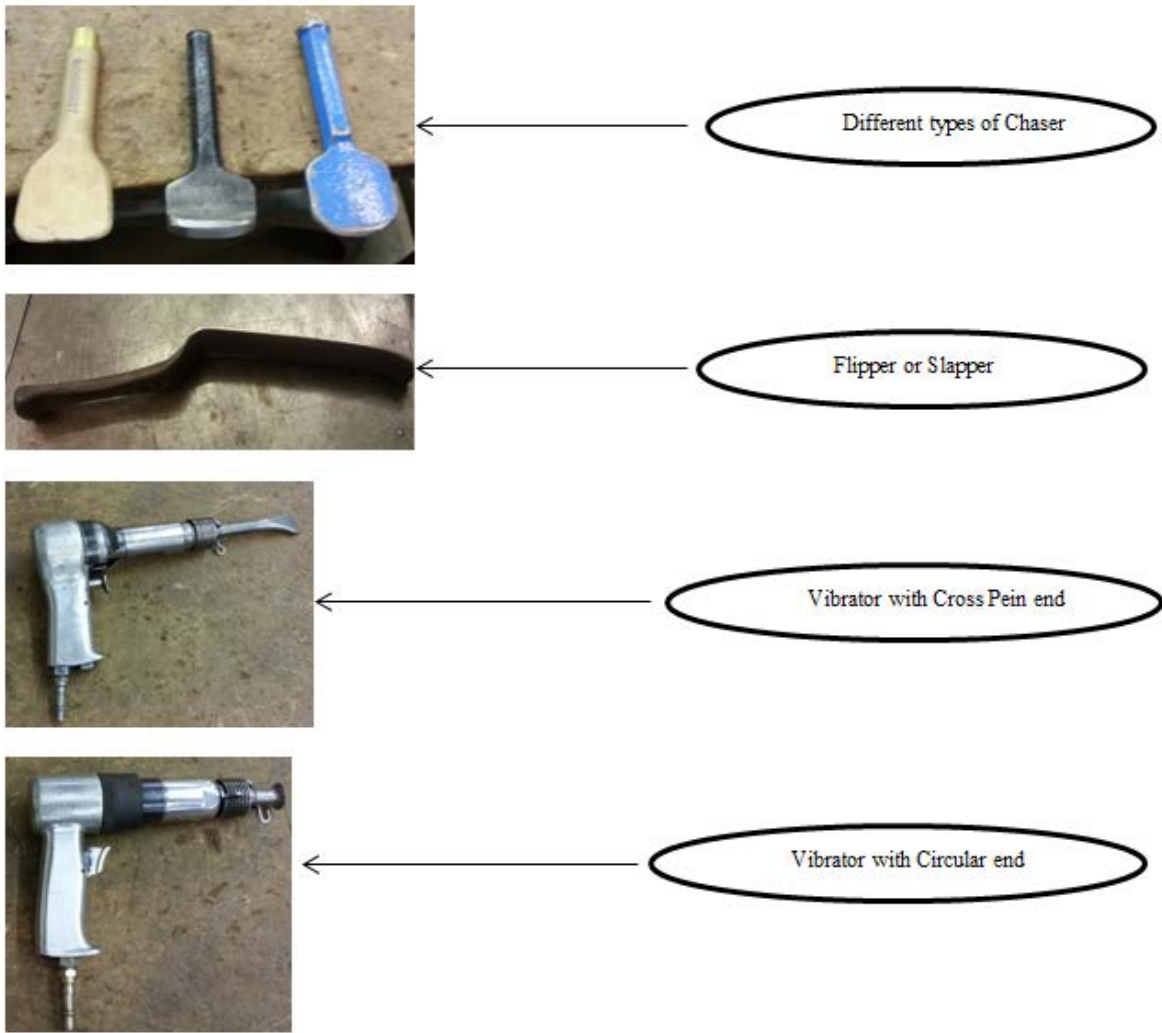


Figure 2.1.4 – Chaser, Slapper & Vibrator

## 2.2 Types of Wheels

Wheeling as discussed earlier involves different wheels which differ in the radii of curvature. The figure (2.2.1) shows the different wheels being used in English Wheels. These wheels are used accordingly to the curvature required in the sheet metal while finishing. The Wheeling mechanism usually stretches the sheet metal, so care should be taken not to over stretch the sheet metal which may result in false shape.



Figure 2.2.1 – Wheels with different radii of curvature

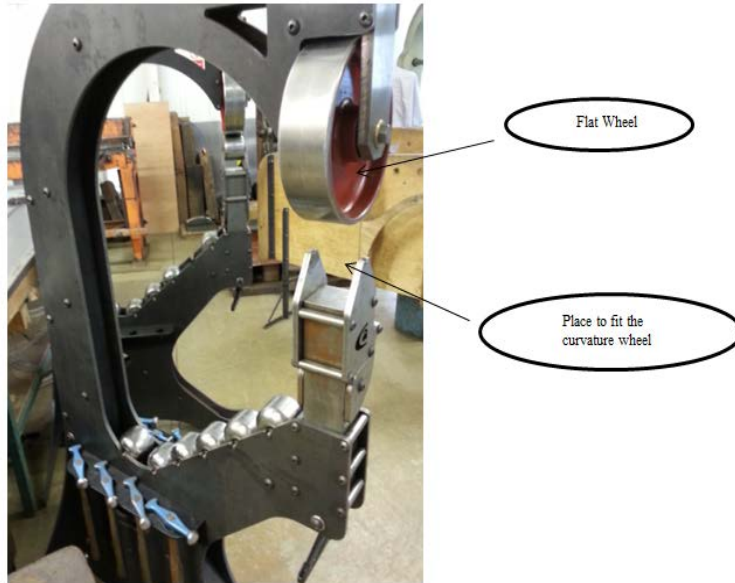


Figure 2.2.2 – English Wheel without Curved Wheel Mounted

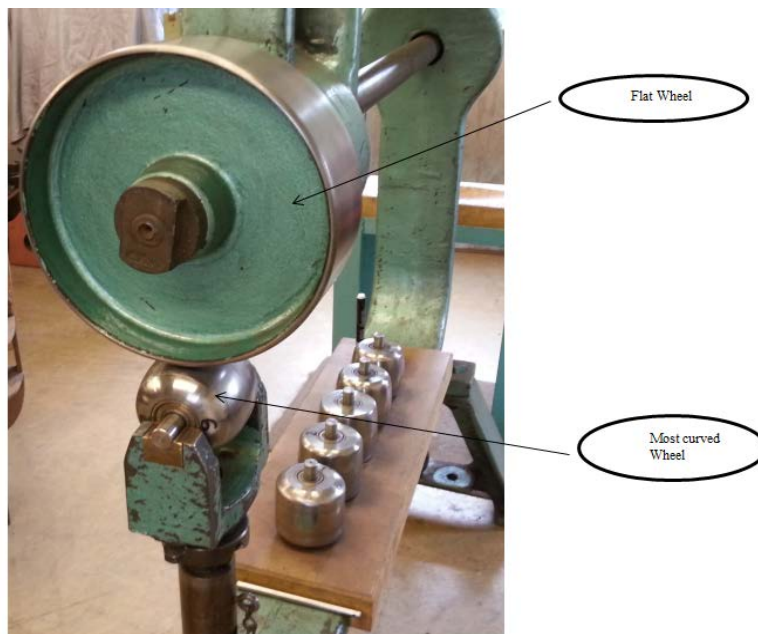


Figure 2.2.3 – English Wheel with Wheel of maximum curvature mounted

Figures (2.2.2 & 2.2.3) illustrate the method of usage of English Wheel.

### 2.3 Measuring & Marking Techniques

Sheet metal forming is a crafting technology. It involves lot of geometrical calculation. Though all the calculations can be easily done theoretically, in practice, it is harder to transfer those measurements due to angular and planar disparity.

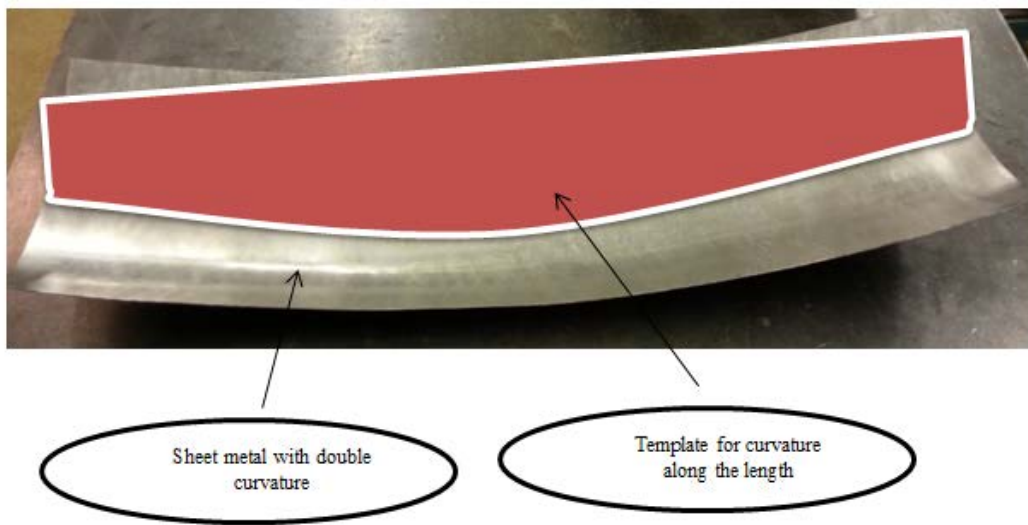


Figure 2.3.1 – Template for curvature along the length

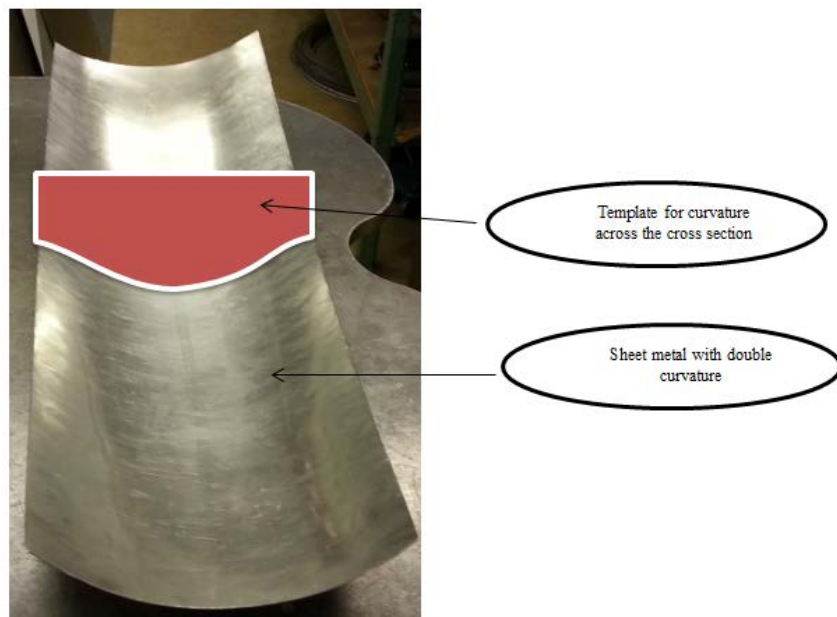


Figure 2.3.2 – Template for curvature along the cross section

The basic technique used by a craftsman is to create templates for making measurements. These templates guide the craftsman in producing a perfect shape required with perfect dimensions. Considering a double curvature sheet metal, two templates are needed to predict the formability of the double curvature. One template is required to be created along the length of the curvature and another along the cross section of the curvature. The figures (2.3.1 & 2.3.2) above illustrate the templates required to measure the formability.

The measuring techniques are very important when considering the crafting involved in sheet metal forming. The measurements are always to be made from Datum Point. Figure (2.3.3) illustrates on how the measurements are to be made from datum point.

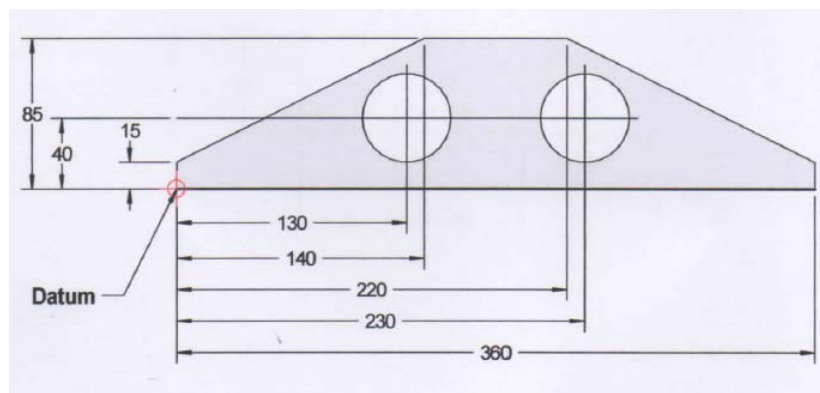


Figure 2.3.3 – Datum Point

When the panel involves two circles, it is also necessary to measure the pitch between two circles in addition to measuring the centre of the circle from datum point. Difference in pitch between circles might cause lot of problems while forming the sheet metal.

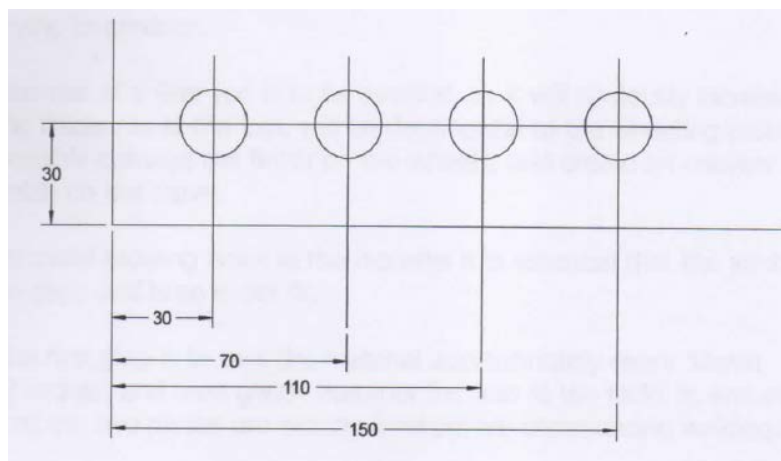


Figure 2.3.4 – Measure of Centre of Circle from Datum Point

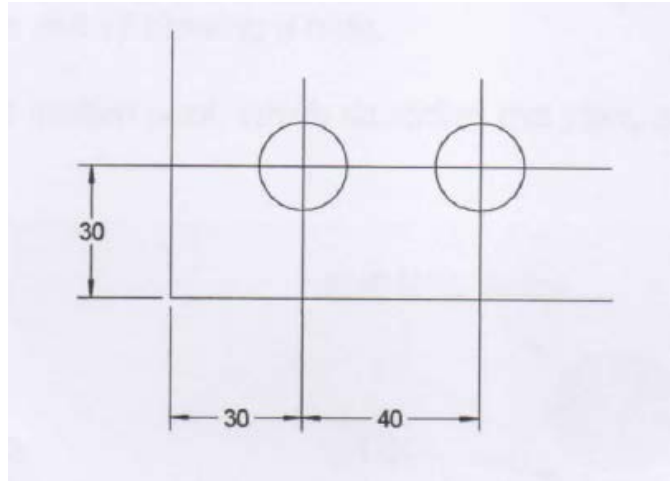


Figure 2.3.5 – Measure of pitch between Circles

Figure (2.3.4) shows the measurement of centre of circle made from datum points. In figure (2.3.5), only the first two circles from left are considered. The pitch between them are measured and found to match the measurement made earlier with the datum point.

It is always important to consider the sheet metal thickness when folding or flanging the sheet metal. The example illustrated in figure (2.3.6) uses a 1mm thickness sheet metal. It is necessary to take the internal measurements only into account when calculating as it accounts for the material thickness as well. In the example, it is 48mm length and 49mm height on both sides. So the summation will be 146mm which is length of the sheet metal required to produce the shape as illustrated in the figure.

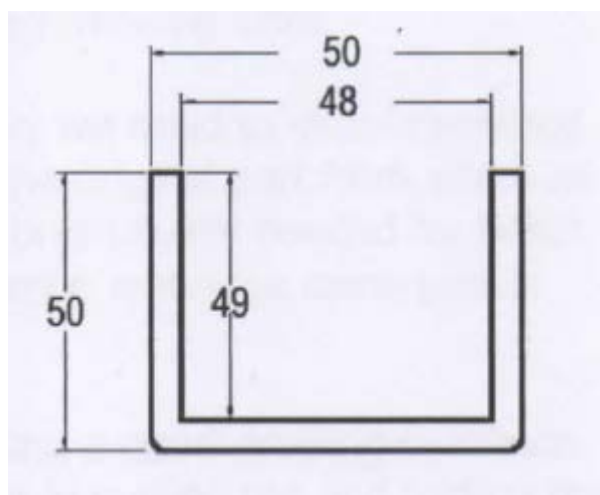


Figure 2.3.6 – Flange allowance



This flange allowance becomes an important factor in determining the dimensions of the sheet metal formed.

Traditional sheet metal manufacturers use scribes to transfer measurements into the sheet metal. There are many chances for human errors while transferring the measure. Even if advanced technology is used in transferring measurements to the sheet metal, there are two important factors that need to be considered. They are angular and planar disparity. In traditional scribing methodology, it is important to maintain the plane of the scribe as shown in figure (2.3.7). If the plane is not maintained, the scribing measure is not in correct dimensions. Also, as shown in figure (2.3.8), it is important to maintain the angle when scribing angular patterns. This applies in advanced technology as well.

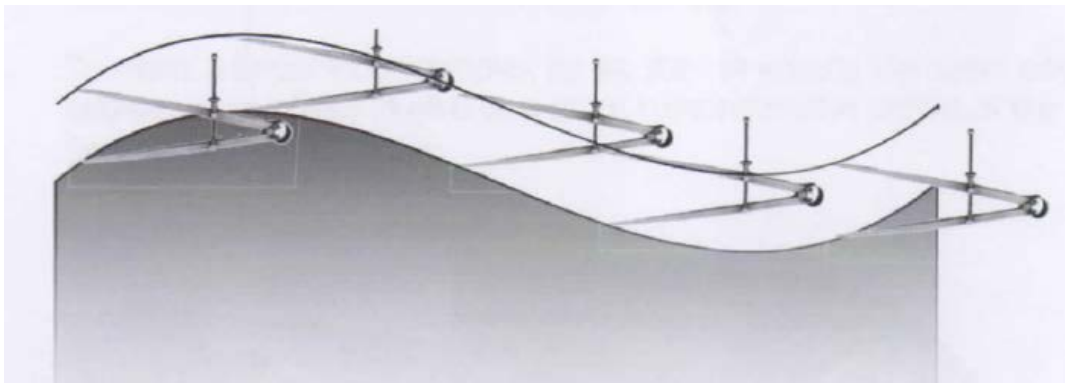


Figure 2.3.7 – Scribing on a plane



Figure 2.3.8 – Scribing at an angle

## 2.4 Filing Techniques

Filing also plays a major role in sheet metal forming. Failing to file a sheet metal edge will result in burr formation at the edges. Hence, it will lead to wrong calculation which results in wrong shape. There are two common types of files used in sheet metal formation. The Dreadnought File which has curved teeth is usually used to file the snapped edges which will remove the burrs off. The diamond file is usually used in filing the surface for sharper finish. Figure (2.4.1) shows these two different types of files.



Figure 2.4.1 – Different types of Files

All the factors discussed in this chapter affect the sheet metal forming. It is important to look at these factors and determine the capability of formability before moving on to the process. These factors also require determination/ measurement throughout the forming process to make sure good formability conditions are maintained.



## **CHAPTER 3 – ENGINEERING FACTORS**

### **3.1 Velocity of the Tool**

As discussed earlier in chapter 2, tooling plays a major role in forming the sheet metal. The impact velocity of the tool determines the deformation of the sheet metal. It is much important to have a controlled velocity/ controllable velocity to produce the required deformation. It should be noted that only if all the kinetic energy (delivered by hammering mechanism through its velocity of impact) is converted into deformation, we could get the deformation required. In reality, it is not possible as there are several factors affecting the delivery of kinetic energy. So, there will be loss of some kinetic energy, hence, a less deformation. The tooling velocity should be compensated for this factor.

Also, much of the energy produced is consumed to deform the material rather to deform the material to required shape. So, the intended shape is not produced. This factor has to be compensated by the velocity of tooling.

### **3.2 Motion of the Work Piece**

In forming the sheet metal, the work piece (i.e. Sheet Metal) is only moved and the tool is kept at the same place producing the impact. The work piece is moved along to get the shape of the panel required. Care is to be taken which portion of the work piece is to be deformed first. The deformation might be shrinking or stretching the sheet metal, so care should be taken the sheet metal is not over stretched or over shrunk.

It is very much important to analyse the work piece movement carrying out an analysis before moving on to real time processing of forming. This could be done using Finite Element Analysis. The deformation analysis could be made and the motion of work piece could be related. It is to be noted that in real time, the deformation will not be as expected so a feedback is necessary to produce the exact deformation through motion of the work piece.

### **3.3 Relative motion of Tool to Work Piece**

The tool is held at the same position producing the impacting force. The work piece is moved to acquire the required shape. It should be considered that the point of impact may sometime require an angular depending on the shape of the material. In that case, there should be an angular motion to tooling to produce the necessary angle of impact.

### **3.4 Ductility, Malleability and Rigidity of the Material**

Material selection as discussed is another factor which determines the formability of the sheet metal. The material selected should be of ductile nature as the sheet metal involves a stretching to produce the required shape. The sheet metal also needs to have good malleable property for it to be shrunk according to the requirements. Also, the material should be of good strength and be rigid to bear all the shrinking and stretching forces. So, ideally the sheet metal should have all the properties. It is very important to find a balance between these properties.

This could be done by calculating the modulus of rigidity and modulus of elasticity of the material and find the best composition for deformation purposes.

### **3.5 Involute Curves**

Involute curves are considerable especially while wheeling the sheet metal or finishing the sheet metal. This may produce some patch problems if the curvature is not maintained properly. The line of contact between the two wheels should always be straight. Alignment between the two wheels (upper flat wheel and lower curved wheel) is to be checked regular to have a smooth finish.

### **3.6 Designing/ Drafting**

As the sheet metal forming involves lot crafting, design considerations are more important to maintain the dimensions of the material. If the design dimensions are not perfect, exact shape will not be produced.

To make things easier, it is good to reverse engineer from the final shape and get the planar dimensions required to produce the 3D shape of the sheet metal. It could be done using NX7.5 or Rhino CAD. This minimises the error to least. All the necessary allowances and tolerances are to be considered before drafting the final design.

## **CONCLUSION**

The practical complexities and benefits of traditional sheet metal forming methodology have been analysed. Though there are complexities, an appropriate design would compensate for the complexities and raise the way for automated incremental sheet metal forming. The conventional methods used in the industry involve lot of cost and lacks flexibility. Automating traditional method and forming the sheet metal incrementally could be a gateway to produce complex shapes with less cost and higher flexibility. It gives raise to accurate and precise manufacturing capabilities. As stated by the traditional sheet metal manufacturers, the traditional method of forming the sheet metal will make the sheet metal more durable and takes a positive edge over the conventional methodologies.

## APPENDIX 2

### Power Hammer Investigation

Investigating into the hammering machine, visits were done to observe how the hammering machine works and observe the constructive formation of sheet metal using hammering machine.

Industrially the hammering machine was known as “Power Hammer”. The initial inquiry was into using a blacksmith’s power hammer (as shown in Fig 1). But these hammers produced heavy impact than what was required and they do not provide control of impact. So, it was concluded that a blacksmith’s power hammer cannot be used.



**Fig 1 - Blacksmith's power hammer**

Exploration into blacksmith's power hammer, lead to the study of several designs of a power hammer which are discussed as below.

### **Planishing hammer**

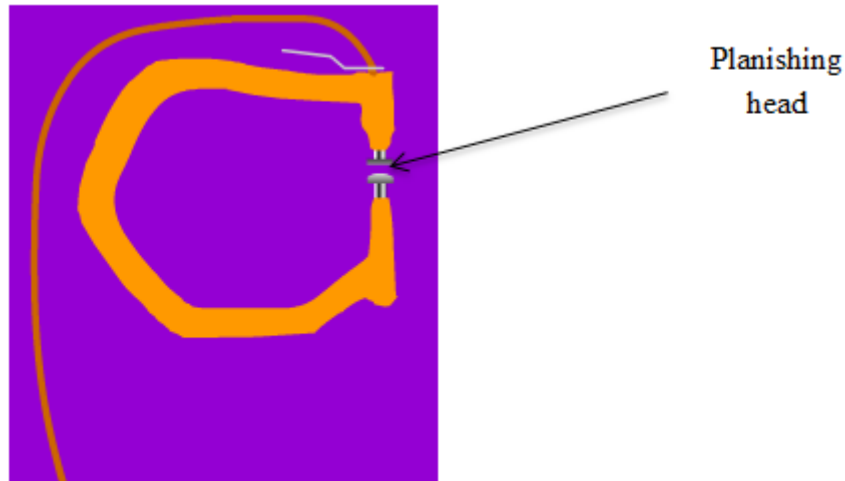


**Fig 2 - Planishing hammer**

A planishing hammer is a pneumatic operated hammer which can only stretch the material. It has got a planishing heads between which the material is fed (Shown in Fig 2). It is usually used for metal finishing purposes. Therefore, it was determined that these type of hammers cannot be used for forming the sheet metal.

### **Pullmax linkage hammer**

Most of the power hammers were driven using an electric motor because the motor created enough power to produce the impact. The pullmax linkage hammer (shown in Fig 3) had several linkages which were constrained in motion to produce an impact using a die by having a linear ram at the end. They used an eccentric to adjust for stroke length and the handle used can also be used to change the linkage slots and produce a different power. These were observed to produce an impact force in the range of 2000 N – 6000 N. These were found to be used by metal workers.

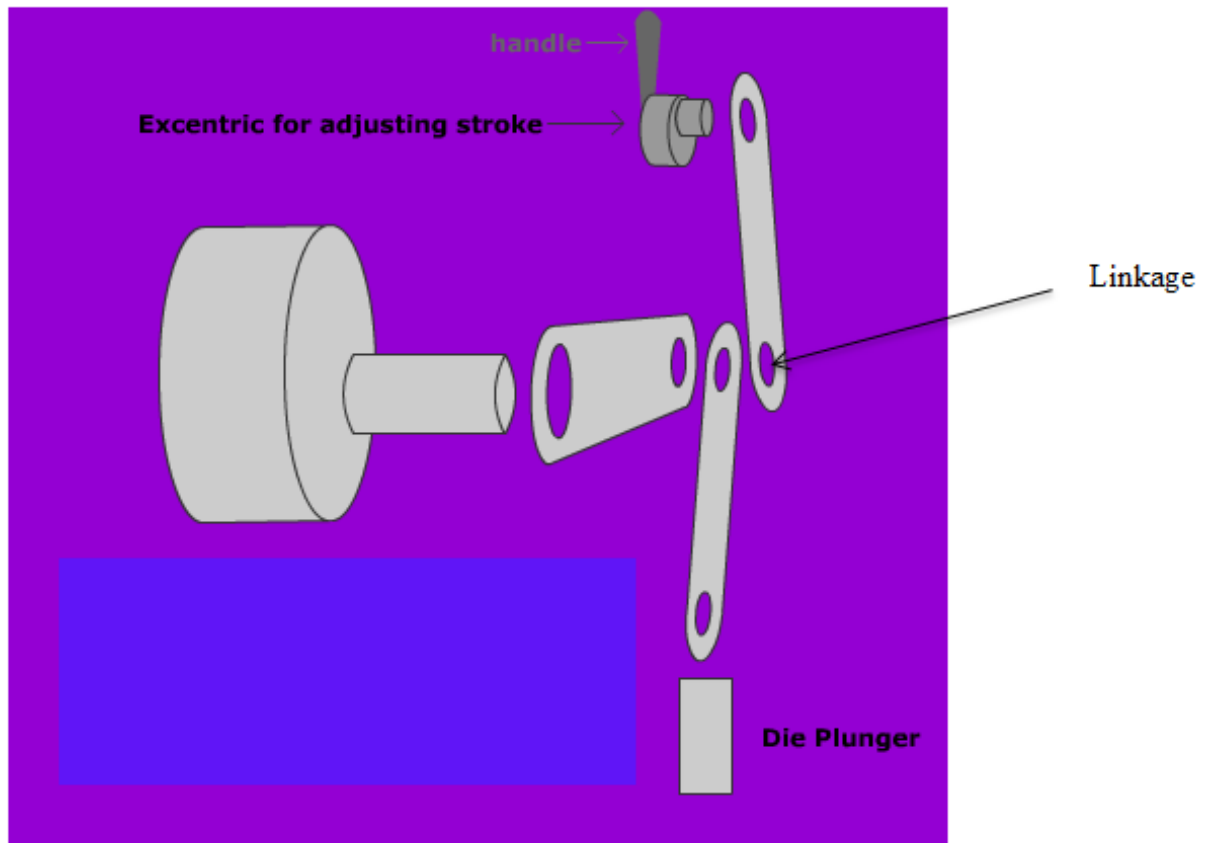


Fig 3 - Pullmax linkage hammer

**Power hammer**

Mostly power hammers were referred to hammers using a crank or toggle mechanism to produce the necessary impact. These types of hammers were driven using an electric motor with the motor connected to an eccentric using belt. The eccentric was then connected to a crank using different slots (for different power) or using a toggle to create the necessary impact. The one shown in Fig 4 is a toggle mechanism. Some of these mechanisms also used a leaf spring which acted as a pivot during slower speeds and a whip during a higher speed. These leaf springs were considered to be necessary not to damage the mechanical links due to the vibrations retracted because of impact.

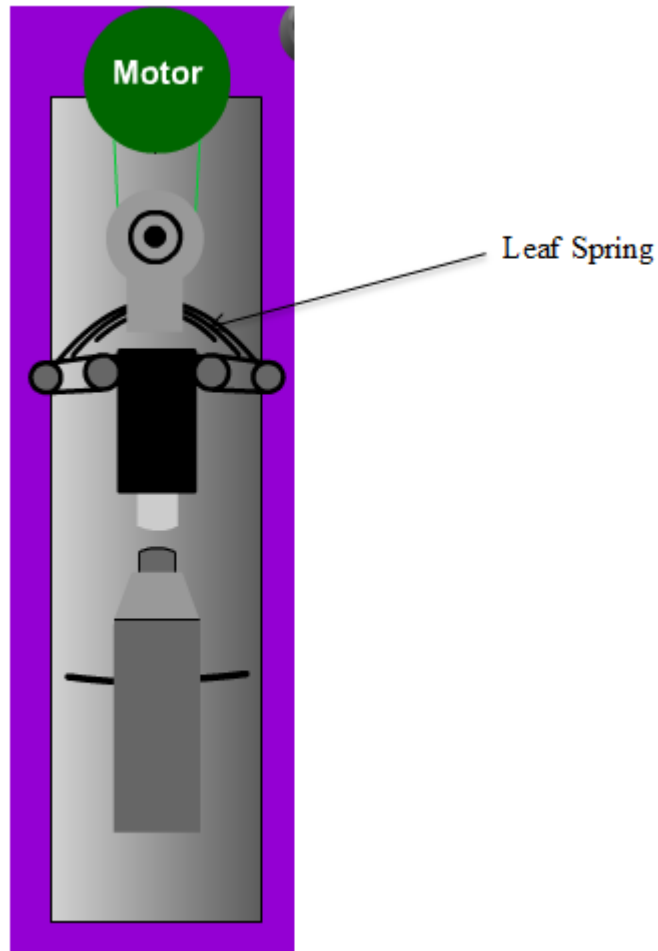
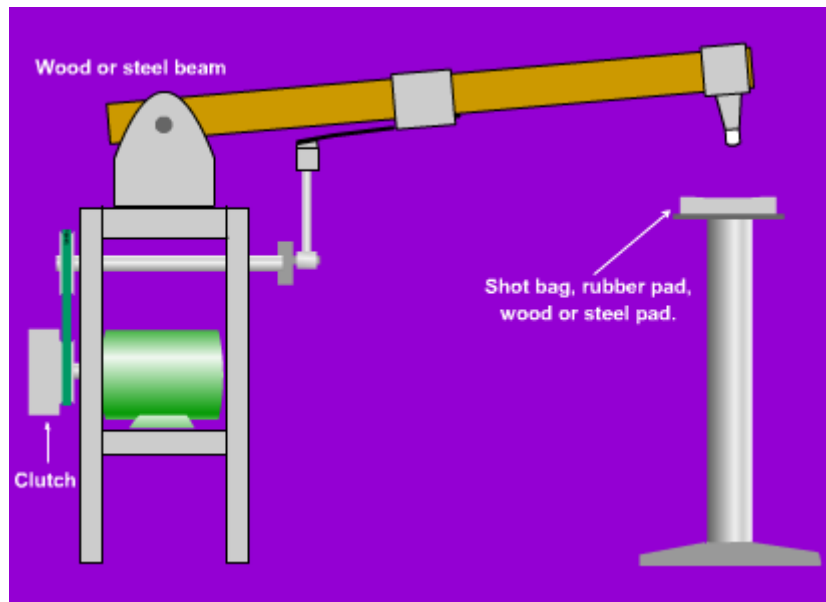


Fig 4 - Power hammer

### Helve hammer

The helve hammer was also driven using an electric motor (shown in Fig 5). A pivot mechanism connected to a motor was used in this case. The impact created by this type of hammer was less in comparative to other types because of the pivoted constraint. In this case, a higher impact would need a higher speed which was not the aim of the research. Also, the hammer's impact was produced in an angle. This angled hammering will have several issues if it is used in prediction of hammering impact.



**Fig 5 - Helve hammer**

As the aim of the research was to find a mechanised hammer which produced impact force between 2000 N and 6000 N even at slower speed or in a single impact (to be precise). Only the pullmax linkage and power hammer was found to deliver the needed power in single impact. As it could be observed both these mechanism have a final push (a very small nudge) during the impact which helps in converting most of the kinetic energy into deformation. Having decided on these types of hammers, workshops were visited to inquire into the real working ability of these hammers.

### **Mechanised hammers in a workshop**

Shown in Fig 6 is a pullmax type power hammer which had several linkages and constrained to produce a linear motion. The mechanism was motor (3 HP motor) driven and used a belt to transfer energy. The motor operation was controlled using a foot pedal which would actually act as a motor ON/ OFF, so the pedal control acted as a clutch and would stop the mechanism once the foot is taken off the pedal. The mechanism any control mechanism over speed. The stroke adjustments were made using linkage slots.

When the variable gear drive to produce different speed using the motor was investigated, it was understood the shear pin the variable drive usually breaks because of its inability to bear the retraction due to impact force. Producing different speed by using conical belt drive also is not viable as slippage causes a huge problem.



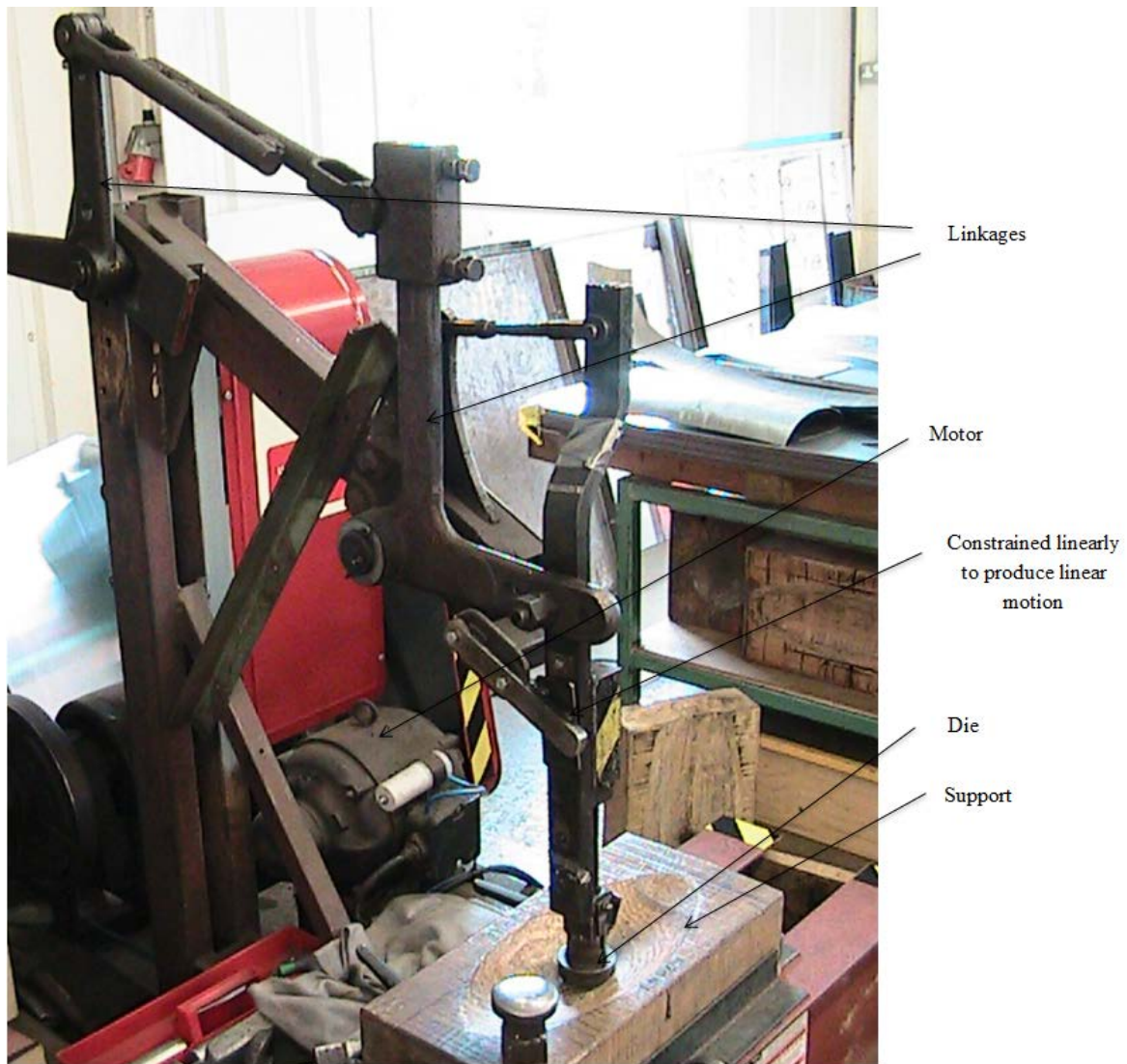


**Fig 6 - Workshop hammer 1**

Another mechanised hammer was also studied (shown in Fig 7). This power hammer was based on “power hammer” type using a flywheel and eccentric. Though the design was varying, the principle used was same. It was driven using a 0.37 KW single phase motor. In this mechanism, a flywheel was used to store the energy and a belt drive was used to transfer the energy to the eccentric. The eccentric had an adjustable link (using a lead screw) which was connected to a leaf spring to transfer the energy to a linear ram. On slower speed the leaf spring would act as a pivot and higher speed it acts as a whip (producing the necessary push). The hammer was pedal controlled. As the energy gets stored in the flywheel, the hammer would not stop immediately when taken foot off the pedal. This was a huge constraint in this mechanism.

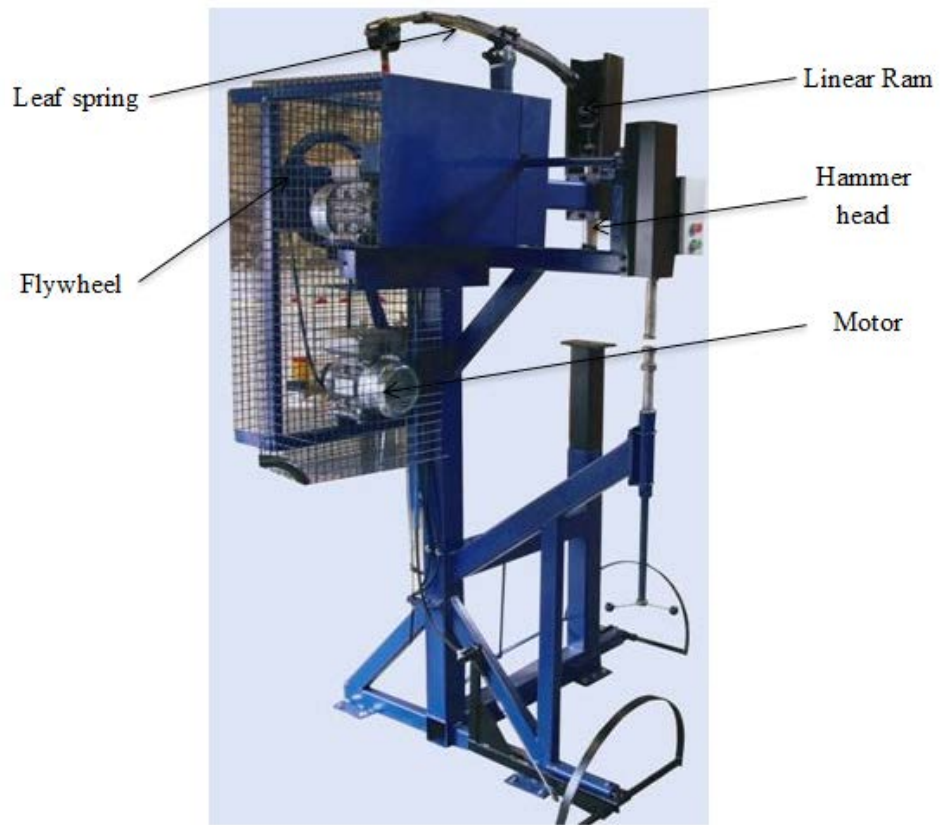


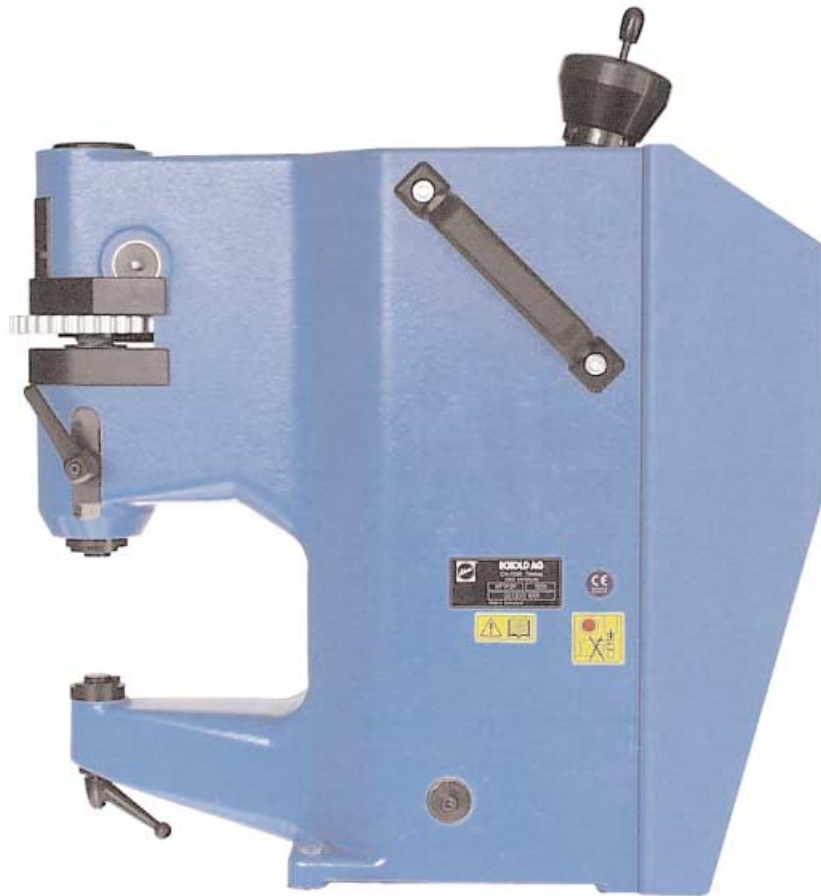
**Fig 7 - Workshop hammer 2**



# ECKOLD AG

---

## Operation Manual Kraftformer Type KF 170 P / KF 170 PD



Illustrations and measurements unbinding. Subject to change without notice.



## Introduction

The purpose of this operation manual is to acquaint yourself with the machine, to learn the proper use, to avoid dangers, unnecessary repair costs and down time and to increase the reliability and machine life.

The operation manual should always be at hand and should be read and followed by every person working with or at the machine.



This machine has been developed, designed and manufactured in accordance with EG-directions 89/392/EWG. This is confirmed by the CE-label fastened to the machine body.



### ECKOLD AG

CH-7203 Trimmis, Schweiz / Suisse / Switzerland

#### EC DECLARATION OF CONFORMITY FOR MACHINERY

Directive 89/392/EEC, 91/368/EEC, 93/44/EEC, 93/68/EEC

Manufacturer: ECKOLD AG

Address: Rheinstrasse, CH 7203 Trimmis / Schweiz

Herewith declares that

make	type	serial number
Krafformer	KF 170 P	021.200.1001
Krafformer	KF 170 PD	021.200.2500
Druckfügezange	MZD 35/3 CH (N)	023.106.0000
TEKO-Druckübersetzer	DPF 125/15/100 S	277.010.0001
Glätthammer	GL 2	023.200.1002
Clinchmaschine	HC 1000 R	021.200.2004
Clinchmaschine	HC 1000 RM	021.200.2003

⇒ is in conformity with the provisions of the Machinery Directive (Directive 89/392/EEC), as amended, and with national implementing legislation,

and furthermore declares that

⇒ the following (parts/clauses of) harmonized standards have been applied:

- EN 292

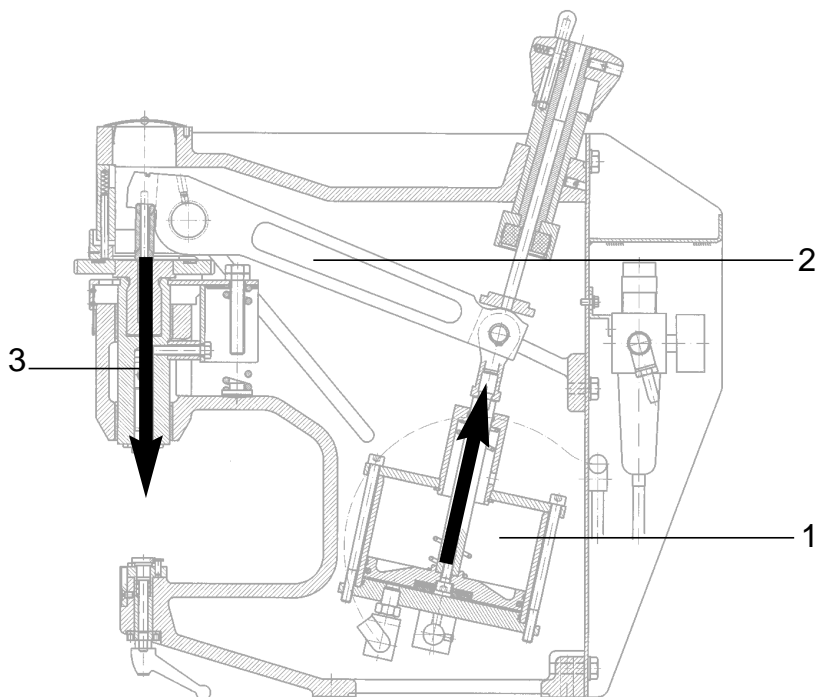
Trimmis, 02.12.2002

**ECKOLD AG**

Marc Eckold  
manager

## Technical Data

### Brief description



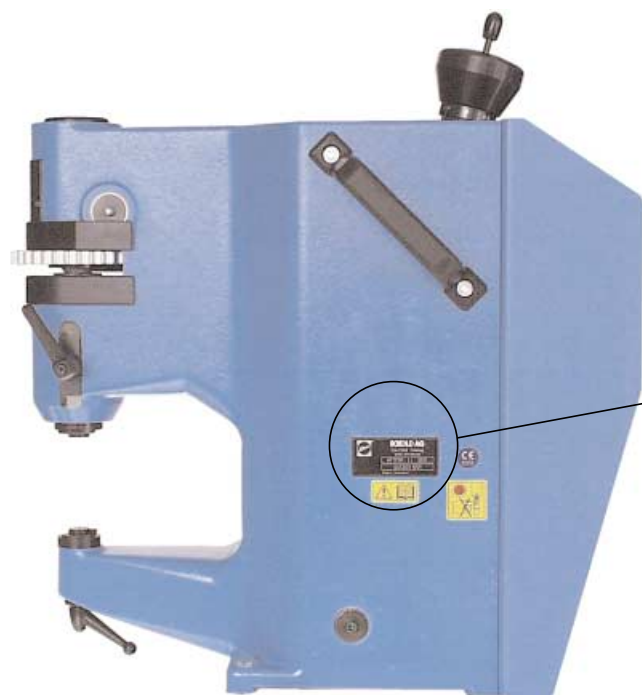
The Eckold Kraffformer KF 170 is a universal machine providing the drive for different, interchangeable tools.

In the KF 170 an air-cylinder (1) drives the pressure lever (2), which converts the radial movement into the vertical stroke of the machine ram (3).

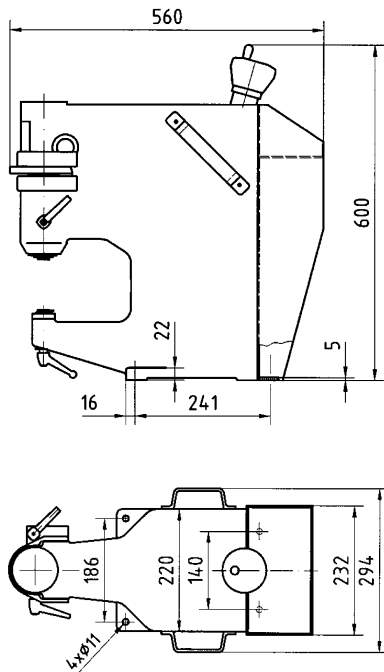
Ram position and stroke length can be precisely preselected and controlled.

The KF 170 PD machine can be switched from single stroke to continuous stroke.

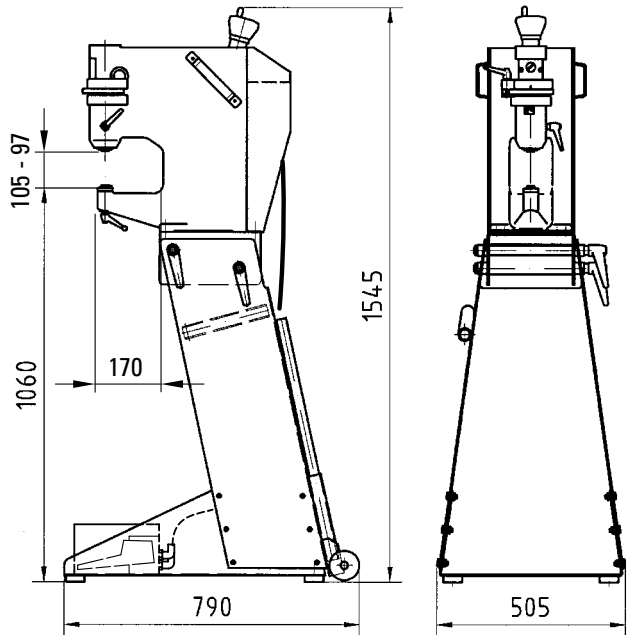
### Type plate position



**Dimensions and weights**



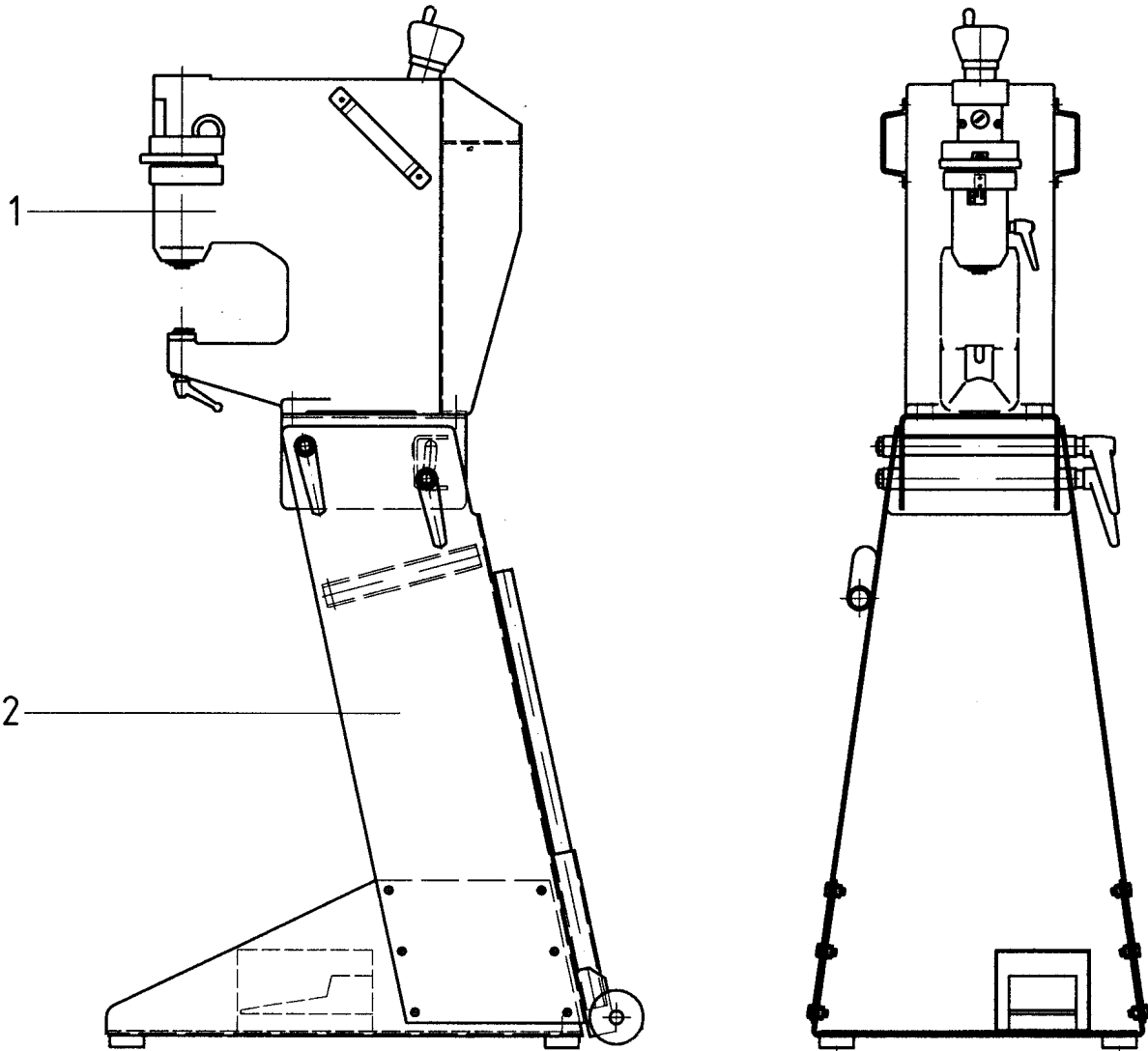
• without stand



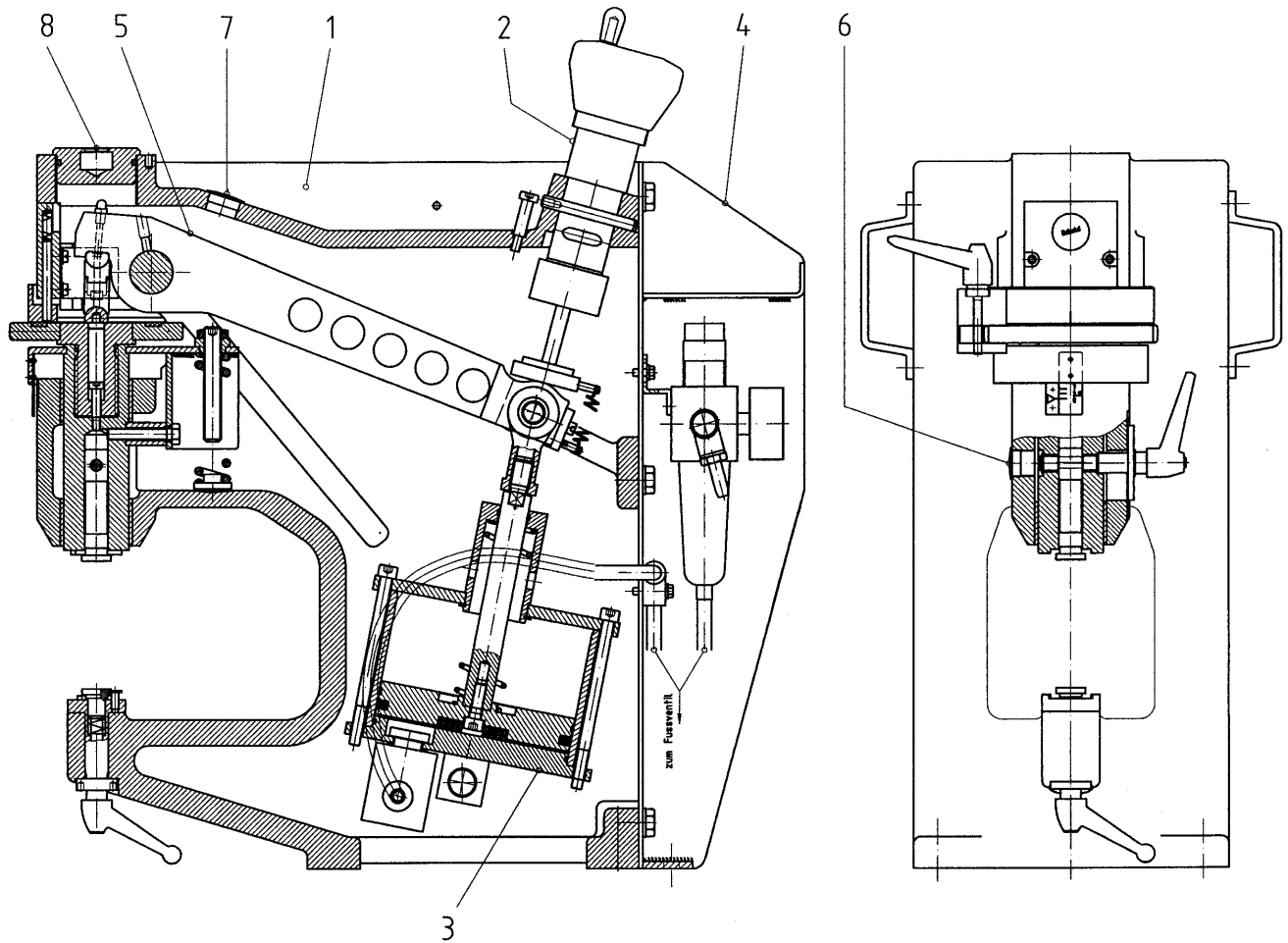
• with stand

Throat depth horizontal		<b>170 mm</b>
Throat height vertical		<b>146 mm</b>
Net weight	- without stand	~ <b>93 kg</b>
	- with stand	~ <b>151 kg</b>
Forming capacity:	- steel	<b>max 2.0 mm</b>
	- aluminium	<b>max 2.0 mm</b>
	- stainless steel	<b>max 1.5 mm</b>

Order no.	KF 170 P single stroke	KF 170 PD continuous stroke
without stand	<b>021.200.1001</b>	<b>021.200.2500</b>
with stand	<b>021.200.1000</b>	<b>021.200.2502</b>



Pos. No.	Stk. Pce	Benennung Description	Artikel Nr. Order No.	DIN Nr. DIN No.	Typ / Abmessungen Type / Dimension
1	1	Gerätekopf Apparatus head	021.200.1001		
2	1	Geräteständer Pedestal	023.127.0000		



Pos. No.	Stk. Pce	Benennung Description	Artikel Nr. Order No.	DIN Nr. DIN No.	Typ / Abmessungen Type / Dimension
1	1	Gehäuse Basisgruppe KF170 P/H Housing	021.300.1002		
2	1	Hubeinstellung Stroke adjustment	021.300.1000		
3	1	Pneumatik - Zylinder Pneumatic cylinder	023.125.0001		
4	1	Abdeckung Covering	023.125.0017		
5	1	Druckhebel Pressure lever	023.125.0019		
6	1	Verschluss - Stopfen Covering	271.450.0010		PG 11
7	1	Verschluss - Stopfen Covering	271.450.0020		PG 16
8	1	Verschluss-Stopfen Covering	023.125.0032		



## APPENDIX 4

### Experiment using wooden hammer and High Speed Camera (400 fps)

#### Experiment:

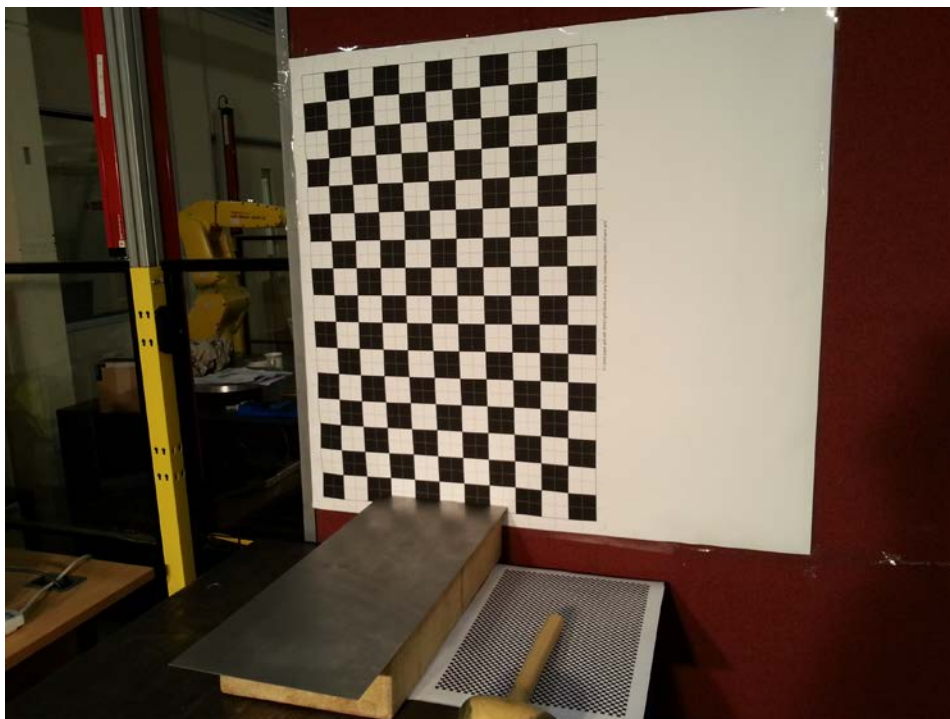
Steel of 1 mm thickness was impacted using a wooden hammer of 0.42 Kg from a height of 0.8 m. The sheet metal (steel) was held on a wooden block anvil which has a hollow double curvature. The action of hammering was captured by a high speed camera which has 400 fps.

#### Objective:

To find the impact velocity and force on a time based analysis.

#### Methodology:

A calibration grid (80x80cm – Black & White) was placed at the back, in close proximity to the hammering action so that the motion of the hammer could be framed using the high speed camera. The high speed camera was set to 400 fps and was triggered to capture the motion of the hammer. The hammer's motion was detected for every 5 millisecond and the distance travelled was also identified.



Knowing the distance travelled and time taken at regular intervals, variable velocity and acceleration could be calculated. Calculating which impact velocity and force could be calculated as well.

#### Results:

The results achieved were not reliable as the frame rate of the camera was less. Some data was lost due to this which gave irrelevant results. So, it was found that a camera with better resolution and frame rate is required to detect the motion of the hammer.

Model: 511F04 IEPE IMPACT HAMMERSerial No.: 106010

Sensitivity ( $\pm 15\%$ ): 0.499 mV/N  
 Measurement Range (Compression): 10 kN  
 Maximum Static Force (Compression): 50 kN  
 Upper Frequency Limit: 36 kHz  
 Non-Linearity:  $\leq 1\%$  FS  
 Temperature Range: -54 to +121 °C  
 Excitation Voltage: 20 to 30 VDC  
 Constant Current Excitation: 2 to 20 mA  
 Output Impedance:  $\leq 100$  ohm

Output Polarity (Compression): Positive  
 Size (Hex x Height x Sensing Surface):  $\phi 26 \times \phi 8 \times 27$  mm  
 Weight: 39 gram  
 Housing Material: Stainless Steel; Sealing Hermetic  
 Electrical Connector: M5  
 Electrical Connection Position: M5 Side  
 Mounting Thread: M8 Female  
 Mounting Torque (Recommended): 181 to 226 N-cm

Model YMC	Measuring Range	Head Weight	Hammer Mass	Head Diameter	Hammer Length	Output Socket	Tips
IH-01	200N	30Gram	-	$\Phi 10$ mm	240mm	BNC	Stainless steel, Aluminum, Rubber, Nylon
IH-02	2,000N	105Gram	-	$\Phi 20$ mm	250mm	BNC	
IH-05	5,000N	105Gram	100Gram	$\Phi 20$ mm	250mm	BNC	
IH-10	10,000N	1,000Gram	500Gram	$\Phi 50$ mm	330mm	BNC	Hard Tip, Medium Tip, Soft Tip
IH-50	50,000N	1,000Gram	500Gram	$\Phi 50$ mm	330mm	BNC	Hard Tip, Medium Tip, Soft Tip, Mass

Test Environment Temperature: 22°C Humidity: 65%Date: 2013-06-18 Reported By: 繪01

## Accelerometer Calibration Sheet

THIS CALIBRATION IS TRACEABLE TO NATIONAL STANDARDS

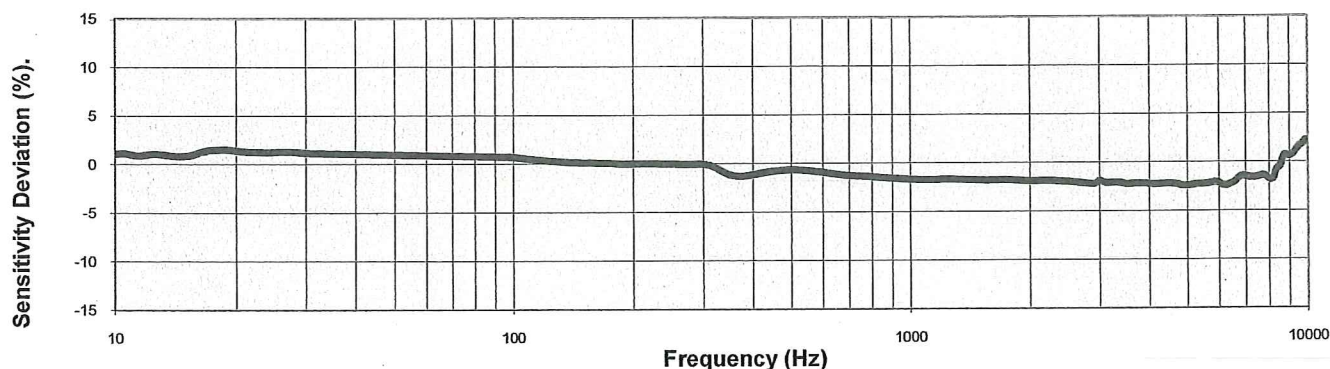
Type:	A/124/E
Serial No:	261
Direction:	Uniaxial

Date:	04/06/2013
Tested by:	Debbie Grant
Job No:	21761

Vibration		Accelerometer	
Level (g)	Freq (Hz)	Sensitivity (mV/g)	Deviation (%)
1	10	10.025	1.10
1	20	10.055	1.40
10	40	10.019	1.04
10	60	10.004	0.89
10	80	9.994	0.79
10	100	9.985	0.70
10	200	9.916	0.00
10	400	9.802	-1.15
10	600	9.825	-0.92
10	800	9.778	-1.39

Vibration		Accelerometer	
Level (g)	Freq (Hz)	Sensitivity (mV/g)	Deviation (%)
10	1000	9.750	-1.67
10	2000	9.730	-1.87
10	3000	9.729	-1.88
10	4000	9.697	-2.21
10	5000	9.678	-2.40
10	6000	9.707	-2.11
10	7000	9.774	-1.44
10	8000	9.743	-1.74
10	9000	9.980	0.65
10	10000	10.136	2.22

Measurements were made in ambient conditions of 22°C ± 3°C



Voltage Sensitivity @ 200Hz (mV/g)	9.92	Test Equipment	
Capacitance (pF)		A/20/N Serial No:	9850
Insulation Resistance (Ω)		Calibration Certificate No:	141514
Polar Cross-Axis @ 100Hz (max %)	5	Charge Sensitivity @ 200Hz (pC/g)	27.54
Cable length (m)		Vibpilot Serial No	A090051
		Calibration Ref	DJB Vibpilot

Calibration Approved:  N. FOREMAN

Date: 04/06/2013

Temperature	± 2°C
Measurement Uncertainty	± 3%
Confidence Probability	95%

The test results refer to measurements made at the time of the test.  
 This certificate may not be reproduced other than in full.  
 This test does not demonstrate the instrument's ability to maintain calibration.



## Accelerometer Calibration Sheet

THIS CALIBRATION IS TRACEABLE TO NATIONAL STANDARDS

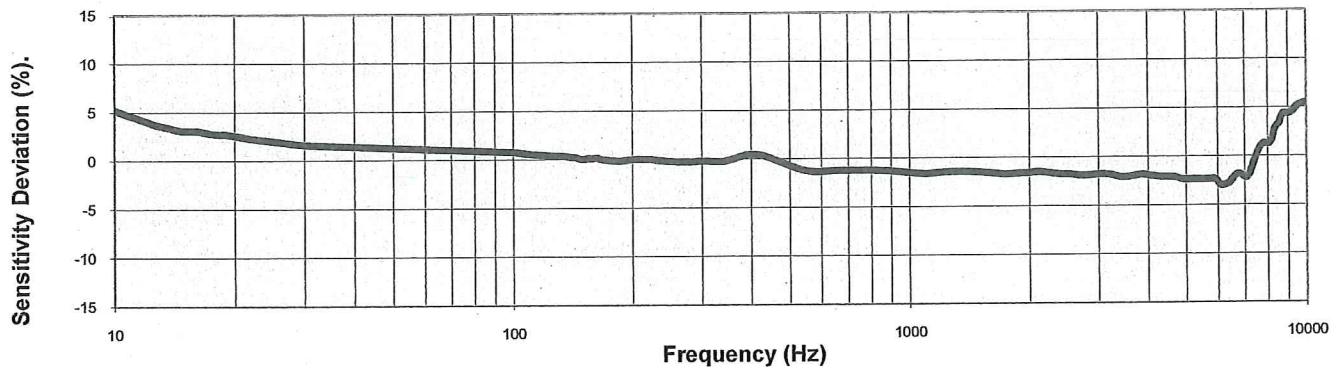
Type:	A/124/E
Serial No:	260
Direction:	Uniaxial

Date:	04/06/2013
Tested by:	Debbie Grant
Job No:	21761

Vibration		Accelerometer	
Level (g)	Freq (Hz)	Sensitivity (mV/g)	Deviation (%)
1	10	10.253	5.14
1	20	10.002	2.56
10	40	9.889	1.40
10	60	9.862	1.13
10	80	9.843	0.93
10	100	9.828	0.78
10	200	9.752	0.00
10	400	9.798	0.47
10	600	9.622	-1.34
10	800	9.634	-1.21

Vibration		Accelerometer	
Level (g)	Freq (Hz)	Sensitivity (mV/g)	Deviation (%)
10	1000	9.606	-1.50
10	2000	9.600	-1.56
10	3000	9.580	-1.77
10	4000	9.569	-1.88
10	5000	9.521	-2.37
10	6000	9.506	-2.52
10	7000	9.543	-2.15
10	8000	9.877	1.28
10	9000	10.177	4.35
10	10000	10.283	5.44

Measurements were made in ambient conditions of 22°C ± 3°C



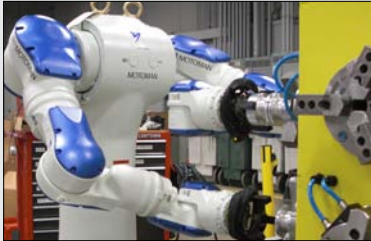
Voltage Sensitivity @ 200Hz (mV/g)	9.75	Test Equipment	
Capacitance (pF)		A/20/N Serial No:	9850
Insulation Resistance (Ω)		Calibration Certificate No:	141514
Polar Cross-Axis @ 100Hz (max %)	5	Charge Sensitivity @ 200Hz (pC/g)	27.54
Cable length (m)		Vibpilot Serial No	A090051
		Calibration Ref	DJB Vibpilot

Calibration Approved:  N. FOREMAN

Date: 04/06/2013

Temperature	± 2°C
Measurement Uncertainty	± 3%
Confidence Probability	95%

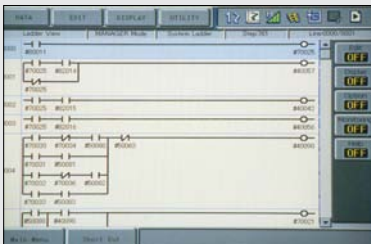
The test results refer to measurements made at the time of the test.  
This certificate may not be reproduced other than in full.  
This test does not demonstrate the instrument's ability to maintain calibration.



MACHINE TENDING



THRU-ARM CABLE AND HOSE ROUTING



LADDER EDITOR

## TOP REASONS TO BUY

- Dexterity to perform complex tasks; dual 7-axis arms work together or independently
- Slim design optimizes space; provides “human-like” flexibility and range of motion, even in tight spaces
- Simplified tooling reduces cost
- Can be used in environments that are hazardous to humans
- Labor savings justifies capital investment

# SDA10D

ASSEMBLY • PACKAGING • HANDLING • MACHINE TENDING • PART TRANSFER

Payload: 10 kg/arm



## Slim, Dual-Arm Robot with “Human-Like” Flexibility

- Powerful actuator-based design provides “human-like” flexibility and fast acceleration.
- Superior dexterity and best-in-class wrist characteristics make slim, dual-arm robot ideally suited for assembly, part transfer, machine tending, packaging and other handling tasks that formerly could only be done by people.
- Highly flexible; 15 axes of motion (7 axes per arm, plus a single axis for base rotation).
- Internally routed cables and hoses (6 - air, 12 - electric) reduce interference and maintenance, and also make programming easier.
- 10 kg (22.1 lb) payload per arm; 720 mm (28.3") horizontal reach per arm; 1,440 mm (56.7") vertical reach per arm;  $\pm 0.1$  mm (0.004") repeatability.
- Both robot arms can work together on one task to double the payload or handle heavy, unwieldy objects. Two manipulators can perform simultaneous independent operations.

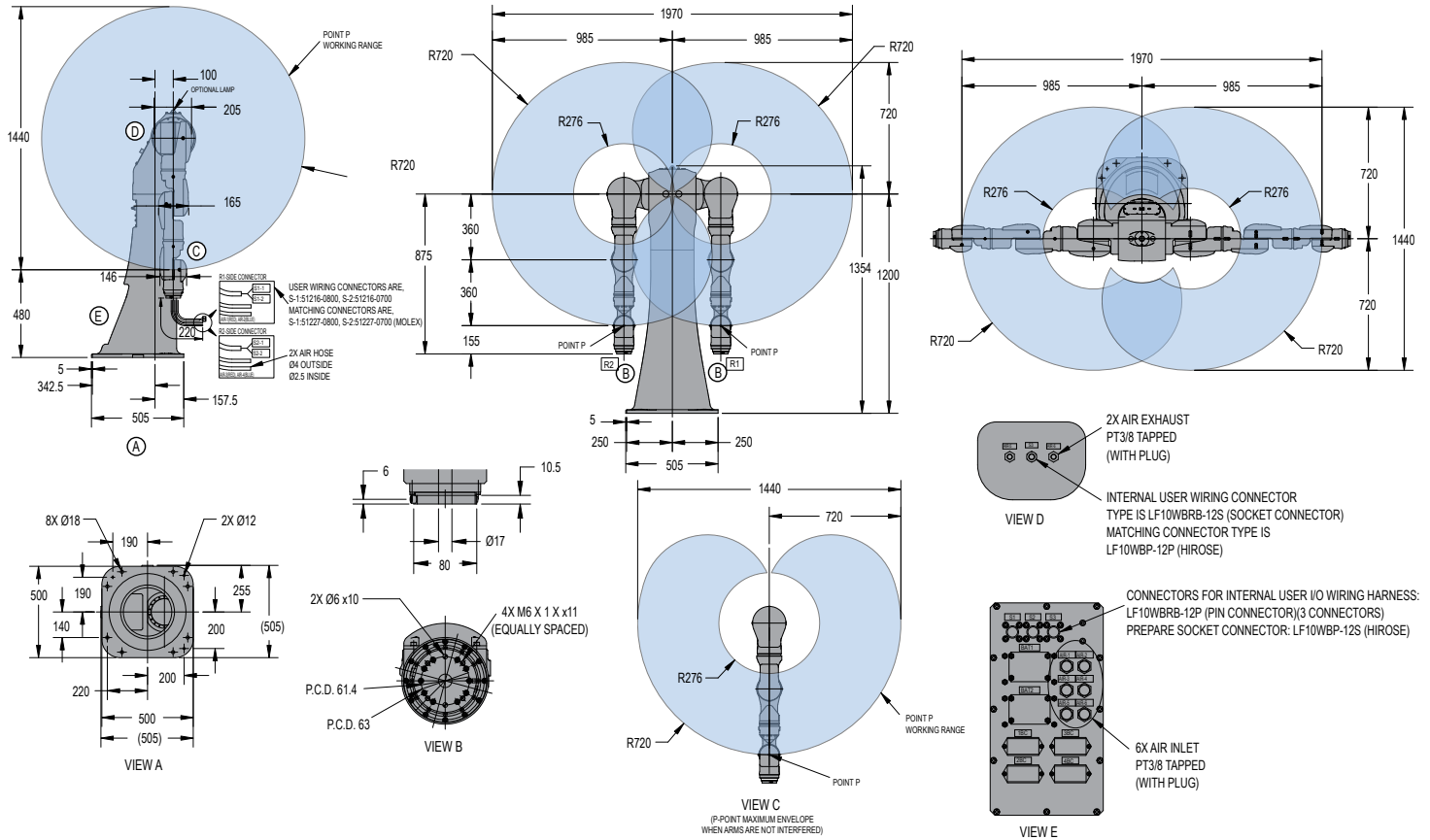
- Ability to hold part with one arm while performing operations on it with other arm. Can transfer a part from one arm to the other with no need to set part down.

## DX100 Controller

- Patented multiple robot control supports up to 8 robots/72 axes.
- Windows® CE programming pendant with color touch screen and USB interface.
- Faster processing speeds for smoother interpolation. Quicker I/O response. Accelerated Ethernet communication.
- Extensive I/O suite includes integral PLC and touch screen HMI, 2,048 I/O and graphical ladder editor.
- Supports all major fieldbus networks, including EtherNet/IP, DeviceNet, Profibus-DP and many others.
- Compliant to ANSI/RIA R15.06-1999 and other relevant ISO and CSA safety standards. Optional Category 3 functional safety unit.

# SDA10D ROBOT

All dimensions are metric (mm) and for reference only. Please request detail drawings for all design/engineering requirements.



## SDA10D SPECIFICATIONS

<b>Structure</b>	Articulated	
<b>Mounting</b>	Floor	
<b>Controlled Axes</b>	15 (7 axes per arm plus base rotation)	
<b>Payload</b>	10 kg (22.1 lbs)/arm	
<b>Horizontal Reach per Arm</b>	720 mm (28.3")	
<b>Horizontal Reach (P-point to P-point)</b>	1,970 mm (77.6")	
<b>Vertical Reach</b>	1,440 mm (56.7")	
<b>Repeatability</b>	±0.1 mm (±0.004")	
<b>Maximum Motion Range</b>	Rotation-Axis (Waist)	±170°
	S-Axis (Lifting)	±180°
	L-Axis (Lower Arm)	±110°
	E-Axis (Elbow)	±170°
	U-Axis (Upper Arm)	±135°
	R-Axis (Upper Arm Twist)	±180°
	B-Axis (Wrist Pitch/Yaw)	±110°
T-Axis (Wrist Twist)	±180°	
<b>Maximum Speed</b>	Rotation-Axis	130°/s
	S-Axis	170°/s
	L-Axis	170°/s
	E-Axis	170°/s
	U-Axis	170°/s
	R-Axis	200°/s
	B-Axis	200°/s
T-Axis	400°/s	
<b>Approximate Mass</b>	220 kg (485.1 lbs)	
<b>Power Consumption</b>	2.7 kVA	
<b>Allowable Moment</b>	R-Axis	31.4 N • m
	B-Axis	31.4 N • m
	T-Axis	19.6 N • m
<b>Allowable Moment of Inertia</b>	R-Axis	1 kg • m <sup>2</sup>
	B-Axis	1 kg • m <sup>2</sup>
	T-Axis	0.4 kg • m <sup>2</sup>

## DX100 CONTROLLER SPECIFICATIONS\*\*

<b>Dimensions (mm)</b>	1,200 (w) x 1,000 (h) x 650 (d) 47.2" x 39.4" x 25.6"
<b>Approximate Mass</b>	250 kg max. (551.3 lbs)
<b>Cooling System</b>	Indirect cooling
<b>Ambient Temperature</b>	During operation: 0° to 45° C (32° to 113° F) During transit and storage: -10° to 60° C (14° to 140° F)
<b>Relative Humidity</b>	90% max. non-condensing
<b>Primary Power Requirements</b>	3-phase, 240/480/575 VAC at 50/60 Hz
<b>Digital I/O</b>	Standard I/O: 40 inputs/40 outputs consisting of 16 system inputs/16 system outputs, 24 user inputs/24 user outputs 32 Transistor Outputs; 8 Relay Outputs Max. I/O (optional): 2,048 inputs and 2,048 outputs
<b>Position Feedback</b>	By absolute encoder
<b>Program Memory</b>	JOB: 200,000 steps, 10,000 instructions CIO Ladder Standard: 15,000 steps Expanded: 20,000 steps
<b>Pendant Dim. (mm)</b>	169 (w) x 314.5 (h) x 50 (d) (6.7" x 12.4" x 2")
<b>Pendant Weight</b>	.998 kg (2.2 lbs)
<b>Interface</b>	One Compact Flash slot; One USB Port (1.1)
<b>Pendant Playback Buttons</b>	Teach/Play/Remote Keypress selector Servo On, Start, Hold, and Emergency Stop Buttons
<b>Programming Language</b>	INFORM III, menu-driven programming
<b>Maintenance Functions</b>	Displays troubleshooting for alarms, predicts reducer wear
<b>Number of Robots/Axes</b>	Up to 8 robots, 72 axes
<b>Multi Tasking</b>	Up to 16 concurrent jobs, 4 system jobs
<b>Fieldbus</b>	DeviceNet Master/Slave, AB RIO, Profibus, Interbus-S, M-Net, CC Link, EtherNet IP/Slave
<b>Ethernet</b>	10 Base T/100 Base TX
<b>Safety</b>	Dual-channel Emergency Stop Pushbuttons, 3-position Enable Switch, Manual Brake Release Meets ANSI/RIA R15.06-1999, ANSI/RIA/ISO 10218-1-2007 and CSA Z434-03

\*\*See DX100 Controller data sheet (DS-399) for complete specifications

www.motoman.com

**YASKAWA**  
MOTOMAN ROBOTICS

MOTOMAN ROBOTICS  
 100 AUTOMATION WAY, MIAMISBURG, OHIO 45342  
 TEL: 937.847.6200 ■ FAX: 937.847.6277

TECHNICAL SPECIFICATIONS SUBJECT TO CHANGE WITHOUT NOTICE  
 DS-403-D ©2011 YASKAWA AMERICA, INC. JUNE 2011

MOTOMAN IS A REGISTERED TRADEMARK  
 WINDOWS IS A REGISTERED TRADEMARK OF MICROSOFT  
 ALL OTHER MARKS ARE THE TRADEMARKS AND  
 REGISTERED TRADEMARKS OF YASKAWA AMERICA, INC.

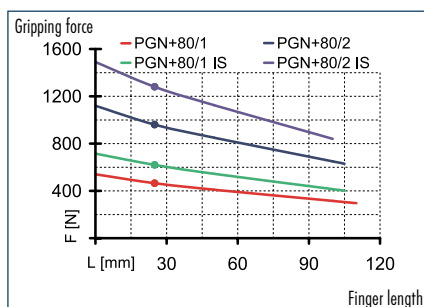


# PGN-plus 80

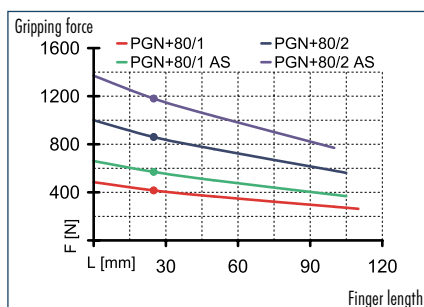
Pneumatic • 2-Finger Parallel Gripper • Universal Gripper



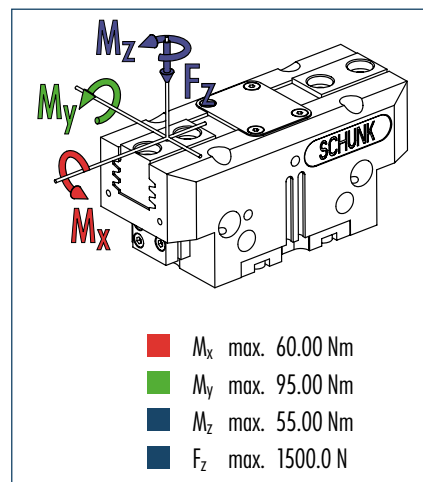
## Gripping force, I.D. gripping



## Gripping force, O.D. gripping



## Finger load



① The indicated moments and forces are static values, apply per base jaw and may occur simultaneously.  $M_y$  may arise in addition to the moment generated by the gripping force itself. If the max. permitted finger weight is exceeded, it is imperative to throttle the air pressure so that the jaw movement occurs without any hitting or bouncing. Service life may be reduced.

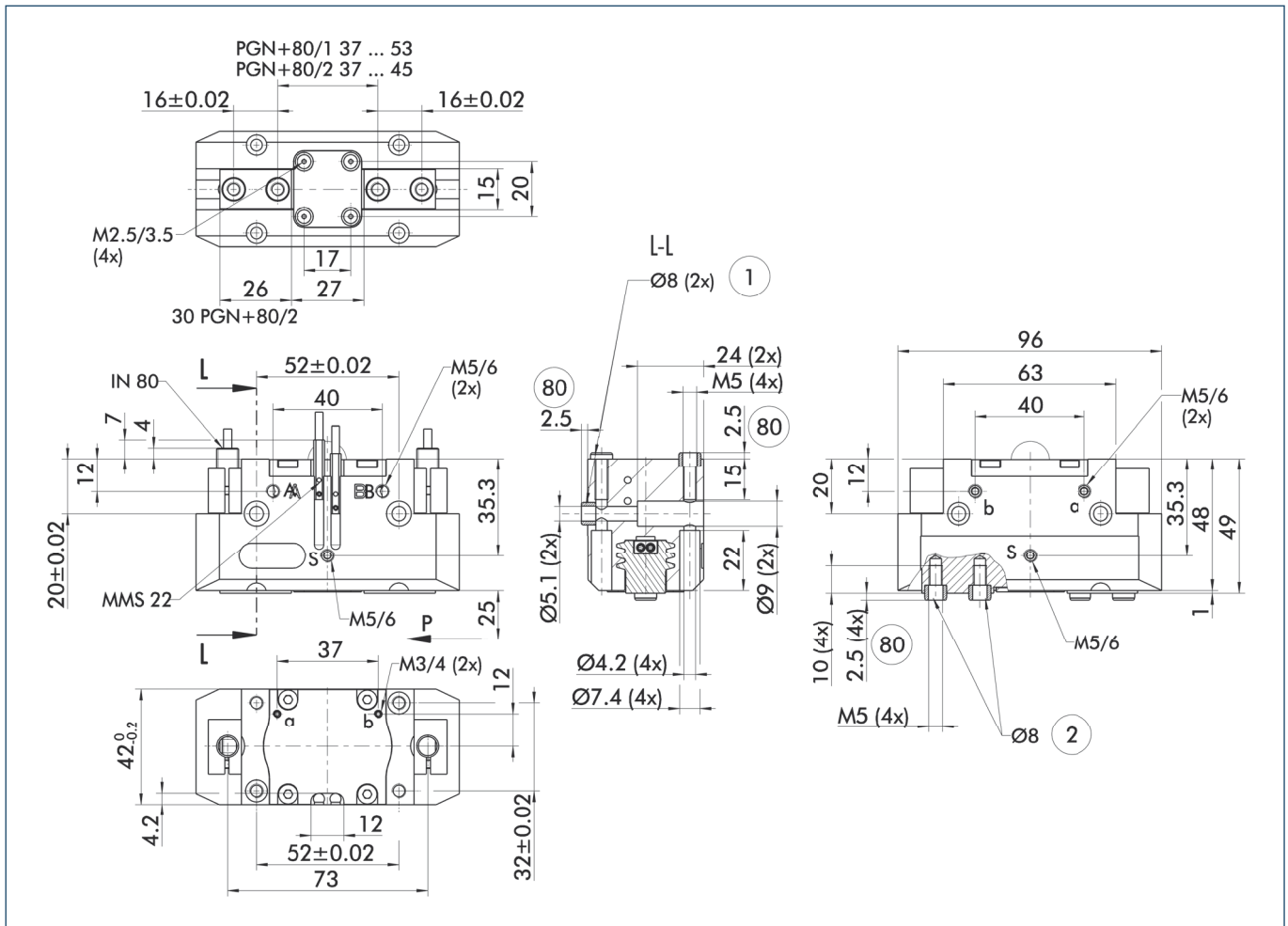
## Technical data

Description	PGN-plus 80-1	PGN-plus 80-2	PGN-plus 80-1-AS	PGN-plus 80-2-AS	PGN-plus 80-1-IS	PGN-plus 80-2-IS
ID	0371101	0371151	0371401	0371451	0371461	0371471
Stroke per finger [mm]	8	4	8	4	8	4
Closing force [N]	415	860	570	1180		
Opening force [N]	465	960			620	1280
Min. spring force [N]			155	320	155	320
Weight [kg]	0.5	0.5	0.6	0.6	0.6	0.6
Recommended workpiece weight [kg]	2.1	4.3	2.1	4.3	2.1	4.3
Air consumption per double stroke [cm <sup>3</sup> ]	21	21	45	45	45	45
Min./max. operating pressure [bar]	2.5/8	2.5/8	4/6.5	4/6.5	4/6.5	4/6.5
Nominal operating pressure [bar]	6	6	6	6	6	6
Closing/opening time [s]	0.04/0.04	0.04/0.04	0.03/0.05	0.03/0.05	0.05/0.03	0.05/0.03
Max. permitted finger length [mm]	110	105	105	100	105	100
Max. permitted weight per finger [kg]	0.6	0.6	0.6	0.6	0.6	0.6
IP class	40	40	40	40	40	40
Min./max. ambient temperature [°C]	-10/90	-10/90	-10/90	-10/90	-10/90	-10/90
Repeat accuracy [mm]	0.01	0.01	0.01	0.01	0.01	0.01
Cleanroom class						
ISO-classification 14644-1	5	5	5	5	5	5

## OPTIONS and their characteristics

Dust-protection version	37371101	37371151	37371401	37371451	37371461	37371471
IP class	64	64	64	64	64	64
Weight [kg]	0.6	0.6	0.7	0.7	0.7	0.7
Anti-corrosion version	38371101	38371151	38371401	38371451	38371461	38371471
High-temperature version	39371101	39371151	39371401	39371451	39371461	39371471
Min./max. ambient temperature [°C]	-10/130	-10/130	-10/130	-10/130	-10/130	-10/130
Force intensified version	PGN-plus 80-1-KVZ	PGN-plus 80-2-KVZ	PGN-plus 80-1-AS-KVZ		PGN-plus 80-1-IS-KVZ	
ID	0372101	0372151	0372401		0372461	
Closing force [N]	745	1550	900			
Opening force [N]	835	1730			990	
Weight [kg]	0.65	0.65	0.75		0.75	
Maximum pressure [bar]	6	6	6		6	
Max. permitted finger length [mm]	100	80	80		80	
Precision version	0371123	0371173	0371423	0371438		

## Main view



The drawing shows the gripper in the basic version with closed jaws, the dimensions do not include the options described below.

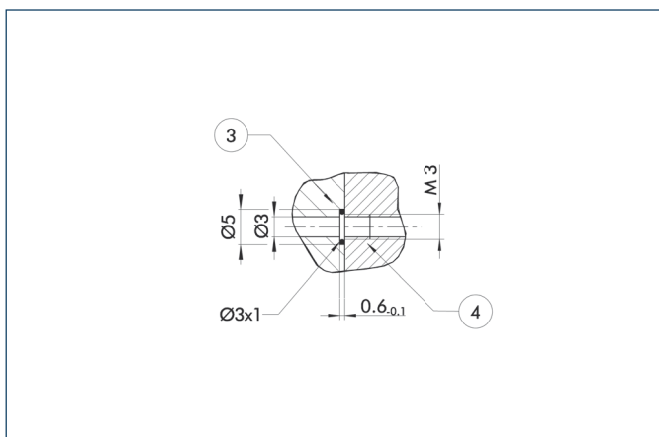
① The SDV-P pressure maintenance valve can also be used for I.D. or O.D. gripping alternatively or in addition to the spring-loaded, mechanical gripping force maintenance device (see "Accessories" catalog section).

A, a Main/direct connection, gripper opening  
 B, b Main/direct connection, gripper closing  
 S Air purge connection, or deaeration bore

② Finger connection  
 Ⓢ Depth of the centering sleeve hole in the matching part

① Gripper connection

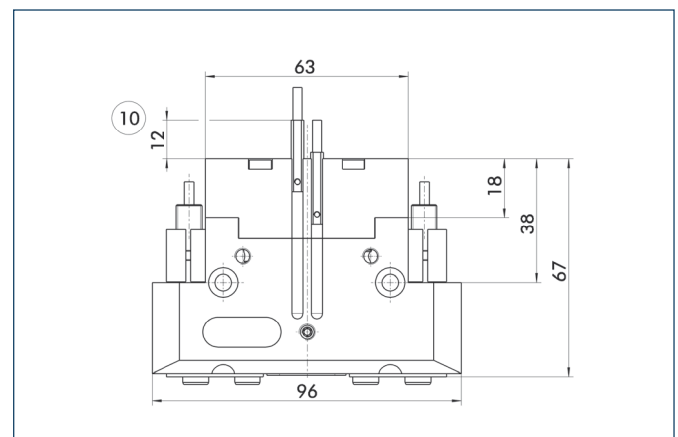
## Hose-free direct connection



③ Adapter  
 ④ Gripper

The direct connection is used for supplying compressed air without hoses. Instead, the pressure medium is fed through bore-holes in the mounting plate.

## AS/IS gripping force maintenance device

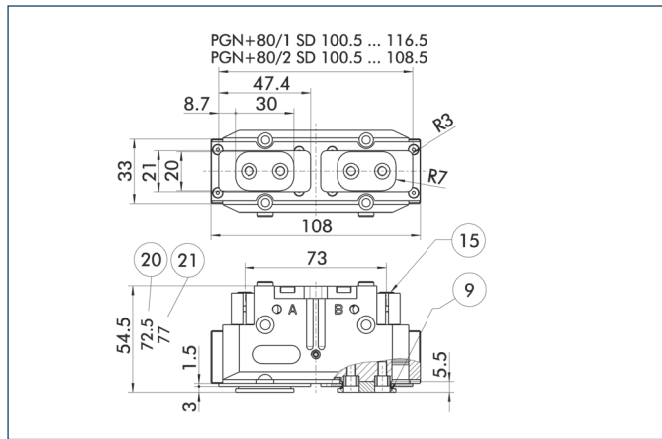


⑩ Projection applies only for AS version

The mechanical gripping force maintenance device ensures a minimum gripping force even in case of pressure drop. This acts as closing force in the AS version, and as opening force in the IS version. In addition, the gripping force maintenance device can also be used for increasing the gripping force or for single-acting gripping.



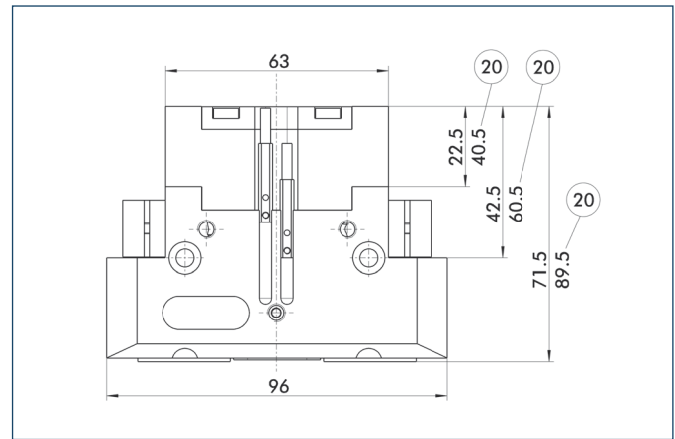
### Dust-protection version



- ⑨ For mounting screw connection diagram, see basic version
- ⑮ Sealing bolt
- ⑳ For AS / IS version
- ㉑ Applies for KVZ version

The "dust-protection" option increases the degree of protection against penetrating substances. The screw connection diagram shifts by the height of the intermediate jaw. The finger length is still measured from the upper edge of the gripper housing.

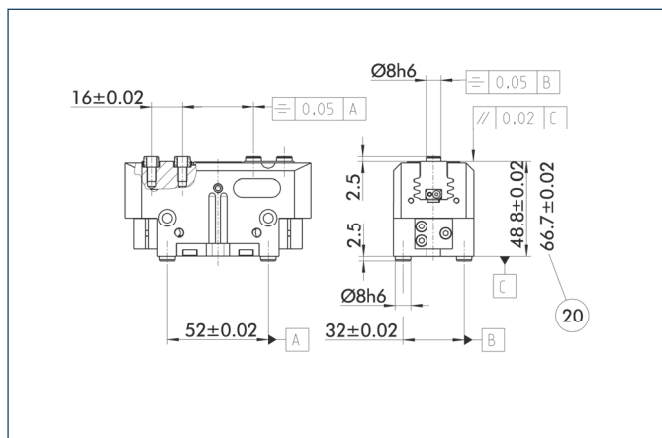
### Force intensified version



- ⑳ For AS / IS version

The KVZ cylinder increases the gripping forces during opening and closing. A second, in series-connected piston also increases the force on the wedge hook. The full gripping force shown in the data table is sometimes only reached after a few hundred gripping cycles. Please consider that grippers which are equipped with a gripping force maintenance device (AS / IS) are higher.

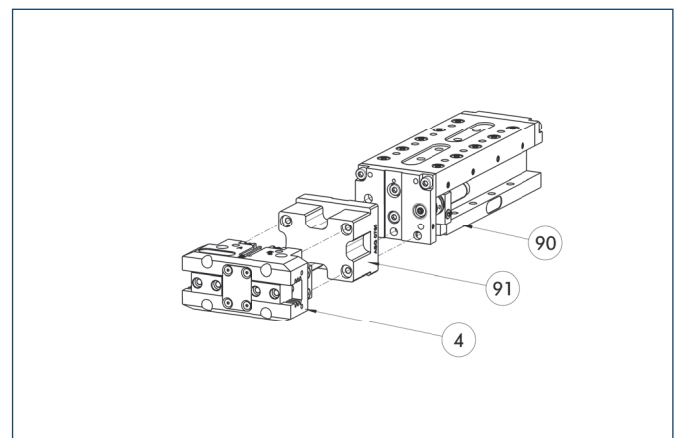
### Precision version



- ⑳ For AS / IS version

The indicated tolerances just refer to the types of precision versions shown in the chart of technical specifications. All other types of precision versions are available on request.

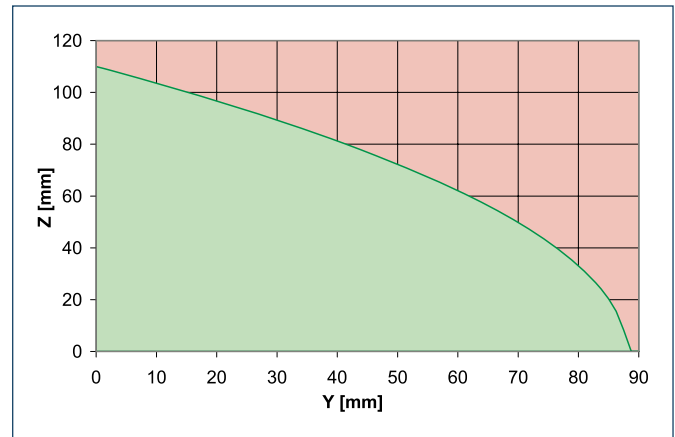
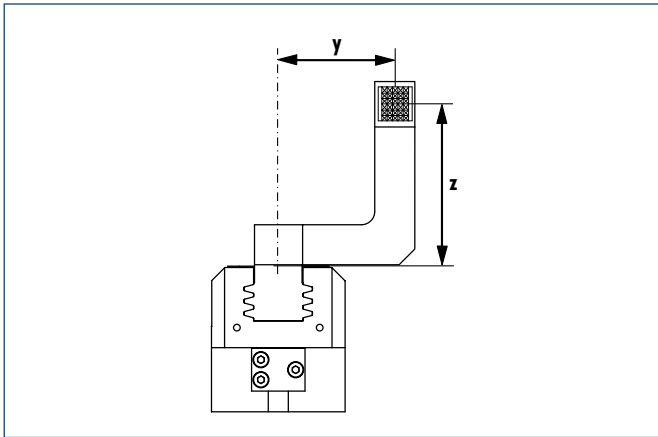
### Modular Assembly Automation



- ④ Gripper
- ⑨⑩ CLM
- ⑨① ASG

This gripper can be combined with the standard linear modules LM, KLM, CLM and ELM of the GEMOTEC modular system. For more information see our main catalog "Modular Assembly Automation".

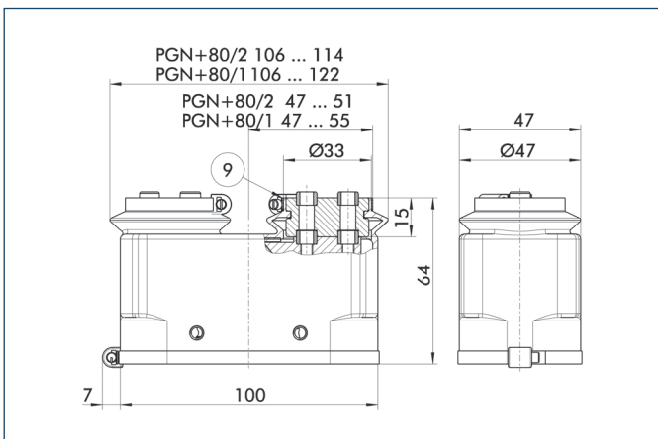
### Maximum permitted finger projection



■ Permitted range  
■ Inadmissible range

The curve applies to the basic version (stroke -1). For other versions, the curve will be parallel but offset in line with the max. permitted finger length.

### Protection cover

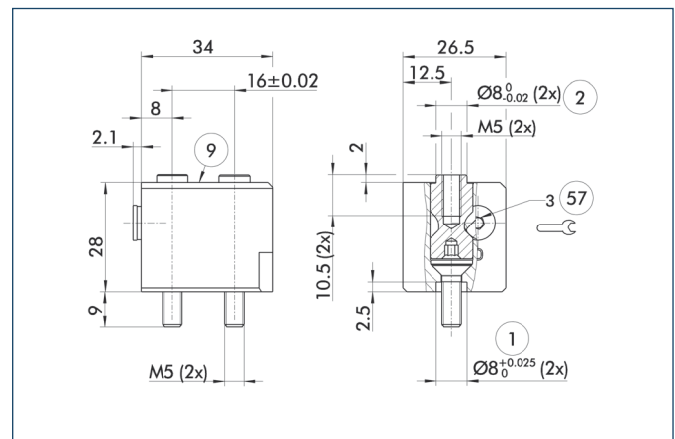


⑨ For mounting screw connection diagram, see basic version

The HUE protective cover completely protects the gripper against external influences up to IP65 if an additional sealing of the cover bottom is provided as part of the application. The mounting diagram shifts by the height of the intermediate jaw.

Description	ID	Cleanroom class ISO-classification 14644-1
Protection cover		
HUE PGN-plus 80	0371481	2

### Quick-change Jaw System



① Gripper connection

② Finger connection

⑨ For mounting screw connection diagram, see basic version

⑤7 Locking

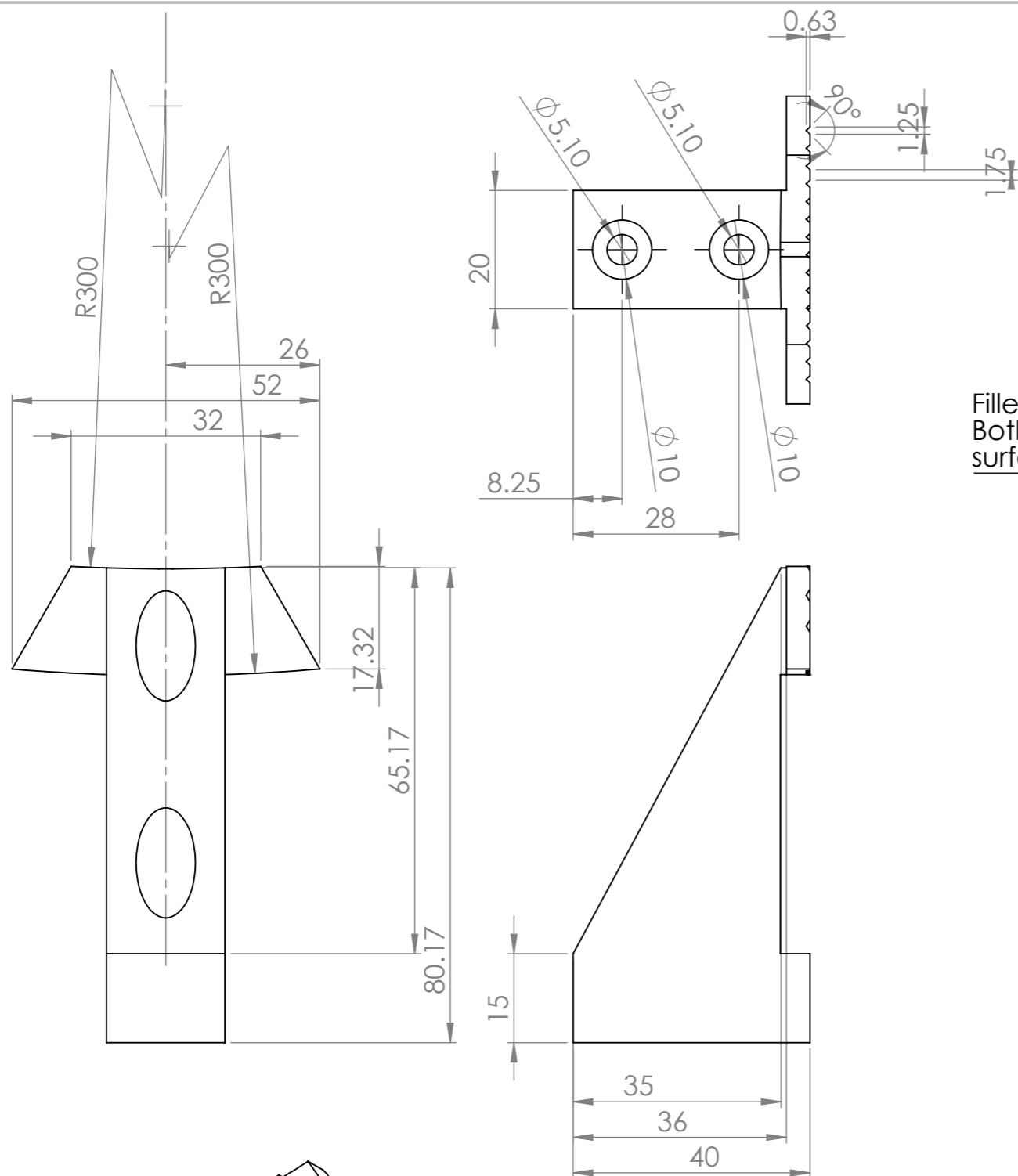
The BSWs quick-change jaw system enables top jaws to be changed on the gripper manually and rapidly. An adapter (BSWS-A) and a base (BSWS-B) are required for each gripper jaw.

For a reverse assembly without height set-up, one adapter (BSWS-A) and a kit (BSWS-U) per gripper jaw are required. Another effect of the BSWS-U is, that there are no disturbing fastening bores in the finger contour.

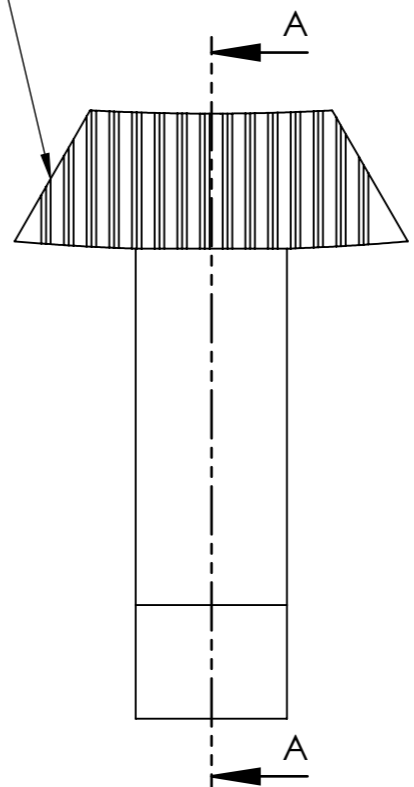
Description	ID
Quick-change Jaw System adapter	
BSWS-A 80	0303024
Quick-change Jaw System base	
BSWS-B 80	0303025
Quick-change Jaw System reversed	
BSWS-U 80	0303042



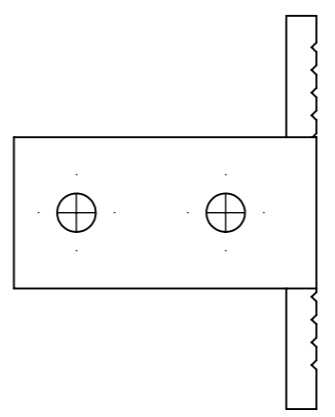
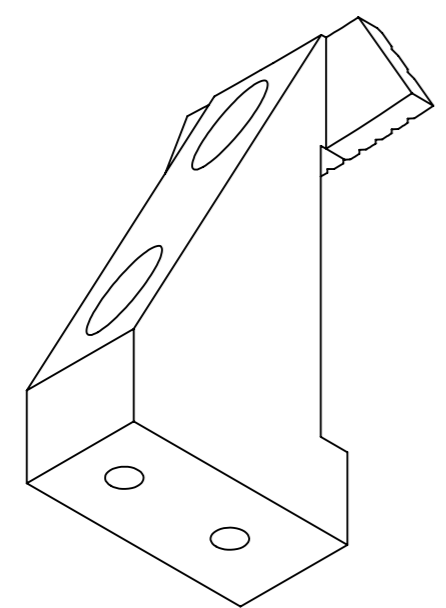
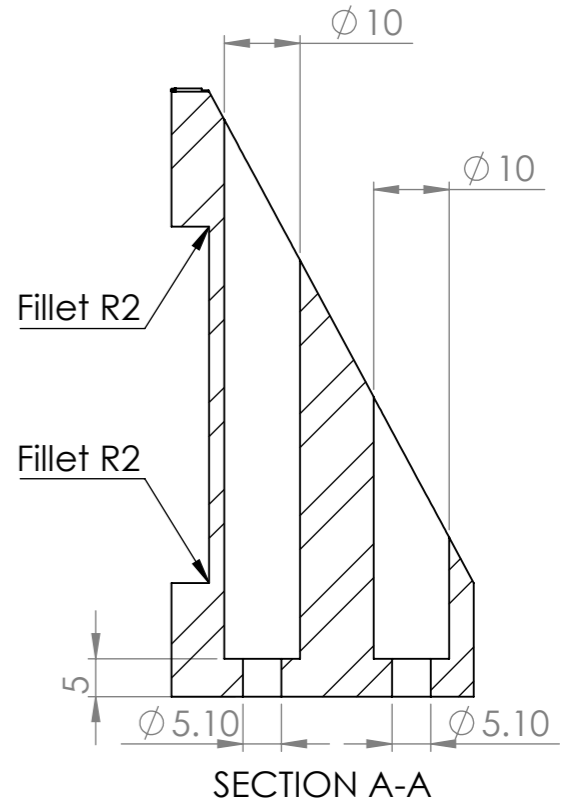
You can find more detailed information and individual parts of the above-mentioned accessories in the "Accessories" catalog section.



Fillet R 0.5  
Both front and back  
surface edges



Chamfer R0.5  
All Edges



UNLESS OTHERWISE SPECIFIED: DIMENSIONS ARE IN MILLIMETERS SURFACE FINISH: TOLERANCES: LINEAR: ANGULAR:				FINISH:		DEBUR AND BREAK SHARP EDGES		DO NOT SCALE DRAWING		REVISION	
								Quantity - 2			
								TITLE: Finger - Panel Forming			
								DWG NO. Drawing 1		A3	
						MATERIAL: EN3B - Steel		SCALE:1:1		SHEET 1 OF 1	
						WEIGHT:					
DRAWN		NAME		SIGNATURE		DATE					
CHK'D											
APPV'D											
MFG											
Q.A											

# 1 Overview

Basler acA1600-20gm				
Item	Symbol	Typ. <sup>1</sup>	Unit	Remarks
<b>Temporal Noise Parameters</b>				
Total Quantum Efficiency (QE)	$\eta$	46	%	$\lambda = 545 \text{ nm}$
Inverse of Overall System Gain	$\frac{1}{K}$	2.1	$\frac{e^-}{\text{DN}}$	
Temporal Dark Noise	$\sigma_{d_0}$	9	$e^-$	
Saturation Capacity	$\mu_{e,\text{sat}}$	8400	$e^-$	
<b>Derived Parameters</b>				
Absolute Sensitivity Threshold	$\mu_{p,\text{min}}$	20	$p\sim$	$\lambda = 545 \text{ nm}$
Dynamic Range	$\text{DYN}_{\text{out.bit}}$	9.8	bit	
Maximum SNR	$\text{SNR}_{y,\text{max.bit}}$	6.5	bit	
	$\text{SNR}_{y,\text{max.dB}}$	39.2	dB	
Item	Symbol	Typ.	Unit	Remarks
<b>Spatial Noise Parameters</b>				
Spatial Offset Noise, $\text{DSNU}_{1288}$	$\sigma_o$	3.0	$e^-$	
Spatial Gain Noise, $\text{PRNU}_{1288}$	$S_g$	0.8	%	

Table 1: Most Important Specification Data

Operating Point		
Item	Symbol	Remarks
Video output format		12 bits/pixel
Gain	Register raw	230
Offset	Register raw	100
Exposure time	$T_{\text{exp}}$	25.0 $\mu\text{s}$ to 18.6 ms

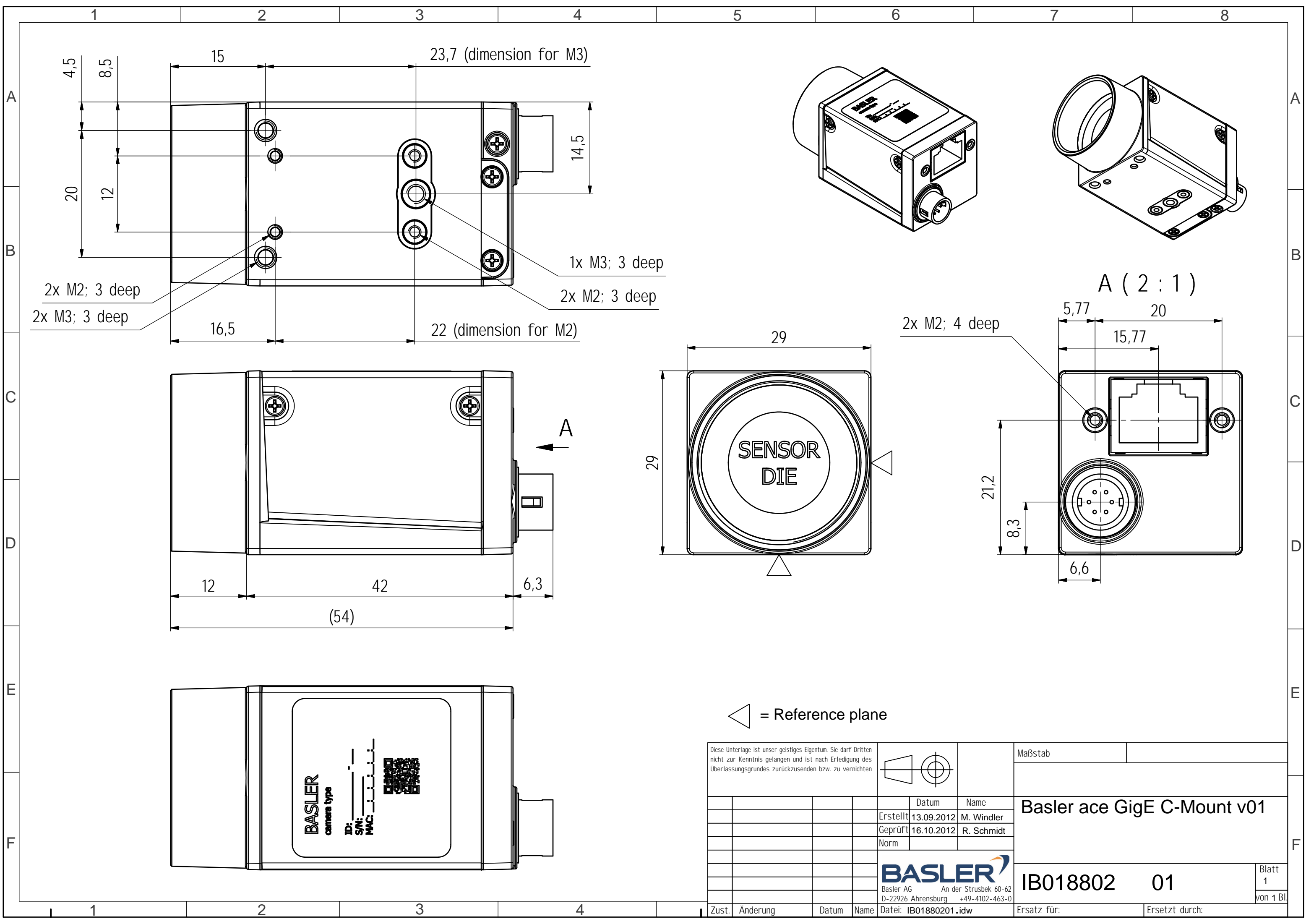
Table 2: Operating Point for the Camera Used

<sup>1</sup>The unit  $e^-$  is used in this document as a statistically measured quantity.

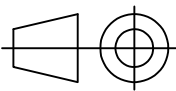

### 3 Basic Information

Basic Information	
Vendor	Basler
Model	acA1600-20gm
Type of data presented	Typical
Number of samples	100
Sensor	ICX274AL
Sensor type	CCD
Sensor diagonal	Diagonal 8.923 mm , Optical Size 1/1.8"
Indication of lens category to be used	C-Mount
Resolution	1628 x 1236 pixel
Pixel width	4.40 $\mu\text{m}$
Pixel height	4.40 $\mu\text{m}$
Readout type	Progressive scan
Transfer type	Interline transfer
Shutter type	-
Overlap capabilities	Overlapping
Maximum readout rate	20 frames/second
General conventions	-
Interface type	Gigabit Ethernet

Table 3: Basic Information



◁ = Reference plane

Diese Unterlage ist unser geistiges Eigentum. Sie darf Dritten nicht zur Kenntnis gelangen und ist nach Erledigung des Überlassungsgrundes zurückzusenden bzw. zu vernichten.						Maßstab	
				Datum		Name	
				Erstellt 13.09.2012		M. Windler	
				Geprüft 16.10.2012		R. Schmidt	
				Norm			
						<b>Basler ace GigE C-Mount v01</b>	
				Basler AG An der Strusbek 60-62 D-22926 Ahrensburg +49-4102-463-0		<b>IB018802 01</b>	
Zust. Änderung				Datum		Name	
Datei: IB01880201.idw				Ersatz für:		Ersetzt durch:	
						Blatt 1 von 1 Bl.	

**Calibration description file**

Below is the calibration description file of the calibration grid used for calibrating the laser scanner set-up. The same data is used in Halcon to generate the calibration grid. Prior to starting the calibration, Halcon (or any other 3D vision software) shall require a description file to be given as an input. This calibration data is used by the 3D vision software to identify the different translations and orientations of the calibration grid. The 3D vision software either accepts or rejects the calibration, based on a matching calibration profile.

---

```

# Plate Description Version 2
# HALCON Version 11.0 -- Fri Jan 09 12:19:56 2015
# Description of the standard calibration plate
# used for the camera calibration in HALCON
# (generated by gen_caltab)
#
#

# 7 rows x 7 columns
# Width, height of calibration plate [meter]: 0.08, 0.08
# Distance between mark centers [meter]: 0.01

# Number of marks in y-dimension (rows)
r 7

# Number of marks in x-dimension (columns)
c 7

# offset of coordinate system in z-dimension [meter] (optional):
z 0

# Rectangular border (rim and black frame) of calibration plate
# rim of the calibration plate (min x, max y, max x, min y) [meter]:
o -0.041 0.041 0.041 -0.041
# outer border of the black frame (min x, max y, max x, min y) [meter]:
i -0.04 0.04 0.04 -0.04
# triangular corner mark given by two corner points (x,y, x,y) [meter]
# (optional):
t -0.04 -0.03 -0.03 -0.04

# width of the black frame [meter]:
w 0.0025

# calibration marks: x y radius [meter]

# calibration marks at y = -0.03 m

```

-0.03 -0.03 0.0025  
-0.02 -0.03 0.0025  
-0.01 -0.03 0.0025  
0 -0.03 0.0025  
0.01 -0.03 0.0025  
0.02 -0.03 0.0025  
0.03 -0.03 0.0025

# calibration marks at  $y = -0.02$  m

-0.03 -0.02 0.0025  
-0.02 -0.02 0.0025  
-0.01 -0.02 0.0025  
0 -0.02 0.0025  
0.01 -0.02 0.0025  
0.02 -0.02 0.0025  
0.03 -0.02 0.0025

# calibration marks at  $y = -0.01$  m

-0.03 -0.01 0.0025  
-0.02 -0.01 0.0025  
-0.01 -0.01 0.0025  
0 -0.01 0.0025  
0.01 -0.01 0.0025  
0.02 -0.01 0.0025  
0.03 -0.01 0.0025

# calibration marks at  $y = 0$  m

-0.03 0 0.0025  
-0.02 0 0.0025  
-0.01 0 0.0025  
0 0 0.0025  
0.01 0 0.0025  
0.02 0 0.0025  
0.03 0 0.0025

# calibration marks at  $y = 0.01$  m

-0.03 0.01 0.0025  
-0.02 0.01 0.0025  
-0.01 0.01 0.0025  
0 0.01 0.0025  
0.01 0.01 0.0025  
0.02 0.01 0.0025  
0.03 0.01 0.0025

# calibration marks at  $y = 0.02$  m

-0.03 0.02 0.0025  
-0.02 0.02 0.0025  
-0.01 0.02 0.0025  
0 0.02 0.0025  
0.01 0.02 0.0025



0.02 0.02 0.0025

0.03 0.02 0.0025

# calibration marks at  $y = 0.03$  m

-0.03 0.03 0.0025

-0.02 0.03 0.0025

-0.01 0.03 0.0025

0 0.03 0.0025

0.01 0.03 0.0025

0.02 0.03 0.0025

0.03 0.03 0.0025

# An automated solution for fixtureless sheet metal forming

Balaji Ilangovan<sup>1,2</sup> · Radmehr P. Monfared<sup>1,2</sup> ·  
Michael Jackson<sup>1,2</sup>

Received: 15 December 2014 / Accepted: 21 May 2015  
© The Author(s) 2015. This article is published with open access at Springerlink.com

**Abstract** Manual forming of sheet metal parts through traditional panel beating is a highly skilled profession used in many industries, particularly for sample manufacturing or repair and maintenance. However, this skill is becoming gradually isolated mainly due to the high cost and lack of expertise. Nonetheless, a cost-effective and flexible approach to forming sheet metal parts could significantly assist various industries by providing a method for fast prototyping sheet metal parts. The development of a new fixtureless sheet metal forming approach is discussed in this article. The proposed approach, named Mechatroforming<sup>®</sup>, consists of integrated mechanisms to manipulate sheet metal parts by a robotic arm under a controlled hammering tool. The method includes mechatronics-based monitoring and control systems for (near) real-time prediction and control of incremental deformations of parts. This article includes description of the proposed approach, the theoretical and modelling backgrounds used to predict the forming, skills learned from manual operations, and proposed automation system being built.

**Keywords** Automation · Flexible manufacturing · Rapid prototyping · Incremental forming

---

✉ Balaji Ilangovan  
B.Ilangovan@lboro.ac.uk

<sup>1</sup> EPSRC Centre for Innovative Manufacturing in Intelligent Automation, Loughborough University, Loughborough, UK

<sup>2</sup> Wolfson School of Mechanical and Manufacturing Engineering, Loughborough University, Loughborough, UK LE11 3TU

## 1 Introduction

In many industries, dies are used for forming sheet metals but they typically lack flexibility and cost-effectiveness when low-volume production or prototyping are considered. For these cases, the traditional manual panel beating is still used. However, manual panel beating is a highly skilled process and unfortunately, due to the lack of interest (by new trainees), high cost, and sporadic industrial applications, is becoming isolated and gradually being lost.

There is not enough research carried out to fully understand and capture the skills of experienced panel beaters and its links with the formal sheet metal forming theories.

Analysing the conventional manual practises has led to an ongoing research work in robotic sheet metal forming which has been discussed in this article. The proposed research methodology could potentially be used by many industries, especially for maintenance and rapid prototyping of sheet metal parts.

There has been some research in die-less incremental forming of sheet metals [1]. Most proposed methods use either stretching or drawing techniques with or without an anvil support. The sheet metal is formed by using a round headed tool which moves down vertically (i.e. in  $Z$  axis). The sheet metal is typically held by fixtures along the edges to avoid movement caused by tool. Either the sheet metal or the tool is moved along  $XY$  axes (i.e. the horizontal plane) to achieve the required contour. The forming is often computer controlled. Employing this technique achieves a smooth finish but may result in fractures due to excessive stretching and often fails while forming complex contours (e.g. having more than  $55^\circ$  wall angle [2]). These methods use fixtures to hold the sheet and typically result in non-uniform thickness of the formed sheet metal, hence, affecting the quality.

## Die-less Automated Sheet Metal Forming



Die-less forming is one of the emerging techniques in the sheet metal forming industry. Research is being carried out to develop a new automated method for sheet metal forming, based on human technique captured from studies of highly skilled panel beaters.

The methodology developed uses a sequential hammering mechanism, the Eckold Kraftformer KF 170 PD. The mechanism incrementally forms the sheet metal which is held and manipulated by a robot to form the required shape. The developed approach includes an in-process monitoring system using machine vision. The vision system feedback is used to accurately control the formation of the material to the three dimensional shape required.

In many industries, dies are used to form sheet metal panels of different contours. Dies lack flexibility and cost effectiveness when low volume production, repair or prototyping is required. In such cases, manual panel beating is typically undertaken for incremental forming of metal panels. This is a highly skilled operation with very little documentation. Unfortunately, due to recruitment issues, high cost and



**By Balaji Ilangovan**  
MISME MIET AMIMECHE  
BEng, MSc.,

**PhD Researcher  
in Automated Sheet Metal Forming**  
EPSRC Centre for Innovative  
Manufacturing in Intelligent  
Automation, Loughborough  
University, UK

**Treasurer**  
IMechE, Leicestershire  
Young Members Panel

**Email:** B.Ilangovan@lboro.ac.uk,  
B.Ilangovan88@gmail.com

**Linkedin:** uk.linkedin.com/pub/  
balaji-ilangovan/40/b82/70a/

## T.M.A. ENGINEERING LTD.

Incorporating Taylor & Challen and CVA High Speed Dieing Presses

### Power Presses

- Serving the power press industry since 1973.
- Service, spares, repairs, overhauls, maintenance.
- Spare parts 'ex stock' for most popular makes of press.
- Team of mechanical & electrical engineers for 'on site' work.
- Fully qualified & trained to carry out HSG236 inspections in line with HSE guidance & recognised by your insurance company.
- Guards – fixed, rising screen, hinged, light guards.
- Electrical control panels, lubrication systems, pneumatics.
- Complete press overhauls, clutch conversions, new electrics.
- Second hand presses, servo feeds, decoilers, straighteners.
- NEW presses & coil feed equipment.

### Locomotives

- Railway Maintenance Support & specialist part manufacture, safety equipment, jigs & fixtures.
- Years of experience with full size & narrow gauge steam & diesel locomotives offering servicing, spares, overhauls & restoration work.
- New narrow gauge steam & diesel locomotives.
- Carriages, bogies, tenders.

### Machining

- One offs & small batch to drawing or sample.
- Large capacity machine & fitting shop.
- Turning, milling, boring, slotting, drilling and welding.
- Fabrication work in steel & aluminium - MIG, TIG & ARC.
- BS EN ISO 9001:2000 Quality Management System



95-111 Tyburn Rd Erdington Birmingham B24 8NQ  
www.TMAeng.co.uk – sales@TMAeng.co.uk  
t. 0121 328 1908 – f. 0121 322 2017

## Ortlinghaus

SINCE 1898  
THE TECHNOLOGY OF CONTROLLED TORQUE

Constant Research & Development into clutch/brake design and manufacture have led to an extensive range of both pneumatic and hydraulic units which are second to none. Full technical backup, engineering support and parts service to OEM Press manufacturers, rebuilders and end users.



Ortlinghaus UK are now official representatives for sales and service of the OPTIMA range of clamping and slide lock systems within the U.K.

**CONTACT: Tony Jepson**  
Telephone: 01527 579123  
Fax: 01527 579077  
E-mail: sales@ortlinghaus.co.uk  
www.ortlinghaus.co.uk



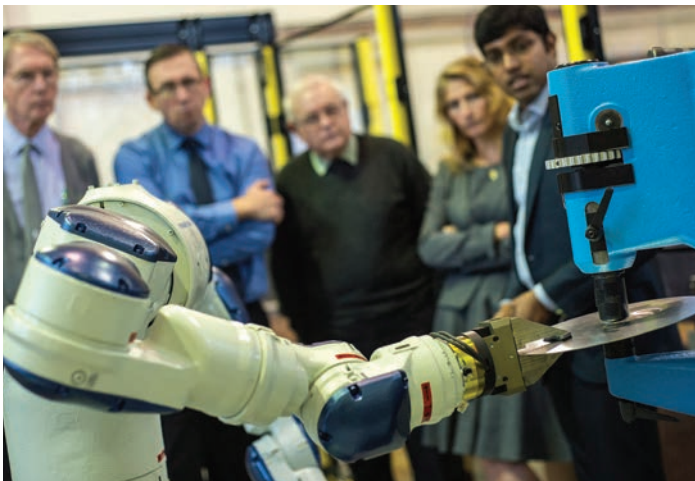
# Die-less Automated Sheet Metal Forming

Die-less forming is one of the emerging techniques in sheet metal forming. Research is being carried out to develop a new automated method for sheet metal forming based on human skill captured from highly skilled panel beaters. The methodology developed uses a sequential hammering mechanism, the Eckold Kraffformer KF 170 PD. The mechanism incrementally forms the sheet metal which is held and manipulated by a robot to form the required shape. The developed approach includes an in-process monitoring system using machine vision. The vision system feedback is used to control the formation of sheet metal accurately to the three dimensional shape required.

In many industries, dies are used to form sheet metal panels of different contours. Dies lack flexibility and cost effectiveness when low volume production, repair or prototyping is required. In such cases, manual panel beating is typically undertaken for incremental forming of metal panels. This is a highly skilled operation with very little documentation. Unfortunately, due to recruitment issues, high cost and sporadic industrial applications, manual panel beating is being isolated and gradually forgotten. It is essential to capture the highly skilled process and preserve the knowledge of metal forming practise.

The EPSRC Centre for Innovative Manufacturing in Intelligent Automation launched a PhD in July 2012 to develop an automated panel forming process. Primarily, the research aimed at understanding and analysing the skills of a manual panel beater. A comprehensive literature review was carried out to understand the industrial and research work in this area. Though there has been a significant research in automated incremental forming processes, the current technology for die-less forming typically uses either stretching or drawing of sheets, usually by pushing the material. This causes a thinning effect on the panel and almost all the current methods require substantial fixtures to hold the panel.

Based on the literature review, the research was focused on forming the sheet metal without using dies and fixtures allowing free formation of sheet metal replicating the skill of a panel beater. The research methodology was developed in three stages, consisting of capturing human skill, semi-automated system and fully automated system. This work included several modelling and experimental process analyses.



Initially, experienced panel beaters were closely observed and their tacit human skill was analysed. It was identified that consecutive shrinking and stretching (through hammering) of sheet metal produces a sheet with uniform thickness. It was also determined that imposing repetitive kinetic energy through hammering allows better control over producing shapes incrementally by consecutive stretching and shrinking without fixtures. This method is also believed to improve release of residual stresses during the forming process. The constructive methodology used by the panel beater improves the quality of the sheet metal by maintaining the uniform distribution of material.

Measurement of the impact force and kinetic energy involved in panel beating of sheet metal was carried out using an instrumented mallet and high speed video to capture data during manual hammering tests conducted in a structured laboratory environment. Based on the impact force determined and corresponding kinetic energy, a hammering machine capable of producing the required force and able to operate at the required frequency was investigated. The Eckold Kraffformer KF 170 PD was purchased as this met the requirements for the automated panel beating test cell.

The semi-automated system utilises the Eckold Kraffformer and manual manipulation of the sheet metal blank between the hammer and the anvil during automatically repetitive hammering to progressively form the desired 3D shape. During the action of forming the shape a Vicon 3D imaging system was used to capture and analyse the movement of the sheet metal blank. Based on several experimental trials, the most suitable movement pattern and path was determined to be used as an input to the robotic manipulation.

The development of an automated system included the integration of an Eckold Kraffformer and Motoman SDA10D on a common control platform. This approach synchronised the sequential hammering of the Eckold Kraffformer with the forming manipulation pattern executed by the robot. A gripper was designed similar to the holding-area of a human grip in manual forming process. The gripper was installed on the robotic arm to be able to hold the sheet metal and provide the required manipulation.

Based on this set-up, experimental trials were performed in developing an automated sheet metal forming process. The trials based on forming a bowl shape were successful and repeatable after several analyses and modifications. The human skills studied and decomposing the video of trials to examine the formation contributed towards performance enhancement.

continued on page 20 >>>>

# MANUFACTURING THE FUTURE CONFERENCE 2013

Free- Form Automated Incremental Panel Forming

Balaji Ilangovan, Radmehr P. Monfared, Michael Jackson

EPSRC Centre for Innovative Manufacturing in Intelligent Automation, Wolfson School of Mechanical & Manufacturing Engineering, Loughborough University, Loughborough, B.ilangovan@lboro.ac.uk

Dies are used in many industries to form metal panels of different contours but they lack flexibility and cost effectiveness when low volume production, repair or prototyping is considered. In such cases, manual panel beating is typically undertaken for incremental forming of metal panels. Manual panel forming is a highly skilled operation with very little documentation and the skill is disappearing due to non-observance and lack of training. There has been a significant amount of research in automated incremental forming processes. However, the current technology for die-less forming typically uses either stretching or drawing of sheets, usually by pushing the material. This causes a thinning effect on the panel which requires substantial fixtures.

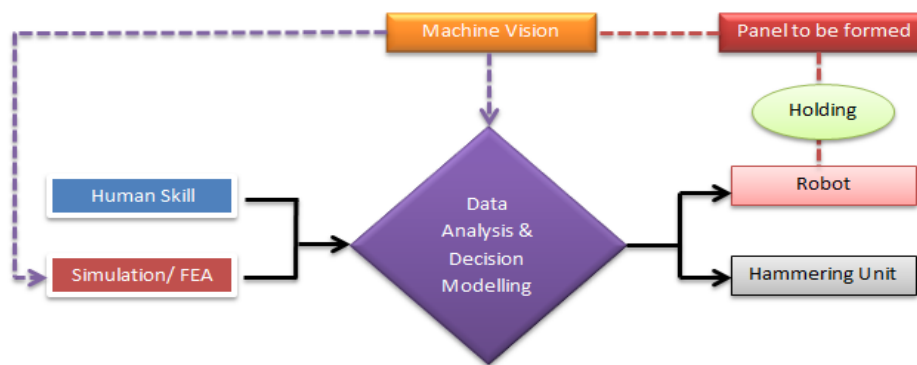


Figure 1

This research is aimed at developing a new automated method for panel formation based on human skill captured from manual operators. The methodology being developed, incrementally forms the material through impacting with continuous control and modification through a fixtureless integrated process. The proposed approach includes automating panel forming with a near real time monitoring system using machine vision. This process is targeted at producing nearly uniform panel thickness by introducing a higher degree of freedom in formation with continuous stress analysis. This research has the potential to optimise the panel formation and reduce reworks in forming irregular shapes. The process model based on human skill capture is illustrated in Figure 1. The scope of this research is limited to 1mm thick aluminium and steel which covers standard industry applications. The formation is carried out by an impact energy delivery unit causing deformation in the panel, which is held by a robot controlling the movement of the panel, adhering to the formation. The distance of deformation is obtained by using point-cloud data, which is generated by using machine vision and analysed through finite elements.

**Significance Statement:** This research will provide a proof of principle for automated one off, flexible production of irregular panels. Highly accurate production will be achieved based on the panel formation skills captured from human operators.